PUBLICATIONS OF
THE UNIVERSITY OF EASTERN FINLAND

Dissertations in Health Sciences

MUHAMMAD ALI SHAHBAZ

CELLULAR INVESTIGATIONS INTO THE INTERPLAY OF PARTICULATE MATTER EXPOSURE, RESPIRATORY INFECTIONS, AND ALZHEIMER'S DISEASE

CELLULAR INVESTIGATIONS INTO THE INTERPLAY OF PARTICULATE MATTER EXPOSURE, RESPIRATORY INFECTIONS, AND ALZHEIMER'S DISEASE

Muhammad Ali Shahbaz

CELLULAR INVESTIGATIONS INTO THE INTERPLAY OF PARTICULATE MATTER EXPOSURE, RESPIRATORY INFECTIONS, AND ALZHEIMER'S DISEASE

To be presented by permission of the Faculty of Health Sciences,
University of Eastern Finland for public examination in SN200
Auditorium, Kuopio on June 12th, 2024, at 12 o'clock noon

Publications of the University of Eastern Finland
Dissertations in Health Sciences
No 832

A.I. Virtanen Institute for Molecular Sciences
University of Eastern Finland, Kuopio
2024

PunaMusta Oy
Joensuu, 2024
Distributor: University of Eastern Finland
Kuopio Campus Library

ISBN: 978-952-61-5235-6 (print/nid.)
ISBN: 978-952-61-5236-3 (PDF)
ISSNL: 1798-5706
ISSN: 1798-5706
ISSN: 1798-5714 (PDF)

Author's address: A.I. Virtanen Institute for Molecular Sciences
University of Eastern Finland
KUOPIO
FINLAND

Doctoral programme: Doctoral Programme in Molecular Medicine

Supervisors: Professor Katja Kanninen, Ph.D.
A.I. Virtanen Institute for Molecular Sciences
University of Eastern Finland
KUOPIO
FINLAND

Professor Pasi Jalava, Ph.D.
Department of Environmental and Biological Sciences, Faculty of Science, Forestry and Technology
University of Eastern Finland
KUOPIO
FINLAND

Professor Marjut Roponen, Ph.D.
Department of Environmental and Biological Sciences, Faculty of Science, Forestry and Technology
University of Eastern Finland
KUOPIO
FINLAND

Reviewers:

Professor Paola Palestini, Ph.D.
School of Medicine and Surgery
University of Milano-Bicocca
Monza
Italy

Professor Jonathan Grigg, Ph.D.
Blizard Institute - Faculty of Medicine and Dentistry
Queen Mary University of London
London
United Kingdom

Opponent:

Principal Investigator, Dr. Juana Maria Delgado-Saborit
School of Medicine
Universitat Jaume I,
Castellón
Spain

Shahbaz, Muhammad Ali
Cellular Investigations into the Interplay of Particulate Matter Exposure, Respiratory Infections, and Alzheimer's Disease
Kuopio: University of Eastern Finland
Publications of the University of Eastern Finland
Dissertations in Health Sciences 832. 2024, 132 p.
ISBN: 978-952-61-5235-6 (print)
ISSNL: 1798-5706
ISSN: 1798-5706
ISBN: 978-952-61-5236-3 (PDF)
ISSN: 1798-5714 (PDF)

ABSTRACT

Environmental agents present in inhaled air, including pollutants and pathogens, present formidable challenges to human health. While components of air pollution, such as high levels of particulate matter (PM), are associated with increased premature deaths, communicable respiratory infections are among the leading causes of death worldwide. In particular, the advent of the COVID-19 pandemic highlighted the profound impact of airborne agents on health, leading to widespread fatalities and raising concerns about long-term health issues. This thesis explores the intersection of two environmental exposures, PM and respiratory infections, and their effects on cellular and molecular mechanisms of the respiratory system.

Particulate matter with a diameter smaller than 2.5 μm ($PM_{2.5}$), particulate matter with a diameter smaller than 10 μm (PM10), and ultrafine particles (UFP) with a diameter smaller than 0.1 μm, not only pose environmental concerns but also potentially exacerbate respiratory infections. Their interaction with the respiratory system, particularly their ability to breach defence mechanisms and impact responses to both bacterial and viral infections, is a complex and underexplored area that is addressed in this thesis. This thesis also highlights the importance of the

olfactory mucosa (OM) as a critical interface in this dynamic. Situated at the rooftop of the nasal cavity and in direct contact with the brain, the OM is linked to the brain translocation of PM, and neurological symptoms of COVID-19, such as anosmia. Moreover, the significance of the OM in neurodegenerative disorders, particularly Alzheimer's Disease (AD), is emphasized by evidence linking impairment in OM function to AD-associated pathological changes. In addressing these challenges, this thesis employs advanced *in vitro* models to replicate complex, physiologically relevant scenarios. This approach allows for a more nuanced exploration of how PM impacts the body's response to respiratory pathogens, with a particular focus on SARS-CoV-2, which causes COVID-19.

This doctoral thesis investigated the effects of $PM_{2.5-1}$ exposure on innate immune responses at the lung barrier by utilizing a co-culture model of alveolar epithelial cells and macrophages. The findings revealed that $PM_{2.5-1}$ enhances inflammatory responses to bacterial stimuli while diminishing responses to viral ligands, indicating a multifaceted role of PM in respiratory immunity and differential mechanism of altering the immune response toward various pathogens. Then in primary human OM cells, the thesis examined the effects of SARS-CoV-2 infection in cells from both healthy individuals and those with AD using a 3D *in vitro* model mimicking the interface between air and brain. This study revealed that while susceptibility to SARS-CoV-2 remains consistent across groups, AD cells exhibited unique transcriptomic responses, suggesting increased oxidative stress and altered immune responses, and highlighting a specific vulnerability of AD cells to viral infections. Lastly, the thesis explored the effects of urban PM, specifically $PM_{10-2.5}$ and $PM_{0.2}$, on OM cell responses to SARS-CoV-2 in the context of AD. It demonstrated that while PM exposure does not increase viral susceptibility, it significantly alters cellular immune responses, particularly in cells from AD individuals, suggesting intricate interactions between air pollution, viral infection, and neurodegeneration.

This thesis provides crucial insights into the complex interactions between airborne agents, respiratory infections, and neurodegenerative diseases, particularly AD. It elucidates how PM exposure modifies immune responses, enhancing vulnerability to bacterial stimuli while diminishing

the body's defense against viral stimuli. Additionally, the research shows that AD can alter cellular reactions to SARS-CoV-2, possibly exacerbating COVID-19 outcomes. Moreover, it sheds light on the compounded effects of PM exposure and AD on immune responses in COVID-19 cases. These findings highlight the imperative need for integrated approaches that encompass environmental, immunological, and pathological factors. This research lays a solid foundation for future studies and public health strategies aimed at mitigating the impacts of environmental factors on disease susceptibility and progression, with a special focus on populations at risk for AD.

National Library of Medicine Classification: QS 532.5.E7, QS 532.5.M8, QT 140, QU 55.7, QU 475, QU 550.5.S4, WA 754, WC 506, WT 155, WV 302.
Medical Subject Headings: Air Pollution; Particulate Matter; Respiratory Tract Infections; Toll-Like Receptors; COVID-19; SARS-CoV-2; Olfactory Mucosa; Alzheimer Disease; Neurodegenerative Diseases; Environmental Exposure; Neuroinflammatory Diseases; Gene Expression Profiling.

Shahbaz, Muhammad Ali
Kaupunki-ilman pienhiukkaset, hengitystieinfektiot ja Alzheimerin tauti: hengitysilman altisteiden vuoro- ja soluvaikutukset
Kuopio: Itä-Suomen yliopisto
Publications of the University of Eastern Finland
Dissertations in Health Sciences 832. 2024, 132 p.
ISBN: 978-952-61-5235-6 (print)
ISSNL: 1798-5706
ISSN: 1798-5706
ISBN: 978-952-61-5236-3 (PDF)
ISSN: 1798-5714 (PDF)

TIIVISTELMÄ

Ympäristötekijät, kuten ilman epäpuhtaudet ja taudinaiheuttajat hengitysilmassa, ovat merkittävä haaste ihmisten terveydelle. Altistuminen ilmansaasteille on yhdistetty ennenaikaisiin kuolemantapauksiin, ja tarttuvat hengitystieinfektiot ovat yksi maailman johtavista kuolinsyistä. Erityisesti koronaviruksen aiheuttama COVID-19 pandemia on johtanut laajoihin kuolemantapauksiin ja herättänyt huolta pitkäaikaisista terveysongelmista. Tämä väitöskirja tutkii hengitysilmassa olevien altisteiden, erityisesti pienhiukkasten (PM), ja hengitystieinfektioiden välistä vuorovaikutusta ja niiden vaikutuksia hengityselimistölle.
Altistuminen ilmansaasteiden pienhiukkasille aiheuttaa terveysriskejä, mutta voi myös pahentaa hengitystieinfektioita. Pienhiukkasten ja hengitysilmassa olevien virusten vuorovaikutus on monimutkainen ja pitkälti tutkimaton aihe. Tämä väitöskirja korostaa hajuepiteelin tärkeyttä tämän vuorovaikutuksen tutkimuksessa. Nenäontelon yläosassa sijaitseva hajuepiteeli on suoraan yhteydessä sekä hengitysilmaan että aivoihin. Hajuepiteelin kautta ilman pienhiukkasilla on mahdollisuus kulkeutua aivokudokseen asti ja muutokset hajuepiteelin toiminnassa on liitetty COVID-19 taudin neurologisiin oireisiin, kuten hajuaistin muutoksiin. Lisäksi keskushermostoa rappeuttavissa sairauksissa, kuten Alzheimerin taudissa (AT), on havaittu hajuepiteelin toiminnan heikkenemistä sekä tautiin

liitettyjä patologisia muutoksia hajuepiteelillä. Tässä väitöskirjassa hyödynnetään edistyneitä soluviljelymalleja tutkimukseen siitä, kuinka ilman pienhiukkaset vaikuttavat elimistön vasteeseen hengitysilman patogeenejä vastaan, keskittyen erityisesti COVID-19 taudin aiheuttajan SARS-CoV-2-viruksen vuorovaikutukseen kaupunki-ilman pienhiukkasten kanssa.

Väitöskirjan ensimmäisessä osatyössä tutkittiin pienhiukkasten vaikutuksia elimistön puolustusjärjestelmän vasteisiin keuhkoissa käyttäen alveolaaristen epiteelisolujen ja makrofagien yhteisviljelymallia. Tulokset osoittivat, että kaupunki-ilman pienhiukkaset muokkaavat keuhkojen solujen immuunivastetta eri tavalla bakteeri kuin virusinfektiota vastaan. Toisessa osatyössä vertailtiin hajuepiteelin solujen vasteita SARS-CoV-2-infektiolle viljelemällä hajuepiteelin soluja kolmiulotteisissa soluviljelymalleissa. Hajuepiteelin solut olivat peräisin henkilöiltä, joilla on todettu AT sekä kognitiivisesti terveiltä kontrollihenkilöiltä. Tämä tutkimus paljasti, että vaikka alttius SARS-CoV-2 infektiolle ei ollut muuttunut tutkimusryhmien välillä, AT solujen vasteet poikkesivat terveistä soluista. Henkilöiden soluissa, joilla oli todettu AT, havaittiin muutoksia geenien ilmentymisessä, jotka viittasivat lisääntyneeseen hapetusstressiin ja solujen muuttuneisiin puolustusvasteisiin. Kolmannessa osatyössä altistuminen kaupunki-ilman hiukkaspäästöille ei lisännyt hajuepiteelin solujen infektioherkkyyttä SARS-CoV-2 virukselle, mutta se muutti merkittävästi solujen puolustusvasteita, erityisesti AT-potilaiden soluissa. Tämä väitöskirja tuo uutta solutason tietoa ilmansaasteiden, hengitystieinfektioiden ja AT:n monimutkaisista yhteyksistä. Se selventää, miten altistuminen kaupunki-ilman hiukkaspäästöille muokkaa immuunivasteita keuhkoissa ja hajupiteelillä. Lisäksi tutkimus osoittaa, että AT voi vaikuttaa solujen vasteisiin SARS-CoV-2 virusinfektiolle, ja tuo uutta tietoa pienhiukkasten ja SARS-CoV-2 viruksen yhteisvaikutuksista hajuepiteelillä. Väitöskirjan tulokset luovat vankan perustan jatkotutkimuksille, joiden tavoitteena on lieventää ilmansaastealtistuksen ja hengitystieinfektioiden haittavaikutuksia erityisesti riskiryhmiin, kuten AT, kuuluvien henkilöiden osalta.

Luokitus: QS 532.5.E7, QS 532.5.M8, QT 140, QU 55.7, QU 475, QU 550.5.S4, WA 754, WC 506, WT 155, WV 302.
Yleinen suomalainen ontologia: ilman saastuminen; hiukkaspäästöt; hengitystiet; tulehdus; toll:in kaltaiset reseptorit; COVID-19; SARS-CoV-2-virus; hajuaisti; Alzheimerin tauti; altistuminen; tulehdukselliset hermoston sairaudet; oksidatiivinen stressi; geenieksprессio

ACKNOWLEDGEMENTS

This doctoral dissertation was conducted at the Cellular Neurobiology research group in the A. I. Virtanen Institute for Molecular Sciences, Faculty of Health Sciences, University of Eastern Finland. I am profoundly grateful to Allah for the strength and perseverance bestowed upon me to complete this work. My heartfelt thanks go to the Academy of Finland, the Sigrid Juselius Foundation, the Päivikki and Sakari Sohlberg Foundation, the Juho Vainio Foundation, and the University of Eastern Finland Doctoral Programme in Molecular Medicine for their generous support in my studies.

I extend my deepest appreciation to my principal supervisor, Professor Katja Kanninen, for her invaluable guidance, expertise, and continuous encouragement throughout my studies. Her faith in my abilities and our insightful research discussions have been fundamental in my growth as a scientist and as a person. I am grateful for mentoring me, I learned a lot from you. I am confident that this will help me throughout my career.

I am equally thankful to my co-supervisor, Professor Pasi I. Jalava, Ph.D., for his unwavering support and positive attitude. Professor Marjut Roponen for introducing me to research and her ongoing guidance and support. Working with them and their teams has been an enriching experience.

I want to thank the official reviewers of my thesis, Professor Paola Palestini and Professor Jonathan Grigg for their time and effort in reviewing this thesis.

Special thanks to Sweelin Chew for being an exceptional mentor and guiding me in learning and mastering new techniques. My sincere gratitude to Giuseppe Balistreri and Olli Vapalahti for their valuable contributions and guidance, which have enriched my learning experience. I express my appreciation to all co-authors and collaborators on this project, including Maria-Viola Martikainen, Teemu J Rönkkö, Mika Komppula, Suvi Kuivanen, Riikka Lampinen, Laura Mussalo, Tomáš Hron, Táňa Závodná, Ravi Ojha, Zdeněk Krejčík, Liudmila Saveleva, Juho Kalapudas, Anne M.

Koivisto, Elina Penttilä, Heikki Löppönen, Prateek Singh, Jan Topinka, Alexey M. Afonin, Kajal Kumari, and Donya Behzadpour. Their contributions have been pivotal to the success of my work.

My heartfelt thanks to my colleagues and friends at the University of Eastern Finland and the Cellular Neurobiology Group for their warm welcome, support, and companionship. I am particularly grateful to Clarisse, Kaustubh, Laura, and Kajal for their constant support and encouragement. Their friendship and our discussions have been a source of strength and inspiration. I am immensely thankful to Riikka and Liudmila, who were a great inspiration during this journey. Their guidance and insights have been invaluable in navigating the challenges of research. I am also grateful to Mirka and Jari for their technical support, which has been crucial in ensuring a smooth workflow in the lab and at the office.

I am immensely thankful to my parents, Ch. Shahbaz Ahmed and Farzana Yasmeen, for their unwavering love, support, and prayers. Their guidance and belief in me have laid the foundation of my journey. My in-laws, including my father-in-law, mother-in-law, and sister-in-law Asfa, also deserve my heartfelt gratitude for their continuous support and encouragement.

I am grateful to my dear friends Faheem, Numan, Barkat, Sohaib, Hasan, Safeer, Abid, Tayyab and Junaid for their companionship and support when needed. Vijay and Huda, your friendship and assistance, especially with my children, have been invaluable. I extend my warmest thanks to the entire Pakistani community in Kuopio for their support and for keeping our culture vibrant in Finland.

Lastly, my deepest gratitude is to my wife, Anam, for her unwavering love and support. Her presence in my life has been a beacon of hope and comfort. To my sons, Musa and Haider, your energy and love have been my greatest motivation. Thank you for filling my life with joy and purpose.

Kuopio, April, 2024

Muhammad Ali Shahbaz

LIST OF ORIGINAL PUBLICATIONS

This dissertation is based on the following original publications:

I. Shahbaz, M. A., Martikainen, M. V., Rönkkö, T. J., Komppula, M., Jalava, P. I., & Roponen, M. Urban air PM modifies differently immune defense responses against bacterial and viral infections in vitro. *Environmental Research*, 192, 110244, 2021.

II. Shahbaz, M. A., Kuivanen, S*., Lampinen, R*., Mussalo, L., Hron, T., Závodná, T., Ojha, R., Krejčík, Z., Saveleva, L., Tahir, N. A., Kalapudas, J., Koivisto, A. M., Penttilä, E., Löppönen, H., Singh, P., Topinka, J., Vapalahti, O., Chew, S., Balistreri, G., & Kanninen, K. M. Human-derived air–liquid interface cultures decipher Alzheimer's disease–SARS-CoV-2 crosstalk in the olfactory mucosa. *Journal of Neuroinflammation*, *20*(1), 1–23, 2023.

III. Shahbaz, M. A., Kuivanen, S*., Mussalo, L*., Afonin, A. M., Kumari, K., Behzadpour, D., Kalapudas, J., Koivisto, A. M., Penttilä, E., Löppönen, H., Jalava, P., Vapalahti, O., Balistreri, G., Lampinen, R*., & Kanninen, K. M*. Exposure to urban particulate matter alters responses of olfactory mucosal cells to SARS-CoV-2 infection. *Environmental Research*, 249, 118451, 2024.

Equal contribution *

The publications were adapted with the permission of the copyright owners.

CONTENTS

ABBREVIATIONS

ACE2	Angiotensin-converting enzyme
ARDS	Acute respiratory distress syndrome
AD	Alzheimer’s disease
ALI	Air Liquid Interface
APOE	Apolipoprotein E
Aβ	Amyloid beta
COVID	Coronavirus disease
CNS	Central nervous system
CMA	Cellular metabolic activity
ct	Cycle threshold
3D	three-dimensional
DEG	Differentially expressed gene
DMEM	Dulbecco's Modified Eagle Medium
ELISA	Enzyme-linked immunosorbent assay
FC	Fold change
HBEC	human bronchial epithelial cells
HMOX1	Heme Oxygenase 1
hpi	Hour post infection
IL-6	Interleukin 6
IL-8	Interleukin 8
INF	Interferon
LP	Lamina propria
LDH	Lactate dehydrogenase
LPS	Lipopolysaccharide
NFTs	Neurofibrillary tangles
NRP1	Neuropilin 1
NQO1	NAD(P)H Quinone Dehydrogenase 1

OM	Olfactory mucosa
OM-ALI	Olfactory mucosa cell at air–liquid interface
OB	Olfactory bulb
OE	Olfactory epithelium
OSN	Olfactory sensory neuron
PAMP	Pathogen-associated Molecular Pattern
PAHs	polycyclic aromatic hydrocarbons
PM	Particulate matter
PMA	phorbol 12-myristate 13-acetate
PCR	Polymerase chain reaction
PI	Propidium Iodide
PRR	Pattern Recognition Receptor
PSEN	Presenilin
ROS	Reactive Oxygen Species
TLR	Toll-like receptor
TMPRSS2	Transmembrane Serine Protease 2
TNF	Tumor necrosis factor-alpha
TEER	Transepithelial Electrical Resistance
UFP	Ultra fine particle
VOC	Variant of concern
WT	Wild type
WHO	World Health Organization

1 INTRODUCTION

The global health threat posed by air pollution is starkly evident in World Health Organization (WHO) data, which show that air pollution contributes to approximately 7 million premature deaths annually (WHO, 2024). Alarmingly, nearly 99% of the global population is exposed to pollutant levels exceeding WHO guidelines. A key component of air pollution is Particulate Matter (PM), consisting of microscopic solids or liquid droplets. PM includes particles of different size ranges, including those less than 10 or 2.5 μm in diameter (PM_{10}, $PM_{2.5}$, respectively) and the minute ultrafine particles (UFP), which have a diameter of less than 100 nm. Depending on their physiochemical properties, PM can penetrate deep into the lungs, translocate to the brain via the olfactory nerve, or enter the bloodstream mainly via respiratory epithelium, thereby impacting not only the respiratory system but also cardiovascular and neurological health (Loane et al., 2013; Ain et al., 2021).

Pathogenic respiratory infections, commonly caused by bacteria or viruses, have a significant global impact, affecting millions each year. The connection between these infections and air pollution, especially PM, is increasingly acknowledged as a major health concern. As of February 2024, the Coronavirus disease 2019 (COVID-19) pandemic has led to over 703 million confirmed cases and approximately 6.98 million deaths worldwide (COVID-19 deaths | WHO COVID-19 dashboard, 2024). The diverse etiology of COVID-19, from asymptomatic to severe, highlights the complex interplay of environmental factors, lifestyle choices, and genetic predispositions on the outcome of infection (Zsichla et al., 2023). Among environmental contributors, epidemiological studies have suggested that exposure to PM, particularly $PM_{2.5}$, can worsen COVID-19 symptoms and increase mortality rates (Marquès et al., 2022; Yu et al., 2024). While emerging *in vivo* and *in vitro* evidence has begun to shed light on how PM exposure affects the host response to the SARS-CoV-2 virus (Sagawa et al., 2021; Zhu et al., 2021; Brocke et al., 2022; Miyashita et al., 2023), there remains a significant need for further research. This research is crucial to

understanding the interaction between COVID-19 and different fractions of PM, to better comprehend the impacts of air pollution exposure on the pandemic.

COVID-19, primarily affecting the respiratory system, also presents neurological symptoms, such as loss of smell (Mutiawati et al., 2021). This symptom can be because of high viral loads in the nasal cavity (Kim et al., 2020; Zou et al., 2020), which implicates the olfactory mucosa (OM) as a potential pathway to the brain (Butowt et al., 2021). Alzheimer's Disease (AD) is the most common neurodegenerative disorder, and the number of individuals suffering from dementia is expected to triple by 2050 (Nichols et al., 2022). AD shares symptoms with COVID-19, including olfactory dysfunction (Jung et al., 2019). The relationship between AD and viral infections, especially SARS-CoV-2, is an area of active research. Individuals with AD are at a heightened risk of severe COVID-19, which might exacerbate AD pathologies, potentially linked to inflammatory processes. However, the specific dynamics between COVID-19 and AD progression, particularly concerning OM involvement, are yet to be fully understood.

Air pollution has been identified as a modifiable risk factor for dementia (Livingston et al., 2020). Living in highly polluted areas is linked to an increased risk of AD (Shi et al., 2020; Ran et al., 2021; Urbano et al., 2023). However, the cellular and molecular events responsible for this link remain poorly understood. The OM, with its direct anatomical connection between the brain and the inhaled air, is an important site for studying the interplay between air pollution exposure, AD, and SARS-CoV-2. This intersection provides vital insights into how environmental factors and viral infections interact in the context of neurodegenerative diseases.

Overall, in this thesis, we aim to employ advanced cell models to provide mechanistic insights into the roles of environmental pollutants, particularly PM, in exacerbating respiratory issues and their interplay with viral infections and neurological consequences. By focusing on the nasal cavity, a critical site for PM deposition and viral entry, the research aims to unravel the complex interactions between environmental exposures, and respiratory pathogens like SARS-CoV-2 in underlying neurological pathological conditions such as AD.

2 REVIEW OF THE LITERATURE

2.1 AMBIENT AIR POLLUTION AND HEALTH

Air pollution is a significant environmental challenge that has profound implications for human health. It involves a complex mixture of gaseous and particulate pollutants released into the atmosphere, impacting overall well-being (Finlayson-Pitts et al., 1997; Kelly et al., 2012). The Air Quality Index (AQI) is a critical tool for gauging air quality, yet its impact is limited by a lack of global standardization. While WHO guidelines target individual pollutants, recent data reveals a staggering 99% of the global population is breathing air below recommended standards (WHO Global Air Quality Guidelines, 2021). Shockingly, pollution claimed 9 million lives in 2015 alone, with economic losses totalling a staggering US$ 4.6 trillion as reported by the Lancet Commission report (Fuller et al., 2022). A recent study used advanced atmospheric modelling, satellite data, and a new relative risk model. It is estimated that annually 8.34 million deaths are attributed to $PM_{2.5}$ and ozone pollution alone, primarily from fossil fuel combustion emissions (Lelieveld et al., 2023).

Various sources contribute to air pollution, including natural factors like volcanic activity and wildfires (Kelly et al., 2012), as well as human activities such as industrial processes, transportation emissions, household combustion, waste burning, and agriculture (Popescu et al., 2010). The acceleration of industrialization and urbanization increases the health risks associated with air pollution (Q. Wang, 2018). Recently the term, Traffic-Related Air Pollution (TRAP) was introduced and it refers to pollution from vehicle emissions, comprising pollutants like carbon monoxide (CO), nitrogen oxides (NOx), PM, and volatile organic compounds (VOCs). These emissions, mostly from the exhaust of motor vehicles, disperse as aerosols in the air and are linked to various health issues including respiratory problems, cardiovascular diseases, and adverse neurological effects (Matz et al., 2019; Boogaard et al., 2022). Among all the pollutants, PM is a major

contributor to negative health outcomes (K. H. Kim et al., 2015). Therefore, regulatory authorities worldwide have placed significant emphasis on investigations related to health concerns associated with PM. However, further research is warranted to fully understand how PM exposure impacts the negative outcomes of and is linked to pathological conditions.

2.1.1 Particulate matter (PM) in urban air pollution

Urban aerosol constitutes a complex mixture of solid particles and liquid droplets suspended in the air, showcasing a diverse range of sizes and compositions. In urban air pollution contexts, PM is categorized based on size: PM_{10} (particles with a diameter of 10 μm or smaller), $PM_{2.5}$ (fine particles with a diameter of 2.5 μm or smaller), and ultrafine particles (UFP) (particles with a diameter of 0.1 μm or smaller) (Particulate Matter Basics | US EPA, 2023). The composition of PM varies depending on emission sources and atmospheric processes. Common components include inorganic compounds such as metals, sulfates, nitrates, and ammonium salts, alongside organic compounds like hydrocarbons, polycyclic aromatic hydrocarbons (PAH), and other molecules. Exposure to PM primarily occurs through inhalation, with particles penetrating the respiratory system and potentially entering the bloodstream. Particle size is a critical factor influencing penetration, with smaller particles like $PM_{2.5}$ and UFP reaching the alveoli of the lungs, while larger PM_{10} particles and the smallest nanoparticles typically deposit in the upper respiratory tract.

All sizes of the PM are considered to be a health concern (K. H. Kim et al., 2015). Mainly PM poses a health risk through oxidative stress and genetic damage (R. Chen et al., 2016; Mack et al., 2019). Oxidative stress induced by PM triggers an immune response leading to inflammation, negatively impacting cellular components like lipids, proteins, and DNA (Gangwar et al., 2020) and inducing an imbalance in calcium homeostasis and cytotoxicity (Y. Wang et al., 2020). The extent of oxidative damage depends on the specific type and concentration of PM constituents, and the ability of the target organ to neutralize the oxidative stress by protective scavenging elements (Lodovici et al., 2011). The genotoxicity

mechanism of PM, classified as a Group 1 carcinogen by the International Agency for Research on Cancer (IARC), primarily involves DNA damage through Reactive Oxygen Species (ROS)-induced oxidative stress and the formation of DNA adducts. These effects are particularly prominent due to exposure to PAH, which can induce oxidative stress and form DNA adducts, leading to an increased risk of cancer (Quezada-Maldonado et al., 2021). Furthermore, direct adsorption of the carcinogens on the PM surface indirectly induces mutagenesis and carcinogenesis when coming into contact with the respiratory surface (Knaapen et al., 2004). A recent review of the epidemiological and experimental evidence concluded that mechanisms underpinning adverse health outcomes involve oxidative stress, inflammation, apoptosis, autophagy, and emerging processes like pyroptosis, ferroptosis, and epigenetic modifications (Tianyu Li et al., 2022). These mechanisms contribute to a spectrum of health impacts, with respiratory effects including asthma exacerbation and chronic bronchitis, and cardiovascular effects encompassing an elevated risk of heart attacks and strokes. Furthermore, PM exposure correlates with adverse outcomes in the nervous, immune, and reproductive systems.

While $PM_{2.5}$ has been extensively researched and has been considered as the main culprit in most PM-induced adverse effects (Feng et al., 2016; Forouzanfar et al., 2015), UFP are gaining prominence due to their unique health risks (Politis et al., 2008; Chen et al., 2016; Schraufnagel, 2020). Defined by a diameter of 0.1 μm or smaller, allows deep penetration of these particles into the respiratory system, reaching the lungs' alveoli, and potentially entering the bloodstream. UFP have a larger surface area in comparison to the mass, potentially increasing absorption and exerting toxic effects (G. Oberdörster, 2001). Small mass and higher surface area increase the load of adsorbed toxic contaminants. Higher PAH content on UFP has been associated with elevated oxidative stress and mitochondrial dysfunction induced by the UFP than the other size fractions (N. Li et al., 2003). Furthermore, unlike larger PM, UFP can evade effective capture by existing monitoring systems, emphasizing the necessity for specific attention in research and regulatory standards. UFP also exhibit unique toxicological properties, including the ability to traverse biological barriers

like the blood-brain barrier, raising concerns about potential impacts on neurological health (Calderón-Garcidueñas et al., 2022; Günter Oberdörster et al., 2004, 2005). Therefore, ongoing research is crucial to further understand the distinct health implications associated with different sizes of PM.

2.1.2 Impact of PM on respiratory health

PM pollution significantly impairs respiratory health by compromising natural defense mechanisms, exacerbating existing respiratory conditions, and contributing to chronic lung diseases, posing a particular risk to vulnerable populations such as children and the elderly (Tao Li et al., 2018; Yang et al., 2020; Tran et al., 2023). $PM_{2.5}$ plays a pivotal role in disrupting essential airway epithelial functions, compromising mucociliary clearance, barrier integrity, and antimicrobial peptide secretion (S. Zhang et al., 2019). The smaller size of $PM_{2.5}$ facilitates deeper penetration into the respiratory system, reaching the alveoli and exerting pronounced effects on host defense mechanisms, as mediated through oxidative stress and inflammatory pathways (Liu et al., 2018; Yang et al., 2020)

The impact of PM on pre-existing respiratory conditions is noteworthy, with asthma and chronic obstructive pulmonary disease (COPD) patients experiencing heightened exacerbations (Delavar et al., 2023; C. Hoffmann et al., 2022). Furthermore, exposure to elevated PM concentrations are associated with increased emergency room visits for upper and lower respiratory infections (LRTI) (Xia et al., 2017; Horne et al., 2018; Strosnider et al., 2019; Ziou et al., 2022) This exacerbation extends to vulnerable populations, such as children and the elderly, who exhibit heightened susceptibility to respiratory infections caused by PM exposure (Xia et al., 2017).

Individuals with hereditary or underlying diseases, like cystic fibrosis, face an elevated risk of respiratory infections due to PM exposure, demonstrating the broad impact of PM on respiratory health (Psoter et al., 2015). Respiratory infections, including acute respiratory outcomes and

upper respiratory tract infections, exhibit an increased risk in conjunction with PM exposure, further emphasizing the need for comprehensive strategies and targeted interventions to mitigate the adverse effects of PM on respiratory health and protect vulnerable populations from associated risks.

2.1.3 Impact of PM on brain health

PM exposure is extensively investigated for its potential impact on neurological health. One primary route for PM-induced effects on the central nervous system (CNS) begins with the inflammatory response resulting from direct PM contact in the lungs (Cipriani et al., 2018). This initial step potentially leads to systemic inflammation that contributes to neuroinflammation and neuronal tissue loss in various brain areas such as the olfactory bulb (OB), frontal cortex, and hippocampus (Brockmeyer and D'Angiulli, 2016). This inflammatory process can disrupt the blood–brain barrier (BBB), allowing adverse impacts on the brain, including subsequent monocyte infiltration, microglia activation, and increased cytokine activity (Calderón-Garcidueñas et al., 2008; Calderón- Garcidueñas et al., 2012).

The nasopharynx serves as the entry point for air and potential particulate matter into the respiratory system. From here, a direct pathway to the brain is established via the olfactory system. Olfactory sensory neurons, located within the olfactory epithelium (OE) of the nasal cavity, extend projections directly to the olfactory bulb at the base of the brain, providing a direct nose-to-brain transport pathway for nanoparticles. (Lucchini et al., 2012; You et al., 2022). This direct route is supported by evidence from both human and rodent studies, demonstrating the deposition of nanosized particles in the OB and its translocation (Heusinkveld et al., 2016; Kao et al., 2012; Maher et al., 2016). PM can penetrate the vascular spaces of filia olfactory – with the OE having paracellular spaces of 10 nm that can directly transport PM to the olfactory bulb. The size of particles that can pass through the OE and reach the olfactory bulb can vary, but typically, particles smaller than 100 nm have a higher likelihood of penetrating the epithelium. Specifically, nanoparticles

with diameters ranging from 1 to 100 nm are more likely to be transported through the paracellular spaces or intracellular transport via olfactory sensory neurons, allowing them to reach the olfactory bulb (Günter Oberdörster et al., 2004).

Additionally, UFP may reach the brain through systemic absorption and entry through the BBB. Studies have demonstrated the systemic translocation of inhaled UFP to the brain through blood circulation, suggesting a potential role of the BBB in PM translocation (Nemmar et al., 2002; Qi et al., 2022). These findings underscore the intricate pathways through which PM, including specific components like $PM_{2.5}$ and UFPs, can influence neurological health.

2.1.4 In vitro models to study cellular effects of PM

In vitro cell culture models are indispensable tools to study cellular and molecular mechanisms, and to advance our understanding of the intricate interactions between PM and cellular events that influence human health. These models provide a controlled experimental setting for researchers to dissect specific cellular and molecular mechanisms underlying PM toxicity with precision. In comparison to *in vivo* models, *in vitro* approaches present distinct advantages, aligning with the 3Rs (Replacement, Reduction, Refinement) in research ethics by eliminating the need for animal experimentation (Tannenbaum et al., 2015). Cell models can be established from different organisms such as humans, rats, and mice. *In vitro* studies are common in the air pollution field and offer a foundational understanding of PM-induced effects before progressing to more complex *in vivo* investigations. The *in vitro* systems empower researchers to manipulate critical variables like PM concentration and composition, allowing a meticulous exploration of the intricate cellular and molecular pathways involved in PM-induced health impacts (Günter Oberdörster et al., 2005).

The respiratory system consists of the nasopharyngeal, tracheobronchial, and alveolar regions, each subdivided into multiple sub-regions (Günter Oberdörster et al., 2005). This complexity underscores the

importance of exploring various cell models to understand inhalation exposure implications. Several immortalized secondary cell lines from the human respiratory tract are commonly used for exploring inhalation exposure implications. Notably, human alveolar and human bronchial epithelial cell lines (Barron et al., 2021), such as A549 and BEAS-2B cells, have been pivotal in advancing comprehension of the direct impact of PM on lower respiratory tissues (C.-C. Cho et al., 2018). Primary cells derived from human biopsies, such as patient-derived cells, significantly enhance physiological relevance in studies. For example, human bronchial epithelial cells (HBECs) are crucial in understanding biological responses under stress conditions, as they closely mimic the natural physiological environment (C.-C. Cho et al., 2018). Furthermore, Nasal and olfactory cell models extend the scope, enabling the exploration of pollutant effects on the upper respiratory tract and the brain, respectively (De Rudder et al., 2018; Kanninen et al., 2020).

More complex cell models have been developed by utilizing co-culture systems involving the cultivation of diverse cell types in tandem, offering an advanced means to investigate intricate interactions within various respiratory cell types, capturing the complexity of the respiratory microenvironment. Co-cultures with immune cells, such as monocytes or macrophages, contribute to a holistic understanding of the immune response to PM exposure (Kasurinen et al., 2018), adding complexity to simple *in vitro* models. Animal-derived cells provide insights into cross-species variations in PM responses, broadening the understanding of potential health impacts. Despite their fundamental role, the evolution of research necessitates more sophisticated methodologies mirroring respiratory system complexities. Innovative techniques, including air-liquid interface (ALI) cultures, co-culture systems, and organ-on-a-chip platforms, emerge as indispensable tools for creating physiologically relevant and intricate models in respiratory research. ALI cultures, representing three-dimensional (3D) models, faithfully mimic respiratory system conditions, providing a closer approximation of cellular responses to PM exposure (Upadhyay et al., 2018). Lately, Organ-on-a-chip platforms further elevate sophistication, simulating dynamic physiological conditions of the

respiratory system within a controlled environment (M. Zhang et al., 2018). These cutting-edge methodologies significantly enhance the relevance of *in vitro* findings by bridging the gap between traditional cell cultures and the holistic organism.

2.2 RESPIRATORY INFECTIONS

Respiratory infections are a persistent global health challenge, causing concern already long before the arrival of the COVID-19 pandemic (Dasaraju et al., 1996). Each year, well before the pandemic, approximately 4 million lives were claimed by acute respiratory infections. These infections spread rapidly through the air, via droplets and aerosols. Research reveals that environmental factors like air quality, humidity, and temperature play crucial roles in the life and transmission of respiratory pathogens (Chan et al., 2011; S. Kumar et al., 2021). The body defends against respiratory pathogens through physical barriers like mucociliary clearance of the epithelial surfaces in the respiratory tract. Additionally, antimicrobial peptides (AMPs) in the mucosal layer directly target pathogens and modulate immune responses, enhancing protection against respiratory threats. The immune system, comprising innate and adaptive components, deploys macrophages, T and B lymphocytes, and antibodies to recognize and eliminate pathogens (Johnstone et al., 2022). Inflammatory responses and immunological memory further enhance the body's ability to protect against respiratory insults (Tosta, 2021). Evidence suggests that vulnerability to respiratory infections is not uniform. Infants and young children, still developing their immune and respiratory systems, are more susceptible (Williams et al., 2002; Liao et al., 2011; Adane et al., 2020; Avendaño Carvajal et al., 2020), while older adults and those with weakened immunity face higher risks of severe outcomes (Wu et al., 2021). Additionally, individuals with existing respiratory conditions like asthma and COPD are at increased risk. Modifiable risk factors for respiratory tract infections include smoking showing an increased likelihood of acquiring infections (C. Jiang et al., 2020; McGeoch et al., 2023). Additionally, environmental risk factors, such as exposure to ambient air pollution

increase the risk of respiratory infections as emphasized by the WHO (Loaiza-Ceballos et al., 2022).

2.2.1 Bacterial and viral infections

Respiratory infections are primarily categorized into bacterial and viral infections, eliciting unique responses from the innate immune system of the host. *Streptococcus pneumoniae, Haemophilus influenzae, and Moraxella catarrhalis* are recognized as the primary bacterial pathogens commonly associated with infections affecting both the upper and lower respiratory tracts (Cappelletty 1998). Respiratory viruses play a crucial role in causing influenza-like illnesses and the common cold. Noteworthy respiratory viruses include respiratory syncytial virus (RSV), rhinovirus, enterovirus, coronaviruses (including SARS and MERS CoV), adenoviruses, and parainfluenza viruses (Kesson, 2007). The interaction between pathogens and the body involves bacteria using toxins and viruses employing evasion strategies against the immune system. The innate immune response, involving cells like natural killer cells and macrophages, serves as the first line of defense. In viral infections, the innate immune response is initiated by pattern recognition receptors (PPRs), such as Toll-like receptors (TLRs) specific to detect viral nucleic acids and proteins (R. Zhou et al., 2021). This activation leads to the release of interferons (INF), inhibiting viral replication (Kawai et al., 2006). Conversely, in Gram-negative bacterial infections, the host employs PRRs like TLR4 to recognize bacterial components, triggering a localized inflammatory response. This activates phagocytic cells, including neutrophils and macrophages, contributing to the elimination of bacterial threats (Aderem, 2003; B. S. Park et al., 2013; Stokes et al., 2015). In addition to direct bacterial and viral interactions, the immune response in the respiratory system can be influenced by environmental factors such as pollutants including PM (Nozza et al., 2021; Rebuli et al., 2021) and pollen (Gilles et al., 2020; Hajighasemi et al., 2023; Martikainen et al., 2023). $PM_{2.5}$ has been identified as a potential modulator of immune responses (Wei et al., 2018). PM can carry microbial components that activate TLRs, particularly TLR2 and TLR4, adding an

environmental dimension to immune modulation. Studies suggest that exposure to PM can contribute to immune dysregulation by activating TLRs, leading to enhanced inflammatory responses. For instance, PM components may engage TLR2, recognizing microbial patterns such as lipopeptides, or stimulate TLR4 through the presence of endotoxins (Shoenfelt et al., 2009). This activation, occurring in conjunction with bacterial and viral encounters, creates a complex interplay between microbial and environmental stimuli in shaping immune responses(Bauer et al., 2012).

2.2.2 SARS-CoV-2 and COVID-19 etiology

SARS-CoV-2, a novel coronavirus that emerged in late 2019, belongs to the coronavirus family, sharing lineage with significant viruses like SARS-CoV and MERS-CoV. Initially identified in Wuhan, China, SARS-CoV-2 infection swiftly evolved into a global pandemic, as declared by the WHO and to date, in January 2024, the virus has claimed 6.98 millions lives (COVID-19 deaths|COVID-19 dashboard, 2024). The ongoing global health crisis faces added complexity with the emergence of new viral variants, such as Alpha, Beta, Gamma, Delta, and Omicron, which have exhibited increased transmissibility and antigenic changes (Carabelli et al., 2023).

The virus primarily spreads through respiratory routes, facilitated by respiratory droplets (Jayaweera et al., 2020). The angiotensin-converting enzyme 2 (ACE2) receptor, acting as the entry point for SARS-CoV-2 (M. Hoffmann et al., 2020), is expressed across the respiratory tract. In the upper respiratory tract, ACE2 is present in the nasal epithelium (Sungnak et al., 2020) and OM (Brann et al., 2020), establishing the initial interaction site between the virus and the host. As the infection progresses to the lower respiratory tract, ACE2 is prominently expressed in the type II alveolar cells of the lungs, underscoring the vulnerability of the lungs to SARS-CoV-2 (Hamming et al., 2004). This widespread distribution of ACE2 contributes to the understanding of COVID-19 pathophysiology. Moreover, tissues beyond the respiratory system, including the heart, kidneys, and

gastrointestinal tract, also express ACE2, highlighting the intricate interplay between SARS-CoV-2 and various organs.

The respiratory manifestations of the virus vary, ranging from asymptomatic or mild cases to severe respiratory distress and acute respiratory distress syndrome (ARDS). ARDS, a critical condition marked by impaired lung function and oxygen exchange, often presents with pneumonia, characterized by inflammatory changes and fluid accumulation in the lung tissue. This spectrum of respiratory outcomes is a crucial aspect of the complexity of the impact of SARS-CoV-2 on the human body.

Current evidence for the recognition of SARS-CoV-2 by PRRs and innate immune response in the host is reviewed in (Diamond et al., 2022; Maison et al., 2023). Briefly, Upon SARS-CoV-2 infection, the host initiates a robust innate immune response involving PRRs such as TLRs, retinoic acid-inducible gene-like receptors (RLRs), and nucleotide-binding oligomerization domain-like receptors (NLRs) (Diamond et al., 2022). TLRs, including TLR2 and TLR3, play crucial roles in recognizing viral components and initiating immune responses, resulting in the release of key cytokines like tumor necrosis factor-alpha (TNF-α) and IFN-γ (Maison et al., 2023). Activation of the TLR2 subsequently also activates NOD-like receptor family pyrin domain containing 3 (NLRP3) inflammasome leading to the release of IL-1β and IL-18. Additionally, TLR7, and TLR8 activation because of viral RNA can also trigger a surge in the cytokines (Manik et al., 2022). The immune response also engages the cGAS-STING pathway and proteasome-mediated degradation of viral proteins (Diamond et al., 2022). However, the dysregulated immune response can contribute to a cytokine storm, causing significant tissue damage.

2.2.3 Role of TLR in immune modulation

PRRs constitute a vital aspect of the innate immune system, acting as vigilant sensors that identify specific molecular patterns linked to pathogens. Among these, the TLRs emerge as pivotal contributors to immune surveillance and response. Expressed by diverse immune cells,

including macrophages, dendritic cells, and B cells, TLRs play a widespread role in immune surveillance. Their functions involve recognizing pathogen-associated molecular patterns (PAMPs) and initiating a signalling cascade that activates immune responses. TLRs are categorized based on their specificity for molecular patterns associated with bacteria and viruses.

For bacterial threats, TLR4 takes the lead, recognizing lipopolysaccharides (LPS), a key component of the outer membrane of Gram-negative bacteria (Amemiya et al., 2021; Beutler, 2002). This recognition by TLR4 is instrumental in detecting bacterial infections and triggering subsequent immune responses. In the viral domain, TLR3 specializes in identifying double-stranded RNA, a common feature in the genomes of certain viruses (Alexopoulou et al., 2001). Activation of TLR3 contributes significantly to the host's defense against viral infections. Additionally, TLR7 and TLR8, responsive to single-stranded RNA prevalent in RNA viruses, are strategically positioned in endosomes and on the cell surface, respectively (Diebold et al., 2004; Heil et al., 2004). Both TLR7 and TLR8 play crucial roles in detecting viral nucleic acids and instigating immune responses to combat viral invaders. This orchestrated interplay highlights the nuanced yet effective role of TLRs in distinguishing and responding to bacterial and viral pathogens. In studies mimicking bacterial and viral stimulation, researchers utilize specific TLR ligands to replicate the molecular patterns associated with bacterial or viral infections. For instance, bacterial LPS can be used to simulate bacterial stimulation, while synthetic viral RNA or DNA mimics viral stimulation (Diebold et al., 2004; A. Kumar et al., 2006; Weidinger et al., 2014). These ligands serve as tools for investigating immune responses and developing a deeper understanding of the intricacies of TLR-mediated immune modulation.

2.3 ALZHEIMER'S DISEASE (AD)

AD is a neurodegenerative disorder characterized by intricate pathological features that gradually erode the neural landscape. At the core of AD pathology is the accumulation of toxic amyloid beta (Aβ) in the brain (O'Brien et al., 2011). Aβ peptides, resulting from the cleavage of amyloid

precursor protein (APP), form aggregates known as amyloid plaques. These plaques gather in the extracellular spaces between cells, disrupting intercellular communication and contributing to cognitive decline.

Within neurons, tau proteins undergo abnormal phosphorylation, leading to the formation of neurofibrillary tangles (NFTs) in the AD brain. Tau, a microtubule-associated protein crucial for maintaining cell structure, loses its normal function and aggregates into twisted filaments within neurons. NFTs contribute to neuronal dysfunction, accentuating cognitive deficits (Metaxas et al., 2016). The combined impact of amyloid plaques and NFTs inflicts significant damage on neurons, compromising the integrity of neural circuits responsible for memory formation and storage. As these structural changes progress, memory impairment ensues.

The classification of AD into familial (FAD) and sporadic forms adds further complexity. FAD is linked to specific genetic mutations in APP, Presenilin 1 (PSEN1), and Presenilin 2 (PSEN2) genes, unfolding predominantly before the age of 65. In contrast, sporadic AD, the more prevalent form, emerges later in life and is influenced by a myriad of genetic, environmental, and lifestyle factors. The intricate interplay of these factors contributes to the multifactorial nature of sporadic AD (Chakrabarti et al., 2015).

2.3.1 Air pollution exposure as a modifiable risk factor for AD

The Lancet Commission recently added air pollution to the list of the 12 modifiable risk factors for dementia (Livingston et al., 2020). The intricate relationship between PM exposure and AD has been extensively investigated across diverse studies, encompassing epidemiological, *in vivo*, *ex vivo*, and *in vitro* research. Epidemiological studies indicate a direct correlation between PM exposure and AD pathology, with various cohorts exhibiting heightened risks, particularly among the elderly in global regions such as the United States, Europe, and Asia (Ran et al., 2021; Shi et al., 2020; Urbano et al., 2023). Cohort studies have also suggested a correlation between PM exposure and cognitive decline (Aretz et al., 2021; Duchesne et al., 2022). High $PM_{2.5}$ concentrations have been associated

with increased Aβ plaques in individuals with cognitive impairment (Iaccarino et al., 2021). In addition, AD-like cortical atrophy and decline in cognitive function have been observed in individuals exposed to high levels of PM_{10} ((J. Cho et al., 2023). *In vivo* studies on transgenic models and standard mice demonstrate an escalation of AD-related biomarkers, cognitive decline, neuroinflammation, and oxidative stress following PM exposure (Hullmann et al., 2017; Calderón-Garcidueñas et al., 2020; Sahu et al., 2021; Saveleva et al., 2022). Additionally, *ex vivo* and *in vitro* studies highlight the role of oxidative stress and neuroinflammation in specific brain regions and OM areas associated with AD (Jang et al., 2018; B. R. Wang et al., 2018). Although some conflicting data are available, overall the convergence of evidence from these diverse approaches underscores PM exposure as a significant risk factor for AD. However, the precise mechanisms underlying PM-induced adverse effects and their association with neurological implications, such as AD or the augmentation of pathology in individuals already suffering from AD, remain less understood.

2.3.2 Olfactory Mucosa (OM) and AD

The OM is situated in the olfactory cleft and plays a crucial role in our sense of smell. It comprises two main parts: the olfactory epithelium (OE) and the lamina propria (LP). The OE, positioned at the rooftop of the nasal cavity, includes various cell types such as olfactory sensory neurons (OSNs), sustentacular cells, microvillar cells, duct cells of the olfactory (Bowman's) glands, and basal cells (Costa et al., 2020). Adjacent to the OE, the LP accommodates essential components for olfactory function. Airborne odorants interact with the olfactory receptors (OR) of the OSNs in the OE, initiating an axon potential that travels to the OB and subsequently to the brain. The OB, a crucial component of the primary olfactory brain network, processes olfactory signals received by OSNs, transmitting them to different parts of the central nervous system for further processing, modulation, and interpretation of smell (Pinto, 2011).

The OM is a sensitive tissue exposed to environmental insults, and basal cells play a pivotal role in regenerating lost cell types, including OSNs. In pathological implications or environmental insults, the recovery of olfaction could be attributed to the presence of progenitor cells in the OE, such as globose basal cells (GBCs) and horizontal basal cells (HBCs), giving rise to SUS cells and neurons, respectively (Choi et al., 2018; Fletcher et al., 2017; Schwob, 2002). However, with age, the regenerative potential of basal cells diminishes, leading to age-related smell impairment. Furthermore, ageing-related smell impairment is associated with a decreased volume of the hippocampus, reduced thickness of the entorhinal cortex, and memory impairment (Growdon et al., 2015).

Evidence suggests that the loss of smell is an early clinical indicator of AD (Roberts et al., 2016; Lafaille-Magnan et al., 2017; Woodward et al., 2017; Jung et al., 2019) and several other neurodegenerative diseases (Marín-Palma et al., 2023). Additionally, AD-associated changes have been observed in the OM. A study on postmortem OM from individuals with AD reveals the presence of hyperphosphorylated tau and Aβ, pathological proteins significantly elevated compared to individuals without neuropathology or with other neurodegenerative diseases (Arnold et al., 2010). This positions OM as a potential window into early pathological changes associated with AD. Utilizing cells derived from the OM, researchers can gain unique insights into disease-related alterations *in vitro*. This encompasses variations associated with AD, such as modifications in APP metabolism and heightened levels of oxidative stress markers (Nelson et al., 2009; Stewart et al., 2013). Notably, recent studies demonstrated AD-related alterations in OM cells obtained from biopsies of individuals with AD (Lampinen et al., 2022a; Lampinen et al., 2022b), suggesting that these cells exhibit similar changes observed in AD-affected brains.

2.3.3 Linking AD and Air Pollution at the OM

The OM assumes a pivotal role not only in unravelling the intricacies of AD but also due to its strategic location in the upper airways, rendering it

susceptible to direct exposure to environmental insults and positioning it as a potential gateway to the brain for airborne substances (Amouei Torkmahalleh et al., 2022; Elder et al., 2006; Garcia et al., 2015; González-Maciel et al., 2017; Günter Oberdörster et al., 2004). Research, exemplified by studies from Oberdörster and coauthors and Gonzalez-Maciel and coauthors., has elucidated the translocation of UFP to the brain through the olfactory nerve, spotlighting the potential role of the OM as a gateway for airborne pollutants. While existing studies have primarily focused on the impact of air pollutants on the human nasal epithelium, investigations into the exposure of various PM fractions to human nasal and OM cells have revealed heightened oxidative stress, inflammatory responses, epithelial barrier dysfunction, and mitochondrial dysfunction, unravelling potential mechanisms through which pollutants affect the OM (Chew et al., 2020; Hong et al., 2016; N. Kim et al., 2019; R. W. Zhao et al., 2019). Furthermore, exposure to different engine emissions containing reactive nitrogen species and PAH induces significant disruptions in the inflammatory response, xenobiotic metabolism, and processes regulating OM integrity, raising alarming concerns about the compromised olfactory barrier (Mussalo et al., 2023).

The link between AD and OM, coupled with its susceptibility to pollutant exposure, establishes this region as an intriguing interface for studying the intersection of AD and air pollution. Olfactory information processing engages key brain regions which are affected in AD, such as the hippocampus and prefrontal cortex, and dysfunction of olfaction has been reported in individuals exposed to high PM levels (Ekström et al., 2022). The observed damage in the OM of AD individuals underscores its potential role in comprehending the complex relationship between AD and the effects of air pollutants (Borgmann-Winter et al., 2015).

2.4 LINK BETWEEN AD AND COVID-19

Increasing evidence suggests that individuals with AD face an elevated risk of COVID-19 infection, with retrospective analyses in the US and the UK revealing higher odds of COVID-19 diagnosis and increased mortality rates

in AD patients (Chung et al., 2022; Hu et al., 2022; Q. Q. Wang et al., 2021a). This heightened susceptibility is attributed to factors such as existing cognitive impairment, compliance challenges, genetic predisposition, and underlying inflammation. Notably, the Apolipoprotein E4e4 (APOE4e4) allele, a major AD risk factor, is associated with increased risk of severity (Kuo et al., 2020a) and mortality (Kuo et al., 2020b) to SARS-CoV-2, with individuals possessing the e4 allele showing lower antiviral gene expression (Chung et al., 2022; Mok et al., 2022).

The bidirectional relationship extends to severe COVID-19 cases, marked by inflammation and cytokine storms, posing concerns for exacerbating pre-existing cognitive impairment in AD patients (Beghi et al., 2022; Crivelli et al., 2022). Evidence indicates that COVID-19 may induce long-term neurodegeneration, manifesting as cognitive dysfunction, memory issues, and structural brain abnormalities (Klein et al., 2021; Charnley et al., 2022; Douaud et al., 2022; W. Zhang et al., 2024). Charnley et al. further identified SARS-CoV-2 peptides that self-assemble into amyloid structures similar to toxic Aβ in AD (Charnley et al., 2022). The virus-induced cytokine storm can disrupt the BBB, damage neural cells, and foster amyloid plaque accumulation, a hallmark of AD. Furthermore, SARS-CoV-2-induced hypoxic alterations and hypercoagulation may contribute to brain ischemia, tau phosphorylation, and cognitive decline (Reiken et al., 2022).

Anosmia, a prevalent neurological symptom in both COVID-19 (Mutiawati et al., 2021) and AD (Murphy, 2018), provides insights into the consequences of SARS-CoV-2 infection in AD. Furthermore, the discussion of SARS-CoV-2 neurological manifestations as a consequence of viral translocation through the olfactory bulb route cannot be ruled out, although existing evidence supporting this hypothesis is lacking. However, the OM demonstrates signs of neuroinflammation, and changes in the OM can manifest effects on the brain. While common inflammatory processes may underlie their crosstalk between AD and COVID-19, further investigation is essential to elucidate the interplay between AD and COVID-19 at the OM.

2.5 LINK BETWEEN PM EXPOSURE AND COVID-19

An accumulating body of evidence since the onset of the pandemic continues to strengthen the substantial link between PM exposure and various dimensions of COVID-19, encompassing incidence, risk, severity, and mortality (Fattorini et al., 2020; Y. Jiang et al., 2020; H. Li et al., 2020; Linares et al., 2021; Travaglio et al., 2021). Recent systematic reviews of epidemiological evidence suggest that both short-term and chronic exposures to PM_{10} and $PM_{2.5}$ significantly contribute to the incidence and severity of adverse outcomes in COVID-19 (Marquès et al., 2022; Sheppard et al., 2023; Yu et al., 2024). Despite the robust evidence supporting this association, the precise mechanisms governing the interplay between PM exposure and the severity of COVID-19 remain an active area of research. As PM enters the respiratory system, it can induce oxidative stress and trigger inflammatory responses, potentially compromising the host's immune defenses and exacerbating the severity of COVID-19 (Mishra et al., 2020; Brocke et al., 2022; Marín-Palma et al., 2023; Upadhyay et al., 2024). Additionally, alterations in the expression of angiotensin-converting ACE2, the primary receptor for SARS-CoV-2, have been observed in response to PM exposure, influencing susceptibility to viral infection (Sagawa et al., 2021; Miyashita et al., 2023). Despite investigations into various PM fractions, including urban PM, diesel $PM_{2.5}$, and PM_{10}, the understanding of how exposure to the smallest particles affects SARS-CoV-2 infection remains a critical research gap. Importantly, the nasal cavity emerges as a crucial battleground for both SARS-CoV-2 and PM exposure, with the OE potentially acting as a site for UFP translocation and neurologic manifestations of the virus. While the primary focus has been on the lungs for both agents, the specific size distribution of PM_{10} tends to accumulate in the upper respiratory tract. PM exposure has been shown to induce alterations in cytokine production, oxidative stress, and mitochondrial dysfunction in human OM providing valuable insights into the potential adverse effects associated with PM exposure (Chew et al., 2020; Santurtún et al., 2022; Mussalo et al., 2023). However, understanding how these

alterations might modulate SARS-CoV-2 infection requires further investigation.

.

3 AIMS OF THE STUDY

The overarching aim of the thesis is to investigate the cellular and molecular events induced by PM exposure in cells of the respiratory system, focusing on the immune response to respiratory infections and the potential implications for AD. The specific aim of the studies I-III are:

I. To determine how exposure to urban air $PM_{2.5-1}$ influences innate immune responses to bacterial and viral stimuli *in vitro*, using a co-culture model of alveolar epithelial cells and monocyte-derived macrophages. The study seeks to uncover the differential modulation of immune responses by PM and its implications for bacterial and viral stimuli.

II. To explore the effects of SARS-CoV-2 infection in primary human OM cells, and to decipher the interaction between SARS-CoV-2 and AD using a 3D *in vitro* model. This includes examining the susceptibility of OM cells to SARS-CoV-2 and analyzing the transcriptomic alterations induced by the virus in cells of cognitively healthy individuals and those with AD.

III. To assess the impact of subacute exposure to urban PM (specifically $PM_{0.2}$ and $PM_{10–2.5}$) on the cellular and immune responses of OM cells to SARS-CoV-2 infection, with a focus on comparisons between cells from healthy individuals and those diagnosed with AD. The study aims to understand how PM exposure influences the progression and severity of SARS-CoV-2 infection in the context of AD.

SUBJECTS AND METHODS

3.1 HUMAN SECONDARY CELL CULTURES (I)

3.1.1 Type II alveolar epithelial cell line (A549)

In study I, we used the type II human alveolar epithelial cell line (A549) which was obtained from ATCC (ATCCRCCL-185™). A549 cells were routinely cultured in Dulbecco's Modified Eagle Medium (DMEM) supplemented with 10% fetal bovine serum (FBS), 2 mM L-glutamine (L-glut), and 100 U/ml penicillin/streptomycin (all Sigma Aldrich, USA).

3.1.2 Monocytic cell line THP-1

The human monocytic cell line THP-1 was acquired from the German Collection of Microorganisms and Cell Cultures (DSMZ, Germany). THP-1 cells were routinely cultured in Roswell Park Memorial Institute (RPMI) 1640 culture medium (Life Sciences, Gibco) supplemented with 10% FBS, 2 mM L-glut, and 100 U/ml penicillin/streptomycin. Prior to co-culture experiments, THP-1 monocytic cells were differentiated into active macrophage-like cells using phorbol 12-myristate 13-acetate (PMA), following the procedure established by Kasurinen et al. (2018). Briefly, the differentiation process of THP-1 cells involved seeding 15,000,000 to 20,000,000 cells in a T75 flask with a surface area of 75 cm^2. These cells were subjected to treatment with 0.5 µg/ml PMA and allowed to incubate for 90 minutes. Following this incubation period, detached cells were carefully removed, subjected to a washing step to eliminate residual PMA, and subsequently utilized in the co-culture experiments

3.1.3 A549 and THP-1 co-culture

The A549-THP1 co-culture system, previously described by Kasurinen et al. (2018), was employed in our study. Briefly, A549 cells were initially seeded at a density of 120,000 cells per well (with a surface area of 3.5 cm^2) in 12-

well plates using DMEM supplemented with 10% FBS, 2 mM L-glutamine, and 100 U/ml penicillin/streptomycin. After allowing attachment for 4 hours, activated macrophage-like THP-1 cells, differentiated using 0.5 µg/ml PMA, were seeded onto the attached A549 cells at a density of 24,000 cells per well. The co-cultured A549 and THP-1 cells were incubated in DMEM at 37°C in a 5% CO_2 environment for 40 hours, allowing the establishment of the co-culture system.

3.2 HUMAN PRIMARY OM CELL CULTURES (II AND III)

3.2.1 Human OM biopsy donors and ethical considerations

For studies II and III, olfactory biopsies were obtained from both cognitively healthy individuals and those diagnosed with AD under the approved ethical permit from the Human Research Ethics Committees (HRECs) of Northern Savo Hospital District (permit number 536/2017). Written informed consent was obtained from all subjects, with proxy consent from family members of individuals with AD. The participants included three cognitively healthy individuals and three with AD, with an average age of 74.3 years and 62.3 years, respectively, comprising both male and female donors. Individuals diagnosed with AD were recruited via the Brain Research Unit, Department of Neurology, University of Eastern Finland, while cognitively healthy individuals were recruited via the Department of Otorhinolaryngology, Kuopio University Hospital, Finland.

3.2.2 Human OM cell culture (II and III)

The procedure for collecting and processing OM biopsies collected from the rooftop of the nasal cavity was utilized with some modification from the protocol described in (Lampinen, Fazaludeen, et al., 2022; Murrell et al., 2005). Briefly, the OM tissue collected from the nasal cavity was transferred to a Biosafety Level 2 (BSL2) facility in PneumaCult - Ex Plus (Stemcell Technologies) supplemented with hydrocortisone (96 ng/mL; Stemcell Technologies) and 1% Penicillin–Streptomycin (Gibco). Initially, the tissue was rinsed in cold Hank's Balanced Salt Solution (HBSS) to remove blood

and cartilage. Then, it was enzymatically digested with dispase II (2.4 U/mL) to separate the OE from the LP. The LP fraction was mechanically triturated and treated with collagenase H (0.25 mg/mL; Sigma Aldrich). After complete digestion, the OE and LP were combined and seeded on poly-D-lysine-coated wells. The cultures were incubated to allow cell migration and proliferation, with regular media changes every 2–3 days. After 8–14 days, the cultures were passaged using TrypLE Express enzyme (Thermo Fisher Scientific) and expanded or frozen for later use. For studies II and III, cryopreserved human primary OM cells at passages 2–3 were thawed and grown in submerged cultures in supplemented PneumaCult-Ex Plus media for 4–6 days under submerged conditions before plating the cells for exposures in study III and utilized for ALI cultures in study II.

3.2.3 Establishment and maintenance of air-liquid interface culture (ALI) (II)

For establishing ALI cultures, transparent inserts for a 24-well plate were used, coated with Matrigel Growth Factor Reduced (GFR) Basement Membrane Matrix (Corning) dilution (1:100). Submerged OM cells were seeded on coated transwell inserts and cultured in PneumaCult-Ex Plus media for 2–4 days with media in both apical and basal chambers. Once confluent, cells were airlifted by replacing media in the basal chamber with PneumaCult ALI medium (Stemcell Technology) supplemented with final concentrations of 4 µg/mL heparin (Paranova), 0.48 µg/mL hydrocortisone, and 1% penicillin–streptomycin. Cultures were maintained in ALI for an additional 21 days for differentiation into pseudostratified epithelium, with regular media changes and washing to remove mucus secretion. These cultures, termed olfactory mucosa cell at air–liquid interface (OM-ALI), were utilized for exposures performed for study II

3.3 EXPOSURE PROTOCOLS

3.3.1 Detailed protocols for PM exposure (I and III)

For Studies I and III, PM samples were obtained from a sampling campaign conducted in China in 2014 at Nanjing University's Xianlin campus (NJU). A detailed methodology describing the collection method, sample source, PM composition, and size-segregation process has been previously reported (Jalava et al., 2015; Rönkkö et al., 2018, 2020). In summary, PM samples were acquired using a high-volume cascade impactor during nighttime operations, gathering four distinct size ranges (Sillanpää et al., 2003). Specifically, for Study I, $PM_{2.5\text{-}1}$ (diameter<2.5 µm) samples were utilized, while Study III incorporated $PM_{0.2}$ (diameter<0.2 µm) and $PM_{10\text{-}2.5}$ (diameter<10µm) and $PM_{10\text{-}2.5}$ samples. These samples were preserved at −20 °C until the day of the exposure.

$PM_{2.5\text{-}1}$ were selected for Study I due to their well-established association with adverse respiratory health effects, including increased susceptibility to respiratory infections and exacerbation of existing respiratory conditions. On the other hand, $PM_{0.2}$ and $PM_{10\text{-}2.5}$ particles were chosen for Study III to explore their differential impacts on immune responses within olfactory mucosa cells. This decision was based on considering their deposition patterns in the respiratory tract. $PM_{0.2}$ includes finer particles that may translocate to various tissues, including the brain, while $PM_{10\text{-}2.5}$ encompasses larger particles that tend to accumulate in the upper respiratory tract.

On the exposure day, the samples were suspended in 10% DMSO (Sigma Aldrich, USA) in endotoxin-tested water (Sigma, W1503) and subjected to 30 minutes of sonication before use in the exposures. Following the administration of PM samples into the cell culture medium, the final DMSO concentration was maintained at <0.3%.

The exposure protocol for Study I and III involved a two-step submerged exposure. In Study I, A549/THP1 co-cultured cells were exposed to varying concentrations of $PM_{2.5\text{-}1}$ (25 µg/ml, 50 µg/ml, and 100 µg/ml equivalent to 6.6, 13.2, and 26.3 µg/cm2) for 24 hours at 37 °C and 5% CO_2. In Study III,

OM cells were exposed to either $PM_{0.2}$ or $PM_{10\text{-}2.5}$ particles at a concentration of 50 µg/ml (equivalent to 13.2 µg/cm^2) for 24 hours.

3.3.2 Bacterial and viral ligands exposure (I)

In Study I, cells exposed to $PM_{2.5\text{-}1}$ underwent a subsequent 24-hour co-exposure to fixed doses of three distinct ligands aiming to mimic viral and bacterial infections. These ligands included 1 µM of ORN R-0006 (TLR7/8 ligand, Miltenyi Biotech), 25 µg/ml of Poly IC (TLR3 ligand, Miltenyi Biotech), and 50 ng/ml of lipopolysaccharide (LPS) (TLR4 ligand).

3.3.3 SARS-CoV-2 infection (II and III)

The SARS-CoV-2 viral strains were acquired and exposures were conducted under the Helsinki University Hospital laboratory research permit 30 HUS/32/2018 § 16 in the Biosafety level 3 (BSL3) facility at the University of Helsinki. The viruses were propagated in VeroE6-TMPRSS2 (Transmembrane Serine Protease 2) cells, stored at -80 °C, and their titers were determined by plaque assay. In Study II, OM-ALI cultures from control and AD individuals were infected with WT SARS-CoV-2 (1×10^5 PFUs/insert), delta variant (1×10^5 PFUs/insert), or omicron variant (1×10^5 PFUs/insert). Apical OM-ALI cultures were exposed to 50 µL of SARS-CoV-2. A SARS-CoV-2 negative medium was used as mock infection, while an investigation into the inhibition of WT-SARS-CoV-2 cell entry was conducted using the TMPRSS2 inhibitor Nafamostat (25 µM).

For Study III, OM cells exposed to PM were transferred to a BSL3 facility and then inoculated with WT SARS-CoV-2. After a 90-minute incubation at 37°C, the infected cells were washed with phosphate-buffered saline and incubated for either 48 or 72 hours at 37°C and 5% CO_2, maintaining pollutant exposure throughout the experiment. Controls included unexposed, PM-exposed, ligand-exposed (Study I), and virus-only (Study III) setups.

3.4 FUNCTIONAL TOXICOLOGICAL IN VITRO ASSAYS

3.4.1 Metabolic Activity Assay (I and III)

The cellular metabolic activity (CMA) was assessed using the MTT (3-(4,5-dimethylthiazol-2-yl)-2,5-diphenyltetrazolium bromide) assay in studies 1 and 3. In Study I, A549/THP1 cells were examined for changes in metabolic activity following exposures to $PM_{2.5\text{-}1}$, and $PM_{2.5\text{-}1}$ along with bacterial and viral ligands, as detailed previously. In Study III, the impact on metabolic activity was specifically studied in OM cells exposed only to $PM_{0.2}$ and $PM_{10\text{-}2.5}$.

The MTT assay involved replacing the cell medium with fresh medium containing 1.2 mM MTT (Sigma-Aldrich). Subsequently, the cells were incubated at +37°C for 2 hours. In negative control samples, cells were treated with 30% (v/v) Triton X-100 for 5 minutes before adding the MTT-supplemented medium. Following incubation, the formazan crystals indicating metabolically active cells were dissolved using sodium dodecyl sulfate (SDS) lysis buffer in Study I and pure dimethyl sulfoxide in Study III.

The absorbance of the solubilized cells was measured at 595 nm using a Wallac Victor 1420 microplate reader (Perkin Elmer, Waltham, USA) for Study I and a Synergy H1 Microplate reader (BioTek, USA) for Study 3. The CMA was assessed by normalizing absorbance values of exposed cells against untreated controls.

3.4.2 2',7'-dichlorodihydrofluorescein diacetate assay (I)

In Study I, cellular oxidative stress was assessed using the fluorescent dye 2',7'-dichlorodihydrofluorescein diacetate (H2DCF-DA), which measures ROS accumulation within cells. Cells were treated with H2DCF-DA and the resulting fluorescence was measured at 0, 30, and 60 minutes using a microplate reader with excitation at 485 nm and emission at 530 nm. The area under the curve (AUC) for fluorescence over time was calculated to quantify ROS levels. The AUC values for treated samples were then normalized against the unexposed control, enabling a comparative analysis of oxidative stress induced by different treatments.

3.4.3 Propidium Iodide Exclusion Test (I)

In Study I, the Propidium Iodide (PI) Exclusion test was employed to evaluate cell viability. PI, a fluorescent dye, permeates cells with compromised plasma membranes (such as dead or damaged cells), while live cells typically exclude PI due to their intact membranes. Cells previously assessed for cellular ROS underwent the PI exclusion test. The PI solution was added to each well, gently mixed, and incubated for 20 minutes. Baseline PI fluorescence was measured at excitation/emission wavelengths of 540 nm and 610 nm, respectively, using a Synergy H1 Microplate reader (BioTek, USA). Subsequently, 10% Triton X-100 was added to lyse the cells, and the plate was further incubated at room temperature for an additional 20 minutes. Maximum PI fluorescence was then measured under the same excitation/emission settings used for the baseline measurements. These fluorescence readings were utilized to calculate the percentage of live cells among the different treatments.

3.4.4 Viability test (I)

In Study I, cell viability and proliferation post various exposures were assessed by nuclear staining using 4',6-diamidino-2-phenylindole (DAPI). The samples underwent staining with a combination of Acridine Orange (AO) and DAPI, using solution 13. Subsequently, the stained samples were analyzed using the Nucleocounter NC-3000 (Chemometec, Denmark) according to the manufacturer's protocol.

3.4.5 Measurements of the cellular thiols (I)

In Study I, we examined the redox status of cellular thiols, an indicator of apoptosis in cells exposed to PM, TLR ligands, and both. Live cells suspended in PBS were stained with Solution 5 (VitaBright-48 (VB-48), AO, and PI. These samples were loaded onto NC-Slide A8 and analyzed using the Nucleocounter NC-3000 (ChemoMetec, Denmark) following the manufacturer's protocol. The scatter plots generated by the Nucleocounter

were processed using FlowJo software version 10 (FlowJo LLC, USA). Live and dead cell populations were distinguished, and among the live cells, those displaying low-intensity VB-48 staining were identified. This low-intensity staining suggests cells undergoing apoptosis or having reduced thiol levels, indicative of apoptosis. The percentage of cells exhibiting this characteristic low-intensity VB-48 staining was quantified as the apoptotic cell population.

3.4.6 Lactase dehydrogenase assay (III)

In Study III, the lactate dehydrogenase (LDH) assay was employed to evaluate cell damage induced by exposures. After the exposures, culture media were collected and stored at -80°C until analysis. The CyQUANT™ LDH Cytotoxicity Assay Kit from Invitrogen was utilized for this purpose, following the manufacturer's recommended protocol. Triton-X-100 treated cells were utilized as a marker for cell death and served as a positive control. Absorbance values were measured at both 490 nm and 650 nm using the Wallac Victor 1420 plate reader. The results were analyzed and presented as the percentage of LDH release following the respective exposures.

3.5 MOLECULAR BIOLOGY ASSAYS

3.5.1 Cell cycle analysis (I)

In Study I, we examined the cell cycle distribution of cells exposed to $PM_{2.5\text{-}1}$, TLR ligands, and their combined exposure. After the exposures, cells were fixed using 70% ethanol and stored at −20°C for subsequent analysis. Following this, the fixed cells underwent centrifugation at 400–500 RCF at 4°C to remove the ethanol without disturbing the cell pellets. The pellets were washed with PBS, centrifuged again, and suspended in PBS. The cells were then treated with RNAse-A (15 µg/ml concentration dissolved in DNAse/RNAse-free water) for 1 hour at 50°C in a dark environment. Subsequently, PI staining (0.01 mg/ml final concentration) was performed, followed by a 30-minute incubation at 37°C. After staining,

the samples were stored at 4°C in the dark until analysis using a BD FACSCanto™ II flow cytometer (BD Biosciences, USA). FlowJo software was used to analyze the data obtained from the flow cytometer. The results were presented as percentages of cells in various cell cycle phases such as Sub-G1, G1-G0, and G2-M.

3.5.2 Quantitative Real-time PCR (III)

In Study 3, OM cells were initially plated in 12-well plates at a density of 70,000 cells per well before being exposed to PM and SARS-CoV-2 infection. Following exposure, the cells were treated with TRI Reagent and stored at -70°C for later analysis. RNA extraction was conducted following the manufacturer's protocol, and the concentration and purity of the obtained RNA samples were assessed using a NanoDrop 1000 spectrophotometer (Thermo Fisher Scientific, USA). Subsequently, cDNA synthesis was performed utilizing the High-Capacity Reverse Transcription Kit. The mRNA levels of specific genes were then measured in duplicate using the StepOnePlus™ Real-Time PCR System (Thermo Fisher Scientific, USA) following the manufacturer's instructions.

To normalize the cycle threshold (Ct) values, the housekeeping gene Glyceraldehyde-3-phosphate dehydrogenase (GAPDH) was utilized as an internal reference. The relative gene expression was quantified utilizing the $2^{-\triangle\triangle Ct}$ method, with Ct representing the threshold cycle number, and the results were presented relative to the control conditions. For a comprehensive list of the TaqMan gene expression assays employed in this study, please refer to Table 1.

Table 1. Taqman primers were obtained from ThermoFisher Scientific for study III.

Gene Symbol	Gene Name	Assay ID
ACE2	Angiotensin I Converting Enzyme 2	Hs01085333_m1

TMPRSS2	Transmembrane Protease, Serine 2	Hs01122322_m1
NQO1	NAD(P)H Quinone Dehydrogenase 1	Hs00168547_m1
HMOX1	Heme Oxygenase 1	Hs01110250_m1
NRP1	Neuropilin 1	Hs00826128_m1
GAPDH	Glyceraldehyde-3-Phosphate Dehydrogenase	Hs02758991_g1

3.5.3 Quantification of viral RNA (RT PCR) (II and III)

In Studies II and III, we assessed the release of SARS-CoV-2 RNA into the culture medium at 1, 48, and 72 hours post-infection (hpi) to monitor viral propagation within the OM cells. In Study II, apical washes from infected cells in transwell inserts, and Study III, cell-exposed media from various treatment conditions, were collected at the same time points from both SARS-CoV-2 infected and mock-infected OM-ALI cultures for RNA extraction. RNA extraction was performed using the QIAamp Viral RNA Minikit (Qiagen) following the manufacturer's instructions. The isolated RNA samples underwent quantitative reverse transcription polymerase chain reaction (RT-PCR) targeting the SARS-CoV-2 RNA-dependent RNA polymerase (RdRp) gene. This analysis utilized established primers, a probe, and an *in vitro* synthesized RdRp control. SARS-CoV-2 RNA copies were quantified at each time point to determine the relative increase in viral load.

3.5.4 Measurement of Transepithelial Electrical Resistance (II)

In Study II, Transepithelial Electrical Resistance (TEER) measurements were regularly taken throughout the establishment and maturation of the OM-ALI cultures. TEER serves as a crucial indicator of the functional integrity and tightness of the cellular barrier. Using the EVOM2 epithelial volt/ohm meter with STX2 chopsticks electrodes (World Precision Instruments), TEER was monitored for a duration of up to 5 weeks. TEER values were

determined using the formula: TEER (Ω/cm^2) = (total resistance (Ω) – blank resistance (Ω) multiplied by the surface area of the transwell insert in cm^2. By the 21st day, TEER values had reached their highest values, suggesting the achievement of a plateau and indicating optimal barrier stability. Consequently, the cell cultures at this stage were selected for subsequent exposure studies due to their established tight junctions and enhanced barrier functionality.

3.5.5 mRNA sequencing (II)

In Study II, mRNA sequencing was performed to analyze the gene expression changes in OM-ALI cultures following SARS-CoV-2 infection. Total RNA samples were collected post-infection and extracted using the AllPrep DNA/RNA/miRNA Universal Kit (Qiagen). Subsequent assessments for RNA integrity were conducted using the Agilent 2100 Bioanalyzer, and RNA concentrations were measured using the Qubit fluorometer (Invitrogen). Computational analyses and RNA sequencing were conducted in collaboration with Professor Jan Topinka (Institute of Experimental Medicine of the Czech Academy of Sciences, Czech Republic), as detailed in Study II. Specifically, ribosomal RNA was removed using the QIAseq FastSelect RNA Removal Kit (Qiagen). From the resulting RNA, 300 ng per sample was utilized to construct RNA libraries employing the QIAseq Stranded Total RNA Library Kit (Qiagen) following the manufacturer's guidelines. The amplified libraries underwent a quality assessment on the Agilent 2100 Bioanalyzer using the High Sensitivity DNA Kit (Agilent), and their concentrations were determined with the Qubit fluorometer and dsDNA HS assay kit (Invitrogen). Subsequently, the libraries were sequenced on an Illumina NovaSeq 6000 platform (200 cycles), generating approximately 50 million reads per sample. Computational analysis involved adapter trimming using Trimmomatic, alignment to the hg38 human genome with the STAR aligner, and gene annotation with FeatureCounts. Differential gene expression (DEG) analysis across various experimental conditions was conducted. Furthermore, the DEGs were

utilized for pathway analysis offering valuable insights into the gene expression alterations in OM-ALI cells post-SARS-CoV-2 infection.

3.5.6 Immunocytochemistry (II)

In Study II, OM-ALI cells subjected to SARS-CoV-2 infection were fixed and immunostained to investigate cellular markers at 72 hpi. The fixed cells underwent 4% paraformaldehyde treatment in both apical and basal chambers, followed by washing and permeabilization with Triton X-100. After blocking and overnight incubation with primary antibodies, secondary antibodies (Table 2) were applied for 3 hours at room temperature. Nuclei were visualized using Hoechst or bisbenzimide staining. Transwell membranes with OM cells were mounted on glass slides for imaging using the CellVoyager™ CQ1 Benchtop High-Content Analysis System (Yokogawa) and Zeiss Axio Observer inverted microscope with LSM800 confocal module (Carl Zeiss AG). Image analysis of 3D-confocal image stacks was performed using the Cell Path Finder software embedded in the CQ1 microscope. Nuclei were automatically detected and fluorescence intensity of epithelial cell markers quantified within a nuclear volume expanded by 10 pixels. Cell classification based on marker positivity utilized manually determined fluorescence thresholds within the same software. Image processing was carried out using ZEN Blue version 3.2 and ImageJ version 1.53q.

Table 2. Primary and secondary antibodies were used in Study II.

Antibodies	**Dilution**	**Catalogue Number**	**Source**
Monoclonal anti-tubulin, acetylated antibody produced in mouse	1:2000	T6793-100UL	Sigma-Aldrich

Mouse monoclonal MUC5AC antibody (45M1)	1:200	MA5-12178	Thermo Fisher Scientific
Mouse monoclonal human Cytokeratin 18 antibody (810811)	1:50	MAB7619	R&D Systems
Goat anti-ACE-2 polyclonal antibody	5 µg/mL	AF933-SP	R&D Systems
Recombinant Rabbit monoclonal Anti-Neuropilin 1 antibody [EPR3113]	1:250	ab81321	Abcam
ZO-1 Polyclonal Antibody	5 µg/mL	40-2200	Invitrogen
SARS-CoV/SARS-CoV-2 Nucleocapsid	1:2000	-	Kind gift by Jussi Hepojoki, Cantuti-Castelvetri et al., Science, 2020
Donkey anti-goat Alexa Fluor-488	1:1000	A-11055	Invitrogen
Donkey anti-mouse Alexa Fluor555	1:500	A-32773	Invitrogen
Goat anti-rabbit Alexa Fluor-647	1:500	A-31573	Invitrogen
Alexa Fluor-488 conjugated phalloidin	1: 200	A-12379	Invitrogen
Hoechst DNA stain	1: 2000	62249	Thermo Fisher Scientific

3.5.7 Enzyme-linked immunosorbent assay (I and III)

In Study I, a sandwich enzyme-linked immunosorbent assay (ELISA) was used to measure pro-inflammatory markers, including interleukin 6 (IL-6)

and TNF-α with ELISA Ready-SET-Go kits from Invitrogen, along with interleukin 8 (IL-8) from R&D Systems, USA. These assays were conducted using A549/THP1 co-culture cell supernatant samples. Conversely, Study III employed Invitrogen ELISA kits for Aβ1-42 and Aβ1-40 to assess the levels of secreted Aβ1-42 and Aβ1-40 in OM cells post-exposure to PM, SARS-CoV-2 infection, or a combined exposure. Medium samples were collected, stored at -70°C, and analyzed using the respective ELISA kits following the recommended protocols.

Table 3. ELISA kits were used for studies 1 and 3.

Protein Name	**Catalogue Number**	**Source**
IL-6	ELISA Ready-SET-Go kit	Invitrogen
TNF-α	ELISA Ready-SET-Go kit	Invitrogen
IL-8	ELISA	R&D Systems, USA
Aβ1-42	KHB3544	Invitrogen
Aβ1-40	KHB3481	Invitrogen

3.5.8 Cytokine proteome profiler (III)

The Proteome Profiler Human XL Cytokine Array Kit (R&D Systems) was employed in Study 3 to analyze 105 cytokines, chemokines, and acute phase proteins in medium samples from different treatments of control and AD OM cells. The aim was to comprehensively profile these biomolecules. Samples were pooled per treatment, and processed according to the kit instructions. Subsequently, processed samples from each exposure were exposed to membranes that contained immobilized capture antibodies specific to biomolecules overnight at +4^{o}C. Following this incubation, the membranes underwent washing steps and were then incubated with detection antibodies. Streptavidin-HRP was subsequently applied to the membrane before imaging using the Bio-Rad ChemiDoc MP (Bio-Rad, USA). Image Lab 5.1 software (Bio-Rad) facilitated spot normalization and quantification on the membrane. The outcomes were presented as Log2 transformed fold changes (FC) relative to the vehicle treatments for both control and AD OM cells.

3.6 STATISTICAL ANALYSIS

For statistical analyses in Study I, IBM SPSS statistics software, version 25, was used, while in Studies 2 and 3, GraphPad Prism version 9.4.1 (GraphPad Software Inc.) was the primary software employed. Details of the statistical method used to analyse the results are indicated in the original publication. Briefly, error bars represented the standard deviation (SD) for Study II and the standard deviation (SEM) for Studies I and III. Significance for functional analyses was considered for values of $p \leq 0.05$, and RNA sequencing data, significance was determined for genes with an adjusted p-value less than or equal to 0.05. Additionally, RNA sequencing datasets underwent analysis Panther overrepresentation analysis, and the QIAGEN Ingenuity Pathway Analysis Software (QIAGEN IPA, QIAGEN Inc., USA) to investigate alterations in canonical pathways. Graphical illustrations in Studies II and III were created using BioRender.com.

4 RESULTS

4.1 URBAN AIR PM MODULATES IMMUNE RESPONSES TO RESPIRATORY INFECTIONS

Exposure to $PM_{2.5}$ has consistently been correlated with an increased susceptibility to bacterial and viral respiratory infections, as evidenced by epidemiological studies. While the detrimental health impacts of fine $PM_{2.5}$ are well-established (Feng et al., 2016), its specific immunomodulatory effects in the context of respiratory bacterial and viral infections remain inadequately understood. Study I sought to bridge this knowledge gap by investigating how acute exposure to varying concentrations of urban air $PM_{2.5\text{-}1}$ influences the immune response to bacterial and viral stimuli in an *in vitro* model mimicking initial respiratory pathogen exposure.

This investigation employed an *in vitro* co-culture model comprising A549 epithelial cells and THP1 monocytes differentiated into macrophage-like cells to replicate the interaction between alveolar epithelium and macrophages. Toll-like receptor (TLR) ligands, chosen to activate specific pathways associated with respiratory infections, were utilized to simulate viral and bacterial stimuli. Cells underwent exposure to various doses of $PM_{2.5\text{-}1}$ and were subsequently exposed to distinct TLR ligands. Key findings from Study I are summarized below.

4.1.1 Inflammatory and Immune Response

$PM_{2.5}$ exposure has been linked to compromised lung immune responses. Our study demonstrated similar findings; dose-dependent increase in pro-inflammatory cytokines (IL-6, TNF-α, IL-8) following $PM_{2.5\text{-}1}$ stimulation in A549-THP1 co-cultures. This led us to further investigate whether $PM_{2.5\text{-}1}$ exposure could elicit pro-inflammatory responses in A549/THP1 cells that mimic the innate immune barrier in the lung, consequently affecting responses to bacterial and viral challenges.

To simulate bacterial and viral challenges *in vitro*, we employed viral TLR ligands (TLR 3 and TLR 7/8) and a bacterial TLR ligand (TLR4). Interestingly, these ligands independently modulated pro-inflammatory cytokines. TLR7/8 induced the highest IL-6 production, followed by TLR4, while TLR3 had limited effects compared to controls. Surprisingly, $PM_{2.5-1}$-primed co-cultures exhibited altered responses to bacterial and viral TLR ligands.

Co-exposure of PM with viral ligands TLR 7/8 and TLR3 revealed substantial alterations in expected pro-inflammatory cytokine responses associated with these viral ligands. Contrary to anticipated cytokine release induced by individual exposures to these ligands or PM alone, the combined exposure resulted in intriguing modifications of cytokine production. For instance, co-exposure to PM and TLR7/8 reduced IL-6 concentrations compared to the response triggered by the TLR7/8 ligand alone. Moreover, at higher PM doses, cytokine levels not only decreased compared to the response from TLR7/8 ligand alone but were also lower relative to PM-only exposure. Similarly, co-exposure to PM and TLR3 induced lower cytokine secretion than PM alone, indicating a deviation from the expected cytokine response. These findings suggest that prior $PM_{2.5-1}$ exposure might diminish the co-culture's ability to mount an effective immune response, potentially exacerbating viral infections.

Conversely, co-exposure of PM with the bacterial TLR4 ligand demonstrated a contrasting effect on the inflammatory response compared to individual exposures. When combined with PM, TLR4 enhanced the pro-inflammatory response, notably increasing TNF-α production compared to exposures to PM or the TLR4 ligand alone. This amplified cytokine production suggests potential immune cell sensitization upon co-exposure. These observations underscore a distinct modulation in the immune response, highlighting the interplay between PM exposure and bacterial stimuli through TLR4 activation.

4.1.2 Cellular metabolic alterations and viability

Our investigation into cellular metabolic alterations following $PM_{2.5}$ exposure revealed a significant dose-dependent reduction in cellular

metabolic activity (CMA), consistent with prior observations (Kasurinen et al., 2018). Interestingly, our study did not reveal any significant impact on CMA when cells were exposed solely to TLR ligands, suggesting that the observed reduction in CMA primarily stems from $PM_{2.5-1}$ exposure. Moreover, subsequent exposures failed to ameliorate CMA, indicating a persistent influence of $PM_{2.5-1}$ on CMA.

Assessment of cellular thiols, notably glutathione (GSH), depicted an increase in cells exhibiting low free thiol levels post-$PM_{2.5-1}$ exposure. While viral ligands displayed minimal impact on thiol levels, exposure to bacterial TLR4 ligands notably depleted free thiols, correlating with an augmented pro-inflammatory response. Intriguingly, $PM_{2.5-1}$ pre-exposure mitigated TLR4-induced effects on thiol depletion, suggesting a potential alteration in cellular responses to bacterial ligands due to $PM_{2.5-1}$ priming. These outcomes suggest that $PM_{2.5-1}$ pre-exposure induced early apoptosis on the acute challenge to bacterial TLR4 ligand as suggested through reduced CMA and cellular thiol levels.

Contrary to expectations, our study did not reveal significant changes in ROS stress or viability. It is plausible that the co-culture model, fostering immune cell interaction with lung epithelial cells, mitigated oxidative stress, consistent with previous findings (Kasurinen et al., 2018; Persson et al., 2013). This observation underscores the intricate interplay between immune cells and epithelial cells, potentially functioning to buffer oxidative stress within the co-culture context.

4.1.3 Cell cycle dynamics

Our investigation into cell cycle dynamics following $PM_{2.5-1}$ exposure revealed striking alterations in cell phase distributions. $PM_{2.5-1}$ exposure induced an increase in cells in the Sub-G1 phase, indicative of apoptosis, and concurrently reduced cells in the G2-M phase, implying cell cycle arrest and apoptosis induction, aligning with previous literature (Lambert et al., 2003). Viral TLR ligands had distinct effects on cell cycle dynamics, particularly in the G2-M phase, potentially associated with viral strategies manipulating the cell cycle for replication (Davy and Doorbar, 2007).

However, $PM_{2.5\text{-}1}$ priming appeared to modify viral ligand-induced effects on the cell cycle, suggesting alterations in viral virulence mechanisms. Interestingly, bacterial TLR4 ligand exposure increased cells in the Sub-G1 phase, indicating an apoptotic response potentially exacerbated due to $PM_{2.5\text{-}1}$ priming. This observation suggests PM-induced alterations in immune responses to viral and bacterial stimuli, emphasizing the complex interactions between PM exposure, TLR stimulation, and subsequent cellular responses.

4.2 SARS-COV-2 INFECTION DYNAMICS IN 3D HUMAN OM MODEL IN THE CONTEXT OF AD

The OM stands as a crucial entry point for inhaled air and its particles, making it a prime interface for pathogen exposure, including neurotropic viruses like SARS-CoV-2. Understanding its role gains prominence in the context of neurodegenerative diseases such as AD, which often presents olfactory dysfunction as an early symptom. Furthermore, AD OM has been shown to express changes associated with the disease. Therefore, exploring the effects of SARS-CoV-2 infection on the OM, particularly in the context of AD, assumes paramount importance in deciphering the potential links between viral infections and neurodegeneration. In Study II, we aimed to establish a physiologically relevant *in vitro* OM model to mimic the *in vivo* tissue by replicating crucial cellular components, and functional barriers to aid in the investigation of SARS-CoV-2 infection in the patient-derived human OM. Key results from the investigation in Study II are summarized below.

4.2.1 Establishment and characterization of 3D OM ALI Cultures

We successfully established a novel 3D ALI culture model using human OM biopsies obtained from both cognitively healthy individuals and those affected by AD. After three weeks in ALI culture, thorough characterization revealed the presence of pseudostratified epithelium with ciliated cells, sustentacular cells, basal cells, and mucous-producing cells. Notably, the

ALI cultures demonstrated barrier formation, as confirmed by measurements of TEER and the expression of tight junction markers.

4.2.2 Expression of SARS-CoV-2 entry proteins and cellular targets

Our investigation aimed to comprehensively characterize the expression profile of key receptors and proteins crucial for SARS-CoV-2 entry and infection within the OM-ALI cultures. Understanding the significance of the ACE-2 receptor, known to be primarily targeted by SARS-CoV-2 for binding to host cell membranes (M. Hoffmann et al., 2020), and Neuropilin-1 receptor (NRP-1), which has been shown to facilitate the infection of SARS-CoV-2 (Cantuti-Castelvetri et al., 2020), is vital in deciphering the susceptibility of cells to the virus. Utilizing global mRNA sequencing data analysis from uninfected cells, we identified the presence of *ACE-2, NRP-1*, *TMPRSS2*, *Cathepsin B* (*CTSB*), *Cathepsin L* (*CTSL*), *basigin* (*BSG*), and *furin* mRNAs in the OM cultures. These genes are well-documented for their involvement in facilitating SARS-CoV-2 infection (V'kovski et al., 2021). To further validate the expression of these crucial entry receptors, ACE-2 and NRP-1 proteins, we conducted immunocytochemical staining of differentiated OM-ALI cultures which showed ACE-2 and NRP1 positive cells expressed in OM-ALI cultures. This molecular investigation was pivotal in comprehensively characterizing the OM-ALI cultures and evaluating their susceptibility to SARS-CoV-2 infection, particularly by assessing the presence and expression of these key receptors and proteins.

4.2.3 SARS-CoV-2 infection in OM cells: effects of variants and disease state

At the outset, our primary focus was to evaluate the effects of the wild-type (WT) SARS-CoV-2 variant on OM cells obtained from both cognitively healthy subjects and individuals diagnosed with AD. Our results indicate that up to 72 hpi, there were no discernible differences in viral replication patterns between the OM cells derived from the control group and those afflicted by AD. This evaluation was conducted through comprehensive immunocytochemistry and quantitative analysis of viral RNA load

determined with qPCR from the media samples collected in a time series following infection. Results collectively suggest a similar level of viral presence in both control and AD-derived OM cells.

Moreover, we investigated the impact of different SARS-CoV-2 variants (e.g., omicron, delta, WT) on the infectivity of OM-ALI cultures derived from cognitively healthy individuals. Surprisingly, OM-ALI cells exhibited higher susceptibility to the WT virus in comparison to the omicron variant. No significant differences were observed between susceptibility to the delta variant in comparison to the WT virus. Importantly, our findings suggest that the underlying AD pathology did not render the AD OM-ALI cells more vulnerable to SARS-CoV-2 infection when compared to cells derived from cognitively healthy controls. These outcomes corroborated emerging epidemiological and *in vivo* evidence, supporting varying susceptibility among distinct SARS-CoV-2 variants in infecting OM cells (Rodriguez-Sevilla et al., 2022; von Bartheld et al., 2023).

4.2.4 Differential gene expression patterns in SARS-CoV-2 infected OM cells of individuals with AD

Transcriptomic analysis was conducted on OM cultures derived from individuals with AD and cognitively healthy controls following SARS-CoV-2 infection. A comparative analysis of gene expression patterns unveiled 1971 DEGs unique to infected AD cells. These DEGs indicated distinct molecular responses exclusive to AD pathology upon viral exposure. The exploration of DEGs highlighted the activation of critical pathways intricately linked to AD pathology within the infected AD OM cells. Noteworthy pathways included integrin signalling, the AD-presenilin pathway, and the Wnt-signaling cascade. These findings suggest potential crosstalk between viral infection and AD-specific molecular mechanisms, indicating a possible exacerbation of AD-associated pathology consequent to SARS-CoV-2 exposure.

4.2.5 Impaired immune responses in AD OM cells post-infection

The AD OM cells exhibited a subdued immune response post-SARS-CoV-2 infection, in contrast to the robust antiviral response observed in cells derived from cognitively healthy controls. This subdued reaction was characterized by the downregulation of key immune signalling molecules, notably *IFN-γ* and *TNF*, underscoring a potential vulnerability of AD cells to the prolonged viral presence and heightened inflammation occurring upon AD pathology in the OM.

4.2.6 Insights into neurological consequences and AD progression

Distinct transcriptomic alterations observed in the infected AD OM cells suggested a plausible exacerbation of AD pathology triggered by SARS-CoV-2 infection. Elevated oxidative stress and compromised immune responses within the infected AD cells hint at an intricate interplay between viral-induced mechanisms and pre-existing AD-related pathophysiology, potentially influencing disease progression and neurological consequences.

4.3 URBAN PM INFLUENCES CELLULAR AND IMMUNE RESPONSES TO SARS-COV-2 IN OM CELLS OF INDIVIDUALS WITH AD

Building upon prior research, Study I delved into the immunomodulatory effects of $PM_{2.5\text{-}1}$ exposure in an *in vitro* A549 and THP-1 derived macrophages co-culture model stimulated with TLR ligands resembling respiratory infections. Study II explored the impact of SARS-CoV-2 infection on human OM cells. In the continuum of this investigation, Study III aimed to elucidate the complex relationship between PM exposure and susceptibility to SARS-CoV-2 infection in human OM cells.

Previous findings have indicated that PM can modify susceptibility to infection in *vitro* cell models of both upper and lower respiratory tracts (Brocke et al., 2022; Miyashita et al., 2023; Yamamoto et al., 2023). Additionally, in animal models, exposure to $PM_{2.5}$ has demonstrated the

capacity to induce variations in ACE2 and/or ACE levels across diverse organs (Botto et al., 2023). This understanding assumes significance, particularly considering the adverse health effects caused by SARS-CoV-2 infection.

Therefore, Study III sought to decipher the potential impact of PM exposure, specifically $PM_{0.2}$ and $PM_{10\text{-}2.5}$, on the susceptibility of OM cells to SARS-CoV-2 infection. Physiologically, the OM stands as a crucial tissue due to the importance of the inhalational route and its role as a potential site for neurotropic effects associated with smaller-sized PM deposited in the nasal area. Given the significance of the OM as a potential site of infection, unraveling this connection has become pivotal, especially considering the neurotropic nature of the virus, and its potential associations with neurodegenerative conditions, as highlighted in prior studies.

4.3.1 No significant influence of PM exposure on SARS-CoV-2 susceptibility in OM Cells

In study III, we first investigated the impact of exposure to $PM_{0.2}$ and $PM_{10\text{-}2.5}$ on the expression of critical genes associated with SARS-CoV-2 entry (*ACE2, TMPRSS2, and NRP1*). Our findings revealed no significant alterations in ACE2 or NRP1 expression in cognitively healthy control or AD cells following exposure to either PM fraction. However, a notable increase in TMPRSS2 expression was observed only in AD cells after a 24-hour $PM_{0.2}$ exposure, suggesting a potential disease-specific response. Subsequent investigation aimed to understand how PM exposure influences SARS-CoV-2 infection ability within OM cells. Our analysis indicated a transient impact of PM on viral RNA load at 1 hpi, yet this effect did not persist over later time points (24, 48, and 72 hours). The absence of alterations in viral RNA levels at later time points suggested minimal biological consequence of PM exposure on the infectibility of OM cells. Although PM particles potentially adhering to OM cells might transiently increase viral load at the onset, the consistent viral load patterns over time point to an absence of enhanced viral entry due to PM exposure. Additionally, the comparable effects of combined PM and SARS-CoV-2 exposure in both control and AD OM cells

suggest a similar impact on viral propagation, highlighting a lack of discernible susceptibility changes in AD OM cells exposed to PM in conjunction with viral infection.

4.3.2 Transient oxidative stress response and cellular toxicity upon co-exposure to PM and SARS-CoV-2 in OM cells

Our study also focused on examining the impact of PM exposure in combination with SARS-CoV-2 infection on cell health. LDH assays revealed that at 24 hours post-infection, both control and AD cells exposed to $PM_{0.2}$ and $PM_{10\text{-}2.5}$ exhibited a slight increase in cytotoxicity. However, a significant rise in cytotoxicity was observed only in cells exposed to $PM_{10\text{-}2.5}$ alongside the virus. At 72 hours post-infection, cells solely infected with SARS-CoV-2, in both control and AD groups, displayed increased cytotoxicity. Similarly, cells exposed to $PM_{0.2}$ followed by SARS-CoV-2 infection also exhibited elevated cytotoxicity, especially in AD cells compared to cognitively healthy control cells. Remarkably, exposure to $PM_{10\text{-}2.5}$ slightly mitigated cytotoxicity in AD cells post-viral infection.

Examining the interplay of PM and SARS-CoV-2 on oxidative stress marker genes revealed increased expression of *NQO1* and *HMOX1* after 24 hours of combined exposure in both control and AD cells. However, by 72 hours, a substantial decrease in mRNA expression levels for these genes was observed in cells co-exposed to PM and the virus compared to cells treated solely with PM.

In summary, our findings suggest that PM exposure, especially $PM_{10\text{-}2.5}$, influences virus-induced cell death. Additionally, while combined exposure initially increased oxidative stress marker expression, this effect diminished over time, indicating a transient nature in the cellular response to PM and SARS-CoV-2 co-exposure. These findings suggest a potential suppression of cellular defences by the virus, emphasizing the need for further exploration into complex PM-viral interactions and cellular responses.

4.3.3 PM and SARS-CoV-2 co-exposure effects on amyloid beta (Aβ) metabolism in OM cells

In study 3, we also superficially explored the dynamics of Aβ metabolism in OM cells, important due to its strong association with AD pathogenesis. Our results revealed that while PM exposure alone did not notably affect Aβ secretion, the virus independently increased the Aβ1-42/Aβ1-40 ratio in both control and AD cells. Intriguingly, co-exposure to PM and the virus intensified Aβ secretion, indicating a potential combined impact on AD pathogenesis. This suggests a complex interaction between PM exposure and viral infection in shaping Aβ dynamics relevant to AD.

4.3.4 Interplay between PM exposures and AD-related inflammation: impact on cytokine profiles following SARS-CoV-2 infection

The study utilized the Proteome Profiler Human XL Cytokine Array, evaluating approximately 105 cytokines, chemokines, and growth factors to comprehensively examine cellular cytokine profiles following treatments. This analysis uncovered complex alterations in cytokine expression when OM cells were exposed to $PM_{0.2}$ and $PM_{10\text{-}2.5}$ concurrently with SARS-CoV-2 infection. Numerous cytokines exhibited notable shifts in their expression patterns in response to these combined treatments.

In control OM cells, prior exposure to $PM_{0.2}$ before SARS-CoV-2 infection attenuated many of the virus-induced cytokine responses observed in cells infected solely with the virus. $PM_{10\text{-}2.5}$ treatment showed similar trends, indicating distinct alterations in cytokine expression levels, particularly in certain markedly downregulated cytokines. In Alzheimer's disease (AD) OM cells, the baseline inflammatory status influenced cytokine profiles across different conditions. Upon SARS-CoV-2 infection, significant changes in cytokine expression were noted compared to cells derived from cognitively healthy individuals. $PM_{0.2}$ and virus treatment induced a trend of downregulation in AD cells, whereas $PM_{10\text{-}2.5}$ elicited an enriched cytokine response.

To explore the impact of existing AD pathology on inflammation and antiviral immune response concerning PM and viral treatment, we compared the relative expression of inflammation-associated proteins in AD cells to control cells across various treatment groups. Remarkably, AD cells exhibited a significantly higher baseline level of cytokine expression compared to controls when treated with the vehicle alone, indicating a pronounced elevation in baseline cytokines in AD cells. Specifically, the top three most altered cytokines in vehicle-treated AD cells, compared to control cells, were RANTES, RAGE, and endoglin, suggesting an inherent inflammatory state in AD.

Furthermore, in AD OM cells infected with the virus, more significant changes were observed in the levels of Granulocyte-Macrophage Colony-Stimulating Factor (GM-CSF), Trefoil Factor 3 (TFF3), and RANTES compared to control cells treated with the virus, indicating a heightened response to viral infection in the AD context. This baseline inflammation in AD cells notably influenced the cytokine profile in co-treatment conditions as well. Specifically, in response to $PM_{0.2}$ and virus treatment, a general trend of downregulation was observed compared to treated control cells, with notable alterations in Interferon-Inducible Protein 10 (IP10), Retinol-Binding Protein 4 (RBP-4), and kallikrein expression levels.

Conversely, prior exposure to $PM_{10\text{-}2.5}$ induced a significantly enriched general cytokine response in AD compared to the respective control treatment. Notably, cytokines like RANTES, Angiogenin, Stromal cell-derived factor 1 alpha (SDF-1a), and Interleukin-6 (IL-6) were among the topmost altered cytokines, indicating a distinct cytokine profile in AD cells exposed to $PM_{10\text{-}2.5}$. These findings underscore the complex interplay between AD pathology, environmental exposures, and viral infection, emphasizing the critical role of considering AD-specific inflammation in understanding immune responses to environmental and viral stimuli.

5 DISCUSSION

The thesis presents a comprehensive overview of findings that illuminate the intricate interplay between environmental exposures, specifically PM and respiratory infections, with a particular emphasis on immune responses and neurological consequences. The significance of the research lies in its interdisciplinary nature, integrating methodologies from environmental science, immunology, and neurobiology to address crucial gaps in understanding. By employing advanced *in vitro* models of the respiratory system and investigating complex physiological scenarios, this approach yields valuable insights into the molecular and cellular mechanisms underlying the impact of air pollution on respiratory infections and neurological health and disease. These findings collectively deepen our comprehension of the complex mechanisms governing respiratory immunity and neurological well-being in the presence of environmental pollutants and viral infections.

5.1 IMPACT OF $PM_{2.5-1}$ POLLUTION ON IMMUNE DYSREGULATION AND INCREASED RISK OF BACTERIAL RESPIRATORY INFECTIONS

Recent studies have shown that $PM_{2.5}$ exposure is linked to an increased risk of bacterial respiratory infections, such as *Streptococcus pneumoniae* and *Staphylococcus aureus*, by impairing host defenses (Y.-W. Chen et al., 2020; Hussey et al., 2017; Mushtaq et al., 2011; H. Zhao et al., 2014). However, the specific mechanisms by which $PM_{2.5}$ exposure alters immune responses at a cellular level remain inadequately explored. This gap in understanding presents a crucial area for investigation, especially considering the global prevalence of $PM_{2.5}$ exposure and its potential impact on public health.

Our study contributes to this understanding by simulating the host-lung barrier interaction, specifically examining A549 epithelial cells and THP1 macrophages. By utilizing co-cultures, we aimed to provide a more

comprehensive picture of $PM_{2.5}$ adverse effects, acknowledging the limitations of single-cell line studies (Kasurinen et al., 2018). We observed that $PM_{2.5\text{-}1}$ exposure leads to a dose-dependent alteration in the innate immune response. Specifically, it causes a marked increase in the production of pro-inflammatory cytokines like IL-6, IL-8, and TNF-α. This dysregulation potentially makes individuals more susceptible to bacterial respiratory infections, particularly at high $PM_{2.5}$ exposure levels.
Our study's hypothesis suggests that exposure to $PM_{2.5}$ primes immune cells, particularly alveolar macrophages, to hyper-react to bacterial stimuli by activating TLR4 receptors, possibly through endotoxins present in the PM fraction (Alexis et al., 2006). This activation likely triggers heightened NF-κB signalling and cytokine production. Recent research employing TLR4-enriched mammal models, like sheep, has reinforced the importance of TLR4 in bacterial infections. Specifically, it has been demonstrated that elevated TLR4 levels exacerbate the innate immune response to bacterial LPS-induced apoptosis in monocytes/macrophages by disrupting autophagic flux via NF-κB and MAPK signalling pathways (Gawda et al., 2018; S. Wang et al., 2023). This discovery suggests a plausible mechanism by which heightened TLR4 expression could increase susceptibility to gram-negative bacterial respiratory infections, particularly in environments characterized by elevated $PM_{2.5}$ levels. Consequently, individuals exposed to high concentrations of $PM_{2.5}$ may exhibit increased vulnerability to bacterial respiratory infections due to dysregulated immune responses.

The ramifications of our study are multi-dimensional and significant. Recent research has consistently identified a link between $PM_{2.5}$ exposure and the rise of antibiotic resistance in various bacteria globally, with these correlations intensifying over time (Z. Zhou et al., 2023). Our findings contribute to this growing body of evidence, suggesting a proactive public health strategy. By aiming to reduce $PM_{2.5}$ levels, we could potentially lower the incidence of bacterial respiratory infections. Such a reduction would not only lessen the dependence on antibiotics but also address the escalating challenge of antibiotic resistance. Furthermore, a key implication is the necessity for healthcare professionals to recognize the increased risk of bacterial respiratory infections in people exposed to high concentrations

of $PM_{2.5}$. This understanding is crucial for accurate diagnosis and effective treatment, particularly in regions burdened by heavy air pollution. Further investigation into the mechanisms of $PM_{2.5}$-induced immune dysregulation in bacterial infections is essential. Such investigations could lead to effective interventions to mitigate the adverse health effects of $PM_{2.5}$ exposure, benefiting both individual health and public health policy.

5.2 $PM_{2.5\text{-}1}$ INDUCED ALTERATIONS IN VIRAL IMMUNE RESPONSE DYNAMICS

$PM_{2.5}$ exposure has been closely linked with increased risk and severity of viral respiratory infections. This heightened susceptibility is attributed to the compromised lung immune responses that arise from various mechanisms, such as immune exhaustion (Tao et al., 2020), oxidative stress (Lee et al., 2014), and the inactivation of essential immune cells, including macrophages (Migliaccio et al., 2013). Among the critical facets of the immune response to viruses are the TLRs, specifically TLR7/8 and TLR3, which play a pivotal role in recognizing viral PAMPs (Bortolotti et al., 2021; Martínez-Espinoza et al., 2022; Stegemann-Koniszewski et al., 2018; Triantafilou et al., 2005). However, the precise influence of $PM_{2.5}$ exposure on TLR-mediated immune responses against different viruses remains poorly understood, despite its importance given the global prevalence of viruses and $PM_{2.5}$ exposure.

The study specifically highlights the nuanced impact of $PM_{2.5\text{-}1}$ on the immune responses mediated by different TLRs. Notably, TLR7/8, associated with detecting single-stranded RNA viruses such as influenza and HIV, demonstrated a dampened cytokine production in $PM_{2.5\text{-}1}$ primed co-cultures, suggesting a potential suppression of the immune response to these viruses. It suggests that $PM_{2.5\text{-}1}$ exposure can specifically modulate the immune system response to TLR7/8 ligand, implying that prior exposure to $PM_{2.5\text{-}1}$ might precondition the immune system, potentially affecting its ability to respond effectively to single-stranded RNA viruses (Tao et al., 2020). This could lead to a change in the severity or nature of

respiratory infections caused by such viruses, particularly in polluted environments.

Conversely, TLR3, which is activated in response to double-stranded RNA viruses like RSV and reoviruses, elicited only low cytokine levels following $PM_{2.5-1}$ exposure. This distinct response pattern indicates that $PM_{2.5-1}$ exposure might affect the immune response to double-stranded RNA viruses differently than to single-stranded RNA viruses. This complex interaction between $PM_{2.5-1}$ exposure and viral pathogen type could be pivotal for comprehending the diverse clinical outcomes in respiratory viral infections, especially in regions characterized by high levels of air pollution.

Furthermore, the study observed that TLR3 and TLR7/8 ligands increased the percentage of cells in the G2-M phase of the cell cycle, a strategy often employed by viruses to create favorable conditions for replication (Fan et al., 2018). However, this cell cycle response was altered in $PM_{2.5-1}$ primed co-cultures, indicating that prior $PM_{2.5-1}$ exposure could influence viral replication and virulence.

The study's findings offer crucial insights into the complex interaction between environmental pollutants such as $PM_{2.5-1}$ and the body's response to viral infections, particularly relevant in the COVID-19 pandemic. Our observations on immune response alterations to various viral ligands post-$PM_{2.5-1}$ exposure contribute to the growing evidence, prompting a reassessment of public health strategies, especially in highly polluted regions. Further research is urgently needed to identify the viruses most affected by PM2.5 and understand the specific mechanisms driving these responses, essential for developing targeted interventions, particularly in polluted areas, to mitigate respiratory viral infections' risks. Moreover, the study acknowledges the need to consider a broader spectrum of factors, including genetic predispositions, environmental influences, and lifestyle choices, in understanding the full impact of air pollution on health. This comprehensive approach is necessary for gaining a deeper insight into how these various elements interact and contribute to the overall scenario of respiratory health, particularly in the context of prevalent viral infections. Additionally, exploring Toll-like receptor (TLR) ligands' therapeutic potential presents a promising avenue for combating viral

infections (Dyavar et al., 2021). Leveraging TLR agonists to modulate the innate immune response, alongside traditional antiviral therapies, offers diverse therapeutic opportunities across medical fields like inflammation, cancer, infection, allergy, and autoimmunity. This underscores the importance of innovative strategies targeting TLR signalling pathways to improve health outcomes in various conditions (Hennessy et al., 2010).

5.3 IN VITRO MODELING OF THE HUMAN OM: INSIGHTS INTO ENVIRONMENTAL EXPOSURE AND NEUROLOGICAL HEALTH

The new cell culture model developed in this project consists of primary human OM cells cultured in ALI conditions and addresses a pressing need stemming from the significance of the olfactory-brain connection concerning environmental exposure and disease pathology. The olfactory system serves as a direct conduit for environmental agents and pathogens to access the brain, establishing itself as a pivotal interface between external exposures and neurological health. However, the intricate dynamics of this route and its implications for disease pathogenesis have been hindered by the absence of physiologically relevant *in vitro* models of the OM.

The observed increase in TEER over time, coupled with the confirmation of tight junctions and the presence of cilia, signifies the successful differentiation of OM cells into pseudostratified epithelium, closely resembling the physical barrier of the OM. This characterization underscores the model's ability to replicate essential features of the nasal cavity microenvironment, facilitating the exploration of infection, inflammation, and immune responses within the OE. Moreover, the identification of specific cell types within the OM-ALI cultures, such as goblet cells and sustentacular cells, further enhances the model's physiological relevance, enabling the investigation of cell-type-specific responses to environmental stimuli and pathogens (Barrila et al., 2018). Furthermore, the expression of entry receptors essential for SARS-CoV-2 infection in differentiated OM-ALI cultures underscores the model's potential for studying viral pathogenesis and host-virus interactions.

Overall, these findings support the notion that the developed *in vitro* model of the OM holds promise for advancing our understanding of neuroinvasive infections, neurological outcomes, and potential interventions targeting the olfactory route. Leveraging patient-derived cells in this model also enables researchers to explore how underlying neurological conditions influence susceptibility to infection and responses to environmental exposures, paving the way for targeted therapeutic strategies. Moreover, there is an exciting opportunity to further enhance this model to establish an *in vitro* system that recapitulates the entire nose-brain axis. By improving upon the current model, researchers could incorporate additional components such as olfactory bulb neurons or brain organoids connected to the OE, allowing for the study of bidirectional signalling between the nose and the brain. This advancement could revolutionize our understanding of how environmental exposures and pathogens impact neurological health in brain cells, providing invaluable insights for the development of novel therapeutic interventions targeting the olfactory route and beyond. Ultimately, the establishment of such a comprehensive *in vitro* model holds the potential to accelerate research in neurology.

5.4 SARS-COV-2 INFECTION DYNAMICS IN THE OM AND ITS NEUROLOGICAL IMPLICATIONS

Recent research has significantly advanced our understanding of SARS-CoV-2, particularly its potential to cause neurological symptoms (Wan et al., 2021). Among these, anosmia, or loss of smell, has been a prominent symptom, suggesting the virus might affect the CNS via the trans olfactory route (Meinhardt et al., 2021). While previous studies *in vivo* and *ex vivo* have shown that SARS-CoV-2 infects sustentacular cells in the OM, direct infection of the OSNs, which are responsible for smell perception, has been less evident (Shahbaz et al., 2022). Our study is the first to demonstrate *in vitro* that SARS-CoV-2 primarily infects non-neural cells in the human OM, including apical ciliary cells and sustentacular cells. Sustentacular cells also

known as supporting cells, provide structural and metabolic support to OSN in the OM.

Infection of the supporting cells resulting in death and loss of cilia results in desquamation of the OM as observed in animal models (Bryche et al., 2020). This damage could disrupt normal olfactory function, contributing to anosmia. Furthermore, our study highlights the potential of Nafamostat, a TMPRSS2 inhibitor, in preventing SARS-CoV-2 infection in an OM as previously demonstrated in several susceptible cell lines from both human and animal origins (M. Hoffmann et al., 2020). This points to the crucial role of the TMPRSS2 enzyme in viral entry into cells via the ACE2 receptor and suggests that inhibiting this pathway could be a viable strategy for preventing or reducing the severity of anosmia and potentially other neurological impacts of the virus.

Moreover, our transcriptomic analysis of SARS-CoV-2-infected OM cells offers deeper insights into the virus's effects at the molecular level. We observed the activation of the COVID-19 pathogenesis pathway, with significant changes in genes related to inflammation, antiviral immune response, oxidative phosphorylation, and mitochondrial function. While this response is part of the bodily defense mechanism against the virus, it can inadvertently damage the OM and could impair the function of OSNs, exacerbating the problem of anosmia.

Furthermore, these alterations may contribute to a wide range of COVID-19 symptoms and complications. Particularly noteworthy is the downregulation of genes linked to neuronal plasticity, axonal guidance, and neuronal survival in infected OM cells. This suggests that SARS-CoV-2 infection could have long-term effects on neuronal health and function (Brockington et al., 2010), providing a potential explanation for some aspects of 'long COVID' and highlighting the need for further research into protective strategies for neural cells.

In summary, our study not only enhances our understanding of how SARS-CoV-2 affects the olfactory system but also opens new avenues for potential treatments. It emphasizes the importance of focusing on the supporting cells in the OE and managing the body's inflammatory response to the virus. Furthermore, the insights into the molecular changes induced

by the virus could have significant implications for understanding and addressing the broader neurological effects of COVID-19.

5.5 VARIABILITY IN THE OM RESPONSE TO DIFFERENT SARS-COV-2 VARIANTS

The prevalence of anosmia during the COVID-19 pandemic has varied with different SARS-CoV-2 variants, indicating variable olfactory impacts. These variants, including Alpha, Beta, Gamma, Delta, and Omicron, identified as variants of concern (VOCs) by the WHO, each possess distinct modifications in their spike proteins (Andre et al., 2023). These mutations can lead to increased infectivity, transmissibility, and immune evasion, which are critical factors in the emergence of new VOCs (Andre et al., 2023). The Omicron variant shows a reduced impact on olfactory dysfunction, with a lower incidence of anosmia compared to variants like delta, possibly due to its spike protein affecting their ability to infect OM cells or penetrate the mucus layer (Butowt et al., 2022; Rodriguez-Sevilla et al., 2022). Our study demonstrated varying susceptibility to infection among OM-ALI cultures exposed to different SARS-CoV-2 variants. The original WT strain showed greater infectivity compared to the Omicron variant in these cultures. This variation in infectivity among the variants, particularly in the context of the OM, is crucial for understanding not only the transmission patterns of the virus but also the clinical outcomes associated with infection. It suggests that the specific mutations in the spike proteins of these variants significantly influence their impact on the olfactory system (de Melo et al., 2023). In conclusion, the variability in the SARS-CoV-2 variants and their consequent differences in infectivity in the OM are key to understanding the varied clinical manifestations of COVID-19, including changes in the sense of smell. This knowledge is essential for devising targeted interventions and public health strategies, especially as new variants continue to emerge. The ongoing study of these variants, focusing on their specific spike protein mutations, remains crucial for effectively managing and mitigating the impacts of the pandemic.

5.6 INTERSECTING PATHWAYS OF COVID-19 AND AD AT THE OM

Recent studies have brought to light the intricate relationship between COVID-19 and dementia, particularly AD. It has been observed that individuals with pre-existing dementia are at a heightened risk of experiencing severe COVID-19 symptoms and have increased mortality rates compared to those without dementia (Q.Q Wang et al., 2021b; Bianchetti et al., 2022). Conversely, COVID-19 has been associated with an elevated likelihood of new AD diagnoses (Rudnicka-Drożak et al., 2023; L. Wang et al., 2022), suggesting a bidirectional link between the two conditions. While the presence of the SARS-CoV-2 virus in the brain remains a topic of debate among researchers, there is growing evidence to suggest that post-COVID-19 AD-like dementia is becoming increasingly prevalent as a long-term complication (S. Zhao et al., 2023). Recent investigations have also uncovered a potential connection between AD and the OM, the tissue responsible for smell perception. Anosmia, or loss of smell, has emerged as a common neurological symptom in COVID-19 patients and may serve as an early indicator of neurodegeneration associated with AD (Jung et al., 2019; Lampinen et al., 2022a; Lampinen et al., 2022b; Rantanen et al., 2022; Roberts et al., 2016). This suggests that the OM could be a key site for understanding how SARS-CoV-2 impacts AD pathology.

Studies proposed that elevated ACE-2 expression in brain cells of AD individuals may enhance neurotropism in individuals with AD (Reveret et al., 2023). However, in contrast, this study demonstrates that in the OM, the susceptibility to SARS-CoV-2 infection may not differ significantly between AD patients and cognitively healthy individuals. This observation can be primarily attributed to the fact that OM cells, both in control subjects and in individuals with AD, express similar mRNA levels of ACE-2 and TMPRSS2 and other main proteins which are implicated in the virus to gain entry into the cells. Since their expression levels do not differ markedly between AD patients and healthy individuals, it suggests that the vulnerability of OM cells to SARS-CoV-2 infection is comparable in both groups.

Furthermore, there is a working hypothesis proposed that neuroinflammation and oxidative stress in AD patients may exacerbate the inflammatory response to COVID-19, potentially leading to more severe outcomes (W. Li et al., 2023). In our study, DEG analysis not only highlighted several key genes associated with AD but also higher basal levels of innate immune response genes and INF-stimulated genes suggesting underlying disease pathology could potentially influence the response of the host and contribute to disease severity. Interestingly, post-infection transcriptomic analysis revealed that AD cells showed differential gene expression patterns in comparison to healthy control cells, potentially influencing disease outcomes. AD cells exhibited increased oxidative stress, altered mitochondrial function, desensitized inflammation and immune responses, and altered genes associated with olfaction. SARS-CoV-2 infection enriched AD-associated pathways in AD cells, indicating a deeper involvement of AD pathology in response to the infection. Although this study reflects the acute response of the AD cells to the SARS-CoV-2 infection, initial studies with long COVID reported changes in brain structure (Douaud et al., 2022), cognitive health (Braga et al., 2023; He et al., 2023; Taquet et al., 2023), and neuroinflammation (Roczkowsky et al., 2023). Our findings propose that the immediate cellular changes triggered by SARS-CoV-2 in the context of AD might underpin the prolonged and complex neurological manifestations seen in long COVID. However, further investigation is warranted in this regard.

This study uncovered crucial findings regarding anosmia in the context of both SARS-CoV-2 and AD. We identified a significant upregulation of UGTA2A in AD cells, suggesting a heightened risk of olfactory dysfunction in AD individuals compared to healthy controls. This enzyme, typically expressed in the sustentacular cells of the OM, has been linked to COVID-19-induced anosmia (Khan et al., 2021; Shelton et al., 2022), indicating a shared pathophysiological mechanism between AD and COVID-19-related anosmia. Additionally, our data showed a notable reduction in ciliary cells and downregulation of key olfactory receptor genes in AD OM-ALI cultures following SARS-CoV-2 infection, reflecting a potential vulnerability in AD individuals to olfactory damage from COVID-19. These findings not only

provide insights into the shared aspects of anosmia in COVID-19 and AD but also suggest the need for targeted olfactory health monitoring and treatment approaches in AD patients during the pandemic.

5.7 PM EXPOSURE EFFECTS ON VIRAL INFECTIONS IN THE CONTEXT OF AD OM

The investigation of PM exposure and its effects on viral infections, particularly with a focus on AD at the OM presents a comprehensive narrative on the effects of agents derived from the inhaled air on respiratory health and neurodegenerative disease. In this study an emphasis was placed on different PM fractions, notably $PM_{10\text{-}2.5}$ and $PM_{0.2}$ (including UFP), to enrich our understanding of their distinct deposition behaviors and cellular implications. $PM_{10\text{-}2.5}$ particles, known to predominantly deposit in the upper respiratory tract, can influence local immune responses within the OM. In contrast, UFPs, due to their minute size, have the potential for translocation to the brain, exploiting the olfactory route for systemic impacts, as demonstrated in studies like (Günter Oberdörster et al., 2004)

The findings that $PM_{0.2}$ and $PM_{10\text{-}2.5}$ do not alter ACE-2 expression or viral replication in OM cells offer a new perspective on the relationship between PM exposure and SARS-CoV-2 susceptibility. Contrary to previous *in vitro* studies primarily conducted on nasal epithelial, alveolar lung cell lines, which suggested that PM exposure might increase susceptibility to viral infections through upregulation of entry receptors (Sagawa et al., 2021; Marchetti et al., 2023; Miyashita et al., 2023). The study instead highlights significant alterations in cellular and immune responses in OM cells, especially in cells derived from individuals with AD. This suggests that PM might modulate the cellular response post-infection rather than directly impacting initial infection rates at the OM. This observation aligns with prior *in vitro* investigations involving alveolar epithelial cells and co-culture models, which have documented alterations in immune responses to SARS-CoV-2 and Avian Influenza viruses following exposure to PM (Marín-Palma et al., 2023; Mishra et al., 2020). Moreover, exposure to

woodsmoke particles before SARS-CoV-2 infection alters host immune gene expression in primary human nasal epithelial cells in a sex-dependent manner, dampening antiviral and INF responses, and potentially suppressing host defense mechanisms against viral infection.

Lastly, exposure to PM fractions such as $PM_{10-2.5}$ and $PM_{0.2}$ is associated with distinct increases in pro-inflammatory cytokines, crucial for combating infections, yet capable of inducing excessive inflammation or desensitizing epithelial cells to viral infections. This study further extends this understanding by demonstrating that PM exposure results in altered immune and cellular responses following SARS-CoV-2 infection, particularly evident in AD cells with elevated baseline cytokine levels. In OM of AD individuals, elevated baseline transcriptomic signatures were also observed in study II and other studies reported OM to show AD-associated pathological changes as mentioned earlier. Therefore, in study III the observed changes in cytokine release and oxidative stress markers suggest that exposure to PM fractions may modulate the body's response to the virus, potentially contributing to the heightened severity of COVID-19 observed in populations exposed to high levels of air pollution, especially among individuals with pre-existing conditions like AD.

5.8 LIMITATIONS OF THE STUDIES AND FUTURE PERSPECTIVES

It is essential to acknowledge the inherent limitations in our study design, including the need for further validation through *in vivo* studies and larger clinical cohorts. Integrating findings from the *in vitro* studies with epidemiological data and clinical observations could facilitate the translation of research findings into practice, informing preventive strategies and therapeutic interventions targeting susceptible individuals (Seyhan, 2019; Steger-Hartmann et al., 2020). Despite these challenges, our research lays a robust foundation for future investigations into the links between environmental factors, immune responses, and neurological health.

In Study I, the A549-THP1 co-culture model provides a valuable platform for studying the effects of $PM_{2.5-1}$ on innate immune responses,

representing the innate physical barrier at the alveolar lung level. However, this model inherently lacks the complexity of *in vivo* systems, potentially limiting its ability to fully capture the dynamic interplay between different cell types, immune responses, and environmental factors present in the human respiratory system. In addition, while TLR agonists used in the study offer insights into the sequence of events, infections with actual viruses could provide a more accurate representation of real-life exposure scenarios.

The utilization of primary human OM cells in Study II and Study III is important given human *in vitro* data with controlled experimental conditions is scarce to date. In Study II, we explored the effects of SARS-CoV-2 in OM cells and the potential link to AD. However, Study II encountered constraints due to the limited availability of OM biopsies and donor variability, potentially impacting the generalizability of findings. Additionally, the emphasis on the non-neural epithelial cell fraction of OM cells overlooked the potential direct infection of OSNs and the intricate crosstalk between neural and non-neural cells, highlighting the importance of exploring the broader cellular landscape within the olfactory system.

Study III focused on the impact of PM exposure on SARS-CoV-2 infection, and specifically on immune responses within OM cells. Study III primarily examined specific PM fractions present in urban air, neglecting the broader spectrum of pollutants and their varied impacts on immune responses. Additionally, it's worth noting that the source of PM can heavily influence its composition, thereby substantially impacting the effects triggered by these particles (Park et al., 2018; Rönkkö et al., 2020, 2021). More information is thus needed on the effects of specific components present in inhaled air.

In the future, integrating more diverse cell types, conducting comprehensive immune response analyses, and employing advanced experimental models could enhance our understanding of respiratory health and susceptibility to infections. Further research on the crosstalk between neural and non-neural cells upon PM exposure and infection is warranted, given the potential implications for transmission to the brain. Such investigations hold promise for elucidating the physiological

relevance and complexity of the nose–brain axis in response to exposure to pathogens and environmental agents, including SARS-CoV-2.

While our study marks a significant milestone, there are additional avenues for exploration. For example, longitudinal studies are warranted to assess the cumulative impact of chronic PM exposures over time, elucidating the persistence of immune alterations, susceptibility to infections, and development of respiratory diseases. In addition, the employment of 3D *in vitro* models for a deeper understanding of cellular integrity and the role of AMPs will be important in providing new avenues for future work. Furthermore, assessing the interplay of genetic and environmental factors is important. For example, the APOE ε4 allele plays a pivotal role in both AD and the severity, and mortality of COVID-19 (Kuo et al., 2020a; Kuo et al., 2020b; Kurki et al., 2021). Carriers of the ε4 allele face a substantially increased risk of developing AD, with homozygous carriers experiencing even greater susceptibility. Moreover, individuals with the ε4 allele are at a heightened risk of severe COVID-19 outcomes, including a more than fivefold increase in severity and a seventeen-fold increase in severe symptom development for homozygous carriers (Safdari Lord et al., 2022).

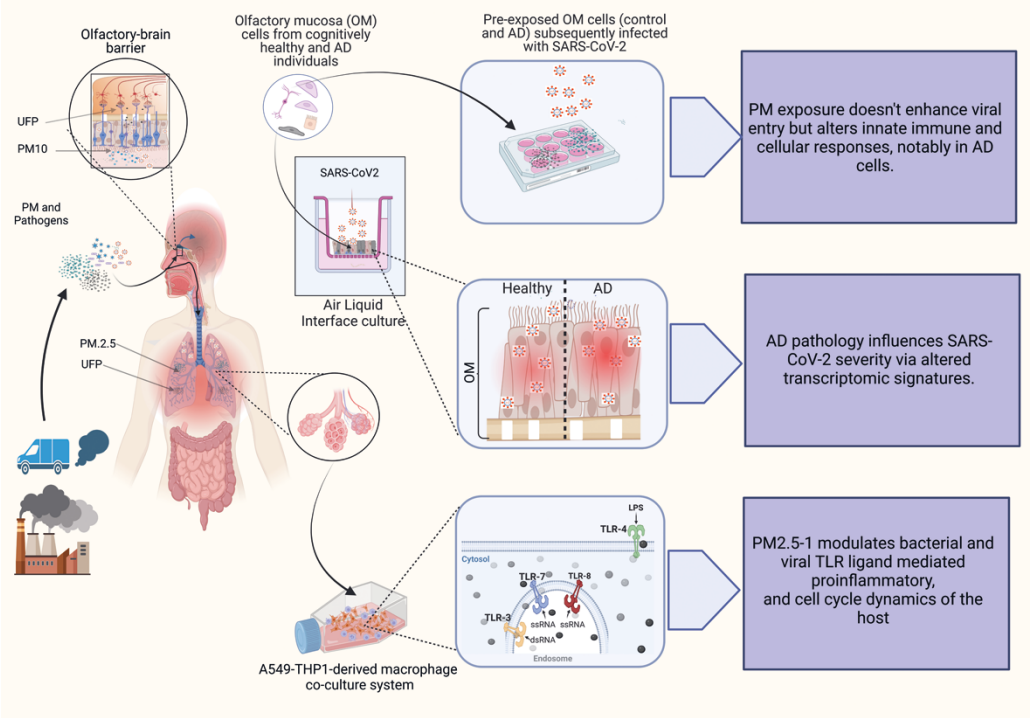

Figure 1. Illustration of the study I-III and key findings. Created with bio render.

6 CONCLUSIONS

This thesis provides a comprehensive cellular exploration of the complex interplay between ambient PM exposure, respiratory infections, and their link to AD. Integrating environmental science, immunology, and neurobiology, the research sheds light on the molecular and cellular mechanisms by which air pollution affects respiratory and neurological health.

In the first publication, $PM_{2.5\text{-}1}$ exposure is shown to alter immune responses, increasing pro-inflammatory cytokines and potentially heightening susceptibility to bacterial respiratory infections. This study also reveals a suppression of immune responses to viral infections, indicating a differential impact of $PM_{2.5\text{-}1}$ on bacterial versus viral threats.

The second publication delves into the intersection of AD and SARS-CoV-2, using an innovative 3D *in vitro* model of the human OM. It uncovers that while AD does not affect SARS-CoV-2 susceptibility, it does lead to distinct transcriptomic responses in infected cells, suggesting more severe COVID-19 outcomes in AD patients due to pre-existing neuroinflammation.

The third study examines the effects of PM exposure on SARS-CoV-2 infection in the context of AD. It finds that while PM exposure does not increase infection susceptibility, it significantly alters cellular immune responses, particularly in AD patients. This implies that environmental factors, coupled with underlying disease pathology, may contribute to the variability in COVID-19 severity and manifestations.

Overall, these findings emphasize the critical need for integrated approaches that consider environmental, immunological, and pathological factors. This research lays a foundation for future studies and public health strategies aimed at mitigating the impacts of environmental factors on disease susceptibility and progression, especially in vulnerable populations like those with AD.

REFERENCES

Adane, M. M., Alene, G. D., Mereta, S. T., & Wanyonyi, K. L. (2020). Prevalence and risk factors of acute lower respiratory infection among children living in biomass fuel using households: A community-based cross-sectional study in Northwest Ethiopia. *BMC Public Health*, *20*(1), 1–13. doi: 10.1186/S12889-020-08515-W/TABLES/4

Aderem, A. (2003). Phagocytosis and the Inflammatory Response. *The Journal of Infectious Diseases*, *187*(s2), S340–S345. doi: 10.1086/374747

Ain, N. U., & Qamar, S. U. R. (2021). Particulate Matter-Induced Cardiovascular Dysfunction: A Mechanistic Insight. *Cardiovascular Toxicology*, *21*(7), 505–516. doi: 10.1007/s12012-021-09652-3

ALEXIS, N., LAY, J., ZEMAN, K., BENNETT, W., PEDEN, D., SOUKUP, J., DEVLIN, R., & BECKER, S. (2006). Biological material on inhaled coarse fraction particulate matter activates airway phagocytes in vivo in healthy volunteers. *Journal of Allergy and Clinical Immunology*, *117*(6), 1396–1403. doi: 10.1016/j.jaci.2006.02.030

Alexopoulou, L., Holt, A. C., Medzhitov, R., & Flavell, R. A. (2001). Recognition of double-stranded RNA and activation of NF-κB by Toll-like receptor 3. *Nature*, *413*(6857), 732–738. doi: 10.1038/35099560

Amemiya, K., Dankmeyer, J. L., Bernhards, R. C., Fetterer, D. P., Waag, D. M., Worsham, P. L., & DeShazer, D. (2021). Activation of Toll-Like Receptors by Live Gram-Negative Bacterial Pathogens Reveals Mitigation of TLR4 Responses and Activation of TLR5 by Flagella. *Frontiers in Cellular and Infection Microbiology*, *11*. doi: 10.3389/fcimb.2021.745325

Amouei Torkmahalleh, M., Naseri, M., Nurzhan, S., Gabdrashova, R., Bekezhankyzy, Z., Gimnkhan, A., Malekipirbazari, M., Jouzizadeh, M., Tabesh, M., Farrokhi, H., Mehri-Dehnavi, H., Khanbabaie, R., Sadeghi, S., khatir, A. A., Sabanov, S., Buonanno, G., Hopke, P. K., Cassee, F., & Crape, B. (2022). Human exposure to aerosol from indoor gas stove

cooking and the resulting nervous system responses. *Indoor Air*, *32*(2), e12983. doi: 10.1111/INA.12983

Andre, M., Lau, L.-S., Pokharel, M. D., Ramelow, J., Owens, F., Souchak, J., Akkaoui, J., Ales, E., Brown, H., Shil, R., Nazaire, V., Manevski, M., Paul, N. P., Esteban-Lopez, M., Ceyhan, Y., & El-Hage, N. (2023). From Alpha to Omicron: How Different Variants of Concern of the SARS-Coronavirus-2 Impacted the World. *Biology*, *12*(9), 1267. doi: 10.3390/biology12091267

Aretz, B., Janssen, F., Vonk, J. M., Heneka, M. T., Boezen, H. M., & Doblhammer, G. (2021). Long-term exposure to fine particulate matter, lung function and cognitive performance: A prospective Dutch cohort study on the underlying routes. *Environmental Research*, *201*. doi: 10.1016/J.ENVRES.2021.111533

Avendaño Carvajal, L., & Perret Pérez, C. (2020). Epidemiology of Respiratory Infections. *Pediatric Respiratory Diseases*, 263. doi: 10.1007/978-3-030-26961-6_28

Barrila, J., Crabbé, A., Yang, J., Franco, K., Nydam, S. D., Forsyth, R. J., Davis, R. R., Gangaraju, S., Ott, C. M., Coyne, C. B., Bissell, M. J., & Nickerson, C. A. (2018). Modeling Host-Pathogen Interactions in the Context of the Microenvironment: Three-Dimensional Cell Culture Comes of Age. *Infection and Immunity*, *86*(11). doi: 10.1128/IAI.00282-18

Barron, S. L., Saez, J., & Owens, R. M. (2021). In Vitro Models for Studying Respiratory Host–Pathogen Interactions. *Advanced Biology*, *5*(6). doi: 10.1002/adbi.202000624

Bauer, R. N., Diaz-Sanchez, D., & Jaspers, I. (2012). Effects of air pollutants on innate immunity: The role of Toll-like receptors and nucleotide-binding oligomerization domain–like receptors. *Journal of Allergy and Clinical Immunology*, *129*(1), 14–24. doi: 10.1016/j.jaci.2011.11.004

Beghi, E., Giussani, G., Westenberg, E., Allegri, R., Garcia-Azorin, D., Guekht, A., Frontera, J., Kivipelto, M., Mangialasche, F., Mukaetova-Ladinska, E. B., Prasad, K., Chowdhary, N., & Winkler, A. S. (2022). Acute and post-acute neurological manifestations of COVID-19: present findings, critical appraisal, and future directions. *Journal of Neurology*, *269*(5), 2265–2274. doi: 10.1007/S00415-021-10848-4

Beutler, B. (2002). *TLR4 as the Mammalian Endotoxin Sensor* (pp. 109–120). doi: 10.1007/978-3-642-59430-4_7

Bianchetti, A., Rozzini, R., Bianchetti, L., Coccia, F., Guerini, F., & Trabucchi, M. (2022). Dementia Clinical Care in Relation to COVID-19. *Current Treatment Options in Neurology*, *24*(1), 1–15. doi: 10.1007/s11940-022-00706-7

Boogaard, H., Patton, A. P., Atkinson, R. W., Brook, J. R., Chang, H. H., Crouse, D. L., Fussell, J. C., Hoek, G., Hoffmann, B., Kappeler, R., Kutlar Joss, M., Ondras, M., Sagiv, S. K., Samoli, E., Shaikh, R., Smargiassi, A., Szpiro, A. A., Van Vliet, E. D. S., Vienneau, D., … Forastiere, F. (2022). Long-term exposure to traffic-related air pollution and selected health outcomes: A systematic review and meta-analysis. *Environment International*, *164*, 107262. doi: 10.1016/J.ENVINT.2022.107262

Borgmann-Winter, K., Willard, S. L., Sinclair, D., Mirza, N., Turetsky, B., Berretta, S., & Hahn, C. G. (2015). Translational potential of olfactory mucosa for the study of neuropsychiatric illness. *Translational Psychiatry*, *5*(3), e527. doi: 10.1038/TP.2014.141

Bortolotti, D., Gentili, V., Rizzo, S., Schiuma, G., Beltrami, S., Strazzabosco, G., Fernandez, M., Caccuri, F., Caruso, A., & Rizzo, R. (2021). TLR3 and TLR7 RNA Sensor Activation during SARS-CoV-2 Infection. *Microorganisms*, *9*(9), 1820. doi: 10.3390/microorganisms9091820

Botto, L., Lonati, E., Russo, S., Cazzaniga, E., Bulbarelli, A., & Palestini, P. (2023). Effects of PM2.5 Exposure on the ACE/ACE2 Pathway: Possible Implication in COVID-19 Pandemic. *International Journal of Environmental Research and Public Health 2023, Vol. 20, Page 4393*, *20*(5), 4393. doi: 10.3390/IJERPH20054393

Braga, J., Lepra, M., Kish, S. J., Rusjan, Pablo. M., Nasser, Z., Verhoeff, N., Vasdev, N., Bagby, M., Boileau, I., Husain, M. I., Kolla, N., Garcia, A., Chao, T., Mizrahi, R., Faiz, K., Vieira, E. L., & Meyer, J. H. (2023). Neuroinflammation After COVID-19 With Persistent Depressive and Cognitive Symptoms. *JAMA Psychiatry*, *80*(8), 787. doi: 10.1001/jamapsychiatry.2023.1321

Brann, D. H., Tsukahara, T., Weinreb, C., Lipovsek, M., Van Den Berge, K., Gong, B., Chance, R., Macaulay, I. C., Chou, H. J., Fletcher, R. B., Das, D.,

Street, K., De Bezieux, H. R., Choi, Y. G., Risso, D., Dudoit, S., Purdom, E., Mill, J., Hachem, R. A., … Datta, S. R. (2020). Non-neuronal expression of SARS-CoV-2 entry genes in the olfactory system suggests mechanisms underlying COVID-19-associated anosmia. *Science Advances*, *6*(31), 5801–5832. doi: 10.1126/SCIADV.ABC5801/SUPPL_FILE/PAPV4.PDF

Brocke, S. A., Billings, G. T., Taft-Benz, S., Alexis, N. E., Heise, M. T., & Jaspers, I. (2022). Woodsmoke particle exposure prior to SARS-CoV-2 infection alters antiviral response gene expression in human nasal epithelial cells in a sex-dependent manner. *American Journal of Physiology-Lung Cellular and Molecular Physiology*, *322*(3), L479–L494. doi: 10.1152/ajplung.00362.2021

Brockington, A., Heath, P. R., Holden, H., Kasher, P., Bender, F. L., Claes, F., Lambrechts, D., Sendtner, M., Carmeliet, P., & Shaw, P. J. (2010). Downregulation of genes with a function in axon outgrowth and synapse formation in motor neurones of the VEGFδ/δ mouse model of amyotrophic lateral sclerosis. *BMC Genomics*, *11*(1), 203. doi: 10.1186/1471-2164-11-203

Bryche, B., St Albin, A., Murri, S., Lacôte, S., Pulido, C., Ar Gouilh, M., Lesellier, S., Servat, A., Wasniewski, M., Picard-Meyer, E., Monchatre-Leroy, E., Volmer, R., Rampin, O., Le Goffic, R., Marianneau, P., & Meunier, N. (2020). Massive transient damage of the olfactory epithelium associated with infection of sustentacular cells by SARS-CoV-2 in golden Syrian hamsters. *Brain, Behavior, and Immunity*, *89*, 579–586. doi: 10.1016/J.BBI.2020.06.032

Butowt, R., Bilińska, K., & von Bartheld, C. (2022). Why Does the Omicron Variant Largely Spare Olfactory Function? Implications for the Pathogenesis of Anosmia in Coronavirus Disease 2019. *The Journal of Infectious Diseases*, *226*(8), 1304–1308. doi: 10.1093/infdis/jiac113

Butowt, R., & von Bartheld, C. S. (2021). Anosmia in COVID-19: Underlying Mechanisms and Assessment of an Olfactory Route to Brain Infection. *The Neuroscientist*, *27*(6), 582–603. doi: 10.1177/1073858420956905

Calderón-Garcidueas, L., Kavanaugh, M., Block, M., D'Angiulli, A., Delgado-Chávez, R., Torres-Jardón, R., González-Maciel, A., Reynoso-Robles, R.,

Osnaya, N., Villarreal-Calderon, R., Guo, R., Hua, Z., Zhu, H., Perry, G., & Diaz, P. (2012). Neuroinflammation, hyperphosphorylated tau, diffuse amyloid plaques, and down-regulation of the cellular prion protein in air pollution exposed children and young adults. *Journal of Alzheimer's Disease : JAD*, *28*(1), 93–107. doi: 10.3233/JAD-2011-110722

Calderón-Garcidueñas, L., & Ayala, A. (2022). Air Pollution, Ultrafine Particles, and Your Brain: Are Combustion Nanoparticle Emissions and Engineered Nanoparticles Causing Preventable Fatal Neurodegenerative Diseases and Common Neuropsychiatric Outcomes? *Environmental Science & Technology*, *56*(11), 6847–6856. doi: 10.1021/ACS.EST.1C04706

Calderón-Garcidueñas, L., Herrera-Soto, A., Jury, N., Maher, B. A., González-Maciel, A., Reynoso-Robles, R., Ruiz-Rudolph, P., Van Zundert, B., & Varela-Nallar, L. (2020). *Reduced repressive epigenetic marks, increased DNA damage and Alzheimer's disease hallmarks in the brain of humans and mice exposed to particulate urban air pollution*. doi: 10.1016/j.envres.2020.109226

Calderón-Garcidueñas, L., Solt, A. C., Henríquez-Roldán, C., Torres-Jardón, R., Nuse, B., Herritt, L., Villarreal-Calderón, R., Osnaya, N., Stone, I., García, R., Brooks, D. M., González-Maciel, A., Reynoso-Robles, R., Delgado-Chávez, R., & Reed, W. (2008). Long-term air pollution exposure is associated with neuroinflammation, an altered innate immune response, disruption of the blood-brain barrier, ultrafine particulate deposition, and accumulation of amyloid beta-42 and alpha-synuclein in children and young adults. *Toxicologic Pathology*, *36*(2), 289–310. doi: 10.1177/0192623307313011

Cantuti-Castelvetri, L., Ojha, R., Pedro, L. D., Djannatian, M., Franz, J., Kuivanen, S., van der Meer, F., Kallio, K., Kaya, T., Anastasina, M., Smura, T., Levanov, L., Szirovicza, L., Tobi, A., Kallio-Kokko, H., Österlund, P., Joensuu, M., Meunier, F. A., Butcher, S. J., … Simons, M. (2020). Neuropilin-1 facilitates SARS-CoV-2 cell entry and infectivity. *Science*, *370*(6518), 856–860. doi: 10.1126/science.abd2985

Cappelletty, D. (1998). Microbiology of bacterial respiratory infections. *The Pediatric Infectious Disease Journal*, *17*(Supplement), S55–S61. doi: 10.1097/00006454-199808001-00002

Carabelli, A. M., Peacock, T. P., Thorne, L. G., Harvey, W. T., Hughes, J., de Silva, T. I., Peacock, S. J., Barclay, W. S., de Silva, T. I., Towers, G. J., & Robertson, D. L. (2023). SARS-CoV-2 variant biology: immune escape, transmission and fitness. *Nature Reviews Microbiology 2023 21:3*, *21*(3), 162–177. doi: 10.1038/s41579-022-00841-7

Chakrabarti, S., Khemka, V. K., Banerjee, A., Chatterjee, G., Ganguly, A., & Biswas, A. (2015). Metabolic Risk Factors of Sporadic Alzheimer's Disease: Implications in the Pathology, Pathogenesis and Treatment. *Aging and Disease*, *6*(4), 282. doi: 10.14336/AD.2014.002

Chan, K. H., Peiris, J. S. M., Lam, S. Y., Poon, L. L. M., Yuen, K. Y., & Seto, W. H. (2011). The effects of temperature and relative humidity on the viability of the SARS coronavirus. *Advances in Virology*, *2011*. doi: 10.1155/2011/734690

Charnley, M., Islam, S., Bindra, G. K., Engwirda, J., Ratcliffe, J., Zhou, J., Mezzenga, R., Hulett, M. D., Han, K., Berryman, J. T., & Reynolds, N. P. (2022). Neurotoxic amyloidogenic peptides in the proteome of SARS-COV2: potential implications for neurological symptoms in COVID-19. *Nature Communications 2022 13:1*, *13*(1), 1–11. doi: 10.1038/s41467-022-30932-1

Chen, R., Hu, B., Liu, Y., Xu, J., Yang, G., Xu, D., & Chen, C. (2016). Beyond PM2.5: The role of ultrafine particles on adverse health effects of air pollution. *Biochimica et Biophysica Acta (BBA) - General Subjects*, *1860*(12), 2844–2855. doi: 10.1016/J.BBAGEN.2016.03.019

Chen, Y.-W., Huang, M.-Z., Chen, C.-L., Kuo, C.-Y., Yang, C.-Y., Chiang-Ni, C., Chen, Y.-Y. M., Hsieh, C.-M., Wu, H.-Y., Kuo, M.-L., Chiu, C.-H., & Lai, C.-H. (2020). PM2.5 impairs macrophage functions to exacerbate pneumococcus-induced pulmonary pathogenesis. *Particle and Fibre Toxicology*, *17*(1), 37. doi: 10.1186/s12989-020-00362-2

Chew, S., Lampinen, R., Saveleva, L., Korhonen, P., Mikhailov, N., Grubman, A., Polo, J. M., Wilson, T., Komppula, M., Rönkkö, T., Gu, C., Mackay-Sim, A., Malm, T., White, A. R., Jalava, P., & Kanninen, K. M. (2020). Urban air

particulate matter induces mitochondrial dysfunction in human olfactory mucosal cells. *Particle and Fibre Toxicology*, *17*(1), 18. doi: 10.1186/s12989-020-00352-4

Cho, C.-C., Hsieh, W.-Y., Tsai, C.-H., Chen, C.-Y., Chang, H.-F., & Lin, C.-S. (2018). In Vitro and In Vivo Experimental Studies of PM2.5 on Disease Progression. *International Journal of Environmental Research and Public Health*, *15*(7), 1380. doi: 10.3390/ijerph15071380

Cho, J., Jang, H., Noh, Y., Lee, S. K., Koh, S. B., Kim, S. Y., & Kim, C. (2023). Associations of Particulate Matter Exposures With Brain Gray Matter Thickness and White Matter Hyperintensities: Effect Modification by Low-Grade Chronic Inflammation. *Journal of Korean Medical Science*, *38*(16). doi: 10.3346/JKMS.2023.38.E159

Choi, R., & Goldstein, B. J. (2018). Olfactory epithelium: Cells, clinical disorders, and insights from an adult stem cell niche. In Laryngoscope Investigative Otolaryngology (Vol. 3, Issue 1, pp. 35–42). John Wiley and Sons Inc. doi: 10.1002/lio2.135

Chung, S. J., Chang, Y., Jeon, J., Shin, J. Il, Song, T. J., & Kim, J. (2022). Association of Alzheimer's Disease with COVID-19 Susceptibility and Severe Complications: A Nationwide Cohort Study. *Journal of Alzheimer's Disease : JAD*, *87*(2), 701–710. doi: 10.3233/JAD-220031

Cipriani, G., Danti, S., Carlesi, C., & Borin, G. (2018). Danger in the Air: Air Pollution and Cognitive Dysfunction. *Https://Doi.Org/10.1177/1533317518777859*, *33*(6), 333–341. doi: 10.1177/1533317518777859

Costa, K. V. T. da, Carnaúba, A. T. L., Rocha, K. W., Andrade, K. C. L. de, Ferreira, S. M. S., & Menezes, P. de L. (2020). Olfactory and taste disorders in COVID-19: a systematic review. In Brazilian Journal of Otorhinolaryngology (Vol. 86, Issue 6, pp. 781–792). Elsevier Editora Ltda. doi: 10.1016/j.bjorl.2020.05.008

COVID-19 deaths | WHO COVID-19 dashboard. (2024). Retrieved from https://data.who.int/dashboards/covid19/deaths?n=c

Crivelli, L., Palmer, K., Calandri, I., Guekht, A., Beghi, E., Carroll, W., Frontera, J., García-Azorín, D., Westenberg, E., Winkler, A. S., Mangialasche, F., Allegri, R. F., & Kivipelto, M. (2022). Changes in cognitive functioning

after COVID-19: A systematic review and meta-analysis. *Alzheimer's & Dementia*, *18*(5), 1047. doi: 10.1002/ALZ.12644

Dasaraju, P. V., & Liu, C. (1996). Infections of the Respiratory System. *Concise Handbook of Infectious Diseases*, 65–65. doi: 10.5005/jp/books/14120_12

de Melo, G. D., Perraud, V., Alvarez, F., Vieites-Prado, A., Kim, S., Kergoat, L., Coleon, A., Trüeb, B. S., Tichit, M., Piazza, A., Thierry, A., Hardy, D., Wolff, N., Munier, S., Koszul, R., Simon-Lorière, E., Thiel, V., Lecuit, M., Lledo, P.-M., … Bourhy, H. (2023). Neuroinvasion and anosmia are independent phenomena upon infection with SARS-CoV-2 and its variants. *Nature Communications*, *14*(1), 4485. doi: 10.1038/s41467-023-40228-7

De Rudder, C., Calatayud Arroyo, M., Lebeer, S., & Van de Wiele, T. (2018). Modelling upper respiratory tract diseases: getting grips on host-microbe interactions in chronic rhinosinusitis using in vitro technologies. *Microbiome*, *6*(1), 75. doi: 10.1186/s40168-018-0462-z

Delavar, M. A., Jahani, M. ali, Sepidarkish, M., Alidoost, S., Mehdinezhad, H., & Farhadi, Z. (2023). Relationship between fine particulate matter (PM2.5) concentration and risk of hospitalization due to chronic obstructive pulmonary disease: a systematic review and meta-analysis. *BMC Public Health*, *23*(1), 1–9. doi: 10.1186/S12889-023-17093-6/FIGURES/2

Diamond, M. S., & Kanneganti, T. D. (2022). Innate immunity: the first line of defense against SARS-CoV-2. *Nature Immunology 2022 23:2*, *23*(2), 165–176. doi: 10.1038/s41590-021-01091-0

Diebold, S. S., Kaisho, T., Hemmi, H., Akira, S., & Reis e Sousa, C. (2004). Innate Antiviral Responses by Means of TLR7-Mediated Recognition of Single-Stranded RNA. *Science*, *303*(5663), 1529–1531. doi: 10.1126/science.1093616

Douaud, G., Lee, S., Alfaro-Almagro, F., Arthofer, C., Wang, C., McCarthy, P., Lange, F., Andersson, J. L. R., Griffanti, L., Duff, E., Jbabdi, S., Taschler, B., Keating, P., Winkler, A. M., Collins, R., Matthews, P. M., Allen, N., Miller, K. L., Nichols, T. E., & Smith, S. M. (2022). SARS-CoV-2 is

associated with changes in brain structure in UK Biobank. *Nature 2022 604:7907*, *604*(7907), 697–707. doi: 10.1038/s41586-022-04569-5

Duchesne, J., Gutierrez, L. A., Carrière, I., Mura, T., Chen, J., Vienneau, D., de Hoogh, K., Helmer, C., Jacquemin, B., Berr, C., & Mortamais, M. (2022). Exposure to ambient air pollution and cognitive decline: Results of the prospective Three-City cohort study. *Environment International*, *161*. doi: 10.1016/J.ENVINT.2022.107118

Dyavar, S. R., Singh, R., Emani, R., Pawar, G. P., Chaudhari, V. D., Podany, A. T., Avedissian, S. N., Fletcher, C. V., & Salunke, D. B. (2021). Role of toll-like receptor 7/8 pathways in regulation of interferon response and inflammatory mediators during SARS-CoV2 infection and potential therapeutic options. *Biomedicine & Pharmacotherapy*, *141*, 111794. doi: 10.1016/j.biopha.2021.111794

Ekström, I. A., Rizzuto, D., Grande, G., Bellander, T., & Laukka, E. J. (2022). Environmental Air Pollution and Olfactory Decline in Aging. *Environmental Health Perspectives*, *130*(2). doi: 10.1289/EHP9563/SUPPL_FILE/EHP9563.S001.ACCO.PDF

Elder, A., Gelein, R., Silva, V., Feikert, T., Opanashuk, L., Carter, J., Potter, R., Maynard, A., Ito, Y., Finkelstein, J., & Oberdörster, G. (2006). Translocation of Inhaled Ultrafine Manganese Oxide Particles to the Central Nervous System. *Environmental Health Perspectives*, *114*(8), 1172. doi: 10.1289/EHP.9030

Fan, Y., Sanyal, S., & Bruzzone, R. (2018). Breaking Bad: How Viruses Subvert the Cell Cycle. *Frontiers in Cellular and Infection Microbiology*, *8*. doi: 10.3389/fcimb.2018.00396

Fattorini, D., & Regoli, F. (2020). Role of the chronic air pollution levels in the Covid-19 outbreak risk in Italy. *Environmental Pollution*, *264*, 114732. doi: 10.1016/j.envpol.2020.114732

Feng, S., Gao, D., Liao, F., Zhou, F., & Wang, X. (2016). The health effects of ambient PM2.5 and potential mechanisms. *Ecotoxicology and Environmental Safety*, *128*, 67–74. doi: 10.1016/J.ECOENV.2016.01.030

Finlayson-Pitts, B. J., & Pitts, J. N. (1997). Tropospheric air pollution: ozone, airborne toxics, polycyclic aromatic hydrocarbons, and particles.

Science (New York, N.Y.), *276*(5315), 1045–1052. doi: 10.1126/SCIENCE.276.5315.1045

Fletcher, R. B., Das, D., Gadye, L., Street, K. N., Baudhuin, A., Wagner, A., Cole, M. B., Flores, Q., Choi, Y. G., Yosef, N., Purdom, E., Dudoit, S., Risso, D., & Ngai, J. (2017). Deconstructing Olfactory Stem Cell Trajectories at Single-Cell Resolution. *Cell Stem Cell*, *20*(6), 817-830.e8. doi: 10.1016/j.stem.2017.04.003

Forouzanfar, M. H., Alexander, L., Bachman, V. F., Biryukov, S., Brauer, M., Casey, D., Coates, M. M., Delwiche, K., Estep, K., Frostad, J. J., Astha, K. C., Kyu, H. H., Moradi-Lakeh, M., Ng, M., Slepak, E., Thomas, B. A., Wagner, J., Achoki, T., Atkinson, C., … Zhu, S. (2015). Global, regional, and national comparative risk assessment of 79 behavioural, environmental and occupational, and metabolic risks or clusters of risks in 188 countries, 1990-2013: A systematic analysis for the Global Burden of Disease Study 2013. *The Lancet*, *386*(10010), 2287–2323. doi: 10.1016/S0140-6736(15)00128-2

Fuller, R., Landrigan, P. J., Balakrishnan, K., Bathan, G., Bose-O'Reilly, S., Brauer, M., Caravanos, J., Chiles, T., Cohen, A., Corra, L., Cropper, M., Ferraro, G., Hanna, J., Hanrahan, D., Hu, H., Hunter, D., Janata, G., Kupka, R., Lanphear, B., … Yan, C. (2022). Pollution and health: a progress update. *The Lancet Planetary Health*, *6*(6), e535–e547. doi: 10.1016/S2542-5196(22)00090-0

Gangwar, R. S., Bevan, G. H., Palanivel, R., Das, L., & Rajagopalan, S. (2020). Oxidative stress pathways of air pollution mediated toxicity: Recent insights. *Redox Biology*, *34*, 101545. doi: 10.1016/J.REDOX.2020.101545

Garcia, G. J. M., Schroeter, J. D., & Kimbell, J. S. (2015). Olfactory deposition of inhaled nanoparticles in humans. *Inhalation Toxicology*, *27*(8), 394–403. doi: 10.3109/08958378.2015.1066904

Gawda, A., Majka, G., Nowak, B., Śróttek, M., Walczewska, M., & Marcinkiewicz, J. (2018). Air particulate matter SRM 1648a primes macrophages to hyperinflammatory response after LPS stimulation. *Inflammation Research*, *67*(9), 765–776. doi: 10.1007/s00011-018-1165-4

Gilles, S., Blume, C., Wimmer, M., Damialis, A., Meulenbroek, L., Gökkaya, M., Bergougnan, C., Eisenbart, S., Sundell, N., Lindh, M., Andersson, L. M., Dahl, Å., Chaker, A., Kolek, F., Wagner, S., Neumann, A. U., Akdis, C. A., Garssen, J., Westin, J., … Traidl-Hoffmann, C. (2020). Pollen exposure weakens innate defense against respiratory viruses. *Allergy*, *75*(3), 576–587. doi: 10.1111/ALL.14047

González-Maciel, A., Reynoso-Robles, R., Torres-Jardón, R., Mukherjee, P. S., & Calderón-Garcidueñas, L. (2017). Combustion-Derived Nanoparticles in Key Brain Target Cells and Organelles in Young Urbanites: Culprit Hidden in Plain Sight in Alzheimer's Disease Development. *Journal of Alzheimer's Disease : JAD*, *59*(1), 189–208. doi: 10.3233/JAD-170012

Growdon, M. E., Schultz, A. P., Dagley, A. S., Amariglio, R. E., Hedden, T., Rentz, D. M., Johnson, K. A., Sperling, R. A., Albers, M. W., & Marshall, G. A. (2015). Odor identification and Alzheimer disease biomarkers in clinically normal elderly. *Neurology*, *84*(21), 2153. doi: 10.1212/WNL.0000000000001614

Hajighasemi, S., Spann, K., & Davies, J. M. (2023). Does pollen exposure influence innate immunity to SARS-CoV-2 in allergy or asthma? *The Journal of Allergy and Clinical Immunology*, *152*(2), 374–377. doi: 10.1016/J.JACI.2023.05.008

Hamming, I., Timens, W., Bulthuis, M. L. C., Lely, A. T., Navis, G. J., & van Goor, H. (2004). Tissue distribution of ACE2 protein, the functional receptor for SARS coronavirus. A first step in understanding SARS pathogenesis. *The Journal of Pathology*, *203*(2), 631. doi: 10.1002/PATH.1570

He, D., Yuan, M., Dang, W., Bai, L., Yang, R., Wang, J., Ma, Y., Liu, B., Liu, S., Zhang, S., Liao, X., & Zhang, W. (2023). Long term neuropsychiatric consequences in COVID-19 survivors: Cognitive impairment and inflammatory underpinnings fifteen months after discharge. *Asian Journal of Psychiatry*, *80*, 103409. doi: 10.1016/j.ajp.2022.103409

Heil, F., Hemmi, H., Hochrein, H., Ampenberger, F., Kirschning, C., Akira, S., Lipford, G., Wagner, H., & Bauer, S. (2004). Species-Specific Recognition of Single-Stranded RNA via Toll-like Receptor 7 and 8. *Science*, *303*(5663), 1526–1529. doi: 10.1126/science.1093620

Hennessy, E. J., Parker, A. E., & O'Neill, L. A. J. (2010). Targeting Toll-like receptors: emerging therapeutics? *Nature Reviews Drug Discovery*, *9*(4), 293–307. doi: 10.1038/nrd3203

Heusinkveld, H. J., Wahle, T., Campbell, A., Westerink, R. H. S., Tran, L., Johnston, H., Stone, V., Cassee, F. R., & Schins, R. P. F. (2016). Neurodegenerative and neurological disorders by small inhaled particles. *Neurotoxicology*, *56*, 94–106. doi: 10.1016/J.NEURO.2016.07.007

Hoffmann, C., Maglakelidze, M., von Schneidemesser, E., Witt, C., Hoffmann, P., & Butler, T. (2022). Asthma and COPD exacerbation in relation to outdoor air pollution in the metropolitan area of Berlin, Germany. *Respiratory Research*, *23*(1), 1–9. doi: 10.1186/S12931-022-01983-1/FIGURES/3

Hoffmann, M., Kleine-Weber, H., Schroeder, S., Krüger, N., Herrler, T., Erichsen, S., Schiergens, T. S., Herrler, G., Wu, N.-H., Nitsche, A., Müller, M. A., Drosten, C., & Pöhlmann, S. (2020). SARS-CoV-2 Cell Entry Depends on ACE2 and TMPRSS2 and Is Blocked by a Clinically Proven Protease Inhibitor. *Cell*, *181*(2), 271-280.e8. doi: 10.1016/j.cell.2020.02.052

Hong, Z., Guo, Z., Zhang, R., Xu, J., Dong, W., Zhuang, G., & Deng, C. (2016). Airborne fine particulate matter induces oxidative stress and inflammation in human nasal epithelial cells. *Tohoku Journal of Experimental Medicine*, *239*(2), 117–125. doi: 10.1620/tjem.239.117

Horne, B. D., Joy, E. A., Hofmann, M. G., Gesteland, P. H., Cannon, J. B., Lefler, J. S., Blagev, D. P., Kent Korgenski, E., Torosyan, N., Hansen, G. I., Kartchner, D., & Arden Pope, C. (2018). Short-term elevation of fine particulate matter air pollution and acute lower respiratory infection. *American Journal of Respiratory and Critical Care Medicine*, *198*(6), 759–766. doi: 10.1164/RCCM.201709-1883OC/SUPPL_FILE/DISCLOSURES.PDF

Hu, Y., Yang, H., Hou, C., Chen, W., Zhang, H., Ying, Z., Hu, Y., Sun, Y., Qu, Y., Feychting, M., Valdimarsdottir, U., Song, H., & Fang, F. (2022). COVID-19 related outcomes among individuals with neurodegenerative diseases:

a cohort analysis in the UK biobank. *BMC Neurology*, *22*(1), 1–12. doi: 10.1186/S12883-021-02536-7/TABLES/4

Hullmann, M., Albrecht, C., van Berlo, D., Gerlofs-Nijland, M. E., Wahle, T., Boots, A. W., Krutmann, J., Cassee, F. R., Bayer, T. A., & Schins, R. P. F. (2017). Diesel engine exhaust accelerates plaque formation in a mouse model of Alzheimer's disease. *Particle and Fibre Toxicology*, *14*(1), 1–14. doi: 10.1186/S12989-017-0213-5/FIGURES/7

Hussey, Shane. J. K., Purves, J., Allcock, N., Fernandes, V. E., Monks, P. S., Ketley, J. M., Andrew, P. W., & Morrissey, J. A. (2017). Air pollution alters *Staphylococcus aureus* and *Streptococcus pneumoniae* biofilms, antibiotic tolerance and colonisation. *Environmental Microbiology*, *19*(5), 1868–1880. doi: 10.1111/1462-2920.13686

Iaccarino, L., La Joie, R., Lesman-Segev, O. H., Lee, E., Hanna, L., Allen, I. E., Hillner, B. E., Siegel, B. A., Whitmer, R. A., Carrillo, M. C., Gatsonis, C., & Rabinovici, G. D. (2021). Association Between Ambient Air Pollution and Amyloid Positron Emission Tomography Positivity in Older Adults With Cognitive Impairment. *JAMA Neurology*, *78*(2), 197–207. doi: 10.1001/JAMANEUROL.2020.3962

Jalava, P. I., Wang, Q., Kuuspalo, K., Ruusunen, J., Hao, L., Fang, D., Väisänen, O., Ruuskanen, A., Sippula, O., Happo, M. S., Uski, O., Kasurinen, S., Torvela, T., Koponen, H., Lehtinen, K. E. J., Komppula, M., Gu, C., Jokiniemi, J., & Hirvonen, M.-R. (2015). Day and night variation in chemical composition and toxicological responses of size segregated urban air PM samples in a high air pollution situation. *Atmospheric Environment*, *120*, 427–437. doi: 10.1016/j.atmosenv.2015.08.089

Jang, S., Kim, E. W., Zhang, Y., Lee, J., Cho, S. Y., Ha, J., Kim, H., & Kim, E. (2018). Particulate matter increases beta-amyloid and activated glial cells in hippocampal tissues of transgenic Alzheimer's mouse: Involvement of PARP-1. *Biochemical and Biophysical Research Communications*, *500*(2), 333–338. doi: 10.1016/J.BBRC.2018.04.068

Jayaweera, M., Perera, H., Gunawardana, B., & Manatunge, J. (2020). Transmission of COVID-19 virus by droplets and aerosols: A critical review on the unresolved dichotomy. *Environmental Research*, *188*, 109819. doi: 10.1016/J.ENVRES.2020.109819

Jiang, C., Chen, Q., & Xie, M. (2020). Smoking increases the risk of infectious diseases: A narrative review. *Tobacco Induced Diseases*, *18*. doi: 10.18332/TID/123845

Jiang, Y., Wu, X.-J., & Guan, Y.-J. (2020). Effect of ambient air pollutants and meteorological variables on COVID-19 incidence. *Infection Control & Hospital Epidemiology*, *41*(9), 1011–1015. doi: 10.1017/ice.2020.222

Johnstone, K. F., & Herzberg, M. C. (2022). Antimicrobial peptides: Defending the mucosal epithelial barrier. *Frontiers in Oral Health*, *3*. doi: 10.3389/froh.2022.958480

Jung, H. J., Shin, I. S., & Lee, J. E. (2019). Olfactory function in mild cognitive impairment and Alzheimer's disease: A meta-analysis. *The Laryngoscope*, *129*(2), 362–369. doi: 10.1002/LARY.27399

Kanninen, K. M., Lampinen, R., Rantanen, L. M., Odendaal, L., Jalava, P., Chew, S., & White, A. R. (2020). Olfactory cell cultures to investigate health effects of air pollution exposure: Implications for neurodegeneration. *Neurochemistry International*, *136*, 104729. doi: 10.1016/J.NEUINT.2020.104729

Kao, Y. Y., Cheng, T. J., Yang, D. M., Wang, C. T., Chiung, Y. M., & Liu, P. S. (2012). Demonstration of an olfactory bulb-brain translocation pathway for ZnO nanoparticles in rodent cells in vitro and in vivo. *Journal of Molecular Neuroscience : MN*, *48*(2), 464–471. doi: 10.1007/S12031-012-9756-Y

Kasurinen, S., Happo, M. S., Rönkkö, T. J., Orasche, J., Jokiniemi, J., Kortelainen, M., Tissari, J., Zimmermann, R., Hirvonen, M. R., & Jalava, P. I. (2018). Differences between co-cultures and monocultures in testing the toxicity of particulate matter derived from log wood and pellet combustion. *PLOS ONE*, *13*(2), e0192453. doi: 10.1371/JOURNAL.PONE.0192453

Kawai, T., & Akira, S. (2006). Innate immune recognition of viral infection. *Nature Immunology*, *7*(2), 131–137. doi: 10.1038/ni1303

Kelly, F. J., & Fussell, J. C. (2012). Size, source and chemical composition as determinants of toxicity attributable to ambient particulate matter. *Atmospheric Environment*, *60*, 504–526. doi: 10.1016/J.ATMOSENV.2012.06.039

Kesson, A. M. (2007). Respiratory virus infections. *Paediatric Respiratory Reviews*, *8*(3), 240–248. doi: 10.1016/j.prrv.2007.07.003

Khan, M., Yoo, S. J., Clijsters, M., Backaert, W., Vanstapel, A., Speleman, K., Lietaer, C., Choi, S., Hether, T. D., Marcelis, L., Nam, A., Pan, L., Reeves, J. W., Van Bulck, P., Zhou, H., Bourgeois, M., Debaveye, Y., De Munter, P., Gunst, J., … Van Gerven, L. (2021). Visualizing in deceased COVID-19 patients how SARS-CoV-2 attacks the respiratory and olfactory mucosae but spares the olfactory bulb. *Cell*, *184*(24), 5932-5949.e15. doi: 10.1016/J.CELL.2021.10.027

Kim, J. Y., Ko, J. H., Kim, Y., Kim, Y. J., Kim, J. M., Chung, Y. S., Kim, H. M., Han, M. G., Kim, S. Y., & Chin, B. S. (2020). Viral Load Kinetics of SARS-CoV-2 Infection in First Two Patients in Korea. *Journal of Korean Medical Science*, *35*(7). doi: 10.3346/JKMS.2020.35.E86

Kim, K. H., Kabir, E., & Kabir, S. (2015). A review on the human health impact of airborne particulate matter. *Environment International*, *74*, 136–143. doi: 10.1016/J.ENVINT.2014.10.005

Kim, N., Han, H., Suh, M.-W., Lee, J. H., Oh, S.-H., Park, K., & Korea, S. (2019). *Effect of lipopolysaccharide on diesel exhaust particle-induced junctional dysfunction in primary human nasal epithelial cells* *. doi: 10.1016/j.envpol.2019.02.082

Klein, R., Soung, A., Sissoko, C., Nordvig, A., Canoll, P., Mariani, M., Jiang, X., Bricker, T., Goldman, J., Rosoklija, G., Arango, V., Underwood, M., Mann, J. J., Boon, A., Dowrk, A., & Boldrini, M. (2021). COVID-19 induces neuroinflammation and loss of hippocampal neurogenesis. *Research Square*. doi: 10.21203/RS.3.RS-1031824/V1

Knaapen, A. M., Borm, P. J. A., Albrecht, C., & Schins, R. P. F. (2004). Inhaled particles and lung cancer. Part A: Mechanisms. *International Journal of Cancer*, *109*(6), 799–809. doi: 10.1002/IJC.11708

Kumar, A., Zhang, J., & Yu, F. X. (2006). Toll-like receptor 3 agonist poly(I:C)-induced antiviral response in human corneal epithelial cells. *Immunology*, *117*(1), 11–21. doi: 10.1111/j.1365-2567.2005.02258.x

Kumar, S., Singh, R., Kumari, N., Karmakar, S., Behera, M., Siddiqui, A. J., Rajput, V. D., Minkina, T., Bauddh, K., & Kumar, N. (2021). Current understanding of the influence of environmental factors on SARS-CoV-

2 transmission, persistence, and infectivity. *Environmental Science and Pollution Research International*, *28*(6), 6267. doi: 10.1007/S11356-020-12165-1

Kuo, C. L., Pilling, L. C., Atkins, J. L., Masoli, J. A. H., Delgado, J., Kuchel, G. A., & Melzer, D. (2020). APOE e4 Genotype Predicts Severe COVID-19 in the UK Biobank Community Cohort. *The Journals of Gerontology: Series A*, *75*(11), 2231–2232. doi: 10.1093/GERONA/GLAA131

Kuo, C. L., Pilling, L. C., Atkins, J. L., Masoli, J. A. H., Delgado, J., Kuchel, G. A., Melzer, D., & Newman, A. B. (2020). ApoE e4e4 Genotype and Mortality With COVID-19 in UK Biobank. *The Journals of Gerontology: Series A*, *75*(9), 1801–1803. doi: 10.1093/GERONA/GLAA169

Kurki, S. N., Kantonen, J., Kaivola, K., Hokkanen, L., Mäyränpää, M. I., Puttonen, H., Martola, J., Pöyhönen, M., Kero, M., Tuimala, J., Carpén, O., Kantele, A., Vapalahti, O., Tiainen, M., Tienari, P. J., Kaila, K., Hästbacka, J., & Myllykangas, L. (2021). APOE ε4 associates with increased risk of severe COVID-19, cerebral microhaemorrhages and post-COVID mental fatigue: a Finnish biobank, autopsy and clinical study. *Acta Neuropathologica Communications*, *9*(1), 199. doi: 10.1186/s40478-021-01302-7

Lafaille-Magnan, M. E., Poirier, J., Etienne, P., Tremblay-Mercier, J., Frenette, J., Rosa-Neto, P., & Breitner, J. C. S. (2017). Odor identification as a biomarker of preclinical AD in older adults at risk. *Neurology*, *89*(4), 327–335. doi: 10.1212/WNL.0000000000004159

Lampinen, R., Fazaludeen, M. F., Avesani, S., Örd, T., Penttilä, E., Lehtola, J. M., Saari, T., Hannonen, S., Saveleva, L., Kaartinen, E., Acosta, F. F., Cruz-Haces, M., Löppönen, H., Mackay-Sim, A., Kaikkonen, M. U., Koivisto, A. M., Malm, T., White, A. R., Giugno, R., … Kanninen, K. M. (2022). Single-Cell RNA-Seq Analysis of Olfactory Mucosal Cells of Alzheimer's Disease Patients. *Cells*, *11*(4), 676. doi: 10.3390/CELLS11040676/S1

Lampinen, R., Górová, V., Avesani, S., Liddell, J. R., Penttilä, E., Závodná, T., Krejčík, Z., Lehtola, J. M., Saari, T., Kalapudas, J., Hannonen, S., Löppönen, H., Topinka, J., Koivisto, A. M., White, A. R., Giugno, R., & Kanninen, K. M. (2022). Biometal Dyshomeostasis in Olfactory Mucosa

of Alzheimer's Disease Patients. *International Journal of Molecular Sciences*, *23*(8), 4123. doi: 10.3390/IJMS23084123/S1

Lee, G. I., Saravia, J., You, D., Shrestha, B., Jaligama, S., Hebert, V. Y., Dugas, T. R., & Cormier, S. A. (2014). Exposure to combustion generated environmentally persistent free radicals enhances severity of influenza virus infection. *Particle and Fibre Toxicology*, *11*(1), 57. doi: 10.1186/s12989-014-0057-1

Lelieveld, J., Haines, A., Burnett, R., Tonne, C., Klingmüller, K., Münzel, T., & Pozzer, A. (2023). Air pollution deaths attributable to fossil fuels: observational and modelling study. *BMJ*, e077784. doi: 10.1136/bmj-2023-077784

Li, H., Xu, X.-L., Dai, D.-W., Huang, Z.-Y., Ma, Z., & Guan, Y.-J. (2020). Air pollution and temperature are associated with increased COVID-19 incidence: A time series study. *International Journal of Infectious Diseases*, *97*, 278–282. doi: 10.1016/j.ijid.2020.05.076

Li, N., Sioutas, C., Cho, A., Schmitz, D., Misra, C., Sempf, J., Wang, M., Oberley, T., Froines, J., & Nel, A. (2003). Ultrafine particulate pollutants induce oxidative stress and mitochondrial damage. *Environmental Health Perspectives*, *111*(4), 455–460. doi: 10.1289/EHP.6000

Li, Tao, Hu, R., Chen, Z., Li, Q., Huang, S., Zhu, Z., & Zhou, L. F. (2018). Fine particulate matter (PM2.5): The culprit for chronic lung diseases in China. *Chronic Diseases and Translational Medicine*, *4*(3), 176. doi: 10.1016/J.CDTM.2018.07.002

Li, Tianyu, Yu, Y., Sun, Z., & Duan, J. (2022). A comprehensive understanding of ambient particulate matter and its components on the adverse health effects based from epidemiological and laboratory evidence. *Particle and Fibre Toxicology 2022 19:1*, *19*(1), 1–25. doi: 10.1186/S12989-022-00507-5

Li, W., Sun, L., Yue, L., & Xiao, S. (2023). Alzheimer's disease and COVID-19: Interactions, intrinsic linkages, and the role of immunoinflammatory responses in this process. *Frontiers in Immunology*, *14*. doi: 10.3389/fimmu.2023.1120495

Liao, P., Ku, M., Lue, K., & Sun, H. (2011). Respiratory tract infection is the major cause of the ambulatory visits in children. *Italian Journal of Pediatrics*, *37*(1), 1–5. doi: 10.1186/1824-7288-37-43/TABLES/4

Linares, C., Belda, F., López-Bueno, J. A., Luna, M. Y., Sánchez-Martínez, G., Hervella, B., Culqui, D., & Díaz, J. (2021). Short-term associations of air pollution and meteorological variables on the incidence and severity of COVID-19 in Madrid (Spain): a time series study. *Environmental Sciences Europe*, *33*(1), 107. doi: 10.1186/s12302-021-00548-1

Liu, C. W., Lee, T. L., Chen, Y. C., Liang, C. J., Wang, S. H., Lue, J. H., Tsai, J. S., Lee, S. W., Chen, S. H., Yang, Y. F., Chuang, T. Y., & Chen, Y. L. (2018). PM2.5-induced oxidative stress increases intercellular adhesion molecule-1 expression in lung epithelial cells through the IL-6/AKT/STAT3/NF-KB-dependent pathway. *Particle and Fibre Toxicology*, *15*(1), 1–16. doi: 10.1186/S12989-018-0240-X/FIGURES/7

Livingston, G., Huntley, J., Sommerlad, A., Ames, D., Ballard, C., Banerjee, S., Brayne, C., Burns, A., Cohen-Mansfield, J., Cooper, C., Costafreda, S. G., Dias, A., Fox, N., Gitlin, L. N., Howard, R., Kales, H. C., Kivimäki, M., Larson, E. B., Ogunniyi, A., … Mukadam, N. (2020). Dementia prevention, intervention, and care: 2020 report of the Lancet Commission. *The Lancet*, *396*(10248), 413–446. doi: 10.1016/S0140-6736(20)30367-6/ATTACHMENT/DFC82F21-55AB-4950-8828-93F27077EF6D/MMC1.PDF

Loaiza-Ceballos, M. C., Marin-Palma, D., Zapata, W., & Hernandez, J. C. (2022). Viral respiratory infections and air pollutants. *Air Quality, Atmosphere, & Health*, *15*(1), 105. doi: 10.1007/S11869-021-01088-6

Loane, C., Pilinis, C., Lekkas, T. D., & Politis, M. (2013). Ambient particulate matter and its potential neurological consequences. *Reviews in the Neurosciences*, *24*(3), 323–335. doi: 10.1515/REVNEURO-2013-0001/MACHINEREADABLECITATION/RIS

Lodovici, M., & Bigagli, E. (2011). Oxidative stress and air pollution exposure. *Journal of Toxicology*, *2011*. doi: 10.1155/2011/487074

Lucchini, R. G., Dorman, D. C., Elder, A., & Veronesi, B. (2012). NEUROLOGICAL IMPACTS FROM INHALATION OF POLLUTANTS AND

THE NOSE-BRAIN CONNECTION. *Neurotoxicology*, *33*(4), 838. doi: 10.1016/J.NEURO.2011.12.001

Mack, S. M., Madl, A. K., & Pinkerton, K. E. (2019). Respiratory Health Effects of Exposure to Ambient Particulate Matter and Bioaerosols. *Comprehensive Physiology*, *10*(1), 1. doi: 10.1002/CPHY.C180040

Maher, B. A., Ahmed, I. A. M., Karloukovski, V., MacLaren, D. A., Foulds, P. G., Allsop, D., Mann, D. M. A., Torres-Jardón, R., & Calderon-Garciduenas, L. (2016). Magnetite pollution nanoparticles in the human brain. *Proceedings of the National Academy of Sciences of the United States of America*, *113*(39), 10797–10801. doi: 10.1073/PNAS.1605941113

Maison, D. P., Deng, Y., & Gerschenson, M. (2023). SARS-CoV-2 and the host-immune response. *Frontiers in Immunology*, *14*, 1195871. doi: 10.3389/FIMMU.2023.1195871/BIBTEX

Manik, M., Rakesh, |, Singh, K., & Singh, R. K. (2022). Role of toll-like receptors in modulation of cytokine storm signaling in SARS-CoV-2-induced COVID-19. *Journal of Medical Virology*, *94*(3), 869–877. doi: 10.1002/JMV.27405

Marchetti, S., Gualtieri, M., Pozzer, A., Lelieveld, J., Saliu, F., Hansell, A. L., Colombo, A., & Mantecca, P. (2023). On fine particulate matter and COVID-19 spread and severity: An in vitro toxicological plausible mechanism. *Environment International*, *179*, 108131. doi: 10.1016/j.envint.2023.108131

Marín-Palma, D., Tabares-Guevara, J. H., Zapata-Cardona, M. I., Zapata-Builes, W., Taborda, N., Rugeles, M. T., & Hernandez, J. C. (2023). PM10 promotes an inflammatory cytokine response that may impact SARS-CoV-2 replication in vitro. *Frontiers in Immunology*, *14*, 1161135. doi: 10.3389/FIMMU.2023.1161135/BIBTEX

Marquès, M., & Domingo, J. L. (2022). Positive association between outdoor air pollution and the incidence and severity of COVID-19. A review of the recent scientific evidences. *Environmental Research*, *203*, 111930. doi: 10.1016/J.ENVRES.2021.111930

Martikainen, M. V., Tossavainen, T., Hannukka, N., & Roponen, M. (2023). Pollen, respiratory viruses, and climate change: Synergistic effects on

human health. *Environmental Research*, *219*, 115149. doi: 10.1016/J.ENVRES.2022.115149

Martínez-Espinoza, I., & Guerrero-Plata, A. (2022). The Relevance of TLR8 in Viral Infections. *Pathogens*, *11*(2), 134. doi: 10.3390/pathogens11020134

Matz, C. J., Egyed, M., Hocking, R., Seenundun, S., Charman, N., & Edmonds, N. (2019). Human health effects of traffic-related air pollution (TRAP): A scoping review protocol. *Systematic Reviews*, *8*(1), 1–5. doi: 10.1186/S13643-019-1106-5/PEER-REVIEW

McGeoch, L. J., Ross, S., Massa, M. S., Lewington, S., & Clarke, R. (2023). Cigarette smoking and risk of severe infectious respiratory diseases in UK adults: 12-year follow-up of UK biobank. *Journal of Public Health*, *45*(4), e621–e629. doi: 10.1093/PUBMED/FDAD090

Meinhardt, J., Radke, J., Dittmayer, C., Franz, J., Thomas, C., Mothes, R., Laue, M., Schneider, J., Brünink, S., Greuel, S., Lehmann, M., Hassan, O., Aschman, T., Schumann, E., Chua, R. L., Conrad, C., Eils, R., Stenzel, W., Windgassen, M., … Heppner, F. L. (2021). Olfactory transmucosal SARS-CoV-2 invasion as a port of central nervous system entry in individuals with COVID-19. *Nature Neuroscience*, *24*(2), 168–175. doi: 10.1038/s41593-020-00758-5

Metaxas, A., & Kempf, S. (2016). Neurofibrillary tangles in Alzheimer's disease: elucidation of the molecular mechanism by immunohistochemistry and tau protein phospho-proteomics. *Neural Regeneration Research*, *11*(10), 1579. doi: 10.4103/1673-5374.193234

Migliaccio, C. T., Kobos, E., King, Q. O., Porter, V., Jessop, F., & Ward, T. (2013). Adverse effects of wood smoke PM $_{2.5}$ exposure on macrophage functions. *Inhalation Toxicology*, *25*(2), 67–76. doi: 10.3109/08958378.2012.756086

Mishra, R., Krishnamoorthy, P., Gangamma, S., Raut, A. A., & Kumar, H. (2020). Particulate matter (PM10) enhances RNA virus infection through modulation of innate immune responses. *Environmental Pollution*, *266*, 115148. doi: 10.1016/J.ENVPOL.2020.115148

Miyashita, L., Foley, G., Semple, S., Gibbons, J. M., Pade, C., McKnight, Á., & Grigg, J. (2023). Curbside particulate matter and susceptibility to SARS–

CoV-2 infection. *Journal of Allergy and Clinical Immunology: Global*, *2*(4), 100141. doi: 10.1016/j.jacig.2023.100141

Murphy, C. (2018). Olfactory and other sensory impairments in Alzheimer disease. *Nature Reviews Neurology 2018 15:1*, *15*(1), 11–24. doi: 10.1038/s41582-018-0097-5

Murrell, W., Féron, F., Wetzig, A., Cameron, N., Splatt, K., Bellette, B., Bianco, J., Perry, C., Lee, G., & Mackay-Sim, A. (2005). Multipotent stem cells from adult olfactory mucosa. *Developmental Dynamics*, *233*(2), 496–515. doi: 10.1002/DVDY.20360

Mushtaq, N., Ezzati, M., Hall, L., Dickson, I., Kirwan, M., Png, K. M. Y., Mudway, I. S., & Grigg, J. (2011). Adhesion of Streptococcus pneumoniae to human airway epithelial cells exposed to urban particulate matter. *Journal of Allergy and Clinical Immunology*, *127*(5), 1236-1242.e2. doi: 10.1016/j.jaci.2010.11.039

Mussalo, L., Avesani, S., Shahbaz, M. A., Závodná, T., Saveleva, L., Järvinen, A., Lampinen, R., Belaya, I., Krejčík, Z., Ivanova, M., Hakkarainen, H., Kalapudas, J., Penttilä, E., Löppönen, H., Koivisto, A. M., Malm, T., Topinka, J., Giugno, R., Aakko-Saksa, P., … Kanninen, K. M. (2023). Emissions from modern engines induce distinct effects in human olfactory mucosa cells, depending on fuel and aftertreatment. *Science of The Total Environment*, *905*, 167038. doi: 10.1016/j.scitotenv.2023.167038

Mutiawati, E., Fahriani, M., Mamada, S. S., Fajar, J. K., Frediansyah, A., Maliga, H. A., Ilmawan, M., Emran, T. Bin, Ophinni, Y., Ichsan, I., Musadir, N., Rabaan, A. A., Dhama, K., Syahrul, S., Nainu, F., & Harapan, H. (2021). Anosmia and dysgeusia in SARS-CoV-2 infection: incidence and effects on COVID-19 severity and mortality, and the possible pathobiology mechanisms - a systematic review and meta-analysis. *F1000Research*, *10*, 40. doi: 10.12688/f1000research.28393.1

Nelson, V. M., Dancik, C. M., Pan, W., Jiang, Z. G., Lebowitz, M. S., & Ghanbari, H. A. (2009). PAN-811 inhibits oxidative stress-induced cell death of human Alzheimer's disease-derived and age-matched olfactory neuroepithelial cells via suppression of intracellular reactive

oxygen species. *Journal of Alzheimer's Disease : JAD*, *17*(3), 611–619. doi: 10.3233/JAD-2009-1078

Nemmar, A., Hoet, P. H. M., Vanquickenborne, B., Dinsdale, D., Thomeer, M., Hoylaerts, M. F., Vanbilloen, H., Mortelmans, L., & Nemery, B. (2002). Passage of Inhaled Particles Into the Blood Circulation in Humans. *Circulation*, *105*(4), 411–414. doi: 10.1161/HC0402.104118

Nichols, E., Steinmetz, J. D., Vollset, S. E., Fukutaki, K., Chalek, J., Abd-Allah, F., Abdoli, A., Abualhasan, A., Abu-Gharbieh, E., Akram, T. T., Al Hamad, H., Alahdab, F., Alanezi, F. M., Alipour, V., Almustanyir, S., Amu, H., Ansari, I., Arabloo, J., Ashraf, T., … Vos, T. (2022). Estimation of the global prevalence of dementia in 2019 and forecasted prevalence in 2050: an analysis for the Global Burden of Disease Study 2019. *The Lancet. Public Health*, *7*(2), e105–e125. doi: 10.1016/S2468-2667(21)00249-8

Nozza, E., Valentini, S., Melzi, G., Vecchi, R., & Corsini, E. (2021). Advances on the immunotoxicity of outdoor particulate matter: A focus on physical and chemical properties and respiratory defence mechanisms. *Science of The Total Environment*, *780*, 146391. doi: 10.1016/J.SCITOTENV.2021.146391

Oberdörster, G. (2001). Pulmonary effects of inhaled ultrafine particles. *International Archives of Occupational and Environmental Health*, *74*(1), 1–8. doi: 10.1007/S004200000185

Oberdörster, Günter, Oberdörster, E., & Oberdörster, J. (2005). Nanotoxicology: An emerging discipline evolving from studies of ultrafine particles. *Environmental Health Perspectives*, *113*(7), 823–839. doi: 10.1289/EHP.7339

Oberdörster, Günter, Sharp, Z., Atudorei, V., Elder, A., Gelein, R., Kreyling, W., & Cox, C. (2004). Translocation of Inhaled Ultrafine Particles to the Brain. *Inhalation Toxicology*, *16*(6–7), 437–445. doi: 10.1080/08958370490439597

O'Brien, R. J., & Wong, P. C. (2011). Amyloid Precursor Protein Processing and Alzheimer's Disease. *Annual Review of Neuroscience*, *34*(1), 185–204. doi: 10.1146/annurev-neuro-061010-113613

Park, B. S., & Lee, J.-O. (2013). Recognition of lipopolysaccharide pattern by TLR4 complexes. *Experimental & Molecular Medicine*, *45*(12), e66–e66. doi: 10.1038/emm.2013.97

Park, M., Joo, H. S., Lee, K., Jang, M., Kim, S. D., Kim, I., Borlaza, L. J. S., Lim, H., Shin, H., Chung, K. H., Choi, Y.-H., Park, S. G., Bae, M.-S., Lee, J., Song, H., & Park, K. (2018). Differential toxicities of fine particulate matters from various sources. *Scientific Reports*, *8*(1), 17007. doi: 10.1038/s41598-018-35398-0

Particulate Matter (PM) Basics | US EPA. (2023). Retrieved from https://www.epa.gov/pm-pollution/particulate-matter-pm-basics

Pinto, J. M. (2011). Olfaction. *Proceedings of the American Thoracic Society*, *8*(1), 46–52. doi: 10.1513/PATS.201005-035RN

Politis, M., Pilinis, C., & Lekkas, T. D. (2008). Ultrafine particles (UFP) and health effects. Dangerous. Like no other PM? Review and analysis. *Global Nest Journal*, *10*(3), 439–452. doi: 10.30955/GNJ.000579

Popescu, F., Ionel, I., Popescu, F., & Ionel, I. (2010). Anthropogenic Air Pollution Sources. *Air Quality*. doi: 10.5772/9751

Psoter, K. J., De Roos, A. J., Mayer, J. D., Kaufman, J. D., Wakefield, J., & Rosenfeld, M. (2015). Fine particulate matter exposure and initial Pseudomonas aeruginosa acquisition in cystic fibrosis. *Annals of the American Thoracic Society*, *12*(3), 385–391. doi: 10.1513/ANNALSATS.201408-400OC/SUPPL_FILE/DISCLOSURES.PDF

Qi, Y., Wei, S., Xin, T., Huang, C., Pu, Y., Ma, J., Zhang, C., Liu, Y., Lynch, I., & Liu, S. (2022). Passage of exogeneous fine particles from the lung into the brain in humans and animals. *Proceedings of the National Academy of Sciences of the United States of America*, *119*(26). doi: 10.1073/PNAS.2117083119/-/DCSUPPLEMENTAL

Quezada-Maldonado, E. M., Sánchez-Pérez, Y., Chirino, Y. I., & García-Cuellar, C. M. (2021). Airborne particulate matter induces oxidative damage, DNA adduct formation and alterations in DNA repair pathways. *Environmental Pollution*, *287*, 117313. doi: 10.1016/J.ENVPOL.2021.117313

Ran, J., Schooling, C. M., Han, L., Sun, S., Zhao, S., Zhang, X., Chan, K. P., Guo, F., Lee, R. S. yin, Qiu, Y., & Tian, L. (2021). Long-term exposure to fine

particulate matter and dementia incidence: A cohort study in Hong Kong. *Environmental Pollution*, *271*, 116303. doi: 10.1016/J.ENVPOL.2020.116303

Rantanen, L. M., Bitar, M., Lampinen, R., Stewart, R., Quek, H., Oikari, L. E., Cuníl-López, C., Sutharsan, R., Thillaiyampalam, G., Iqbal, J., Russell, D., Penttilä, E., Löppönen, H., Lehtola, J.-M., Saari, T., Hannonen, S., Koivisto, A. M., Haupt, L. M., Mackay-Sim, A., … White, A. R. (2022). An Alzheimer's Disease Patient-Derived Olfactory Stem Cell Model Identifies Gene Expression Changes Associated with Cognition. *Cells*, *11*(20), 3258. doi: 10.3390/cells11203258

Rebuli, M. E., Brocke, S. A., & Jaspers, I. (2021). Impact of inhaled pollutants on response to viral infection in controlled exposures. *Journal of Allergy and Clinical Immunology*, *148*(6), 1420–1429. doi: 10.1016/J.JACI.2021.07.002

Reiken, S., Sittenfeld, L., Dridi, H., Liu, Y., Liu, X., & Marks, A. R. (2022). Alzheimer's-like signaling in brains of COVID-19 patients. *Alzheimer's & Dementia*, *18*(5), 955–965. doi: 10.1002/ALZ.12558

Reveret, L., Leclerc, M., Emond, V., Tremblay, C., Loiselle, A., Bourassa, P., Bennett, D. A., Hébert, S. S., & Calon, F. (2023). Higher angiotensin-converting enzyme 2 (ACE2) levels in the brain of individuals with Alzheimer's disease. *Acta Neuropathologica Communications*, *11*(1), 159. doi: 10.1186/s40478-023-01647-1

Roberts, R. O., Christianson, T. J. H., Kremers, W. K., Mielke, M. M., Machulda, M. M., Vassilaki, M., Alhurani, R. E., Geda, Y. E., Knopman, D. S., & Petersen, R. C. (2016). Association Between Olfactory Dysfunction and Amnestic Mild Cognitive Impairment and Alzheimer Disease Dementia. *JAMA Neurology*, *73*(1), 93–101. doi: 10.1001/JAMANEUROL.2015.2952

Roczkowsky, A., Limonta, D., Fernandes, J. P., Branton, W. G., Clarke, M., Hlavay, B., Noyce, R. S., Joseph, J. T., Ogando, N. S., Das, S. K., Elaish, M., Arbour, N., Evans, D. H., Langdon, K., Hobman, T. C., & Power, C. (2023). <scp>COVID</scp> -19 Induces Neuroinflammation and Suppresses Peroxisomes in the Brain. *Annals of Neurology*, *94*(3), 531–546. doi: 10.1002/ana.26679

Rodriguez-Sevilla, J. J., Güerri-Fernádez, R., & Bertran Recasens, B. (2022). Is There Less Alteration of Smell Sensation in Patients With Omicron SARS-CoV-2 Variant Infection? *Frontiers in Medicine*, *9*, 1044. doi: 10.3389/fmed.2022.852998

Rönkkö, T. J., Hirvonen, M.-R., Happo, M. S., Ihantola, T., Hakkarainen, H., Martikainen, M.-V., Gu, C., Wang, Q., Jokiniemi, J., Komppula, M., & Jalava, P. I. (2021). Inflammatory responses of urban air PM modulated by chemical composition and different air quality situations in Nanjing, China. *Environmental Research*, *192*, 110382. doi: 10.1016/j.envres.2020.110382

Rönkkö, T. J., Hirvonen, M.-R., Happo, M. S., Leskinen, A., Koponen, H., Mikkonen, S., Bauer, S., Ihantola, T., Hakkarainen, H., Miettinen, M., Orasche, J., Gu, C., Wang, Q., Jokiniemi, J., Sippula, O., Komppula, M., & Jalava, P. I. (2020). Air quality intervention during the Nanjing youth olympic games altered PM sources, chemical composition, and toxicological responses. *Environmental Research*, *185*, 109360. doi: 10.1016/j.envres.2020.109360

Rönkkö, T. J., Jalava, P. I., Happo, M. S., Kasurinen, S., Sippula, O., Leskinen, A., Koponen, H., Kuuspalo, K., Ruusunen, J., Väisänen, O., Hao, L., Ruuskanen, A., Orasche, J., Fang, D., Zhang, L., Lehtinen, K. E. J., Zhao, Y., Gu, C., Wang, Q., … Hirvonen, M.-R. (2018). Emissions and atmospheric processes influence the chemical composition and toxicological properties of urban air particulate matter in Nanjing, China. *Science of The Total Environment*, *639*, 1290–1310. doi: 10.1016/j.scitotenv.2018.05.260

Rudnicka-Drożak, E., Drożak, P., Mizerski, G., Zaborowski, T., Ślusarska, B., Nowicki, G., & Drożak, M. (2023). Links between COVID-19 and Alzheimer's Disease—What Do We Already Know? *International Journal of Environmental Research and Public Health*, *20*(3), 2146. doi: 10.3390/ijerph20032146

Safdari Lord, J., Soltani Rezaiezadeh, J., Yekaninejad, M. S., & Izadi, P. (2022). The association of APOE genotype with COVID-19 disease severity. *Scientific Reports*, *12*(1), 13483. doi: 10.1038/s41598-022-17262-4

Sagawa, T., Tsujikawa, T., Honda, A., Miyasaka, N., Tanaka, M., Kida, T., Hasegawa, K., Okuda, T., Kawahito, Y., & Takano, H. (2021). Exposure to particulate matter upregulates ACE2 and TMPRSS2 expression in the murine lung. *Environmental Research*, *195*, 110722. doi: 10.1016/j.envres.2021.110722

Sahu, B., Mackos, A. R., Floden, A. M., Wold, L. E., & Combs, C. K. (2021). Particulate Matter Exposure Exacerbates Amyloid-β Plaque Deposition and Gliosis in APP/PS1 Mice. *Journal of Alzheimer's Disease*, *80*(2), 761–774. doi: 10.3233/JAD-200919

Santurtún, A., Colom, M. L., Fdez-Arroyabe, P., Real, Á. del, Fernández-Olmo, I., & Zarrabeitia, M. T. (2022). Exposure to particulate matter: Direct and indirect role in the COVID-19 pandemic. *Environmental Research*, *206*, 112261. doi: 10.1016/j.envres.2021.112261

Saveleva, L., Vartiainen, P., Górová, V., Chew, S., Belaya, I., Konttinen, H., Zucchelli, M., Korhonen, P., Kaartinen, E., Kortelainen, M., Lamberg, H., Sippula, O., Malm, T., Jalava, P. I., & Kanninen, K. M. (2022). Subacute inhalation of ultrafine particulate matter triggers inflammation without altering amyloid beta load in 5xFAD mice. *NeuroToxicology*, *89*, 55–66. doi: 10.1016/J.NEURO.2022.01.001

Schraufnagel, D. E. (2020). The health effects of ultrafine particles. *Experimental & Molecular Medicine 2020 52:3*, *52*(3), 311–317. doi: 10.1038/s12276-020-0403-3

Schwob, J. E. (2002). Neural regeneration and the peripheral olfactory system. In Anatomical Record (Vol. 269, Issue 1, pp. 33–49). Anat Rec. doi: 10.1002/ar.10047

Seyhan, A. A. (2019). Lost in translation: the valley of death across preclinical and clinical divide – identification of problems and overcoming obstacles. *Translational Medicine Communications*, *4*(1), 18. doi: 10.1186/s41231-019-0050-7

Shahbaz, M. A., De Bernardi, F., Alatalo, A., Sachana, M., Clerbaux, L.-A., Muñoz, A., Parvatam, S., Landesmann, B., Kanninen, K. M., & Coecke, S. (2022). Mechanistic Understanding of the Olfactory Neuroepithelium Involvement Leading to Short-Term Anosmia in COVID-19 Using the

Adverse Outcome Pathway Framework. *Cells*, *11*(19). doi: 10.3390/cells11193027

Shelton, J. F., Shastri, A. J., Fletez-Brant, K., Auton, A., Chubb, A., Fitch, A., Kung, A., Altman, A., Kill, A., Shastri, A. J., Symons, A., Weldon, C., Coker, D., Shelton, J. F., Tan, J., Pollard, J., McCreight, J., Bielenberg, J., Matthews, J., … Auton, A. (2022). The UGT2A1/UGT2A2 locus is associated with COVID-19-related loss of smell or taste. *Nature Genetics*, *54*(2), 121–124. doi: 10.1038/s41588-021-00986-w

Sheppard, N., Carroll, M., Gao, C., & Lane, T. (2023). Particulate matter air pollution and COVID-19 infection, severity, and mortality: A systematic review and meta-analysis. *Science of The Total Environment*, *880*, 163272. doi: 10.1016/J.SCITOTENV.2023.163272

Shi, L., Wu, X., Danesh Yazdi, M., Braun, D., Abu Awad, Y., Wei, Y., Liu, P., Di, Q., Wang, Y., Schwartz, J., Dominici, F., Kioumourtzoglou, M. A., & Zanobetti, A. (2020). Long-term effects of PM2·5 on neurological disorders in the American Medicare population: a longitudinal cohort study. *The Lancet Planetary Health*, *4*(12), e557–e565. doi: 10.1016/S2542-5196(20)30227-8

Shoenfelt, J., Mitkus, R. J., Zeisler, R., Spatz, R. O., Powell, J., Fenton, M. J., Squibb, K. A., & Medvedev, A. E. (2009). Involvement of TLR2 and TLR4 in inflammatory immune responses induced by fine and coarse ambient air particulate matter. *Journal of Leukocyte Biology*, *86*(2), 303–312. doi: 10.1189/jlb.1008587

Sillanpää, M., Hillamo, R., Mäkelä, T., Pennanen, A. S., & Salonen, R. O. (2003). Field and laboratory tests of a high volume cascade impactor. *Journal of Aerosol Science*, *34*(4), 485–500. doi: 10.1016/S0021-8502(02)00214-8

Stegemann-Koniszewski, S., Behrens, S., Boehme, J. D., Hochnadel, I., Riese, P., Guzmán, C. A., Kröger, A., Schreiber, J., Gunzer, M., & Bruder, D. (2018). Respiratory Influenza A Virus Infection Triggers Local and Systemic Natural Killer Cell Activation via Toll-Like Receptor 7. *Frontiers in Immunology*, *9*. doi: 10.3389/fimmu.2018.00245

Steger-Hartmann, T., & Raschke, M. (2020). Translating in vitro to in vivo and animal to human. *Current Opinion in Toxicology*, *23–24*, 6–10. doi: 10.1016/j.cotox.2020.02.003

Stewart, R., Kozlov, S., Matigian, N., Wali, G., Gatei, M., Sutharsan, R., Bellette, B., Wraith-Kijas, A., Cochrane, J., Coulthard, M., Perry, C., Sinclair, K., Mackay-Sim, A., & Lavin, M. F. (2013). A patient-derived olfactory stem cell disease model for ataxia-telangiectasia. *Human Molecular Genetics*, *22*(12), 2495–2509. doi: 10.1093/HMG/DDT101

Stokes, B. A., Yadav, S., Shokal, U., Smith, L. C., & Eleftherianos, I. (2015). Bacterial and fungal pattern recognition receptors in homologous innate signaling pathways of insects and mammals. *Frontiers in Microbiology*, *6*. doi: 10.3389/fmicb.2015.00019

Strosnider, H. M., Chang, H. H., Darrow, L. A., Liu, Y., Vaidyanathan, A., & Strickland, M. J. (2019). Age-Specific Associations of Ozone and Fine Particulate Matter with Respiratory Emergency Department Visits in the United States. *American Journal of Respiratory and Critical Care Medicine*, *199*(7), 882–890. doi: 10.1164/rccm.201806-1147OC

Sungnak, W., Huang, N., Bécavin, C., Berg, M., Queen, R., Litvinukova, M., Talavera-López, C., Maatz, H., Reichart, D., Sampaziotis, F., Worlock, K. B., Yoshida, M., Barnes, J. L., Banovich, N. E., Barbry, P., Brazma, A., Collin, J., Desai, T. J., Duong, T. E., … Figueiredo, F. (2020). SARS-CoV-2 entry factors are highly expressed in nasal epithelial cells together with innate immune genes. *Nature Medicine 2020 26:5*, *26*(5), 681–687. doi: 10.1038/s41591-020-0868-6

Tannenbaum, J., & Bennett, B. T. (2015). Russell and Burch's 3Rs Then and Now: The Need for Clarity in Definition and Purpose. *Journal of the American Association for Laboratory Animal Science : JAALAS*, *54*(2), 120. Retrieved from /pmc/articles/PMC4382615/

Tao, R., Cao, W., Li, M., Yang, L., Dai, R., Luo, X., Liu, Y., Ge, B., Su, X., & Xu, J. (2020). PM2.5 compromises antiviral immunity in influenza infection by inhibiting activation of NLRP3 inflammasome and expression of interferon-β. *Molecular Immunology*, *125*, 178–186. doi: 10.1016/j.molimm.2020.07.001

Taquet, M., Skorniewska, Z., Hampshire, A., Chalmers, J. D., Ho, L.-P., Horsley, A., Marks, M., Poinasamy, K., Raman, B., Leavy, O. C., Richardson, M., Elneima, O., McAuley, H. J. C., Shikotra, A., Singapuri, A., Sereno, M., Saunders, R. M., Harris, V. C., Houchen-Wolloff, L., … Harrison, P. J. (2023). Acute blood biomarker profiles predict cognitive deficits 6 and 12 months after COVID-19 hospitalization. *Nature Medicine*, *29*(10), 2498–2508. doi: 10.1038/s41591-023-02525-y

Tosta, E. (2021). The seven constitutive respiratory defense barriers against SARS-CoV-2 infection. *Revista Da Sociedade Brasileira de Medicina Tropical*, *54*, 2021. doi: 10.1590/0037-8682-0461-2021

Tran, H. M., Tsai, F. J., Lee, Y. L., Chang, J. H., Chang, L. Te, Chang, T. Y., Chung, K. F., Kuo, H. P., Lee, K. Y., Chuang, K. J., & Chuang, H. C. (2023). The impact of air pollution on respiratory diseases in an era of climate change: A review of the current evidence. *Science of The Total Environment*, *898*, 166340. doi: 10.1016/J.SCITOTENV.2023.166340

Travaglio, M., Yu, Y., Popovic, R., Selley, L., Leal, N. S., & Martins, L. M. (2021). Links between air pollution and COVID-19 in England. *Environmental Pollution*, *268*, 115859. doi: 10.1016/j.envpol.2020.115859

Triantafilou, K., Vakakis, E., Orthopoulos, G., Ahmed, M. A. E., Schumann, C., Lepper, P. M., & Triantafilou, M. (2005). TLR8 and TLR7 are involved in the host's immune response to human parechovirus 1. *European Journal of Immunology*, *35*(8), 2416–2423. doi: 10.1002/eji.200526149

Upadhyay, S., & Palmberg, L. (2018). Air-Liquid Interface: Relevant In Vitro Models for Investigating Air Pollutant-Induced Pulmonary Toxicity. *Toxicological Sciences*, *164*(1), 21–30. doi: 10.1093/TOXSCI/KFY053

Upadhyay, S., Rahman, M., Rinaldi, S., Koelmel, J., Lin, E. Z., Mahesh, P. A., Beckers, J., Johanson, G., Pollitt, K. J. G., Palmberg, L., Irmler, M., & Ganguly, K. (2024). Assessment of wood smoke induced pulmonary toxicity in normal- and chronic bronchitis-like bronchial and alveolar lung mucosa models at air-liquid interface. *Respiratory Research*, *25*(1). doi: 10.1186/S12931-024-02686-5

Urbano, T., Chiari, A., Malagoli, C., Cherubini, A., Bedin, R., Costanzini, S., Teggi, S., Maffeis, G., Vinceti, M., & Filippini, T. (2023). Particulate

matter exposure from motorized traffic and risk of conversion from mild cognitive impairment to dementia: An Italian prospective cohort study. *Environmental Research*, *222*, 115425. doi: 10.1016/J.ENVRES.2023.115425

Valderrama, A., Ortiz-Hernández, P., Agraz-Cibrián, J. M., Tabares-Guevara, J. H., Gómez, D. M., Zambrano-Zaragoza, J. F., Taborda, N. A., & Hernandez, J. C. (2022). Particulate matter (PM10) induces in vitro activation of human neutrophils, and lung histopathological alterations in a mouse model. *Scientific Reports*, *12*(1). doi: 10.1038/S41598-022-11553-6

V'kovski, P., Kratzel, A., Steiner, S., Stalder, H., & Thiel, V. (2021). Coronavirus biology and replication: implications for SARS-CoV-2. *Nature Reviews Microbiology*, *19*(3), 155–170. doi: 10.1038/s41579-020-00468-6

von Bartheld, C. S., & Wang, L. (2023). Prevalence of Olfactory Dysfunction with the Omicron Variant of SARS-CoV-2: A Systematic Review and Meta-Analysis. *Cells*, *12*(3), 430. doi: 10.3390/cells12030430

Wan, D., Du, T., Hong, W., Chen, L., Que, H., Lu, S., & Peng, X. (2021). Neurological complications and infection mechanism of SARS-CoV-2. *Signal Transduction and Targeted Therapy*, *6*(1), 406. doi: 10.1038/s41392-021-00818-7

Wang, B. R., Shi, J. Q., Ge, N. N., Ou, Z., Tian, Y. Y., Jiang, T., Zhou, J. S., Xu, J., & Zhang, Y. D. (2018). PM2.5 exposure aggravates oligomeric amyloid beta-induced neuronal injury and promotes NLRP3 inflammasome activation in an in vitro model of Alzheimer's disease. *Journal of Neuroinflammation*, *15*(1), 1–12. doi: 10.1186/S12974-018-1178-5/FIGURES/7

Wang, L., Davis, P. B., Volkow, N. D., Berger, N. A., Kaelber, D. C., & Xu, R. (2022). Association of COVID-19 with New-Onset Alzheimer's Disease. *Journal of Alzheimer's Disease*, *89*(2), 411–414. doi: 10.3233/JAD-220717

Wang, Q. (2018). Urbanization and Global Health: The Role of Air Pollution. *Iranian Journal of Public Health*, *47*(11), 1644. Retrieved from /pmc/articles/PMC6294869/

Wang, Q. Q., Davis, P. B., Gurney, M. E., & Xu, R. (2021). COVID-19 and dementia: Analyses of risk, disparity, and outcomes from electronic

health records in the US. *Alzheimer's & Dementia*, *17*(8), 1297–1306. doi: 10.1002/ALZ.12296

Wang, Q. Q., Xu, R., & Volkow, N. D. (2021). Increased risk of COVID-19 infection and mortality in people with mental disorders: analysis from electronic health records in the United States. *World Psychiatry*, *20*(1), 124–130. doi: 10.1002/WPS.20806

Wang, S., Zhang, K., Song, X., Huang, Q., Lin, S., Deng, S., Qi, M., Yang, Y., Lu, Q., Zhao, D., Meng, F., Li, J., Lian, Z., Luo, C., & Yao, Y. (2023). TLR4 Overexpression Aggravates Bacterial Lipopolysaccharide-Induced Apoptosis via Excessive Autophagy and NF-κB/MAPK Signaling in Transgenic Mammal Models. *Cells*, *12*(13), 1769. doi: 10.3390/cells12131769

Wang, Y., Wu, T., & Tang, M. (2020). Ambient particulate matter triggers dysfunction of subcellular structures and endothelial cell apoptosis through disruption of redox equilibrium and calcium homeostasis. *Journal of Hazardous Materials*, *394*. doi: 10.1016/J.JHAZMAT.2020.122439

Wei, T., & Tang, M. (2018). Biological effects of airborne fine particulate matter (PM 2.5) exposure on pulmonary immune system. *Environmental Toxicology and Pharmacology*, *60*, 195–201. doi: 10.1016/j.etap.2018.04.004

Weidinger, E., Krause, D., Wildenauer, A., Meyer, S., Gruber, R., Schwarz, M. J., & Müller, N. (2014). Impaired activation of the innate immune response to bacterial challenge in Tourette syndrome. *The World Journal of Biological Psychiatry : The Official Journal of the World Federation of Societies of Biological Psychiatry*, *15*(6), 453–458. doi: 10.3109/15622975.2014.907503

WHO global air quality guidelines. (2021). *Particulate matter (PM2.5 and PM10), ozone, nitrogen dioxide, sulfur dioxide and carbon monoxide.* Geneva.

Williams, B. G., Gouws, E., Boschi-Pinto, C., Bryce, J., & Dye, C. (2002). Estimates of world-wide distribution of child deaths from acute respiratory infections. *The Lancet. Infectious Diseases*, *2*(1), 25–32. doi: 10.1016/S1473-3099(01)00170-0

Woodward, M. R., Amrutkar, C. V., Shah, H. C., Benedict, R. H. B., Rajakrishnan, S., Doody, R. S., Yan, L., & Szigeti, K. (2017). Validation of olfactory deficit as a biomarker of Alzheimer disease. *Neurology: Clinical Practice*, *7*(1), 5–14. doi: 10.1212/CPJ.0000000000000293

World Health Organization. (2024). *Air pollution*. Retrieved from https://www.who.int/health-topics/air-pollution#tab=tab_2

Wu, Y., Goplen, N. P., & Sun, J. (2021). Aging and respiratory viral infection: from acute morbidity to chronic sequelae. *Cell and Bioscience*, *11*(1), 1–13. doi: 10.1186/S13578-021-00624-2/FIGURES/4

Xia, X., Zhang, A., Liang, S., Qi, Q., Jiang, L., & Ye, Y. (2017). The Association between Air Pollution and Population Health Risk for Respiratory Infection: A Case Study of Shenzhen, China. *International Journal of Environmental Research and Public Health*, *14*(9), 950. doi: 10.3390/ijerph14090950

Yamamoto, A., Sly, P. D., Chew, K. Y., Khachatryan, L., Begum, N., Yeo, A. J., Vu, L. D., Short, K. R., Cormier, S. A., & Fantino, E. (2023). Environmentally persistent free radicals enhance SARS-CoV-2 replication in respiratory epithelium. *Experimental Biology and Medicine (Maywood, N.J.)*, *248*(3), 271–279. doi: 10.1177/15353702221142616

Yang, L., Li, C., & Tang, X. (2020). The Impact of PM2.5 on the Host Defense of Respiratory System. *Frontiers in Cell and Developmental Biology*, *8*. doi: 10.3389/fcell.2020.00091

You, R., Ho, Y.-S., & Chang, R. C.-C. (2022). The pathogenic effects of particulate matter on neurodegeneration: a review. *Journal of Biomedical Science*, *29*(1), 15. doi: 10.1186/s12929-022-00799-x

Yu, K., Zhang, Q., Wei, Y., Chen, R., & Kan, H. (2024). Global association between air pollution and COVID-19 mortality: A systematic review and meta-analysis. *Science of The Total Environment*, *906*, 167542. doi: 10.1016/J.SCITOTENV.2023.167542

Zhang, M., Xu, C., Jiang, L., & Qin, J. (2018). A 3D human lung-on-a-chip model for nanotoxicity testing. *Toxicology Research*, *7*(6), 1048–1060. doi: 10.1039/C8TX00156A

Zhang, S., Huo, X., Zhang, Y., Huang, Y., Zheng, X., & Xu, X. (2019). Ambient fine particulate matter inhibits innate airway antimicrobial activity in

preschool children in e-waste areas. *Environment International*, *123*, 535–542. doi: 10.1016/j.envint.2018.12.061

Zhang, W., Gorelik, A. J., Wang, Q., Norton, S. A., Hershey, T., Agrawal, A., Bijsterbosch, J. D., & Bogdan, R. (2024). Associations between COVID-19 and putative markers of neuroinflammation: A diffusion basis spectrum imaging study. *Brain, Behavior, & Immunity - Health*, *36*, 100722. doi: 10.1016/J.BBIH.2023.100722

Zhao, H., Li, W., Gao, Y., Li, J., & Wang, H. (2014). Exposure to particular matter increases susceptibility to respiratory Staphylococcus aureus infection in rats via reducing pulmonary natural killer cells. *Toxicology*, *325*, 180–188. doi: 10.1016/j.tox.2014.09.006

Zhao, R. W., Guo, Z. Q., Zhang, R. X., Deng, C. R., Dong, W. Y., & Zhuang, G. S. (2019). [The role of autophagy in PM2.5-induced inflammation in human nasal epithelial cells]. *Zhonghua Er Bi Yan Hou Tou Jing Wai Ke Za Zhi = Chinese Journal of Otorhinolaryngology Head and Neck Surgery*, *54*(7), 510–516. doi: 10.3760/CMA.J.ISSN.1673-0860.2019.07.006

Zhao, S., Toniolo, S., Hampshire, A., & Husain, M. (2023). Effects of COVID-19 on cognition and brain health. *Trends in Cognitive Sciences*, *27*(11), 1053–1067. doi: 10.1016/j.tics.2023.08.008

Zhou, R., Liu, L., & Wang, Y. (2021). Viral proteins recognized by different TLRs. *Journal of Medical Virology*, *93*(11), 6116–6123. doi: 10.1002/jmv.27265

Zhou, Z., Shuai, X., Lin, Z., Yu, X., Ba, X., Holmes, M. A., Xiao, Y., Gu, B., & Chen, H. (2023). Association between particulate matter (PM)2·5 air pollution and clinical antibiotic resistance: a global analysis. *The Lancet Planetary Health*, *7*(8), e649–e659. doi: 10.1016/S2542-5196(23)00135-3

Zhu, P., Zhang, W., Feng, F., Qin, L., Ji, W., Li, D., Liang, R., Zhang, Y., Wang, Y., Li, M., Wu, W., Jin, Y., & Duan, G. (2022). Role of angiotensin-converting enzyme 2 in fine particulate matter-induced acute lung injury. *Science of The Total Environment*, *825*, 153964. doi: 10.1016/J.SCITOTENV.2022.153964

Zhu, T.-Y., Qiu, H., Cao, Q.-Q., Duan, Z.-L., Liu, F.-L., Song, T.-Z., Liu, Y., Fang, Y.-Q., Wu, G.-M., Zheng, Y.-T., Ding, W.-J., Lai, R., & Jin, L. (2021). Particulate matter exposure exacerbates susceptibility to SARS-CoV-2

infection in humanized ACE2 mice. *Zoological Research*, *42*(3), 335–338. doi: 10.24272/j.issn.2095-8137.2021.088

Ziou, M., Tham, R., Wheeler, A. J., Zosky, G. R., Stephens, N., & Johnston, F. H. (2022). Outdoor particulate matter exposure and upper respiratory tract infections in children and adolescents: A systematic review and meta-analysis. *Environmental Research*, *210*, 112969. doi: 10.1016/J.ENVRES.2022.112969

Zou, L., Ruan, F., Huang, M., Liang, L., Huang, H., Hong, Z., Yu, J., Kang, M., Song, Y., Xia, J., Guo, Q., Song, T., He, J., Yen, H.-L., Peiris, M., & Wu, J. (2020). SARS-CoV-2 Viral Load in Upper Respiratory Specimens of Infected Patients. *The New England Journal of Medicine*, *382*(12), 1177. doi: 10.1056/NEJMC2001737

Zsichla, L., & Müller, V. (2023). Risk Factors of Severe COVID-19: A Review of Host, Viral and Environmental Factors. *Viruses*, *15*(1), 175. doi: 10.3390/V15010175/S1

ORIGINAL PUBLICATIONS (I – III)

I

Urban air PM modifies differently immune defense responses against bacterial and viral infections in vitro

Muhammad Ali Shahbaz, Maria-Viola Martikainen, Teemu J Rönkkö, Mika Komppula, Pasi I Jalava, Marjut Roponen

Environmental Research, 192, 110244, 2021.

Environmental Research 192 (2021) 110244

Contents lists available at ScienceDirect

Environmental Research

journal homepage: www.elsevier.com/locate/envres

Urban air PM modifies differently immune defense responses against bacterial and viral infections in vitro

Muhammad Ali Shahbaz [a,*], Maria-Viola Martikainen [a], Teemu J. Rönkkö [a], Mika Komppula [b], Pasi I. Jalava [a], Marjut Roponen [a]

[a] University of Eastern Finland, Department of Environmental and Biological Sciences, Yliopistonranta 1, P.O. Box 1627, FI-70211, Kuopio, Finland
[b] Finnish Meteorological Institute, Yliopistonranta 1F, P.O. Box 1627, FI-70211, Kuopio, Finland

ARTICLE INFO

Keywords:
Ambient particulate matter
Toll-like receptor
Lipopolysaccharides
Poly: IC
ORN R-0006
Respiratory infections

ABSTRACT

Epidemiological evidence has shown the association between exposure to ambient fine particulate matter (PM) and increased susceptibility to bacterial and viral respiratory infections. However, to date, the underlying mechanisms of immunomodulatory effects of PM remain unclear. Our objective was to explore how exposure to relatively low doses of urban air PM alters innate responses to bacterial and viral stimuli in vitro. We used secondary alveolar epithelial cell line along with monocyte-derived macrophages to replicate innate lung barrier in vitro. Co-cultured cells were first exposed for 24 h to $PM_{2.5\text{-}1}$ (particle aerodynamic diameter between 1 and 2.5 μm) and subsequently for an additional 24 h to lipopolysaccharide (TLR4), polyinosinic-polycytidylic acid (TLR3), and synthetic single-stranded RNA oligoribonucleotides (TLR7/8) to mimic bacterial or viral stimulation. Toxicological endpoints included pro-inflammatory cytokines (IL-8, IL-6, and TNF-α), cellular metabolic activity, and cell cycle phase distribution. We show that cells exposed to $PM_{2.5\text{-}1}$ produced higher levels of pro-inflammatory cytokines following stimulation with bacterial TLR4 ligand than cells exposed to $PM_{2.5\text{-}1}$ or bacterial ligand alone. On the contrary, $PM_{2.5\text{-}1}$ exposure reduced pro-inflammatory responses to viral ligands TLR3 and TLR7/8. Cell cycle analysis indicated that viral ligands induced cell cycle arrest at the G2-M phase. In PM-primed co-cultures, however, they failed to induce the G2-M phase arrest. Contrarily, bacterial stimulation caused a slight increase in cells in the sub-G1 phase but in $PM_{2.5\text{-}1}$ primed co-cultures the effect of bacterial stimulation was masked by $PM_{2.5\text{-}1}$. These findings indicate that $PM_{2.5\text{-}1}$ may alter responses of immune defense differently against bacterial and viral infections. Further studies are required to explain the mechanism of immune modulation caused by PM in altering the susceptibility to respiratory infections.

1. Introduction

Exposure to ambient air pollution causes up to 4.2 million annual premature deaths worldwide (Cohen et al., 2017). One major component of air pollution is particulate matter (PM). PM is a mixture of solid and liquid particles (organic and inorganic-derived particles) dispersed in ambient air. Its size, shape, and composition vary depending on the source of origin. Generally, PM originates from natural (e.g. airborne dust, volcanic activity, and pollen) or anthropogenic sources (e.g. industry and traffic primarily by different combustion processes). It has been classified according to aerodynamic diameter into coarse (≤10 μm), Fine (≤2.5 μm), and ultra-fine (≤0.1 μm) PM (US EPA, 2016). The size of the particles directly links with the potential of PM for causing detrimental health outcomes. PM with an aerodynamic diameter less than 2.5 μm ($PM_{2.5}$) are among the most studied air pollutants of health concern since smaller particles are more likely to penetrate deeper in the lungs and encounter lung surface (Xing et al., 2016). $PM_{2.5}$ is not a self-contained pollutant; it contains a heterogeneous combination of solid and liquid particles, which not only includes chemicals but also biological fractions (Kelly and Fussell, 2012). Epidemiological evidence suggests that there is an increasing risk of developing bacterial and viral respiratory infection with exposure to ambient air pollution, in particular, fine particulate matter (Ciencewicki and Jaspers, 2007; Croft et al., 2019; Horne et al., 2018; Zhang et al., 2019). Furthermore, the recent coronavirus epidemic emphasizes the need for a detailed understanding of the link between air pollution and respiratory infection. Nationwide U.S cross-sectional study has highlighted the association between a small increase in long term exposure to $PM_{2.5}$ and an increased risk of

* Corresponding author.
E-mail addresses: ali.shahbaz@uef.fi, ali.varya123@gmail.com (M.A. Shahbaz).

https://doi.org/10.1016/j.envres.2020.110244
Received 2 July 2020; Received in revised form 9 September 2020; Accepted 17 September 2020
Available online 25 September 2020

mortality due to COVID-19 infection (Wu et al., 2020). In experimental models, fine PM exposure has increased the risk of pneumonia due to the deleterious effect on alveolar macrophages and alveolar epithelium (Migliaccio et al., 2013; Mushtaq et al., 2011). As reviewed in Wei and Tang (2018) few studies have focused on the immune-modulatory effect of fine PM and its effects on the immune response to respiratory infections. Therefore, it is crucial to explore links between fine PM exposure and alteration in the immune response to bacterial and viral respiratory infections since large populations are exposed to air pollutants and respiratory infections may spread more rapidly in the densely populated areas.

Alveolar epithelium and alveolar macrophages serve as pillars in the innate immune system of the respiratory tract. Inhaled pathogens must evade the innate immune system to establish infections (Bhattacharya and Westphalen, 2016). In vitro co-culture of secondary epithelial cells (A549 cells) and THP1 monocytes, differentiated into macrophage-like cells have been used in immunological and toxicological studies on the respiratory health to better understand the effect of cell-cell interaction and to better mimic the first line of defense i.e., alveolar epithelium and macrophages (Dehai et al., 2014; Holownia et al., 2015).

Family of Toll-like receptors (TLRs) expressed by epithelial and dedicated immune cells are an important component in pathogen recognition and innate immune response (Medzhitov, 2001). Activation of TLRs on airway epithelial cells has been shown to induce the production of several cytokines, chemokines, and antimicrobial peptides (Guillot et al., 2005; Hertz et al., 2003; Sha et al., 2004). The importance of TLRs for the host defense in the lung has been demonstrated by the increased susceptibility of TLR knockout mice towards viral or bacterial infections (Takeuchi et al., 2000; Wetzler, 2003). This is because each member of TLR family recognizes specific pathogen-associated molecular patterns (PAMPs), e.g., TLR3 is activated by virus-derived double-stranded RNA (Alexopoulou et al., 2001) and TLR4 by bacterial lipopolysaccharides (Beutler, 2002), whereas TLR7 and TLR8 recognize single-stranded viral RNA (Diebold et al., 2004; Heil et al., 2004). In our study, TLR ligands were used to mimic bacterial and viral stimuli, i.e., polyinosinic-polycytidylic acid (Poly I:C), which represents virus-derived double-stranded RNA and activates TLR3, lipopolysaccharide (LPS) (Gram-positive bacteria, TLR4), and synthetic single-stranded RNA oligoribonucleotide (ORN R-0006) (single--stranded viral RNA, TLR7/8). Previously, ligands have been also used for mimicking bacterial and viral stimuli (Diebold et al., 2004; Kumar et al., 2006; Park and Lee, 2013).

In the present study, we aimed to unravel how acute exposure to relatively low doses of fine PM alters the immune response to bacterial and viral stimuli. We used urban air $PM_{2.5\text{-}1}$ (fraction of PM that have an aerodynamic diameter of 2.5–1.0 μm) to expose the co-cultured cells in a two-step submerged exposure model. First, cells were primed with a dose range of $PM_{2.5\text{-}1}$ for 24 h, and in the second step, they were exposed to bacterial TLR4 ligand (LPS), viral ligand TLR3 (Poly I:C), and TLR7/8 ligand (ORN R 006).

2. Methods

2.1. Particulate matter samples

We used PM samples obtained from a sampling campaign conducted in China during 2014. PM samples were collected at Nanjing University (NJU) Xianlin campus. Details of the collection method, the origin of the sample, PM composition, and method of size-segregation have been described earlier by Jalava et al. (2015) and Rönkkö et al. (2018). In brief, we used $PM_{2.5\text{-}1}$ samples collected with high volume cascade impactor during night time. The sampler collects four different size ranges, from which the fine particle size was chosen for this study. $PM_{2.5\text{-}1}$ samples were stored at −20 °C until the day of the exposure. On the day of exposure $PM_{2.5\text{-}1}$ samples were suspended in 10% dimethyl sulfoxide (DMSO) (Sigma Aldrich, USA) in endotoxin tested water (Sigma, W1503) and sonicated for 30 min before utilization for exposure. After administrating the samples to cell culture medium, the final DMSO concentration was <0.3%.

2.2. Co-culture model

We utilized the A549-THP1 co-culture, which has been previously described by Kasurinen et al. (2018). Briefly, type II human alveolar epithelial cell line (A549) and human monocytic cell line THP-1 were purchased from ATCC ($ATCC^{R}CCL\text{-}185^{TM}$) and German Collection of Microorganisms and Cell Cultures (DSMZ, Germany) respectively. A549 cells were routinely maintained in Dulbecco's Modified Eagle Medium (DMEM), supplemented with 10% fetal bovine serum (FBS), 2 mM L-glutamine (L-glut), and 100 U/ml penicillin/streptomycin. THP-1 cells were maintained in Roswell Park Memorial Institute (RPMI) 1640 culture medium (Life Sciences, Gibco) supplemented with 10% FBS, 2 mM L-glut, and 100 U/ml pen/strep. THP-1 monocytic cells were differentiated to active macrophage-like cells before co-culture experiments with phorbol 12-myristate 13-acetate (PMA) (Kasurinen et al., 2018). After establishing co-culture, both cell lines were cultured in DMEM. All reagents were purchased from Sigma-Aldrich (USA) unless noted otherwise.

For the co-culture experiments, A549 cells were seeded in 12-well plates at a seeding density of 120,000 cells per well in FBS supplemented media and allowed them to attach for 4 h. Once the A549 cells were attached to the bottom of the well, media in the wells was aspirated and activated macrophage-like THP-1 cells were seeded at a seeding density of 24,000 cells per well on top of attached A549 cells. The co-cultured cells were incubated at 37 °C and 5% CO_2 for 40 h before exposing the cells to the first exposure. The seeded co-culture yields approximately 400,000–600,000 cells per well after the end of the exposure. One hour before the exposure the co-culture medium was replaced with fresh medium supplemented with 5% FBS, 2 mM L-Glut, and 100 U/ml (pen/strep).

2.3. Cell exposure

The study was designed as a two-step submerged exposure. Co-cultured cells were exposed to three concentrations of $PM_{2.5\text{-}1}$ (25 μg/ml, 50 μg/ml, and 100 μg/ml corresponding to 6.6, 13.2, and 26.3 μg/cm^2) in duplicate wells for 24 h at 37 °C and 5% CO_2.

The $PM_{2.5\text{-}1}$-exposed cells were then co-exposed for next 24 h to fixed doses of three different ligands: 1 μM of ORN R-0006 (TLR7/8 ligand, Miltenyi Biotech), 25 μg/ml of Poly IC (TLR3 ligand, Miltenyi Biotech), and 50 ng/ml of lipopolysaccharide (LPS) (TLR4 ligand). All the ligands were reconstituted and used according to the manufacturers' instructions. Various controls were included in the experimental setup, i.e. unexposed control, $PM_{2.5\text{-}1}$ control (for each concentration), ORN R-0006 control, Poly IC control, and LPS control.

At the end of co-exposure, cell culture media was retrieved and stored at −80 °C for the cytokine analysis. The cells were then detached using 1 ml trypsin-EDTA and 5 min incubation at 37 °C, followed by adding 100 μl of FBS to inactivate trypsin. 300 μl of the cell suspension was then separated for MTT (3-(4,5-dimethylthiazol-2-yl)-2,5-diphenyltetrazoliumbromide) assay and viability assay. The remaining 700 μl of cell suspension was centrifuged at 4000 RCF for 5 min at 4 °C. The supernatant was carefully removed, and the cell pellet was then suspended in PBS. FBS-free cell suspension was used for 2′,7′-dichlorodihydrofluorescein diacetate (H2DCF-DA) assay, propidium iodide (PI) exclusion assay, and thiol assay.

2.4. Inflammatory cytokine analysis

We performed the sandwich enzyme-linked immunosorbent assay (ELISA) for quantitative cytokine analysis from the co-culture cell supernatant samples stored at −80 °C. Measured pro-inflammatory

markers included interleukin 6 (IL-6), tumor necrosis factor-alpha (TNF-α) (all ELISA Ready-SET-Go kit, Invitrogen), interleukin 8 (IL-8) (ELISA, R&D-Systems, USA). All the ELISA's were performed according to the manufacturer's instruction for each kit.

2.5. Cellular metabolic activity

Cellular metabolic activity (CMA) was analyzed by treating 100 μl aliquots of cell suspension from each sample in duplicates with 25 μl of MTT solution (5 mg/ml in PBS) in 96 well plate for 2 h at 37 °C and 5% CO_2. During incubation, live cells uptake yellow MTT and metabolize it to purple formazan. After incubation, 100 μl of sodium dodecyl sulfate (SDS) lysis buffer was added to each well. Cells were then lysed for 2 h at 37 °C and 5% CO_2 followed by 30 min at room temperature on a plate shaker to release formazan from the cells. After incubation, absorbance was measured at 570 nm using a Synergy H1, Microplate reader (BioTek, USA). The absorbance values of the exposed cells were then normalized against the untreated controls and the percentage of cellular metabolic activity was calculated by the following formula: ((absorbance exposed/absorbance control) *100%).

2.6. Oxidative stress

2′,7′-dichlorodihydrofluorescein diacetate (H2DCF-DA) was used to measure the cellular oxidative stress. Cells suspended in PBS (100 μl aliquots) were pipetted to 96 well plate wells in duplicates. 8 μl of H2DCF-DA (0.5 μM in DMSO) was added to each well and 2′, 7' –dichlorofluorescein (DCF) fluorescence was measured at 3-time points (0, 30, and 60 min) using 485 nm excitation and 530 nm emission with Synergy H1 Microplate reader (BioTek, USA). Area under the curve (AUC) for the increasing fluorescence values against time was calculated using ((15*T60) + (30*T30) - (45*T0)) for all treated and control samples. The values for exposed samples were then normalized against unexposed control.

2.7. Membrane permeability

After the cellular oxidative stress measurement, the same 96-well plated cells were used for the PI exclusion test. We added 7.2 μl of PI solution (0.5 mg/ml in PBS) to each well and mixed the plate for 2 min on a plate shaker. The cells were incubated for 20 min at 37 °C and 5% CO_2 in a humidified incubator before measuring baseline PI fluorescence (540 nm excitation and 610 nm emission using Synergy H1 Microplate reader (BioTek, USA). Then 20 μl of lysis solution (10% Triton X-100 in double-distilled water) was added and the cells were incubated room temperature. After 20 min of incubation, maximum PI fluorescence was measured at the same settings as for baseline. The percentage of live cells was calculated by using formula (100-(($PI_{baseline}$/PI_{max})*100%)).

2.8. Viability with DAPI staining

Cell viability and proliferation were analyzed using DAPI staining. Every cell sample was stained with solution 13 (Acridine Orange (AO) and 4′6-diamidino-2-phenylidinole (DAPI) (Chemometec, Denmark) in a ratio of 19:1. Stained samples were analyzed with Nucleocounter NC-3000 (Chemometec, Denmark) using protocol provided by the manufacturer.

2.9. Cell cycle analysis

Duplicate experiments on separate culture plates were performed to obtain cells for cell cycle analysis. Briefly, cells were harvested after exposures and fixed using 70% ethanol. Fixed cells were then stored at −20 °C until analysis was performed. For analysis, cells were centrifuged at 400–500 RCF at 4 °C, and ethanol was discarded without disturbing the cell pellets. Cell pellets were washed with PBS, centrifuged, and suspended again in PBS before treating them with 15 μg/ml of RNAse-A dissolved in DNAse/RNAse-free water (Sigma-Aldrich, Italy) for 1 h at 50 °C on heat block in a darkroom. After incubation cells were then stained with propidium iodide (final concentration in sample tube 0.01 mg/ml) and incubated at 37 °C for 30 min. Samples were kept at 4 °C and in the dark until analyzed using a BD FACSCanto™ II (BD Biosciences, San Jose, CA, USA). Results were analyzed further using FLOWJO. Results were presented as percentages of cells in Sub-G1, G1-GO, and G2-M phase.

2.10. Apoptosis marker analysis

We analyzed the redox status of cellular thiols as a marker for apoptosis. 19 μl of the cell suspended in PBS was mixed with 1 μl of Solution 5 (VitaBright-48 (VB-48), Acridine Orange (AO), and Propidium Iodide (PI), ChemoMetec, Denmark). Samples were loaded on NC-Slide A8 and analyzed on Nucleocounter NC-3000 (ChemoMetec, Denmark) using a premade protocol provided by the manufacturer. The scatter plots obtained from Nucleocounter were analyzed using FlowJo software version 10 (FlowJo LLC, USA). Live and dead cells were gated, and then live cell populations were further marked to separate the low intensity and high intensity VB-48 stained cells. Cells that are apoptotic or with low levels of reduced thiols have low VB-48 stains. The percentage of cell with low-intensity VB-48 stains were considered as apoptotic cell population.

2.11. Statistical analyses

All experiments were performed three times and all analysis were run in duplicates. The data have been presented as means and standard error of means (SEM). The data of all studied variables were normally distributed and thus fulfilled assumptions of parametric testing. Levene's test was used to test the homogeneity of variances. Since they were unequal, comparisons between exposed samples and control samples as well as comparisons between different exposures were made using Welch's analysis of variance, followed by Dunnett's T3 post hoc test. Values of $P < 0.05$ were considered statistically significant. IBM SPSS statistics software, version 25 was used for all statistical analyses.

3. Results

PM stimulation increased the production of IL-6 in a dose-dependent manner in the co-cultured cells. Of the studied viral ligands, TLR7/8 induced the highest production of IL-6 whereas TLR3 induced a marginal increase in IL-6 production compared to unexposed control cells. TLR4 also significantly increased the IL-6 production relative to the unexposed control. In co-exposure to PM and TLR7/8, the IL-6 release of the cells increased significantly at the lowest PM dose when compared to responses of the cells after PM exposure only. However, PM and TLR7/8 co-exposure resulted in much lower IL-6 concentrations than for TLR 7/8 ligand alone. With the highest PM dose, IL-6 levels were not only lower than after exposure to TLR-7/8 ligand alone but they were also decreased when compared to IL-6 release after the cells were exposed to same PM mass without the ligand. Co-exposure to PM and TLR3 induced lower cytokine secretion than PM alone. In contrast, co-exposure to PM and TLR4 caused IL-6 production that was higher than that of cells exposed to either PM or TLR4 alone (Fig. 1).

PM increased the production of TNF-α dose-dependently. TLR7/8 induced the highest production of TNF-α, whereas TLR3 was not able to induce TNF-α production in our cell model. TLR4 induced slight but non-significant increase in TNF-α production. In PM and TLR7/8 co-exposures, production of TNF-α was approximately the same for all PM doses and comparable to the response after exposure to highest PM dose alone, but significantly lower than after exposure to TLR7/8 alone. Interestingly, when the cell model was co-exposed to PM and TLR3, cytokine secretion was lower than in stimulation with PM alone, but the

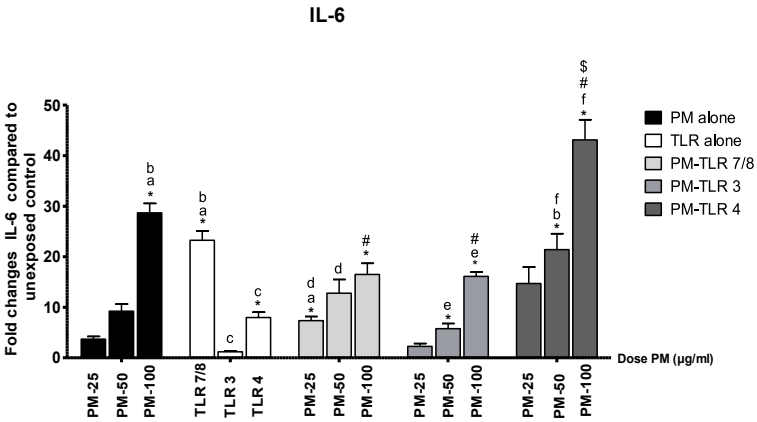

Fig. 1. IL-6 pro-inflammatory cytokine production was assessed after two-step submerged exposure. Co-cultured cells were first exposed to three doses (25, 50, 100 µg/ml) of $PM_{2.5\text{-}1}$ and after 24 h, to three different Toll-like receptor ligands (TLR7/8, TLR3, TLR4) for another 24 h. Figure shows mean ± SEM, n = 3. Significance was assumed at $p < 0.05$. * indicates significance from unexposed control. a indicates significance from PM-25. b indicates significance from PM-50. c indicates significance from PM-100. d indicates significance from TLR7/8. e indicates significance from TLR3. f indicates significance from TLR4. # indicates significance from ligand-PM-25. $ indicates significance from ligand-PM-50. ¤ indicates significance from ligand-PM100.

difference was not statistically significant. In contrast to other two ligands, cells primed PM responded to TLR4 exposure by significantly enhanced TNF-α production (Fig. 2).

In co-exposure to PM and TLR7/8, the production of IL-8 increased slightly for the lowest two doses when compared to respective PM dose alone. However, no significant indication of additive effects of PM and TLR7/8 was observed at any of the dose levels. Similar to TLR7/8, co-exposure to PM and TLR3 induced roughly the same level of cytokine secretion than PM. In contrast, co-exposure to PM and TLR4 caused IL-8 production that was higher than that of cells exposed to PM or TLR4 alone (Fig. 3).

PM alone induced a dose-dependent decrease in CMA. Studied TLR ligands alone did not affect the CMA when compared to the unexposed control. CMA following co-exposure to PM and TLR ligands did not differ from that observed after exposure to PM alone (Fig. 4).

PM alone, TLR ligands alone or co-exposure of PM and TLR did not induce any changes in intracellular ROS production compared to unexposed control cells (Fig. 5).

PM alone caused a slight dose-dependent decrease in cell membrane integrity. The studied ligands (TLR7/8, TLR3, and TLR4) did not affect the integrity of cell membranes as compared to unexposed control. The results of combined exposures were not different from PM alone exposures (Fig. 6A). Co-exposure to PM and TLR ligands slightly decreased cell viability compared to unexposed control and the respective PM dose alone, however, none of the changes were statistically significant (Fig. 6B).

PM alone increased dose-dependently the percentage of cells in the Sub-G1 phase. Of the studied TLR ligands, only TLR4 ligand caused a slight increase in the percentage of cells in the Sub-G1 phase. PM-TLR7/8 co-exposure increased the percentage of cells in the Sub-G1 phase and they induced slightly higher responses than the respective PM doses alone. (Fig. 7A).

Interestingly, PM alone, TLR7/8, TLR4 alone, or any of the PM-TLR co-exposures did not affect the percentages of cells in the G1-G0 phase. TLR3 alone significantly decreased the number of cells in the G1-G0 phase (Fig. 7B).

PM exposure induced a slight dose-dependent decrease in cells in G2-M phase, which was however statistically non-significant. Of the studied TLRs, only TLR3 caused a significant increase in cells in the G2-M phase when compared to control. Pre-exposure to PM reduced cellular responses to TLRs; the percentage of cells in the G2-M phase was significantly lower following co-exposure of PM-TLR7/8 and PM-TLR3 when compared to the respective exposures to ligands alone. (Fig. 7C).

PM alone induced a dose-dependent increase in the live cells with low levels of reduced thiols. Viral ligands TLR7/8 and TLR3 alone did not significantly affect the percentage of cells with reduced thiols when compared to unexposed control. However, when PM-treated cultures were treated with TLR ligands, there was a slight trend towards an

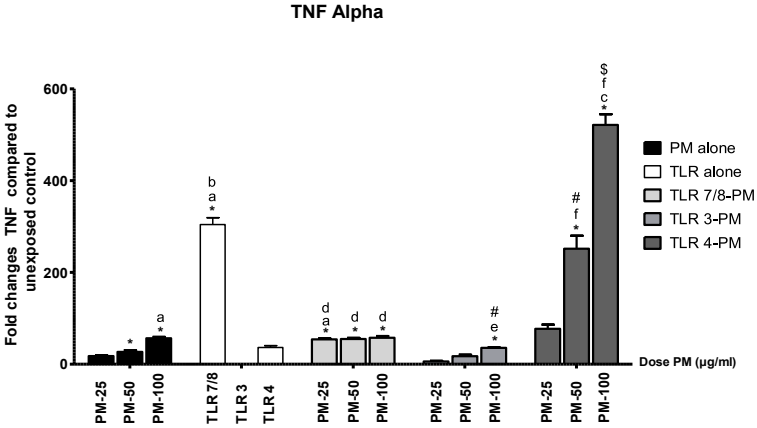

Fig. 2. TNF-α pro-inflammatory cytokine production was accessed after two-step submerged exposures described in Fig. 1. Figure shows mean ± SEM, n = 3. Significance was assumed at $p < 0.05$. * indicates significance from unexposed control. a indicates significance from PM-25. b indicates significance from PM-50. c indicates significance from PM-100. d indicates significance from TLR7/8. e indicates significance from TLR3. f indicates significance from TLR4. # indicates significance from ligand-PM-25. $ indicates significance from ligand-PM-50. ¤ indicates significance from ligand-PM100.

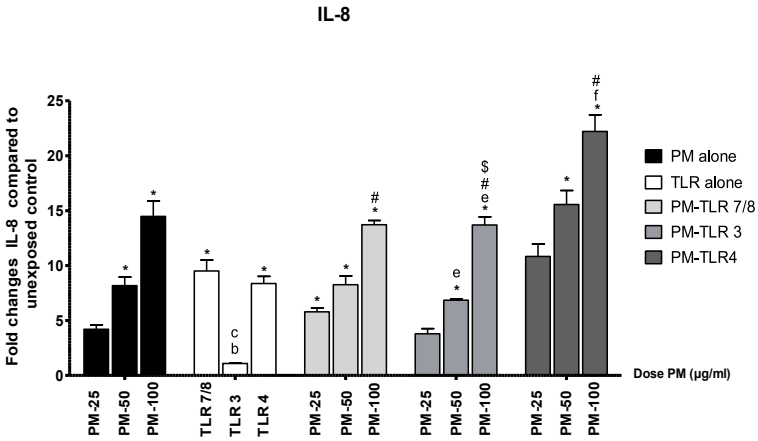

Fig. 3. IL-8 pro-inflammatory cytokine production was accessed after two-step submerged exposures described in Fig. 1. Figure shows mean ± SEM, n = 3. Significance was assumed at $p < 0.05$. * indicates significance from unexposed control. a indicates significance from PM-25. b indicates significance from PM-50. c indicates significance from PM-100. d indicates significance from TLR7/8. e indicates significance from TLR3. f indicates significance from TLR4. # indicates significance from ligand-PM-25. $ indicates significance from ligand-PM-50. ¤ indicates significance from ligand-PM100. PM alone increased the production of IL-8 dose-dependently. Of the studied ligands, TLR7/8 induced the highest, and TLR3 the lowest IL-8 production.

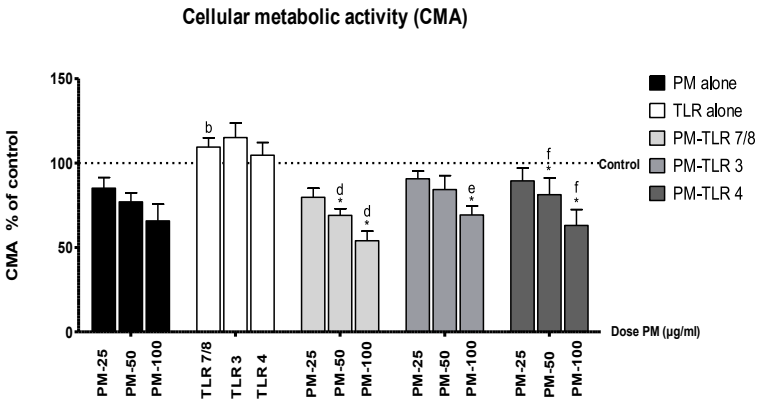

Fig. 4. Cellular metabolic activity (CMA) was assessed using the MTT after two-step submerged exposures described in Fig. 1. Figure shows mean ± SEM, n = 4. Significance was assumed at $p < 0.05$. * indicates significance from unexposed control. a indicates significance from PM-25. b indicates significance from PM-50. c indicates significance from PM-100. d indicates significance from TLR7/8. e indicates significance from TLR3. f indicates significance from TLR4. # indicates significance from ligand-PM-25. $ indicates significance from ligand-PM-50. ¤ indicates significance from ligand-PM100.

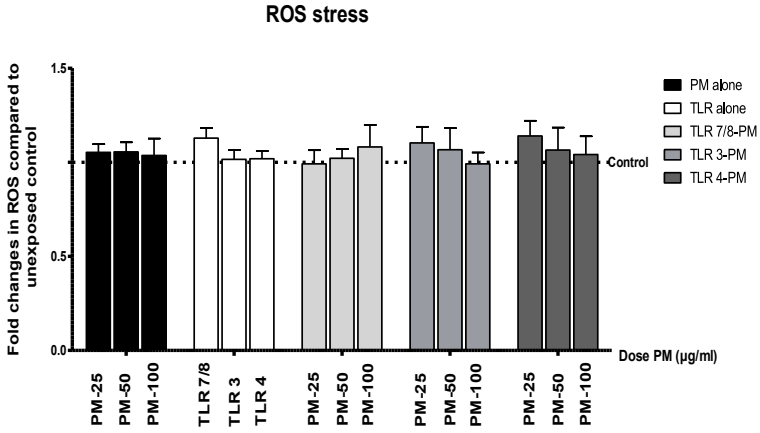

Fig. 5. Oxidative stress was assessed by using DCF-test after two-step submerged exposures described in Fig. 1. Figure shows mean ± SEM, n = 4.

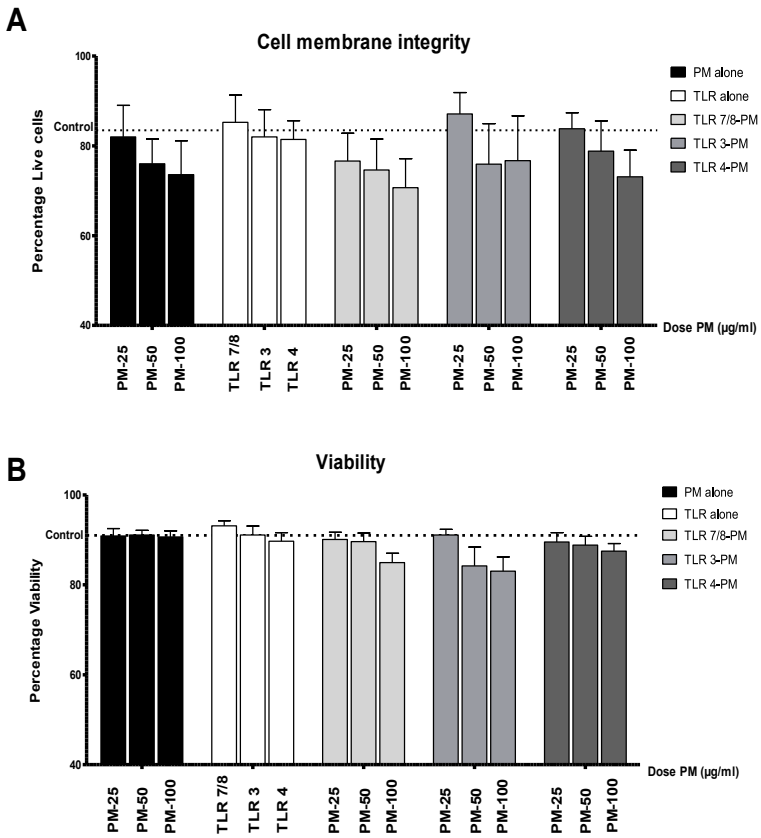

Fig. 6. A. Cell membrane integrity was assessed by using PI exclusion B. Viability was assessed by using DAPI staining after two-step submerged exposures described in Fig. 1. Figure shows mean ± SEM, n = 4.

increase in cells with depleted thiol levels as compared to the respective PM dose, but differences were not significant. Bacterial ligand (TLR4) alone induced a significant increase in cells with reduced thiol levels. However, when cell cultures were co-exposed to PM and TLR4, the percentage of cells with reduced thiol levels did not differ from those induced by respective doses of PM (Fig. 8).

4. Discussion

$PM_{2.5}$ exposure has been considered to impair the normal immune responses of the lung, rendering it susceptible to infections (Feng et al., 2016). In this study, we evaluated how exposure to $PM_{2.5\text{-}1}$ affects innate immune responses of A549-THP1 co-cultures against viral and bacterial stimuli. Alveolar epithelial cells serve as a physical barrier, which alongside the presence of immune cells constitutes an innate immune response. A comparative study on mono and co-culture of A549 epithelial cells and THP1 activated macrophages has concluded that the use of only one cell line can underestimate or overestimate the magnitude of adverse effects caused by PM (Kasurinen et al., 2018). Therefore, to better understand cell-cell communication, co-cultures were used as an in vitro model to mimic the lung barrier. Furthermore, previous studies have shown that $PM_{2.5}$ can induce pro-inflammatory cytokine expression in the lung epithelium and human macrophage cells by stimulating overexpression of genes for transcription factors and cytokines (Zhou et al., 2015; Zhu et al., 2019). In an in vivo study conducted by Zhao et al. (2016), $PM_{2.5}$ exposure disrupted the balance between M1 and M2 polarized macrophages, which caused an increase in the pro-inflammatory cytokines. Our results confirmed that relatively low doses of $PM_{2.5\text{-}1}$ can cause a modest increase in pro-inflammatory responses, measured as the production of IL-8, IL-6, and TNF-α, in A549 and THP1 co-culture.

We characterized the cytokine response of A549-THP1 co-culture to viral TLR ligands (TLR3, TLR7/8) and bacterial TLR ligand (TLR4). Results showed that both viral ligands caused an increase in IL-6 and IL-8 levels compared to control. However, response to TLR7/8 ligand was very high compared TLR3 ligand response. Our results are partially consistent with the study on primary airway epithelial cells, showing that exposure to TLR3 ligand increased IL-6, IL-8, and TNF-α production of the cells (Lever et al., 2015). Interestingly, in our study TLR3 ligand did not induce TNF-α production. TNF-α serves an important physiological role of activation of nuclear factor kappa-light-chain-enhancer of activated B cells (NF-Kβ) and influx of neutrophils to the site of inflammation (Schütze et al., 1995). A study on the A549-THP1 co-culture has concluded that TNF-α was secreted by activated macrophages and A549-THP1 co-culture when exposed to PM but not by PM-exposed A549 cells (Kasurinen et al., 2018). Furthermore, TNF-α has been detected in neither control A549 cells nor the cells exposed to cigarette smoke (Holownia et al., 2016). To our knowledge synthetic TLR7/8 ligand ORN R 006 has not been previously used in any other study on respiratory epithelial cells, however, TLR7 ligation with loxoribine or TLR8 ligation with Poly U has led to atypical activation of nuclear factor kappa-B (NFkB) pathway (Cherfils-Vicini et al., 2010). In

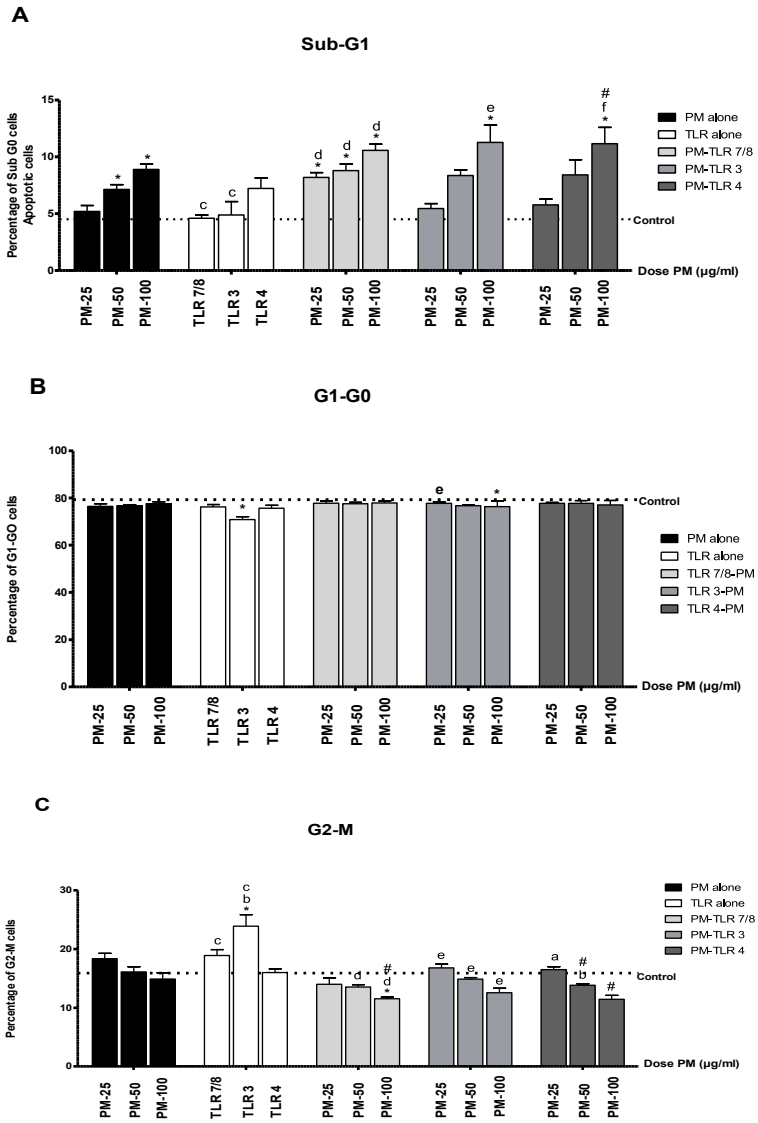

Fig. 7. Cell cycle analysis was performed using PI staining after two-step submerged exposure described in Fig. 1. A. Sub-G1 phase, Fig B. G1-G0 phase, and Fig C. G2-M phase. Figure shows mean ± SEM, n = 3. * indicates significance from unexposed control. a indicates significance from PM-25. b indicates significance from PM-50. c indicates significance from PM-100. d indicates significance from TLR7/8. e indicates significance from TLR3. f indicates significance from TLR4. # indicates significance from ligand-PM-25. $ indicates significance from ligand-PM-50.

our study, we assume that TLR7/8 activated NFkB has led to the induction of downstream inflammatory cytokines including IL-6 and IL-8, and TNF-α. On the other hand, TLR4 ligand (LPS) alone induced IL-6, IL-8, and TNF-α in the A549-THP1 co-culture, which is consistent with the results of the study that has been conducted on human lung mucoepidermoid carcinoma (H292) and THP-1 cells. LPS stimulation induced significant pro-inflammatory cytokines in both cell lines (Liu et al., 2018).

Co-cultures primed with $PM_{2.5\text{-}1}$ on subsequent exposure with viral ligand TLR7/8 showed no additive effect on the response of pro-inflammatory cytokines as the response remained roughly the same as for $PM_{2.5\text{-}1}$ alone. This indicates that in $PM_{2.5\text{-}1}$ primed co-cultures the pro-inflammatory response was altered against TLR7/8 ligand. Another viral ligand TLR3 behaved differently as it alone induced very low levels of IL-8 and IL-6 but not induce the production of TNF-α in co-culture. In addition, when PM primed co-cultures were exposed to TLR3 ligand, the production of IL-8 and IL-6 was not further increased. This indicates that in addition to low inflammatory potential of TLR3 ligand, it may also suppress responses induced by PM.

Several studies have indicated that urban particulate matter decreases the ability of the macrophage to phagocytize and weakens the capacity of alveolar macrophages as well as alveolar epithelium to mount an effective immune response against viral stimuli (Migliaccio et al., 2013; Xu et al., 2008; Zhou and Kobzik, 2007). Results from an in vivo study on mice also that ultrafine carbon particle exposure suppresses the early immune response in the lung. However, at day 7 inflammation and viral exacerbation increased drastically (Lambert et al., 2003). Therefore, in our study, it could be assumed that prior exposure to $PM_{2.5\text{-}1}$ decreased the ability of A549-THP1 co-culture to mount an effective immune response which may potentially lead to

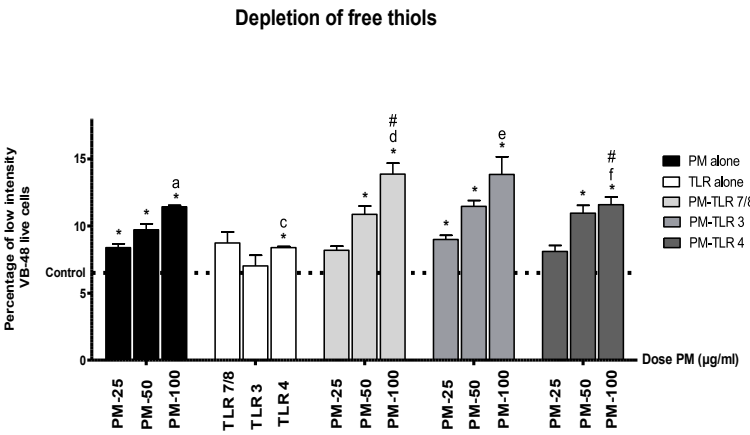

Fig. 8. Cells with depleted free thiols were determined from VB-48™ stain intensity after two-step submerged exposure described in Fig. 1. Figure shows mean ± SEM, n = 3. Significance was assumed at $p < 0.05$. * indicates significance from unexposed control. a indicates significance from PM-25. b indicates significance from PM-50. c indicates significance from PM-100. d indicates significance from TLR7/8. e indicates significance from TLR3. f indicates significance from TLR4. # indicates significance from ligand-PM-25. $ indicates significance from ligand-PM-50.

more exaggerated viral infection. Further studies using real viral exposures are needed to estimate the virulence of the viral infection and to understand the exact mechanisms.

In contrast to viral ligands, bacterial TLR4 ligand added to $PM_{2.5\text{-}1}$ pre-treated co-culture caused a dramatic increase in the IL-8, TNF-α, and IL-6 levels indicating a possible sensitization of the immune cells. Our results are consistent with the study performed on secondary lung epithelial BEAS-2B cells in a co-culture with purified monocytes (Chaudhuri et al., 2010). The study showed that diesel exhaust particles override the nature of the inflammatory response to LPS and produced an exaggerated pro-inflammatory response. In a more recent study, exposure to PM at low concentrations to murine macrophages has caused priming of the respective immune cells resulting in hyper-inflammatory response to subsequent LPS exposure (Gawda et al., 2018). The hyperinflammatory response may be attributed to the fact that $PM_{2.5\text{-}1}$ can also contain bacterial endotoxin in its biological fraction; if present, it can cause the activation of TLR-MYD 88 by activation of TLR4 receptor leading to downstream activation of NF-κB mediated inflammatory response. Once activated it can increase the expression of pro-inflammatory markers and induce expression of more TLR4 receptors (Bauer et al., 2012; Peden, 2011). Therefore, subsequent exposure to bacterial stimuli may lead to a more abrupt pro-inflammatory response in the form of a cytokine storm, rendering individuals susceptible to acquire the worse form of respiratory bacterial exacerbations.

In this study, any of the stimulations did not induce significant changes to ROS stress. Moreover, no drastic changes in viability were seen. Activation of pro-inflammatory pathways are often associated with ROS stress generated by the exposure to PM on lung epithelial cells. However, some studies have previously shown that in co-culture model the presence of immune cells caused a mitigating effect on the oxidative stress in the alveolar epithelial cells (Kasurinen et al., 2018; Persson et al., 2013). Persson et al. (2013) showed that the presence of activated macrophages in A549 culture causes effective sequestering of Fe-ions from the media and thus minimizing Fe driven oxidative reaction. Alternatively, it is possible that the oxidative stress has occurred much earlier than was our measuring time-point. In this study, we used non-cytotoxic doses of $PM_{2.5\text{-}1}$, TLR4, TLR3, and TLR7/8 to eliminate the hindering effect of cytotoxic responses to other measured endpoints. The aim was to investigate the role of $PM_{2.5\text{-}1}$ in modulating the subsequent innate immunity responses i.e., the release of different pro-inflammatory cytokines, which may play a role in the susceptibility to bacterial and viral infection in PM $_{2.5\text{-}1}$ exposed co-culture.

Cellular metabolic activity of A549-THP1 co-cultured cells reduced significantly with the $PM_{2.5\text{-}1}$ exposure at middle and higher doses, whereas TLR ligands alone did not affect CMA negatively. In subsequent exposures, reduction in CMA was associated with doses of PM with slight or no improvement in CMA after the addition of viral ligands TLR3 and TLR7/8 or bacterial ligand TLR4. Previous studies on a similar cell model exposed to PM originating from different sources concluded that reduction in CMA is caused by activation of macrophages in the co-culture, which produces a mitigation effect on the majority of A549 cells (Kasurinen et al., 2018).

Cellular glutathione (GSH) depletion is used as an indicator of early apoptotic cells (Coppola and Ghibelli, 2000). In this study, we determined the level of free thiols such as GSH. Our results suggested, that $PM_{2.5\text{-}1}$ is associated with an increased number of cells with low levels of free thiols, especially at higher doses, whereas viral ligands TLR3 and TLR7/8 alone did not affect the status of reduced thiols in cells. Adjacent to the individual exposures, cells that were first treated with $PM_{2.5\text{-}1}$ and later with TLR3 or TLR7/8 viral ligands showed slight or no changes in free thiol levels when compared to $PM_{2.5\text{-}1}$ alone. On the other hand, bacterial TLR4 ligand-induced a significant increase in the number of cells with depleted free thiols when compared to control. However, the effect of TLR4 diminished in cells, which were pre-exposed to $PM_{2.5\text{-}1}$. This indicated that early apoptosis would be solely due to the activation of macrophages by $PM_{2.5\text{-}1}$, which caused a reduction in CMA leading to a higher number of cells undergoing apoptosis. Furthermore, it could also be assumed that the reduction in cellular thiol levels works independently of ROS stress, since, in our exposure, no significant ROS stress was indicated. This assumption is in line with previous results concluding a necessary and critical role for GSH loss in apoptosis and uncoupling GSH depletion from ROS formation (Rodrigo Franco et al., 2007).

Lastly, we also studied the cell cycle phase distribution of exposed cells. Exposure to $PM_{2.5\text{-}1}$ increased the percentage of cells in the Sub-G1 phase and reduced the percentage of cells in the G2-M phase, indicating an increase in the number of cells undergoing cell cycle arrest at the G1 phase as well as apoptosis. As discussed above, reduction in CMA caused by the presence of activated macrophages in the co-culture may have resulted in an increased number of cells in the Sub-G1 phase. Kaplon et al. (2015) reviewed the interconnection of cellular metabolism and cell cycle arrest and concluded that decreased CMA may lead to cell cycle arrest and eventually apoptosis. Contrary to $PM_{2.5\text{-}1}$ alone, individual exposure to viral ligands TLR3 and TLR7/8 increased the percentage of cells in the G2-M phase. Davy and Doorbar (2007) reviewed various mechanisms by which RNA, DNA, and retroviruses are known to induce cell cycle arrest at the G2-M phase and how this alteration helps viruses in survival and replication within the host cells during infection. For example, avian coronavirus infectious bronchitis virus has induced

G2-M phase arrest to promote favorable conditions for viral replication (Dove et al., 2006). Therefore, we assumed that the increase in the number of cells in the G2-M phase is associated with viral ligand-induced cell cycle arrest to progeny viral production. However, viral ligands failed to induce modifications in the G2-M phase in $PM_{2.5\text{-}1}$ primed co-cultures. From our results, it can be speculated that prior exposure to PM may alter the viral virulence. On the other hand, bacterial ligand TLR4 increased the number of cells in the Sub-G1 phase, with no effect on G1-G0 and G2-M phases. In correlation to the results from thiol assay, which accounts for the early apoptotic cells; pretreatment of cells with $PM_{2.5\text{-}1}$ slightly increased the number of cells in the Sub-G1 phase, especially at higher doses of $PM_{2.5\text{-}1}$. The response was, however, not statistically significant when compared to $PM_{2.5\text{-}1}$ alone but it shows that co-exposure with TLR4 ligand has some effect on the number of cells in the Sub-G1 phase. Therefore, our results indicate that $PM_{2.5\text{-}1}$ priming modifies immune responses against bacterial and viral stimulation in the studied cell model.

5. Conclusion

$PM_{2.5\text{-}1}$ exposure altered the pro-inflammatory cytokine response to both bacterial and viral stimuli in the alveolar lung cell model. $PM_{2.5\text{-}1}$ increased the sensitivity of the A549-THP1 co-culture to produce pro-inflammatory cytokines, which potentially leads to hyperinflammatory response against bacterial infection. Instead, virus-mediated pro-inflammatory effects were suppressed if the co-culture model of the alveolar barrier was primed with $PM_{2.5\text{-}1}$. These findings provide insight into the underlying immunomodulatory effects of fine particulate matter, which potentially leads to susceptibility to respiratory infections.

Funding

The work was supported by Päivikki and Sakari Sohlberg Foundation, Juho Vainio Foundation, and the Academy of Finland grants (319245, 294081, 287982).

Author contribution

Muhammad Ali Shahbaz: Formal analysis, Investigation, Methodology, Data curation, Visualization, Writing-original draft, Writing-review, and editing. Maria-Viola Martikainen: Investigation, Writing-review, and editing. Teemu J. Rönkkö: Investigation, Writing-editing, and reviewing. Mika Kompppula: Resources, Writing-review, and editing. Pasi I. Jalava: Funding acquisition, Methodology, Resources, Supervision, Validation, Writing-review, and editing. Marjut Roponen: Conceptualization, Funding acquisition, Methodology, Project administration, Resources, Supervision, Validation, Writing-review, and editing.

Declaration of competing interest

The authors declare that they have no known competing financial interests or personal relationships that could have appeared to influence the work reported in this paper.

Acknowledgments

The authors wish to thank Ms Hanne Vainikainen, MSc Tuukka Ihantola and MSc Henri Hakkarainen for their technical support.

References

Alexopoulou, L., Holt, A.C., Medzhitov, R., Flavell, R.A., 2001. Recognition of double-stranded RNA and activation of NF-kappaB by Toll-like receptor 3. Nature 413, 732–738. https://doi.org/10.1038/35099560.

Bauer, R.N., Diaz-Sanchez, D., Jaspers, I., 2012. Effects of air pollutants on innate immunity: the role of Toll-like receptors and nucleotide-binding oligomerization domain–like receptors. J. Allergy Clin. Immunol. 129, 14–24. https://doi.org/10.1016/j.jaci.2011.11.004.

Beutler, B., 2002. TLR4 as the mammalian endotoxin sensor. Curr. Top. Microbiol. Immunol. 270, 109–120. https://doi.org/10.1007/978-3-642-59430-4_7.

Bhattacharya, J., Westphalen, K., 2016. Macrophage-epithelial interactions in pulmonary alveoli. Semin. Immunopathol. 38, 461–469. https://doi.org/10.1007/s00281-016-0569-x.

Chaudhuri, N., Paiva, C., Donaldson, K., Duffin, R., Parker, L.C., Sabroe, I., 2010. Diesel exhaust particles override natural injury-limiting pathways in the lung. Am. J. Physiol. Lung Cell Mol. Physiol. 299, L263–L271. https://doi.org/10.1152/ajplung.00297.2009.

Cherfils-Vicini, J., Platonova, S., Gillard, M., Laurans, L., Validire, P., Caliandro, R., Magdeleinat, P., Mami-Chouaib, F., Dieu-Nosjean, M., Fridman, W., Damotte, D., Sautès-Fridman, C., Cremer, I., 2010. Triggering of TLR7 and TLR8 expressed by human lung cancer cells induces cell survival and chemoresistance. J. Clin. Invest. 120, 1285–1297. https://doi.org/10.1172/JCI36551.

Ciencewicki, J., Jaspers, I., 2007. Air pollution and respiratory viral infection. Inhal. Toxicol. 19, 1135–1146. https://doi.org/10.1080/08958370701665434.

Cohen, A.J., Brauer, M., Burnett, R., Anderson, H.R., Frostad, J., Estep, K., Balakrishnan, K., Brunekreef, B., Dandona, L., Dandona, R., Feigin, V., Freedman, G., Hubbell, B., Jobling, A., Kan, H., Knibbs, L., Liu, Y., Martin, R., Morawska, L., Pope, C.A., Shin, H., Straif, K., Shaddick, G., Thomas, M., van Dingenen, R., van Donkelaar, A., Vos, T., Murray, C.J.L., Forouzanfar, M.H., 2017. Estimates and 25-year trends of the global burden of disease attributable to ambient air pollution: an analysis of data from the Global Burden of Diseases Study 2015. Lancet 389, 1907–1918. https://doi.org/10.1016/S0140-6736(17)30505-6.

Coppola, S., Ghibelli, L., 2000. GSH extrusion and and the mitochondrial pathway of apoptotic signalling. Biochem. Soc. Trans. 28, 56–61. https://doi.org/10.1042/bst0280056.

Croft, D.P., Zhang, W., Lin, S., Thurston, S.W., Hopke, P.K., Masiol, M., Squizzato, S., van Wijngaarden, E., Utell, M.J., Rich, D.Q., 2019. The association between respiratory infection and air pollution in the setting of air quality policy and economic change. Annals of the American Thoracic Society 16, 321–330. https://doi.org/10.1513/AnnalsATS.201810-691OC.

Davy, C., Doorbar, J., 2007. G2/M cell cycle arrest in the life cycle of viruses. Virology 368, 219–226. https://doi.org/10.1016/j.virol.2007.05.043.

Dehai, C., Bo, P., Qiang, T., Lihua, S., Fang, L., Shi, J., Jingyan, C., Yan, Y., Guangbin, W., Zhenjun, Y., 2014. Enhanced invasion of lung adenocarcinoma cells after co-culture with THP-1-derived macrophages via the induction of EMT by IL-6. Immunol. Lett. 160, 1–10. https://doi.org/10.1016/j.imlet.2014.03.004.

Diebold, S.S., Kaisho, T., Hemmi, H., Akira, S., Reis e Sousa, C., 2004. Innate antiviral responses by means of TLR7-mediated recognition of single-stranded RNA. Science 303, 1529–1531. https://doi.org/10.1126/science.1093616.

Dove, B., Brooks, G., Bicknell, K., Wurm, T., Hiscox, J.A., 2006. Cell cycle perturbations induced by infection with the coronavirus infectious bronchitis virus and their effect on virus replication. J. Virol. 80, 4147–4156.

Feng, S., Gao, D., Liao, F., Zhou, F., Wang, X., 2016. The health effects of ambient PM2.5 and potential mechanisms. Ecotoxicol. Environ. Saf. 128, 67–74. https://doi.org/10.1016/j.ecoenv.2016.01.030.

Franco, Rodrigo, Panayiotidis, Mihalis I., Cidlowski, John A., 2007. Glutathione depletion is necessary for apoptosis in lymphoid cells independent of reactive oxygen species formation. J. Biol. Chem. 282, 30452–30465. https://doi.org/10.1074/jbc.M703091200.

Gawda, A., Majka, G., Nowak, B., Śróttek, M., Walczewska, M., Marcinkiewicz, J., 2018. Air particulate matter SRM 1648a primes macrophages to hyperinflammatory response after LPS stimulation. Inflamm. Res. 67, 765–776. https://doi.org/10.1007/s00011-018-1165-4.

Guillot, L., Goffic, R.L., Bloch, S., Escriou, N., Akira, S., Chignard, M., Si-Tahar, M., 2005. Involvement of toll-like receptor 3 in the immune response of lung epithelial cells to double-stranded RNA and influenza A virus. J. Biol. Chem. 280, 5571–5580. https://doi.org/10.1074/jbc.M410592200.

Heil, F., Hemmi, H., Hochrein, H., Ampenberger, F., Kirschning, C., Akira, S., Lipford, G., Wagner, H., Bauer, S., 2004. Species-specific recognition of single-stranded RNA via toll-like receptor 7 and 8. Science 303, 1526–1529. https://doi.org/10.1126/science.1093620.

Hertz, C.J., Wu, Q., Porter, E.M., Zhang, Y.J., Weismüller, K., Godowski, P.J., Ganz, T., Randell, S.H., Modlin, R.L., 2003. Activation of Toll-like receptor 2 on human tracheobronchial epithelial cells induces the antimicrobial peptide human beta defensin-2. J. Immunol. 171, 6820–6826. https://doi.org/10.4049/jimmunol.171.12.6820.

Holownia, A., Wielgat, P., Kwolek, A., Jackowski, K., Braszko, J.J., 2015. Crosstalk between Co-cultured A549 cells and THP1 cells exposed to cigarette smoke. Adv. Exp. Med. Biol. 858, 47–55. https://doi.org/10.1007/5584_2015_112.

Holownia, A., Wielgat, P., Rysiak, E., Braszko, J.J., 2016. Intracellular and extracellular cytokines in A549 cells and THP1 cells exposed to cigarette smoke. Adv. Exp. Med. Biol. 910, 39–45. https://doi.org/10.1007/5584_2016_214.

Horne, B.D., Joy, E.A., Hofmann, M.G., Gesteland, P.H., Cannon, J.B., Lefler, J.S., Blagev, D.P., Korgenski, E.K., Torosyan, N., Hansen, G.I., Kartchner, D., Pope, C.A., 2018. Short-term elevation of fine particulate matter air pollution and acute lower respiratory infection. Am. J. Respir. Crit. Care Med. 198, 759–766. https://doi.org/10.1164/rccm.201709-1883OC.

Jalava, P.I., Wang, Q., Kuuspalo, K., Ruusunen, J., Hao, L., Fang, D., Väisänen, O., Ruuskanen, A., Sippula, O., Happo, M.S., Uski, O., Kasurinen, S., Torvela, T., Koponen, H., Lehtinen, K.E.J., Komppula, M., Gu, C., Jokiniemi, J., Hirvonen, M.-, 2015. Day and night variation in chemical composition and toxicological responses

of size segregated urban air PM samples in a high air pollution situation. Atmos. Environ. 120, 427–437. https://doi.org/10.1016/j.atmosenv.2015.08.089.
Kaplon, J., van Dam, L., Peeper, D., 2015. Two-way communication between the metabolic and cell cycle machineries: the molecular basis. Cell Cycle 14, 2022–2032. https://doi.org/10.1080/15384101.2015.1044172.
Kasurinen, S., Happo, M.S., Rönkkö, T.J., Orasche, J., Jokiniemi, J., Kortelainen, M., Tissari, J., Zimmermann, R., Hirvonen, M., Jalava, P.I., 2018. Differences between co-cultures and monocultures in testing the toxicity of particulate matter derived from log wood and pellet combustion. PloS One 13, e0192453. https://doi.org/10.1371/journal.pone.0192453.
Kelly, F.J., Fussell, J.C., 2012. Size, source and chemical composition as determinants of toxicity attributable to ambient particulate matter. Atmos. Environ. 60, 504–526. https://doi.org/10.1016/j.atmosenv.2012.06.039.
Kumar, A., Zhang, J., Yu, F.X., 2006. Toll-like receptor 3 agonist poly(I:C)-induced antiviral response in human corneal epithelial cells. Immunology 117, 11–21. https://doi.org/10.1111/j.1365-2567.2005.02258.x.
Lambert, A.L., Trasti, F.S., Mangum, J.B., Everitt, J.I., 2003. Effect of preexposure to ultrafine carbon black on respiratory syncytial virus infection in mice. Toxicol. Sci. 72, 331–338. https://doi.org/10.1093/toxsci/kfg031.
Lever, A.R., Park, H., Mulhern, T.J., Jackson, G.R., Comolli, J.C., Borenstein, J.T., Hayden, P.J., Prantil-Baun, R., 2015. Comprehensive evaluation of poly(I:C) induced inflammatory response in an airway epithelial model. Physiological Reports 3, e12334–n/a. https://doi.org/10.14814/phy2.12334.
Liu, X., Yin, S., Chen, Y., Wu, Y., Zheng, W., Dong, H., Bai, Y., Qin, Y., Li, J., Feng, S., Zhao, P., 2018. LPS-induced proinflammatory cytokine expression in human airway epithelial cells and macrophages via NF-κB, STAT3 or AP-1 activation. Mol. Med. Rep. 17, 5484–5491. https://doi.org/10.3892/mmr.2018.8542.
Medzhitov, R., 2001. Toll-like receptors and innate immunity. Nat. Rev. Immunol. 1, 135–145. https://doi.org/10.1038/35100529.
Migliaccio, C.T., Kobos, E., King, Q.O., Porter, V., Jessop, F., Ward, T., 2013. Adverse effects of wood smoke PM(2.5) exposure on macrophage functions. Inhal. Toxicol. 25, 67–76. https://doi.org/10.3109/08958378.2012.756086.
Mushtaq, N., Ezzati, M., Hall, L., Dickson, I., Kirwan, M., Png, K.M.Y., Mudway, I.S., Grigg, J., 2011. Adhesion of Streptococcus pneumoniae to human airway epithelial cells exposed to urban particulate matter. e2 J. Allergy Clin. Immunol. 127, 1236–1242. https://doi.org/10.1016/j.jaci.2010.11.039.
Park, B.S., Lee, J., 2013. Recognition of lipopolysaccharide pattern by TLR4 complexes. Exp. Mol. Med. 45, e66. https://doi.org/10.1038/emm.2013.97.
Peden, D.B., 2011. The role of oxidative stress and innate immunity in O(3) and endotoxin-induced human allergic airway disease. Immunol. Rev. 242, 91–105. https://doi.org/10.1111/j.1600-065X.2011.01035.x.
Persson, H.L., Vainikka, L.K., Eriksson, I., Wennerström, U., 2013. TNF–stimulated macrophages protect A549 lung cells against iron and oxidation. Exp. Toxicol. Pathol. 65, 81–89. https://doi.org/10.1016/j.etp.2011.06.004.
Rönkkö, T.J., Jalava, P.I., Happo, M.S., Kasurinen, S., Sippula, O., Leskinen, A., Koponen, H., Kuuspalo, K., Ruusunen, J., Väisänen, O., Hao, L., Ruuskanen, A., Orasche, J., Fang, D., Zhang, L., Lehtinen, K.E.J., Zhao, Y., Gu, C., Wang, Q., Jokiniemi, J., Komppula, M., Hirvonen, M., 2018. Emissions and atmospheric processes influence the chemical composition and toxicological properties of urban air particulate matter in Nanjing, China. Sci. Total Environ. 639, 1290–1310. https://doi.org/10.1016/j.scitotenv.2018.05.260.
Schütze, S., Wiegmann, K., Machleidt, T., Krönke, M., 1995. TNF-induced activation of NF-κB. Immunobiology 193, 193–203. https://doi.org/10.1016/S0171-2985(11)80543-7.
Sha, Q., Truong-Tran, A.Q., Plitt, J.R., Beck, L.A., Schleimer, R.P., 2004. Activation of airway epithelial cells by toll-like receptor agonists. Am. J. Respir. Cell Mol. Biol. 31, 358–364. https://doi.org/10.1165/rcmb.2003-0388OC.
Takeuchi, O., Hoshino, K., Akira, S., 2000. Cutting edge: TLR2-deficient and MyD88-deficient mice are highly susceptible to Staphylococcus aureus infection. J. Immunol. 165, 5392–5396. https://doi.org/10.4049/jimmunol.165.10.5392.
US EPA, O., 2016. Particulate Matter (PM) Pollution, 2019.
Wei, T., Tang, M., 2018. Biological effects of airborne fine particulate matter (PM2.5) exposure on pulmonary immune system. Environ. Toxicol. Pharmacol. 60, 195–201. https://doi.org/10.1016/j.etap.2018.04.004.
Wetzler, L.M., 2003. The role of Toll-like receptor 2 in microbial disease and immunity. Vaccine 21 (Suppl. 2), 55. https://doi.org/10.1016/s0264-410x(03)00201-9.
Wu, X., Nethery, R., Benjamin, M., Braun, D., Dominici, F., 2020. Exposure to Air Pollution and COVID-19 Mortality in the United States: A Nationwide Cross-Sectional Study.
Xing, Y., Xu, Y., Shi, M., Lian, Y., 2016. The impact of PM2.5 on the human respiratory system. J. Thorac. Dis. 8, E69–E74. https://doi.org/10.3978/j.issn.2072-1439.2016.01.19.
Xu, D., Huang, N., Wang, Q., Liu, H., 2008. [Study of ambient PM2.5 on the influence of the inflammation injury and the immune function of subchronic exposure rats]. Wei Sheng Yan Jiu 37, 423–428.
Zhang, D., Li, Y., Chen, Q., Jiang, Y., Chu, C., Ding, Y., Yu, Y., Fan, Y., Shi, J., Luo, Y., Zhou, W., 2019. The relationship between air quality and respiratory pathogens among children in Suzhou City. Ital. J. Pediatr. 45, 1–10. https://doi.org/10.1186/s13052-019-0702-2.
Zhao, Q., Chen, H., Yang, T., Rui, W., Liu, F., Zhang, F., Zhao, Y., Ding, W., 2016. Direct effects of airborne PM2.5 exposure on macrophage polarizations. Biochim. Biophys. Acta 1860, 2835–2843. https://doi.org/10.1016/j.bbagen.2016.03.033.
Zhou, H., Kobzik, L., 2007. Effect of concentrated ambient particles on macrophage phagocytosis and killing of Streptococcus pneumoniae. Am. J. Respir. Cell Mol. Biol. 36, 460–465. https://doi.org/10.1165/rcmb.2006-0293OC.
Zhou, Z., Liu, Y., Duan, F., Qin, M., Wu, F., Sheng, W., Yang, L., Liu, J., He, K., 2015. Transcriptomic analyses of the biological effects of airborne PM2.5 exposure on human bronchial epithelial cells. PloS One 10, e0138267. https://doi.org/10.1371/journal.pone.0138267.
Zhu, J., Zhao, Y., Gao, Y., Li, C., Zhou, L., Qi, W., Zhang, Y., Ye, L., 2019. Effects of different components of PM2.5 on the expression levels of NF-κB family gene mRNA and inflammatory molecules in human macrophage. Int. J. Environ. Res. Publ. Health 16, 1408. https://doi.org/10.3390/ijerph16081408.

II

Human-derived air–liquid interface cultures decipher Alzheimer's disease–SARS-CoV-2 crosstalk in the olfactory mucosa

Shahbaz, M. A, Kuivanen, S*, Lampinen, R*, Mussalo, L, Hron, T, Závodná, T, Ojha, R, Krejčík, Z, Saveleva, L, Tahir, N. A, Kalapudas, J, Koivisto, A. M, Penttilä, E, Löppönen, H, Singh, P, Topinka, J, Vapalahti, O, Chew, S, Balistreri, G, Kanninen, K. M

Journal of Neuroinflammation, 20(1), 1–23, 2023.

Journal of Neuroinflammation

RESEARCH

Open Access

Human-derived air–liquid interface cultures decipher Alzheimer's disease–SARS-CoV-2 crosstalk in the olfactory mucosa

Muhammad Ali Shahbaz[1], Suvi Kuivanen[2,3†], Riikka Lampinen[1†], Laura Mussalo[1], Tomáš Hron[4], Táňa Závodná[5], Ravi Ojha[2], Zdeněk Krejčík[5], Liudmila Saveleva[1], Numan Ahmad Tahir[1], Juho Kalapudas[6], Anne M. Koivisto[6,7,8], Elina Penttilä[9], Heikki Löppönen[9], Prateek Singh[10], Jan Topinka[5], Olli Vapalahti[2], Sweelin Chew[1], Giuseppe Balistreri[2,11] and Katja M. Kanninen[1*]

Abstract

Background The neurological effects of the coronavirus disease of 2019 (COVID-19) raise concerns about potential long-term consequences, such as an increased risk of Alzheimer's disease (AD). Neuroinflammation and other AD-associated pathologies are also suggested to increase the risk of serious SARS-CoV-2 infection. Anosmia is a common neurological symptom reported in COVID-19 and in early AD. The olfactory mucosa (OM) is important for the perception of smell and a proposed site of viral entry to the brain. However, little is known about SARS-CoV-2 infection at the OM of individuals with AD.

Methods To address this gap, we established a 3D in vitro model of the OM from primary cells derived from cognitively healthy and AD individuals. We cultured the cells at the air–liquid interface (ALI) to study SARS-CoV-2 infection under controlled experimental conditions. Primary OM cells in ALI expressed angiotensin-converting enzyme 2 (ACE-2), neuropilin-1 (NRP-1), and several other known SARS-CoV-2 receptor and were highly vulnerable to infection. Infection was determined by secreted viral RNA content and confirmed with SARS-CoV-2 nucleocapsid protein (NP) in the infected cells by immunocytochemistry. Differential responses of healthy and AD individuals-derived OM cells to SARS-CoV-2 were determined by RNA sequencing.

Results Results indicate that cells derived from cognitively healthy donors and individuals with AD do not differ in susceptibility to infection with the wild-type SARS-CoV-2 virus. However, transcriptomic signatures in cells from individuals with AD are highly distinct. Specifically, the cells from AD patients that were infected with the virus showed increased levels of oxidative stress, desensitized inflammation and immune responses, and alterations to genes associated with olfaction. These results imply that individuals with AD may be at a greater risk of experiencing severe outcomes from the infection, potentially driven by pre-existing neuroinflammation.

Conclusions The study sheds light on the interplay between AD pathology and SARS-CoV-2 infection. Altered transcriptomic signatures in AD cells may contribute to unique symptoms and a more severe disease course, with a notable involvement of neuroinflammation. Furthermore, the research emphasizes the need for targeted interventions to enhance outcomes for AD patients with viral infection. The study is crucial to better comprehend the relationship

†Suvi Kuivanen and Riikka Lampinen contributed equally to this work.

*Correspondence:
Katja M. Kanninen
katja.kanninen@uef.fi
Full list of author information is available at the end of the article

between AD, COVID-19, and anosmia. It highlights the importance of ongoing research to develop more effective treatments for those at high risk of severe SARS-CoV-2 infection.

Keywords COVID-19, Alzheimer's disease, Neurological manifestations, SARS-CoV-2, Olfactory, Anosmia, Air–liquid interface, Inflammation, Immune responses

Graphical Abstract

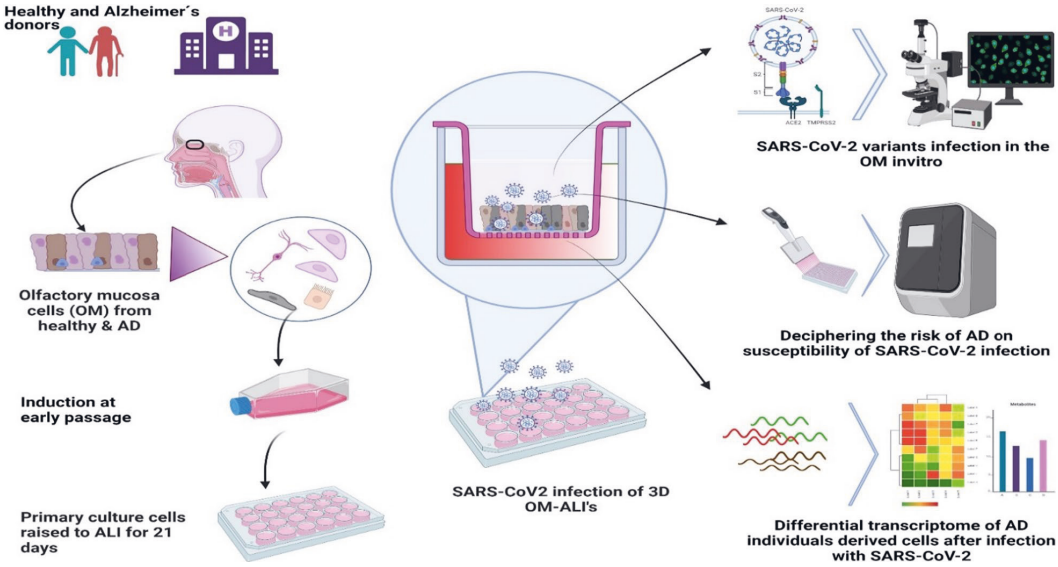

Introduction

Coronavirus disease (COVID-19) caused by severe acute respiratory coronavirus 2 (SARS-CoV-2) persists as a serious global health problem after three years into the pandemic. As of December 2022, there have been 652 million confirmed cases of COVID-19, including 6.7 million deaths, reported to the World Health Organization (WHO). It has been observed since the early days of the pandemic that SARS-CoV-2 predominantly attacks the human respiratory system, but also causes dysfunction in other organs including the central nervous system (CNS). A wide range of neurological symptoms has been reported to accompany the disease and affect its course. Olfactory dysfunction was recognized early in the COVID-19 pandemic [1–3] and is a strong and consistent symptom associated with SARS-CoV-2 infection [4]. Most patients show extensive or complete recovery of the ability to smell within 2–3 weeks of the first symptoms [5, 6]. However, in about 10–20% of cases, loss of the sense of smell persists for months after infection onset [6]. Furthermore, clinical evidence also indicates that a subset of patients bears long-lasting consequences (also known as long COVID) of SARS-CoV-2 infection, including olfactory dysfunction that persists even a year after the initial infection [7].

Given the CNS-related symptoms observed in COVID-19 patients, it is likely that SARS-CoV-2 can target the brain [8, 9]. A potential pathway to induce neurological manifestations occurs intranasally through the olfactory bulb via a trans-synaptic route, as supported by reported loss of olfaction in COVID-19 patients. Since the olfactory mucosa (OM) is situated at the rooftop of the nasal cavity, and directly exposed to the environment, it acts as the first line of defense against inhaled agents including viruses that could potentially enter the brain. It harbors a heterogeneous population of cells including olfactory sensory neurons (OSNs) responsible for initiating olfactory sensations, supporting cells, and cells of regenerative potential. However, evidence from research conducted since the pandemic indicates that human olfactory sensory neurons do not express or exhibit low expression of *TMPRSS2* (transmembrane protease, serine 2), and

ACE-2 (angiotensin-converting enzyme 2), two key genes involved in SARS-CoV-2 entry into the cell [10]. Instead, protein products of these two genes are abundant in samples of the whole olfactory mucosa of humans [10] and in mouse olfactory epithelium (OE) [11]. Emerging evidence suggests that in the OE, sustentacular cells which are known to support olfactory sensory neurons, express relatively high levels of ACE-2 [12, 13]. Infection of the sustentacular cells leads to dysfunction of the olfactory sensory neurons and consequentially loss of smell in COVID-infected individuals [14]. However, infection of the olfactory sensory neurons has not yet been ruled out [15, 16]. Notably, new evidence has shown other proteins such as NRP-1 (neuropilin-1), to serve as important SARS-CoV-2 receptors and thus enhance viral infectivity [17]. NRP-1 is present at high levels in the OE and in brain areas related to olfaction [18, 19]. Therefore, the olfactory pathway may constitute an important route of CNS invasion. However, the consequences of SARS-CoV-2 infection at the OM are not fully understood, partially due to a shortage of robust and effective in vitro models to study viral infection in human cells.

Alzheimer's disease (AD) is one of the most prevalent CNS disorders associated with the comorbidity of COVID-19 [20, 21]. AD is complex and affected by age, heredity, lifestyle, and environmental factors [22]. The disease is pathologically characterized by the deposition of amyloid beta (Aβ) and neurofibrillary tangles in the brain regions responsible for memory and learning, causing a multitude of symptoms associated with dementia [23]. Interestingly, like SARS-CoV-2 infection, olfactory dysfunction is often reported in several neurodegenerative diseases [24], including AD [25–28]. Recently, Lampinen et al. 2022 showed AD-associated changes in OM cells derived from biopsies of individuals with AD [29, 30], suggesting that these cells display similar alterations seen in AD-affected brains.

The connection of AD with viral infections has been postulated for decades and is still controversial despite supporting evidence [31, 32], but little is yet known about the relationship between SARS-CoV-2 and AD [33–35]. On one hand, there appears to be an increased risk of COVID-19 infection in individuals diagnosed with AD [36], and on the other hand, long-lasting neurological consequences of SARS-CoV-2 infection may relate to the onset of AD. Furthermore, severe infection is associated with aging-related molecular features in the brain [37] and the brains of COVID-19 patients display AD-like pathological features [38]. Interestingly, interferon-induced transmembrane protein 3 gene networks are significantly enriched in AD patients and induced by several viruses, including SARS-CoV-2 [39], suggesting a potential crossroad between immune mechanisms and AD pathology. The core of the crosstalk between AD and SARS-CoV-2 could potentially be the inflammatory processes [40, 41]. However, whether COVID-19 could trigger emerging AD or accelerate its onset remains unclear. Furthermore, the effects of SARS-CoV-2 infection at the OM, a mucous membrane interacting with both the external environment and the brain, of individuals with AD have not previously been addressed.

In this study, we collected OM biopsies from cognitively healthy donors and individuals with AD to model the human OM in a 3-dimensional (3D), Air–liquid interface (ALI) culture system and investigated the effects of SARS-CoV-2 infection in the cultured cells. We explored how AD affects susceptibility to SARS-CoV-2 infection and mapped the transcriptomic landscape of SARS-CoV-2 infection both in healthy and diseased cells.

Materials and methods

Ethical considerations

Olfactory biopsies were obtained from the cognitively healthy and AD individuals under the approved ethical permit from the Human Research Ethics Committees (HRECs), of Northern Savo Hospital District (permit number 536/2017). Written informed consent was obtained from all subjects and proxy consent from family members of persons with mild AD dementia.

Human olfactory mucosal biopsies

For the collection of human olfactory mucosal (OM) biopsies a relatively non-invasive procedure was carried out by an ENT surgeon at Kuopio University Hospital, Finland. A total of three cognitively healthy individuals and three individuals diagnosed with mild AD dementia participated in the study. The average age of the cognitively healthy control and AD individuals was 74.3 years and 62.3 years, respectively, representing both male and female donors. For this study, individuals diagnosed with AD had mild dementia according to Clinical Dementia Rating (CDR) and were recruited via the Brain Research Unit, Department of Neurology, University of Eastern Finland. All the individuals with AD fulfilled the NIA-AA clinical criteria of progressive AD and magnetic resonance imaging (MRI) or fluorodeoxyglucose (FDG)-positron emission tomography (PET) had showed degenerative processes, or, in Cerebrospinal fluid (CSF) biomarker examination, biomarker (Aβ, tau, and phos-tau) changes typical to AD were observed [42]. Cognitively healthy individuals were recruited via the Department of Otorhinolaryngology, Kuopio University Hospital, Finland, from donors undergoing a dacryocystorhinostomy (DCR) surgery, or from the already existing registries of the Brain Research Unit of the University of Eastern Finland. The cognition of all the study

participants was evaluated utilizing the Consortium to Establish a Registry for Alzheimer's Disease (CERAD) neuropsychological battery [43, 44].

The detailed protocol for collecting and processing OM biopsy collected from the rooftop of the nasal cavity was previously described [30, 45]. However, some modifications were made to improve the epithelial cell growth. Briefly, the tissue piece collected from the rooftop of the nasal cavity was transferred under an aseptic environment to the Biosafety Level 2 (BSL2) facility in PneumaCult - Ex Plus (Stemcell Technologies) prepared according to the manufacturer's instructions and supplemented with hydrocortisone (final concentration of 96 ng/mL) and 1% Penicillin–Streptomycin (Gibco). Processing of the tissue sample was done immediately, starting with the rinsing in cold Hank's Balanced Salt Solution (HBSS) followed by the removal of blood and cartilage. The clean tissue sample was then enzymatically digested for 45 min with dispase II at 2.4 U/mL (Roche, Basel, Switzerland) to separate OE from lamina propria (LP). Once the OE was separated, the LP fraction was first mechanically triturated followed by treatment with PneumaCult - Ex Plus media containing 0.25 mg/mL collagenase H (Sigma-Aldrich, St. Louis, MO, USA) for up to 10 min. Once the OE and LP were completely digested, both the OE and LP were combined and seeded on poly-D-lysine (Sigma-Aldrich) coated wells of a 6-well plate in supplemented PneumaCult - Ex Plus media. The cultures were then incubated at 37 °C, 5% CO_2 to allow cells to migrate out of the digested tissue pieces and proliferate. Half of the culture media was changed every 2–3 days for a total of 8–14 days before passaging the cultures and freezing the primary cell lines in liquid nitrogen for later use in a freezing media containing 90% PneumaCult-Ex Plus Media and 10% dimethyl sulfoxide (DMSO). Cells in primary passages 2–3 were used for air–liquid interface cultures as described below.

Establishment and maintenance of air–liquid interface culture (ALI)

Cryopreserved human primary olfactory mucosal cells were thawed and grown for 3–5 days in submerged cultures in PneumaCult-Ex Plus media. For air–liquid interface (ALI) cultures, transparent inserts for a 24-well plate were used with a 0.4 µm pore size polyethylene terephthalate (PET) membrane and 0.3 cm^2 culture area (Sarstedt). Inserts were coated with 1:100 Matrigel Growth Factor Reduced (GFR) Basement Membrane Matrix (Corning) dilution. Once confluent, submerged OM cells were passaged and seeded on coated 24-well transwell inserts at a seeding density of 4×10^4–5×10^4 cells and cultured in PneumaCult-Ex Plus media for 2–4 days with media in both apical and basal chambers. Cells were monitored for confluence, and media was changed with fresh expansion media if required. Once a monolayer was observed, the cells were subjected to airlift by removing culture media from the apical side/compartment and at the same time replacing media in basal chamber to PneumaCult ALI medium (Stemcell Technology). The PneumaCult ALI medium was prepared according to the manufacturer's instructions and supplemented with final concentrations of 4 µg/mL heparin (Paranova), 0.48 µg/mL hydrocortisone (Acros Chemicals), and 1% penicillin–streptomycin (Gibco). Cells were maintained in ALI for an additional 21 days for differentiation of primary cells to the pseudostratified epithelium. The ALI differentiation medium in the basal chamber was changed every 2–3 days and the apical chamber with the cells were washed with HBSS every 7 days to remove mucus secreted by the cells. These cells are called olfactory mucosa cell at air–liquid interface (OM-ALI).

SARS-CoV2-propagation and purification

SARS-CoV-2 viral strains; Wuhan strain isolate wild type (WT, strain B.1), delta variant (strain B.1.617.2), omicron variant (B.1.1.529). SARS-CoV-2 was obtained under the Helsinki University Hospital laboratory research permit 30 HUS/32/2018 § 16. All viral work experiments were performed in BSL3 facilities at the University of Helsinki. The original stocks were propagated in VeroE6-TMPRSS2 cells (WT, delta and omicron). Detailed protocol for viral propagation has been previously described [18]. Viral stocks were stored at − 80 °C in Dulbecco's modified Eagle's medium, 2% fetal calf serum (FCS), 2 mM L-glutamine, and 1 × penicillin–streptomycin. Virus titers were determined by plaque assay in VeroE6-TMPRSS2 cells. All viral stocks were sequenced by next-generation sequencing, the presence of the furin cleavage site in the genome was confirmed.

TEER measurements

Transepithelial electrical resistance (TEER) was measured to access the epithelial barrier integrity of the OM cultures at ALI every 7th day till the 21st day. An epithelial volt/ohm meter (EVOM2) from World Precision Instruments (Sarasota) was used with STX2 chopsticks electrodes for the TEER measurements, as described in [46]. TEER readings were obtained in triplicates for each line in OM-ALIs. TEER values were calculated as TEER (Ω/cm^2) = (resistance total (Ω) − resistance blank (Ω)) × transwell insert surface in cm^2.

SARS-CoV-2 infection of the OM-ALI cultures

After 21 days, OM-ALIs in transwell inserts were transported to BSL3 facilities at the University of Helsinki for virus infections. Prior to infections, fresh media was

changed to the basolateral compartments. ALI cultures from healthy donors or Alzheimer's disease individuals were infected in triplicates. Briefly, OM-ALIs were inoculated with 50 µL of SARS-CoV-2 with either WT SARS-CoV-2 (1×10^5 Plaque forming units/insert (PFU's/insert)), delta variant (1×10^5 PFU's/insert), or omicron variant (1×10^5 PFU's/insert). Medium control (mock) was used as a negative control for infection. In addition, inhibition of the WT-SARS-CoV-2 viral cell entry was also tested by treating the cells with TMPRSS2 inhibitor Nafamostat (25 µM). The virus was applied to the apical surface of the OM-ALI to mimic viral infection in vivo. The basal chamber was not infected and contained only fresh PneumaCult ALI media. The infected OM-ALI cultures were incubated at 37 °C and 5% CO_2 for 1 h, followed by aspiration of the virus and washing of the cells with Dulbecco's phosphate buffered saline (D-PBS) three times. The last wash was saved and used for PCR which was carried out for quantification of SARS-CoV-2 viral RNA copies in the media. The infected OM-ALI cultures were then further incubated at 37 °C and 5% CO_2 for 48 or 72 h. D-PBS apical washes were collected at 1, 24, 48, 72 h post-infection (hpi) to measure the viral RNA release from infected cells at later time points. Samples were stored at − 80 °C. Infected cells from OM-ALI cultures were harvested 48 hpi for messenger RNA (mRNA) sequencing or fixed at 72 hpi for immunofluorescence staining depending on the downstream assay.

Quantification of viral RNA after infection

Infected cells from the apical side in transwell inserts were washed with PBS for 10 min. Apical PBS washes obtained from SARS-CoV-2 infected and mock-infected OM-ALI cultures at 1, 48, and 72 hpi were used to extract RNA using QIAamp Viral RNA Minikit (Qiagen) using the manufacturer's protocol. Extracted RNA samples were used to perform SARS-CoV-2 quantitative RT-PCR using primers, a probe, and an in vitro synthesized control for RNA-dependent RNA polymerase (RdRp) as described earlier [47, 48]. SARS-CoV-2 RNA copies were accessed at each time point and a relative increase in viral load was determined.

RNA preparation and RNA sequencing

Upon the completion of the SARS-CoV-2 infection, the basal culture media was removed, and the apical pseudostratified epithelium was washed three times in sterile D-PBS to remove any mucus or traces of leaked media. The OM-ALI cells were then collected in a lysis buffer of the AllPrep DNA/RNA/miRNA Universal Kit (Qiagen). Cells were pooled from three inserts to ensure the harvesting of enough total RNA for the sequencing. The samples were stored in a lysis buffer at − 80 °C prior to RNA extraction. Total RNA was extracted according to the manufacturer's instructions. The Agilent 2100 Bioanalyzer and RNA 6000 Pico Kit were used to evaluate the integrity of the isolated RNA. RNA concentrations were measured with the Qubit fluorometer using the Qubit RNA HS Assay Kit (Invitrogen). 300 ng of total RNA of each sample was used for sequencing library preparation. Prior to the library preparation, ribosomal RNA was depleted with the QIAseq FastSelect RNA Removal Kit (Qiagen) according to the manufacturer's instructions. RNA libraries were prepared using the QIAseq Stranded Total RNA Library Kit (Qiagen) according to the manufacturer's instructions. Amplified libraries were subjected to quality control assessment on the Agilent 2100 Bioanalyzer using the High Sensitivity DNA Kit (Agilent). Concentrations of the libraries were measured with the Qubit fluorometer and the dsDNA HS assay kit (Invitrogen). Libraries were pooled at the equimolar concentration of 4 nM. Sequencing was performed on the Illumina NovaSeq 6000 platform using the S1 Reagent Kit (200 cycles). The 2×100 bp paired-end sequencing resulted in ~ 50 million reads per sample.

RNA sequencing data processing and analyses

Sequencing data were adaptor trimmed using Trimmomatic [49] and aligned to human genome reference version hg38 using RNA-seq aligner STAR v2.7.10a [50]. Alternative contigs were excluded from the reference sequence. Specific parameters of STAR aligner were following: –outFilterType Normal –outFilterMultimapNmax 20 –alignSJoverhangMin 8 –alignSJDBoverhangMin 3 –outFilterMismatchNmax 999 –outFilterMismatchNoverReadLmax 0.2 –outFilterMismatchNoverLmax 0.05 –alignIntronMin 20 –alignIntronMax 1,000,000 –alignMatesGapMax 1,000,000 –outFilterIntronMotifs RemoveNoncanonicalUnannotated –twopassMode Basic. Reads were then assigned to RefSeq gene annotation using FeatureCounts v2.0.1 [51] with the following parameters: -largest Overlap -s 1 -p -B -P -d 30 -D 100000 -C -T 4. The number of reads belonging to genes was counted. From 52.8% to 64.8% of all reads were uniquely assigned to genes in each sample. This corresponds to at least 33.8 million reads per sample.

Differential expression and pathway analysis

We performed the differential gene expression analysis between cells of the mock-treated AD and control libraries, mock-treated control and SARS-CoV-2 infected control cell libraries, mock-treated AD and SARS-CoV-2 infected AD cell libraries, and also between SARS-CoV-2 infected controls and SARs-CoV-2 infected AD cell libraries. For pathway enrichment analysis, we used the differentially expressed genes (DEGs) between control

and AD with mock treatment and/or SARS-CoV-2 infection. PANTHER overrepresentation analysis for pathway enrichment was performed using PANTHER (version 17.0, released 2022-02-22, http://www.pantherdb.org/). Similarly, by using DEGs along with the fold changes we performed Ingenuity pathway analysis (IPA) for the identification of the altered canonical pathways. The IPA Analysis Match CL license used in this study was purchased from QIAGEN (https://www.qiagenbioinformatics.com/products).

Immunocytochemistry and imaging

At 72 hpi with SARS-CoV-2, the OM-ALI cells were fixed using 4% paraformaldehyde (PFA). The PFA was added to both the apical and basal chambers for 10 min and then washed with D-PBS containing 0.2% bovine serum albumin (BSA) (Sigma). Fixed cells on the inserts were permeabilized with Triton X-100 (Sigma) at 1:100 dilution for 20 min and washed three times with the D-PBS + 0.2% BSA. Before primary antibody treatments, cells were blocked with 0.2% BSA in D-PBS for 30 min. Later, incubated overnight at 4 °C with predetermined concentrations of primary antibodies (Table 1) and subsequently washed three times with D-PBS to remove traces of non-binding primary antibodies. To visualize primary antibody binding, cells were treated with secondary antibodies for 3 h at room temperature (Table 1) and then washed with D-PBS + 0.2% BSA. For visualizing the nuclei, cells were stained with Hoechst (1:1000 dilution of 1 mg/mL stock) or bisbenzimide (1:1000 dilution of 1 mg/mL stock). After staining, the transwell membranes containing OM cells were removed from their inserts using a scalpel and peeled off from the bottom of the transwell using tweezers and mounted on glass slides using mounting media (Prolong Gold antifade reagent). The cells were facing upward and covered with 0.17-mm glass coverslips for imaging. Imaging was done using automated spinning disc CellVoyager™ CQ1 Benchtop High-Content Analysis System (Yokogawa) at the Imaging unit of the University of Helsinki at 10 and 20 × objectives, and Zeiss Axio Observer inverted microscope with LSM800 confocal module (Carl Zeiss AG) att the UEF Cell and Tissue Imaging Unit at 20, 40, and 63 × objectives. Image analysis was performed from 3D-confocal image stacks using the Cell Path Finder software inbuilt in the CQ1 microscope. Nuclei were automatically detected in the 3D stacks, and the fluorescence intensity of different epithelial cell markers analyzed within the nuclear volume expanded by 10 pixels in all directions. Classification of cells into positive and negative for a given marker was done with the same software using a manually determined threshold of fluorescence. Processing of the images was done using ZEN Blue version 3.2 (Zeiss) and open-source software ImageJ version 1.53q (Fiji).

Table 1 Key resources for immunostainings

Reagent or resource	Source	Identifier (catalogue number; lot number)
Primary antibodies		
Monoclonal anti-tubulin, acetylated antibody produced in mouse; Dilution: 1:2000	Sigma-Aldrich	T6793-100UL; 108923
Mouse monoclonal MUC5AC antibody (45M1); Dilution 1:200	Thermo Fisher Scientific	MA5-12178; WD3205962
Mouse monoclonal human Cytokeratin 18 antibody (810811); Dilution 1:50	R&D Systems	MAB7619; GR3268718-6
Goat anti-ACE-2 polyclonal antibody; Dilution 5 µg/mL	R&D Systems	AF933-SP; HOK0320051
Recombinant Rabbit monoclonal Anti-Neuropilin 1 antibody [EPR3113] Dilution 1: 250	Abcam	ab81321; 212288-45
ZO-1 Polyclonal Antibody; Dilution: 5 µg/mL	Invitrogen	40-2200; WA317222
SARS-CoV/SARS-CoV-2 Nucleocapsid Dilution: 1:2000	Kind gift by Jussi Hepojoki	Cantuti-Castelvetri et al., Science, 2020 [18]
Secondary antibodies		
Donkey anti-Goat Alexa Fluor-488 Dilution: 1:1000	Invitrogen	A-11055; 2,513,496
Donkey anti mouse Alexa Fluor555 Dilution: 1:500	Invitrogen	A-32773; VB302733
Goat anti rabbit Alexa Fluor-647 Dilution: 1:500	Invitrogen	A-31573; 2497486
Alexa Fluor-488 conjugated phalloidin	Invitrogen	A-12379; 1948083
Hoechst DNA stain	Thermo Fisher Scientific	62249; MF1423541

Statistical methods and graphical illustrations

The GraphPad Prism 9.4.1 (GraphPad Software Inc.) software was used for the statistical analysis of the data. Statistical analysis methods used for different comparisons are indicated in figure legends. Error bars in Figs. 1, 2, 3 and 4 represent standard deviation (SD). Statistical significance was assumed for p-values ≤ 0.05. The graphical illustrations were created with BioRender.com.

Results

Primary human OM cells efficiently differentiate into pseudostratified epithelium in ALI cultures in vitro

To study SARS-CoV-2 infection in differentiated OM-ALIs, we first established ALI culture conditions for cells derived from OM biopsies (Fig. 1a). OM-ALIs were cultured under ALI conditions for 21 days and then characterized for epithelial barrier function and tight junctions. Trans-epithelial resistance (TEER) was measured to determine the polarization and integrity in cultures 7, 14, and 21 days after initiation of the ALI cultures. A significant increase in TEER values ($F=36.39$, $p=0.0004$) was observed at day 21 (mean 325.12 Ω/cm^2, SD = 20.48) as compared to the day 7 TEER values (mean 186.56 Ω/cm^2, SD = 33.21) (Fig. 1b). To characterize the ALI model further, the cells were immunostained for ZO-1 to confirm tight junctions, and for acetylated tubulin to detect the presence of cilia. (Fig. 1c, d, Additional file 1: Fig. S1a, b). Our results showed the presence of pseudostratified epithelium with tight junction to mimic a physical barrier at the OM.

Primary human OM cells express non-neural epithelial cells in ALI cultures and express ACE-2 and other entry receptors required for SARS-CoV-2 infection

We further characterized the cell types expressed in the OM-ALI. Immunocytochemical staining of cell type-specific markers demonstrated that the ALI cultures contain populations of different cell types present in the human OM in vivo, including an average of 12% of goblet cells (Mucin 5AC + cells), and 4–5% sustentacular cells (Cytokeratin-18 + cells) (Fig. 2a, b; Additional file 1: Fig. S1c, d). Quantification of the immunostainings showed an average of 20% of cells within the differentiated OM-ALI cultures express apical ciliary markers (Fig. 2b). We further characterized differentiated OM-ALI cultures for expression of entry receptors required for SARS-CoV-2 infection. Global mRNA sequencing data analysis from uninfected cells indicated the presence of the *ACE-2, NRP-1, TMPRSS2,* Cathepsin B (*CTSB*), Cathepsin *L (CTSL*), basigin (*BSG*), and furin mRNAs (Fig. 2c), all of which are implicated to be important for SARS-CoV-2 infection [52–56]. SARS-CoV-2 is known to primarily target ACE-2; cellular transmembrane receptors for binding to the host cell membrane [52], whereas NRP-1 has also been shown to enhance infection of SARS-CoV-2 in ACE2-expressing cells [18]. Therefore, immunocytochemical staining of differentiated OM-ALI cultures for the ACE-2 receptor and NRP-1 proteins was performed to validate the expression the of most important entry receptors required for SARS-CoV-2 infection (Fig. 2d).

SARS-CoV2 infects OM cells of both cognitively healthy donors and individuals with AD

Having characterized the ALI cultures and knowing they express entry receptors required for SARS-CoV-2 infection, we next sought to determine the infectability of the cells and to compare how cells from individuals with AD may differ from cells derived from cognitively healthy individuals. After growing cells in ALI for three weeks, the AD and cognitively healthy control cells were subjected to apical infection with the SARS-CoV-2-WT (1×10^5 PFU) for 72 h. The representative image of infections with SARS-CoV-2 nucleocapsid protein (NP) co-stained with MUC5AC (Fig. 3a, Additional file1: Fig. S1f), and acetylated tubulin (Fig. 3b), indicating the presence of the virus in the OM-ALIs. Furthermore, co-staining with acetylated tubulin indicated the presence of viral NP in the apical epithelium (Fig. 3b, Additional file 1: Fig. S1e).

Viral infections in OM-ALI cells showed no significant differences in viral NP or MUC5AC (goblet cell marker) positive cells between the groups (Fig. 3c). However, infected OM-ALI cells show a significant reduction in the acetylated tubulin (ciliary marker) in AD individuals-derived OM-ALI cells ($t=3915$, $df=4$, $p=0.0173$ (Fig. 3c).

(See figure on next page.)

Fig. 1 Characterization of the human primary olfactory mucosal cells at air–liquid interface. **a** Representation of the OM-ALI setup derived from human primary OM cells. **b** TEER measurement at days 7, 14, and 21 after initiation of OM-ALI cultures for cells derived from cognitively healthy control subjects. Graph shows mean with SD of $n=3$ study subjects. Ordinary one-way ANOVA with Tukey's multiple comparisons tests. **Indicates a p-value ≤ 0.005, *** indicates p-value ≤ 0.0005. **c**, **d** Representative immunostainings of OM-ALI cultures for the presence of zonula occludens-1 (ZO1), a tight junction marker; acetylated tubulin, a ciliary marker protein; and actin for the cytoskeleton of the cells. All imaged on 10 × objective; scale bar 100 µm

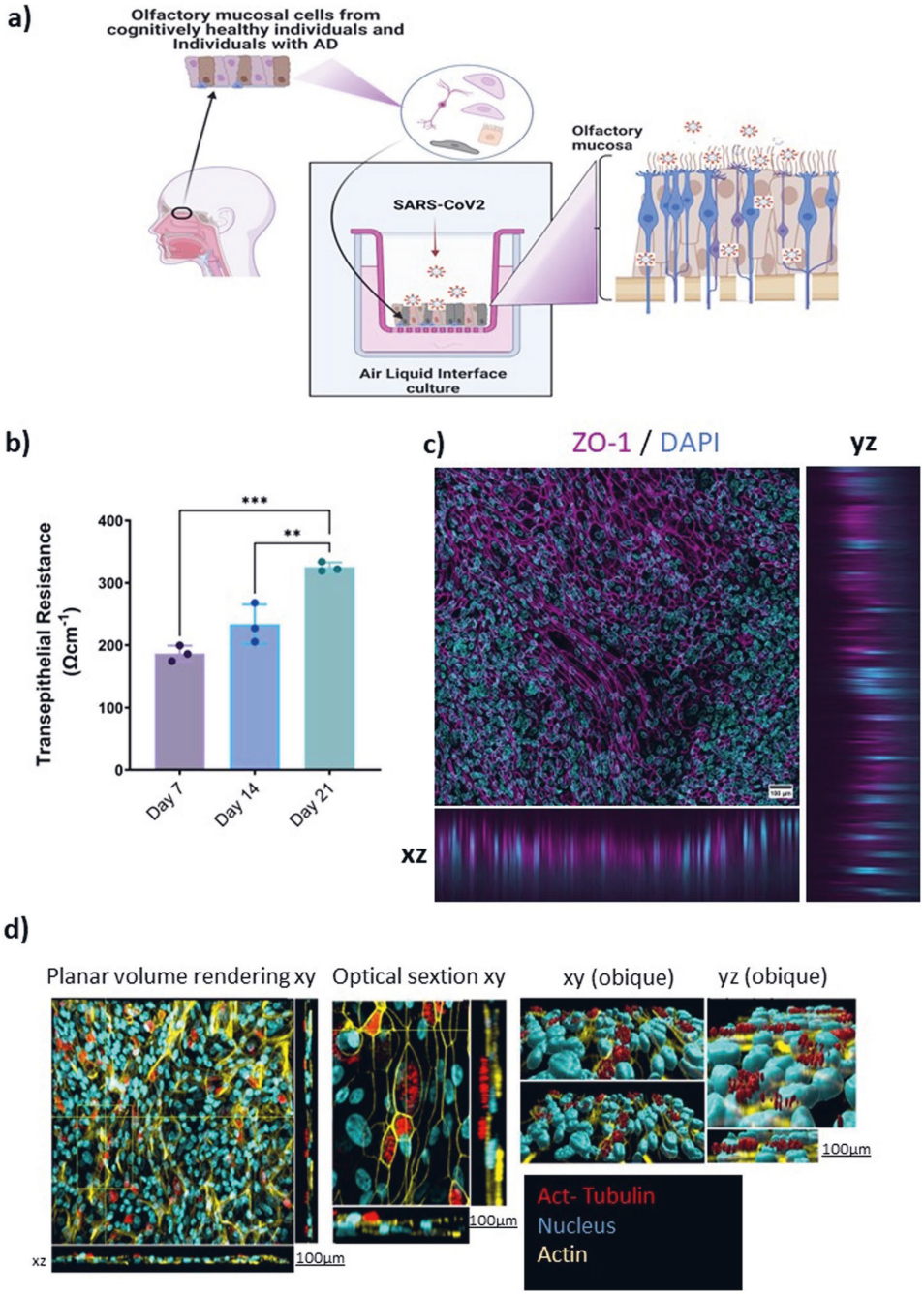

Fig. 1 (See legend on previous page.)

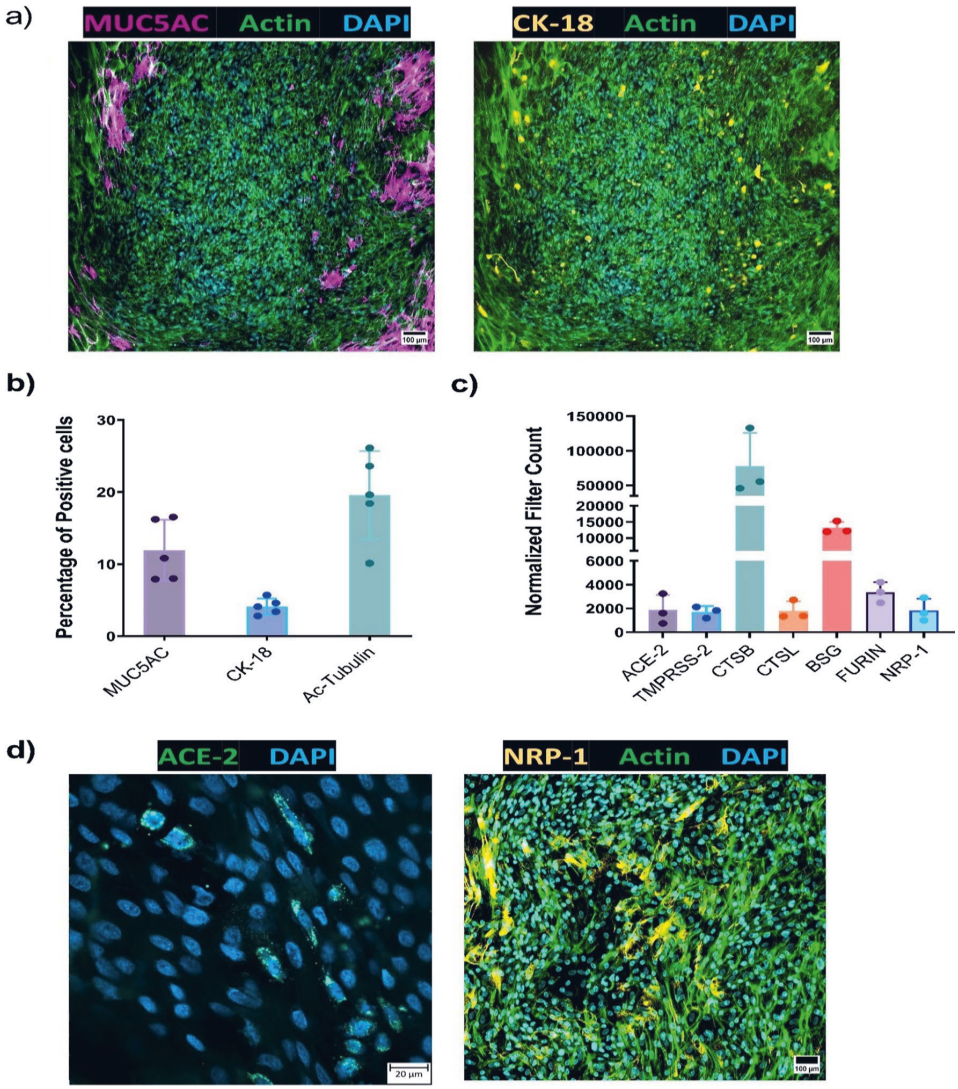

Fig. 2 Human OM-ALI express non-neural epithelial cells and receptor proteins required for SARS-CoV-2 infection. **a** Representative immunostainings of OM-ALI cultures for the presence mucin 5AC (MUC5AC) for goblet cells; Cytokeratin 18 (CK-18) for sustentacular cells; and actin for the cytoskeleton of the cells. All imaged on 10×objective; scale bar 100 µm. **b** Quantification of the immunostainings representing the percentages of positive cells for MUC5AC for goblet cells; Cytokeratin 18 (CK-18) for sustentacular cells; and Ac-tubulin (acetylated tubulin) for ciliated cells. Graph shows mean with SD of $n=3$ for cognitively healthy controls (total of 5 images were analyzed, each dot represents percentage of positive cell in single image). **c** Normalized filter counts of genes involved in SARS-CoV-2 infection, obtained from bulk mRNA sequencing of mock-treated OM-ALI cultures derived from cognitively healthy controls. Graph shows mean with SD of $n=3$. **d** Representative immunostaining images of ACE-2 and NRP-1 expression in the OM-ALIs. Imaged ACE-2 on 63×(scale bar 20 µm), and NRP-1 on 10×objective (scale bar 100 µm)

In addition to quantifying the numbers of SARS-CoV-2 positive cells, we also monitored secreted viral RNA copies released from the apical side of the OM-ALI cultures at 1, 48, and 72 hpi. In both healthy control and AD OM-ALI cultures the viral RNA levels increased after SARS-CoV-2 infection in a time-dependent manner, confirming

the viral replication and propagation with the infected cells. However, no significant differences were observed between viral RNA levels released from the apical side of the OM-ALI cultures at any observed time point between cells derived from cognitively healthy controls and individuals with AD (Fig. 3d). We also determined the expression of SARS-CoV-2-associated genes in infected and mock-treated cell samples. No significant differences in mRNA expression *of ACE-2, TMPRSS2, CTSL, BSG, Furin,* and *NRP-1* were observed between the cells derived from cognitively healthy control subjects and AD individuals in mock-treated or SARS-CoV-2 infected samples (Fig. 3e). Interestingly, the two-way ANOVA test showed that the presence of disease (AD) had a significant effect on alteration in gene expression levels of *CTSL* ($F=5.406$; $p=0.049$) and *NRP-1* ($F=6.432$; $p=0.034$) (Fig. 3e).

Next, cells of the cognitively healthy donor were used to determine the susceptibility of the cultures to different SARS-CoV-2 variants. For this experiment, we infected the OM-ALI cells with WT, delta, and omicron variants of SARS-CoV-2 (Fig. 4). A recent review comparing published data on the contribution of genetic variants to the incidence of anosmia concluded that the omicron variant causes less olfactory dysfunction than the other variants, indicating that WT and delta have a broader invasive potential in the OE [57]. Coinciding with these data, our results also showed differences in the infectibility of OM-ALI with the investigated variants of SARS-CoV-2 with one-way ANOVA ($F=7.202$, $p=0.0028$). Furthermore, the OM-ALI cultures were less susceptible to infection with the omicron variant as compared to the WT SARS-CoV-2 when determined by the percentage of cells positive for the virus variants in question ($p=0.0439$) (Fig. 4); whereas no significant difference was observed in the percentage of positive cells when comparing the WT and delta variants. Lastly, inhibition of the SARS-CoV-2 viral infection with short pre-treatment of cells with TMPRSS2 inhibitor Nafamostat resulted in complete inhibition of infection by the WT SARS-CoV-2 ($p=0.0038$) (Fig. 4). This suggests that in the OM-ALI viral entry into the cell is dependent on proteolytic cleavage of the spike protein with TMPRSS2 after the virus binds to the ACE-2 receptor [58].

Distinct gene expression changes in OM-ALI cells from Alzheimer's individuals infected with SARS-CoV-2

Having established an in vitro representative model for human OM cells that are susceptible to SARS-CoV-2 infection, we sought to elucidate the transcriptomic alterations caused by SARS-CoV-2 infection in cognitively healthy individuals and individuals with AD. For this, we performed bulk mRNA sequencing on OM cells that were either infected with WT SARS-CoV-2 (1×10^5 PFU's) for 48 h or received mock treatment. Principal component analysis and differential gene expression analysis of the sequencing results revealed profound differences between control and AD cells. We discovered a total of 427 (138 upregulated and 289 downregulated) significantly differentially expressed genes (DEGs) (FDR < 0.05) in mock-treated AD OM-ALI cells when compared to mock-treated control OM-ALI cells (Additional file 5: Table S1). Figure 5a depicts the DEGs representing the baseline differences between mock-treated controls and AD individuals. Based on the log2-fold change, the five most upregulated genes in AD individuals are *TUBBP5* (Tubulin beta pseudogene 5), *NOS2* (Nitric Oxide Synthase 2), *UGT2A2* (UDP Glucuronosyltransferase Family 2 Member A2), *NTF3* (Neurotrophin 3), *and KCNJ1* (Potassium Voltage-Gated Channel Subfamily J Member 1), while *POSTN* (Periostin), *FN1* (Fibronectin 1), *NNMT* (Nicotinamide N-Methyltransferase), *PAMR1* (Peptidase Domain Containing Associated with Muscle Regeneration 1), *and COL4A1* (Collagen Type IV Alpha 1 Chain) are the five most downregulated genes. Interestingly, *UGT2A1* and *UGT2A2* have recently been implicated in COVID-19-associated loss of smell and taste [59].

Next, we assessed the impact of SARS-CoV-2 infection on the gene expression of control and AD OM-ALI cells. Infection of cells derived from cognitively healthy controls with SARS-CoV-2 resulted in 1797 DEGs (FDR < 0.05), out of which 1113 were upregulated and 684

(See figure on next page.)

Fig. 3 Human OM-ALI from AD and cognitively healthy individuals have similar susceptibility to SARS-CoV-2 infection. **a**, **b** Representative image of OM-ALIs at 72 hpi with SARS-CoV-2 (1 × 105 PFU). Immunostaining was done with SARS-CoV-2 NP (nucleocapsid protein); acetylated tubulin (ciliated cell marker); MUC5AC (goblet cell marker). Imaged on 10 × objective; scale bar 100 µm. **c** Quantification of the OM-ALIs at 72 hpi with SARS-CoV-2 (1 × 105 PFU) immunostainings representing the percentages of SARS-CoV-2 NP, Act-tubulin; MUC5AC in control and AD cells. Graph shows mean with SD of $n=3$ for both control and AD cells. Unpaired two-tailed t-test. *Indicates p-values ≤ 0.05. **d** Quantification of SARS-CoV-2 RNA copies released from the infected control and AD OM-ALIs at 1, 48, and 72 hpi. Graph shows mean with SD of $n=3$ donors for both control and AD OM-ALIs. **Indicates p-values ≤ 0.01, ***indicates p-values ≤ 0.001 by two-way ANOVA with Tukey multiple comparison. e) Normalized filtered counts of genes for key receptors and proteins involved in SARS-CoV-2 infection obtained from bulk mRNA sequencing of mock and infected OM-ALI cultures from control and AD. Graph shows mean with SD of $n=3$ for both control and AD cells. Ordinary two-way ANOVA test; # indicates the disease effect and p-values ≤ 0.05

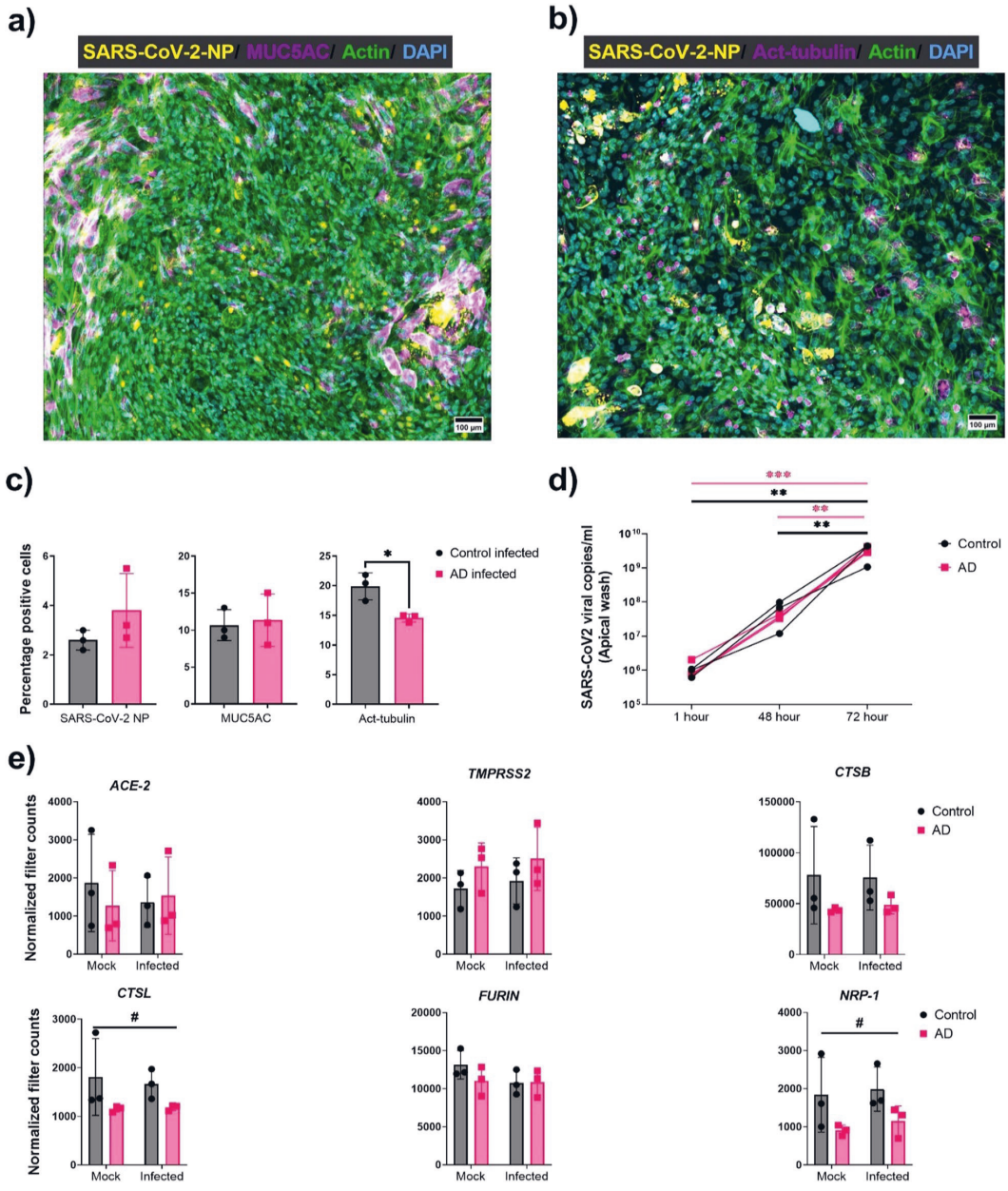

Fig. 3 (See legend on previous page.)

were downregulated in comparison to mock-treated cells (Fig. 5b, Additional file 5: Table S2). In cells derived from individuals with AD, SARS-CoV-2 infection resulted in 1176 DEGs, out of which 624 were upregulated and 552 downregulated (Fig. 5c, Additional file 5: Table S3). Interestingly, our analysis showed 1971 (790 upregulated 790 and 1181 downregulated) differentially expressed genes in infected AD OM-ALI when compared to infected

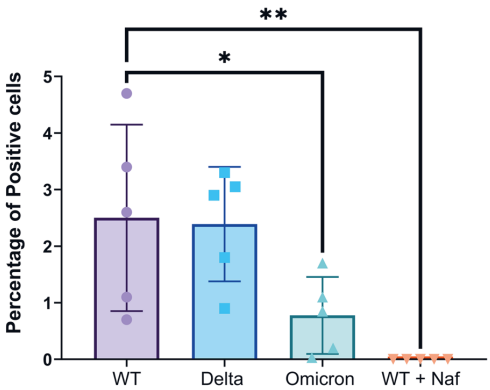

Fig. 4 Human OM-ALI cells from healthy individuals exhibit variant-specific susceptibility to SARS-CoV-2 infection. Quantification of the of viral NP-positive OM-ALIs at 72 hpi with WT-SARS-CoV-2 (1 × 105 PFU), delta variant (1 × 105 PFU's), omicron variant (1 × 105 PFU's), and inhibition of WT infection with pre-treatment of Nafamostat (25 μM). Graph shows mean with SD of $n = 3$ for cognitively healthy controls (total of 5 images were analyzed, each dot represents percentage of positive cell in single image). One-way ANOVA with Dunnett's multiple comparisons tests; *indicates p-values ≤ 0.05 and **indicates p-values ≤ 0.01

control OM-ALI cells (Fig. 5d, Additional file 5: Table S4). Many DEGs suggest that underlying AD pathology altered the responses of cells to SARS-CoV-2 infection.

As expected, SARS-CoV-2 infection in control OM-ALI cells showed that the highest fold changes were observed in genes that are involved in the antiviral immune response*: CXCL11* (C–X–C motif chemokine ligand 11, fc = 4.8), *CXCL10* (C–X–C motif chemokine ligand 10, fc = 4.7), and *IL6* (interleukin 6, fc = 1.76). Moreover, in the antiviral signaling response, *IFI44* (Interferon Induced Protein 44, fc = 3.47), *IFIT1* (Interferon Induced Protein with Tetratricopeptide Repeats 1, fc = 3.4), *RSAD2* (Radical S-Adenosyl Methionine Domain Containing 2, fc = 3.3), *IFIT2 (*Interferon Induced Protein with Tetratricopeptide Repeats 2, fc = 3.15), *OASL* (2'-5'-Oligoadenylate Synthetase Like, fc = 2.4), *MX2* (MX Dynamin Like GTPase 2, fc = 2.4), ISLR2 (Immunoglobulin Superfamily Containing Leucine Rich Repeat Protein 2, fc = 2.3), and *IFIT3* (Interferon Induced Protein with Tetratricopeptide Repeats 3, fc = 2.3) exhibited increased expression. Both antiviral immune response and interferon-mediated signaling are characteristic features of SARS-CoV-2 infection reported in the literature in vitro, ex vivo, and in vivo [60–62]. However, in AD OM cells the upregulation of genes associated with the immune response and interferon-mediated signaling after infection with WT-SARS-CoV-2 were less drastic, and only a few genes were observed in the top 20 significant DEG when compared to mock-treated AD OM-ALI cells, including *CXCL10* (fc = 2,8), *IFI44L* (fc = 2,4), *RSAD2* (fc = 1,9), *IFI6* (fc = 1,3), *IFIT1* (fc = 1,3), and *OASL* (fc = 1,32). Surprisingly, 4 out of 10 most upregulated DEGs, and 8 out of 10 most downregulated DEGs in AD-infected OM-ALI were non-coding RNAs (ncRNA) which was not seen in the control-infected OM. Among the most significant differentially expressed ncRNAs (*NEAT1, TALAM1, GAS5*) have been previously reported to be associated with SARS-CoV-2 infection [63–65].

To investigate the effect of AD pathology in the mock and infected samples, we compared numbers of RNA sequencing reads from mock control and AD cells, and infected controls and AD samples to the Kyoto Encyclopedia of Genes and Genomes (KEGG) database of genes involved in Alzheimer's disease pathway (hsa05010). Figure 5e shows the top 20 DEGs in mock cells from cognitively healthy and AD individuals from the KEGG AD pathway. Similarly, we also identified top DEGs in infected cells from cognitively healthy and AD individuals from the KEGG AD pathway (Fig. 5f). Furthermore, to investigate the SARS-CoV-2 infection effect, we showed top differential transcriptomic signatures of SARS-CoV-2 infection compared to KEGG human Coronavirus disease pathway (hsa05171) in cognitively healthy and AD individuals (Fig. 5g, h). Interestingly, the top AD pathway-associated DEGs between the control mock and AD mock are *PTGS2* (Prostaglandin-Endoperoxide Synthase 2), *DKK* (Dickkopf-related protein), and *APOE* (Apolipoprotein E), whereas AD-pathway-associated DEGs in control infected and AD infected include *SNCA* (α-synuclein), *WNT* (Wingless-related integration) site 4 and *WNT10A*. On the other hand, the top SARS-CoV-2 pathway-associated DEGs between the control mock and control infected

(See figure on next page.)

Fig. 5 AD alters OM-ALI cell response to SARS-CoV-2 via transcriptomic changes. **a**–**d** Volcano plots showing differentially expressed genes (DEGs) between **a** control mock and AD mock, genes with Log2 fc of ≤ -3 or ≥ 3 and FDR ≤ 0.01 are highlighted; **b** control mock and control infected, genes with Log2 fc of ≤ -2 or ≥ 2 and FDR ≤ 0.01 are highlighted; **c** AD mock and AD infected, genes with Log2 fc of ≤ – 2 or ≥ 2 and FDR ≤ 0.01 are highlighted; **d** control infected and AD infected, genes with Log2 fc of ≤ – 5 or ≥ 5 and FDR ≤ 0.01 are highlighted. The red dot indicates Log2 fc cutoff 1 and FDR cutoff 0.05. **e**, **f** Heatmaps showing Alzheimer's disease KEGG pathway (hsa05010) associated top 20 DEGs in; **e** control mock and AD mock; **f** control infected vs AD infected. **g**, **h** Heatmaps showing KEGG human coronavirus disease pathway (hsa05171) associated DEGs in **g** control mock and control infected and in **h** AD mock and AD infected. *fc* fold change, *FDR* false discovery rate

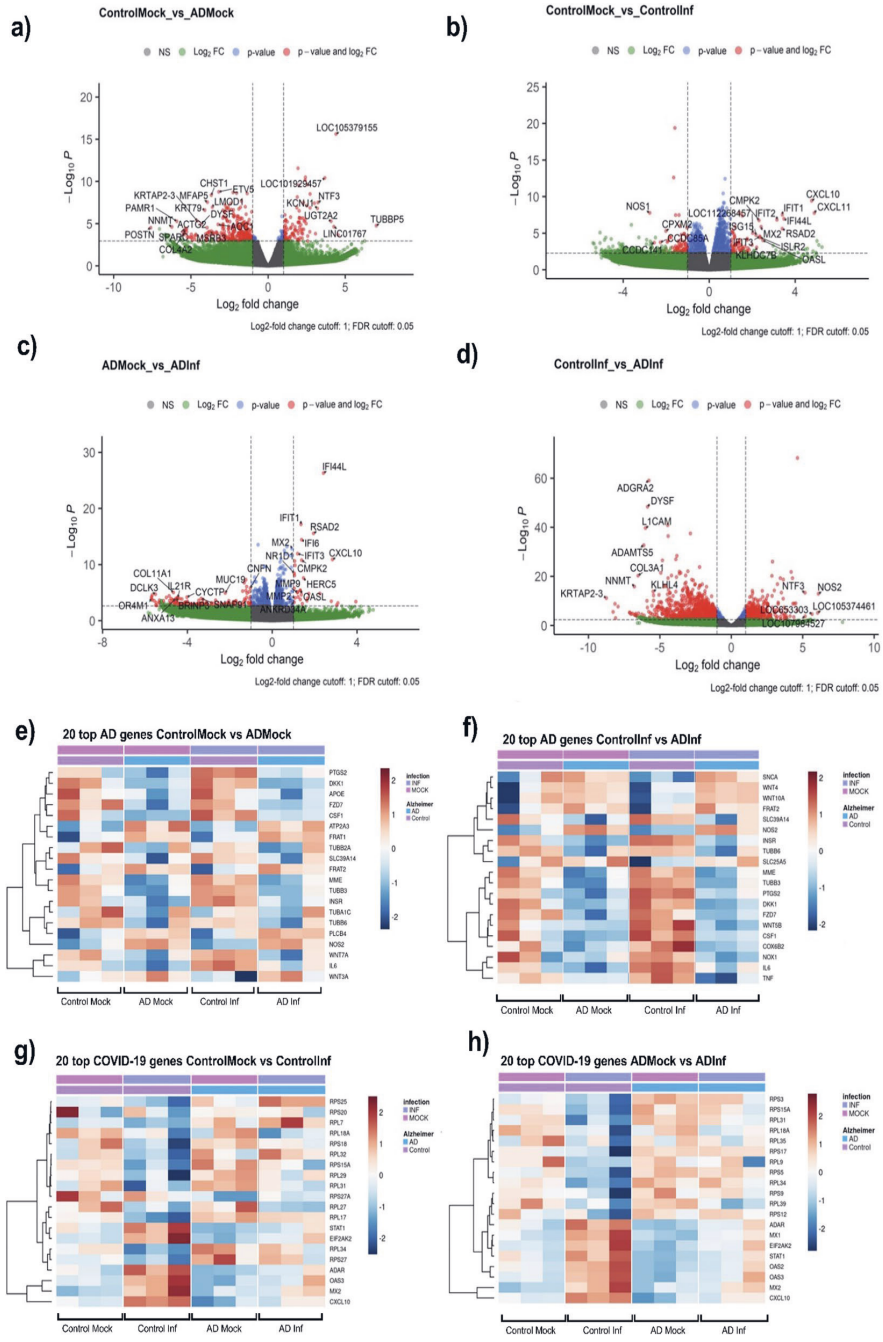

Fig. 5 (See legend on previous page.)

are *RPS* (ribosomal protein) *S25, RPS20*, and *RPL7*, whereas SARS-CoV-2-pathway-associated DEGs in AD mock and AD-infected cells include *RPS3, RPS15A*, and *RPL31.*

We further performed PANTHER pathways overrepresentation analysis on DEGs between infected and non-infected control and AD cells. Interestingly, we found only the integrin signaling pathway and Alzheimer's disease-presenilin pathway that were significantly enriched. In addition, analysis of all the significant DEGs demonstrated other pathways implicated in AD (Additional file 2: Fig. S2A). This indicates the utility of patient-derived cells in understanding SARS-CoV-2 infection. Interestingly, SARS-CoV-2 infection in control and AD cells enriched similar pathways associated with SARS-CoV-2. However, in the SARS-CoV-2-infected AD cells, more AD-associated pathways were enriched (Additional file 2: Fig. S2B). Enriched pathways include Inflammation mediated by chemokine and cytokine signaling pathways, cadherin signaling pathways, and Wnt-signaling pathways. Furthermore, the numbers of DEGs associated with the common AD pathways were significantly increased in SARS-CoV-2 infected AD cells than in the mock-treated AD (Additional file 2: Fig. S2C).

Core analyses in IPA were performed for all the significant DEGs in each data set to identify pathways associated with differential gene expression patterns. Associated networks determined by the analysis were used to identify upstream regulators. Altered pathways that were associated with the DEG in between the mock-treated control and AD OM-ALI cells were related to an extracellular matrix organization, proteoglycans synthesis dysregulation (associated with Aβ deposition), synaptic dysfunction, wound healing, and inflammation (Fig. 6a, Additional file 5: Table S5). Furthermore, we found AD-associated upstream regulators including *ZEB1* (Zinc Finger E-Box Binding Homeobox), *TGFB1* (Transforming Growth Factor Beta 1), and *TNF* (Tumor Necrosis Factor) that are inhibited and *NR3C1* (Nuclear Receptor Subfamily 3 Group C Member 1), and various *EFNA* (ephrin A's) activated in mock AD cells. All these upstream regulators are linked to AD. The figure shows the top five statistically significant inhibited and activated upstream regulators in the mock-treated control and AD OM-ALI cells (Fig. 6e, Additional file 5: Table S6).

In both control and AD cells, as expected, infection with SARS-COV-2 was linked to the Coronavirus Pathogenesis Pathway or the Coronavirus Replication Pathway. In IPA, core analysis for comparison of SARS-CoV-2 infection with the representative mock treatment in control and AD ranked eIF2 signaling as the most affected pathway (Fig. 6b, c). Viruses hijack the host cell machinery to complete viral replication and protein synthesis. In response, host cells turn off these systems, which is thought to be an integrated stress response. The stress response induces translational silencing via phosphorylation of eIF2 (eukaryotic initiation factor-2) [66]. Therefore, sustained phosphorylation of eIF2 inhibits host or viral protein synthesis. Interestingly, a recent study also showed downregulation of the elF2 signaling pathway in the transcriptomic analysis of nasopharyngeal swabs derived from COVID-19-infected patients [67]. Furthermore, IPA analysis showed SARS-CoV-2 infection in control and AD cells to be associated with mitochondrial dysfunction and downregulation of the oxidative phosphorylation pathway (Additional file 5: Tables S7, S8). In both infection groups, a similar trend of alterations in the top three pathways was observed. However, overall coverage of the pathway with the DEGs in control OM-ALI cells was almost double that of the AD OM-ALI cells after infection. Like the canonical pathways, upstream regulators between SARS-CoV-2 infected control and AD OM-ALI cells are the same, indicating a similar pattern of infection (Additional file 5: Tables S9, S10). The upstream regulators are mainly involved in antiviral immune response and inflammation. The top 10 biologically and statistically significant upstream regulators between control mock and control infected (Fig. 6f) and AD mock and AD infected (Fig. 6g) are shown.

Furthermore, core IPA analysis of the DEGs between control and AD cells post-infection confirms significant biological differences between the up- or downregulation of pathways (Fig. 6d). For example, elF2 signaling was downregulated in both control and AD cells upon infection. However, the IPA of DEGs comparing control infection with the AD infection showed less effective

(See figure on next page.)

Fig. 6 AD OM-ALI cells show distinct biological changes post-SARS-CoV-2 infection. Top signaling pathways in canonical pathway comparison between all exposure groups with the percentages overlap of pathway genes with DEGs: **a** mock-treated controls and SARS-CoV-2 infected controls; **b** mock-treated AD and SARS-CoV-2 infected AD; **c** mock-treated control and mock-treated AD; **d** SARS-CoV-2 infected control and SARS-CoV-2 infected AD cells. The rankings were based on Fisher's exact test and pathways are presented with the highest significance on the top and displayed along in decreasing order of significance from the top. The cutoff for statistical significance was a p-value ≤ 0.05 and a biological significance indicated by Z-score ≤ − 2 or ≥ 2. $n = 3$ control and $n = 3$ AD OM-ALI cultures for all data. **e**–**h** Indicates upstream regulators associated to DEG in the **e** control mock and AD mock; **f** control mock and control infected; **g** AD mock and AD infected; h control infected and AD infected. *Y*-axis indicates the upstream regulator network, and the x-axis represents the activation *Z*-score

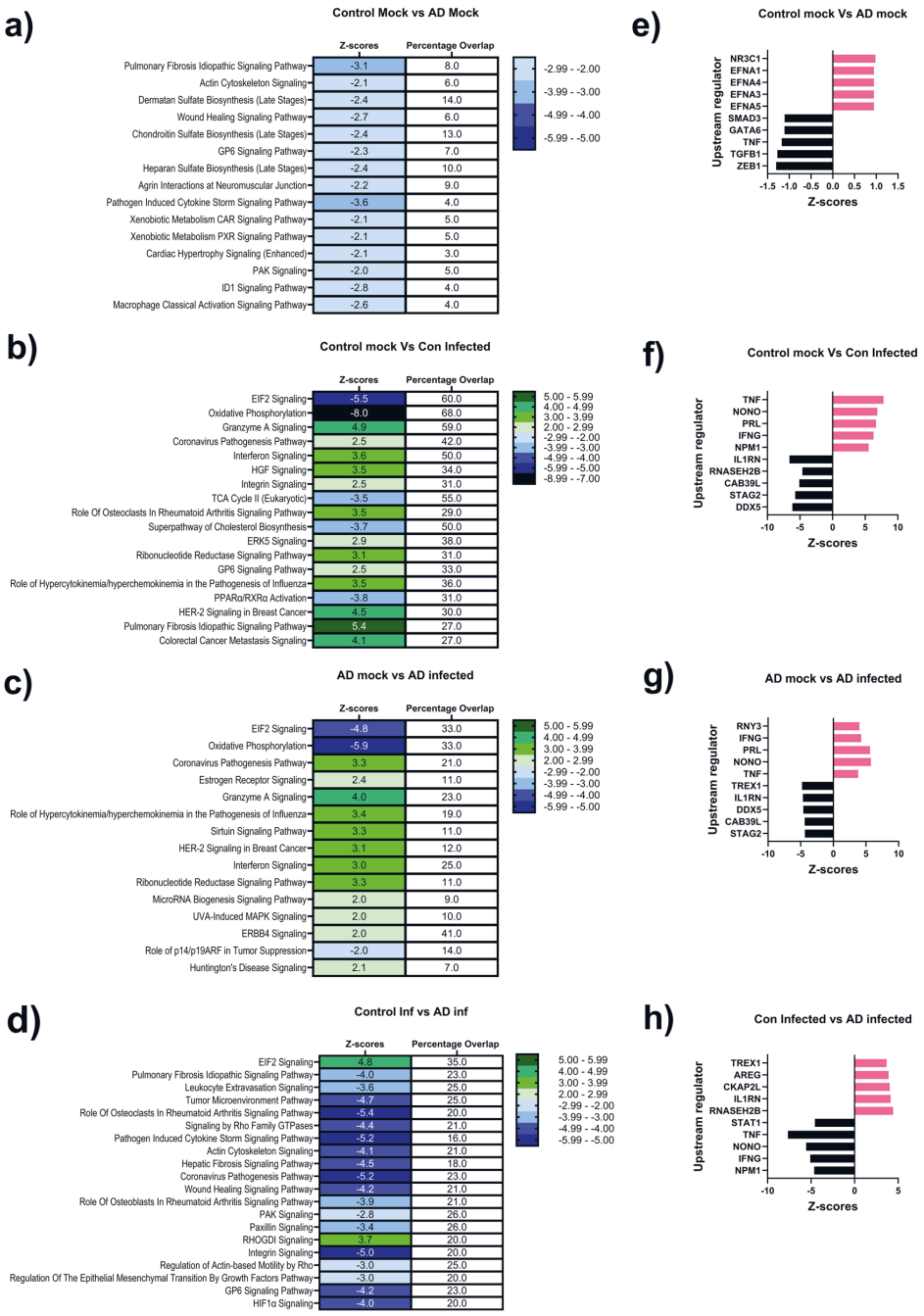

Fig. 6 (See legend on previous page.)

downregulation of the elF2 pathway in the AD OM-ALI cells as compared to control OM-ALI. Interestingly, pathways related to an extracellular matrix organization, wound healing, integrin signaling, and inflammation which were already downregulated in the mock-treated AD cells were further downregulated after infection (Fig. 6d, Additional file 5: Table S11). Although as shown above, the top upstream regulators were common for infection of the control and AD cells, both quantitative and biological activity differences of upstream regulators between SARS-CoV-2 infected control and AD OM-ALI were observed (Fig. 6h, Additional file 5: Table S12).

Discussion

The OM, situated at the rooftop of the nasal cavity, is in direct contact to inhaled air and the particles present in it. Previous studies have shown infection of the OM with the SARS-CoV-2, and this has been investigated in ex vivo human olfactory biopsies from infected individuals [68, 69]. However, analyses of viral replication and pathophysiological processes caused by infection of the OM cells are limited. Furthermore, there is a lack of understanding of viral infection processes and possible differential responses of the infected cells to SARS-CoV-2 in underlying neurological disease conditions, i.e., AD. According to the current information, this paper presents the first efforts to address these knowledge gaps and to develop a physiologically relevant human-derived 3D in vitro model of the OM. We present evidence that human OM biopsies-derived cell cultures, when grown in ALI, recapitulate key features of the OM in vivo, and can be used to model viral infections under controlled experimental conditions. Furthermore, in this study, we present new insight into the infectability of the OM cells derived from AD individuals in comparison to those of cognitively healthy individuals and decipher the transcriptomic crosstalk between AD and SARS-CoV-2 infection at the OM.

In this study, we established a novel 3D ALI culture of the human OM. Characterization of cells derived from OM biopsies taken from cognitively healthy individuals and those affected by AD after three weeks in ALI indicated the presence of pseudostratified epithelium and cells expressing cilia. Furthermore, our results showed that the OM cells grown in ALI formed a barrier, confirmed through TEER measurement and expression of tight junction markers. Although we were unable to identify neither immature nor mature olfactory neurons, we confirm that sustentacular cells, basal cells, and mucous-producing cells are among the different cell types expressed in the OM-ALI cultures.

Our previous evidence from single-cell transcriptomic analysis of traditional 2D cultures of OM cells revealed the presence of AD-associated pathology in the OM cells derived from individuals with AD [30]. Consistent with that, in this study, the transcriptomic profile of the AD OM-ALI cells is also distinct from that of cognitively healthy control cells. We report a total of 427 DEGs between the control mock and AD mock OM-ALI cultures and further shortlist the top 20 DEGs that are associated with Alzheimer's disease KEGG pathway (hsa05010). Interestingly, several of these top DEGs were found to be commonly attributed to AD in other cells or in vivo, i.e., *DKK1* [70], FZD7 (Frizzled-7) [71], *PTGS2* [72], and *APOE* [73]. Furthermore, enrichment of AD-associated pathways, i.e., integrin signaling pathway, Alzheimer's disease-presenilin pathway, and Wnt-signaling pathway, were observed in pathway analysis of DEGs between non-infected control and AD OM-ALI cells. In addition, key upstream regulators that are linked to the DEGs found in non-infected AD cells correspond to the key phenomena in AD including inflammation, oxidative stress, regulation of Aβ deposition, neuronal dysfunction, and synaptic plasticity. Therefore, we believe that the OM-ALI culture of cells of individuals with AD exhibits pathological features associated with the disease.

Importantly, the OM-ALI cultures express ACE-2, the main entry receptor of SARS-CoV-2—the expression of this receptor has also been previously demonstrated ex vivo in the human OE [10, 13, 74]. Aside from the role of ACE-2 in facilitating viral entry, some research has put forth the Neuropilin-1 receptor (NRP-1) as an alternative means of entry for SARS-CoV-2 [17]. The expression of NRP-1 in the OE is not limited to certain cell type and as is the case with ACE-2 [18]. In coherence with the evidence ex vivo, in this study, we confirmed that OM-ALI cells also express the NRP-1 receptor. Furthermore, OM-ALI cells expressed genes for all the characteristic proteins that are important for viral entry and infection, such as TMPRSS-2, CTSB, CTSL, NRP-1, BSG, and furin.

Evidence to date indicates that SARS-CoV-2 infects the non-neural cells of the OE, mainly the sustentacular cells surrounding the olfactory sensory neurons (OSNs) [68, 75]. Sustentacular cells provide functional and structural support to the OSNs and hence play a crucial role in olfaction [76, 77]. Infection of sustentacular cells leads to detrimental effects on the OE, which may lead to olfactory function impairment. This can happen either through a direct impact on the uniformity of the OE or indirectly through affecting the metabolic and functional activity of the OSNs. Research conducted on Syrian hamsters by Bryche et al. showed that the loss of sustentacular cells caused by the virus resulted in the desquamation of the OE, the recruitment of immune cells, and the loss of OSN cilia [78]. Another study by Zazhytska et al. reported significant damage to the OE, although there

was little infection of the OSNs [69]. The study also documented the downregulation of sustentacular cell-specific markers, followed by the downregulation of OSN-specific genes and related signaling pathways that play a role in the sense of smell. Consistent with the others, our study demonstrates infection of apical cells of the OM-ALI, including ciliary cells and non-neuronal epithelial cells.

In addition to the above-mentioned effects, previous research has corroborated the involvement of immune cells in the infection of OM. Infection of sustentacular cells located in the OE prompts the production of pro-inflammatory cytokines as a defensive reaction against viral invasion. However, these pro-inflammatory cytokines could provoke harm to the OE, and thereby induce dysfunction of the OSNs. In this study, acute infection in the OM-ALI cells derived from cognitively healthy controls and AD individuals led to a robust immune response and upregulation of the pro-inflammatory response. It has been observed in patients with long COVID that even after the resolution of SARS-CoV-2 infection in the OM, gene expression changes remain in the sustentacular cells. These changes suggest a reaction to the ongoing inflammation signaling and are accompanied by a reduction in the number of OSNs [79]. Since our ALI culture model does not include neurons, it is possible that in vivo the OSNs can also be infected, although this may be limited, as earlier reported [16, 80]. It is herein not possible to completely understand the crosstalk between sustentacular cells and OSNs, however, our transcriptomic data from infected OM-ALI cells indicate downregulation of several genes that are linked to neuronal plasticity, axonal guidance, and neuronal survival, thereby supporting the hypothesis that infection of the supporting cells of the OM can induce secondary harmful effects on OSN functions.

The current study presents the transcriptomic landscape of WT SARS-CoV-2 infection in human OM cells. As expected, differential gene expression analysis of SARS-CoV-2 infected OM-ALI cells revealed COVID-19 pathogenesis pathway activation along with alterations in genes involved in inflammation and antiviral immune response through interferon signaling. Pathway analysis of DEGs in SARS-CoV-2 infected OM-ALI cells also revealed alterations of genes involved in oxidative phosphorylation and mitochondrial function. Others have reported mitochondrial dysfunction in infected brain cells, which has been attributed to the neuropathogenesis of SARS-CoV-2 infection [81]. Furthermore, mitochondrial dysfunction is a hallmark of many neurodegenerative diseases, including AD, and alterations in mitochondrially located genes and mitochondrial function in OM cells of individuals with AD have been previously demonstrated [30]. It is plausible that increased mitochondrial stress and reduced oxidative phosphorylation resulting from SARS-CoV-2 infection in the OM further intensify oxidative stress and may exacerbate the pro-inflammatory response of the OM, which could potentially be damaging to the epithelial barrier.

A recent study suggested that modification of the SARS-CoV-2 spike protein potentially alters cell tropism and interaction with proteins that promote virus uptake [82]. That also corresponds with the prevalence data from the emerging variants of SARS-CoV-2 which indicate that there are differences in the incidence of anosmia in COVID-19-affected individuals with certain variants [57]. In this study, we demonstrated the changes in the infectibility of the OM-ALI cultures with the different variants of SARS-CoV-2. Interestingly, OM-ALI cells showed greater susceptibility to infection with SARS-CoV-2-WT as compared to the omicron variant of SARS-CoV-2, whereas the delta variant did not differ significantly from the infection with the WT virus. Reduction in the number of infected cells of OM with omicron as compared to the other mentioned variants may explain the reduction in the number of cases of anosmia in individuals with COVID-19. These results are in line with a very recent study that suggests a transition in cellular tropism from OE to the respiratory epithelium with omicron as compared to the WT and delta SARS-CoV-2 in the hamster model [83]. However, further research is required to fully understand how changes in the SARS-CoV-2 spike proteins between the emerging variants alter the viral tropism in the OM.

Since the start of the pandemic, several mechanisms have been hypothesized that are potentially linked to increased susceptibility of SARS-CoV-2 infection in individuals affected by AD (reviewed in [34]). Our results demonstrate that the SARS-CoV-2 virus infects equally OM-ALI cells of both cognitively healthy individuals and those affected by AD. There were no differences observed in terms of the infectability of the OM cells from control and AD individuals or the increase in the viral titer over the infection period. Therefore, our results provide crucial evidence suggesting that underlying AD pathology does not make the OM-ALI cells more vulnerable to infection. Recent research has revealed that individuals suffering from AD have higher levels of ACE-2 protein in the hippocampal region of the brain, as compared to healthy individuals. The elevated levels of ACE-2 in the brain have been linked to an augmented risk of SARS-CoV-2 neurotropism [84]. Apart from its role in facilitating viral entry into the cell, ACE-2 may also have a protective effect against the development and progression of AD by modulating the production and aggregation of Aβ, as suggested by a study in transgenic AD mice [85]. Our study conducted on OM did not reveal changes

in the cellular expression of ACE-2 in AD cells, which could explain the similar infection patterns observed in both control and AD OM-ALI cells. Interestingly, we did observe that certain COVID-19-associated genes, including *CTSL* and *NRP-1*, were significantly downregulated specifically in the AD cells following infection. This supports the idea that even though healthy and AD cells are infected in a similar manner, the cellular responses to the virus may vary.

Even though the susceptibility to the infection was similar in both AD and control OM-ALI cells, the transcriptomic analyses revealed significant differential expression of genes following SARS-CoV-2 infection. In general, the data show that the overall transcriptional footprint of WT SARS-CoV-2 infection is distinct in cognitively healthy control cells in comparison to AD cells, given that 1971 DEGs were observed between SARS-CoV-2 infected control and AD OM-ALI cells. This suggests that although the virus infects the cells in the same way, the response to the infection may differ in individuals with AD, which could potentiate and intensify COVID-19-associated outcomes. It has been reported that an effective antiviral response contributes to viral clearance and improves clinical outcomes [86, 87]. However, in individuals with underlying AD, inflammation and impaired immune function can increase the risk of severe disease outcomes [88]. Interestingly in this study, SARS-CoV-2 infection in the cognitively healthy control cells shows a robust response of antiviral immune response genes and interferon-stimulated genes, which was not observed in infected cells of AD individuals. Even though the AD OM-ALI cultures without viral infection show basal enrichment of innate immune response genes and interferon-stimulated genes (Additional file 3: Fig. S3, Additional file 4: Fig. S4), IPA analysis of the comparison between DEGs in SARS-CoV-2 infected cells from AD individuals and cognitively healthy controls indicated downregulation of *IFN-γ* (interferon-gamma) and *TNF* in the AD OM-ALI cells. In fact, innate immunity deficits, and specifically type 1 interferon signaling perturbations are often observed in AD in various cell types [89–92]. This suggests that like other cell types, the cells of the OM of individuals with AD are impaired in immune responses.

Another study suggested that in moderate-to-severe cases of SARS-CoV-2 infection, insufficient activation of interferon-mediated antiviral immune responses leads to a failure to limit viral replication in a timely manner [93]. Therefore, it is plausible that the existing activation of immune responses present in non-infected AD cells could cause desensitization or milder alterations in the respective genes after infection with SARS-CoV-2. Moreover, dampened antiviral immune and inflammatory response during early convalescence could potentially be inadequate and delay viral clearance. Recent evidence also suggested that persistent viral reservoirs and the continued SARS-CoV-2 specific immune responses during late convalescence may result in uncontrolled inflammation, causing long-lasting adverse outcomes including neurological perturbations [94]. Additionally, reactive oxygen species (ROS) are known to escalate neuroinflammation and lead to excessive production of Aβ, thereby contributing to the development and progression of AD. Notably, the current study found that infected AD cells have elevated oxidative stress as compared to infected controls. It is suggested from recent evidence that the activity of innate immunity is heavily influenced by oxidative stress, which has been identified as a significant contributor to the pathogenesis of COVID-19, due to its perpetuation of the cytokine storm cycles reported by recent data [95]. On the other hand, AD is also associated with multiple etiologies and pathophysiologic mechanisms, and oxidative stress appears to be a major part of the pathophysiologic process [96]. It is reasonable to speculate that elevated oxidative stress with persistent viral reservoirs and dysfunctional inflammatory response could potentially be linked to the worsening of existing AD pathology and progression of AD. However, further evidence is necessary to fully comprehend the long-term consequences of the infection in individuals with AD.

Loss of the sense of smell is a common attribute among many SARS-CoV-2-infected individuals and in non-infected individuals with AD. *UGTA2A* has been known to be expressed in the sustentacular cells of the OE [68, 79] and was recently implicated as a common risk gene among individuals with COVID-19-induced anosmia [59]. Our data showed upregulation of *UGTA2A* (log2fc 4.08, Padj 0.001) in mock AD cells as compared to mock control cells, suggesting an increased risk of loss of smell in AD individuals as compared to healthy controls. In addition to this, our study suggested a significant reduction in the ciliary cells after infection of the AD OM-ALI cells, as compared to infection in healthy cells. Extensive OE damage, due to loss of cells after infection and ciliary desquamation, has been reported for SARS-CoV-2 infection in the OM of mice, and hamsters [15, 75, 78]. Similarly, ciliary loss has also been indicated in the nasal and respiratory epithelium as well after infection with SARS-CoV-2 [97, 98]. Furthermore, bulk transcriptomic data from the SARS-CoV-2 infected OM-ALI cells from AD individuals show significant downregulation of olfactory receptor (OR) family genes *OR4M1*, *OR2T11*, and *OR4N2* after SARS-CoV-2 infection. It is important here to note that although we did not detect neurons in the OM-ALI cultures, downregulation of the OR genes was observed specifically in SARS-CoV-2 infected AD cells.

While the ORs are associated primarily with the sense of smell and primarily expressed by the OSNs, recent studies have suggested that they may play a role in other biological processes in the body [99]. These receptors have been found in non-olfactory tissues such as the gut, kidney, and sperm, however, their functions beyond odorant detection have not been fully elucidated [100]. Interestingly, alterations in ORs have also been reported in the brain and implicated in neurodegenerative diseases [101]. For example, OR4M1 stimulation in mouse primary cortico-hippocampal neurons protects against abnormal tau processing [102], processing that is implicated in AD pathology. However, in this study, downregulation of the OR receptor genes after SARS-CoV-2 infection of the AD OM-ALI could possibly be attributed to hindrance in the perception of a smell. These alterations in OM cells could indicate that the presence of underlying AD may increase the risk of SARS-CoV-2 infection-associated loss of smell.

Conclusions

In conclusion, this study introduced a novel physiologically relevant patient-derived cell model which can facilitate an improved understanding of COVID-19 pathogenesis and allow evaluation of vulnerability and risk associated with pre-existing AD in COVID-19 patients. Additionally, our model offers a pertinent preclinical platform to rapidly evaluate potential drugs and vaccines against COVID-19 and other pathogens that may emerge in the future. However, it is important to note here that our study has some limitations. First, we acknowledge that SARS-CoV-2-associated loss of smell and the infection pathogenesis in the OE can be affected by host genetics, age, ethnicity, and geographical location [103–105], however, this study was performed on primary cells derived from OM biopsies taken from AD patient and cognitively healthy individuals. Furthermore, the number of OM biopsies available for this study was restricted due to the limited availability of donors over the study duration. However, given the similar responses of the OM cells from all donors of the same disease status, we believe these results to be representative of virus-induced alterations in these cells. Second, to our knowledge, this study presents the first efforts to explore the interaction of existing AD pathology and SARS-CoV-2 infection of human-derived OM. Given that AD is a complex disease with several lifestyle and genetic factors implicated in the risk of development and progression of this disease, further studies should aim to assess the impact of confounding factors on cellular responses. Third, it is important to highlight that the scope of the study is limited to the evaluation of the effects of SARS-CoV-2 on the non-neural epithelial cell fraction of the OM cells. Although current literature suggests that direct infection of the OSNs is less probable and that infection-related effects in epithelial cells lead to detrimental effects on the neurons, this was not addressed in the current study. Research on the crosstalk between neural and non-neural cells upon infection should be a topic of further investigation given that the trans-olfactory route may serve as a potential entry route for several pathogens and environmental agents to the brain. Such studies will increase the physiological relevance and complexity to better recapitulate in vivo conditions and enable the investigation of the crosstalk at the nose–brain axis upon exposure to SARS-CoV-2 and other pathogens. Finally, this study did not address the effects of other respiratory viruses or damage-associated molecular pattern (DAMP)-induced induction of inflammation. These topics warrant further studies in the future. In conclusion, this study introduced a novel physiologically relevant patient-derived cell model to facilitate an improved understanding of COVID-19 pathogenesis and allow evaluation of vulnerability and risk associated with pre-existing AD in COVID-19 patients. Additionally, our model offers a pertinent preclinical platform to rapidly evaluate potential drugs and vaccines against COVID-19 and other pathogens that may emerge in the future.

Abbreviations

COVID-19	Coronavirus disease of 2019
AD	Alzheimer's disease
OM	Olfactory mucosa
SARS-CoV-2	Severe acute respiratory syndrome coronavirus 2
ALI	Air–liquid interface
NP	Nucleocapsid protein
OSNs	Olfactory sensory neurons
LP	Lamina propria
OE	Olfactory epithelium
D-PBS	Dulbecco's phosphate buffered saline
HBSS	Hank's balanced salt solution
OM-ALI	Olfactory mucosa cell at air–liquid interface
WT	Wild type
TEER	Trans-epithelial electrical resistance
hpi	Hour post-infection
DEGs	Differentially expressed genes
PFA	Paraformaldehyde
mRNA	Messenger RNA
PFU	Plaque forming unit
BSA	Bovine serum albumin
CNS	Central nervous system
BSL	Biosafety level 2
IPA	Ingenuity pathway analysis
ACE-2	Angiotensin-converting enzyme 2
TMPRSS2	Transmembrane protease, serine 2
NRP-1	Neuropilin-1
CTSB	Cathepsin B
CTSL	Cathepsin L
BSG	Basigin
Furin	Furin
UGT2A2	UDP Glucuronosyltransferase Family 2 Member A2
CXCL10	C–X–C motif chemokine ligand 10
OASL	2′-5′-Oligoadenylate synthetase like
RSAD2	Radical *S*-adenosyl methionine domain containing 2
IFIT1	Interferon induced protein with tetratricopeptide repeats 1

PTGS2	Prostaglandin-endoperoxide synthase 2
eIF2	Eukaryotic translation initiation factor 2
APOE	Apolipoprotein E
OR	Olfactory receptor
MUC5AC	Mucin 5AC
TNF	Tumor necrosis factor

Supplementary Information

The online version contains supplementary material available at https://doi.org/10.1186/s12974-023-02979-4.

Additional file 1. Immunohistochemical staining (single channel images) of OM-ALI cultures from cognitively healthy controls for a) zonula occludens-1 (ZO1) (tight junction marker); b) acetylated tubulin (ciliary marker); c) MUC5AC (mucinproducing cells); d) Cytokeratin 18 (CK-18) (sustentacular cells); e) co-staining of nucleocapsid protein (NP) (SARS-CoV-2 infection marker) with acetylated tubulin; co-staining of nucleocapsid protein (NP) with MUC5AC. Slides were imaged on 10x objective; Scale bar 100μm.

Additional file 2. Significantly enriched Panther pathways at 48 h post-infection in AD cells compared to control cells. (a) ADassociated pathways are significantly enriched in mock AD cells (Control Mock vs AD Mock). (b) Infection with WT SARS-CoV-2 causes enrichment in AD-associated pathways (Control Infected vs AD Infected). (c) Numbers of genes enriched in AD-associated pathways after infection of control and AD cells.

Additional file 3. Changes in expression of genes involved in interferon-stimulated genes at 48 h post-infection with SARS-CoV-2. (a) Heatmap comparing mock control and infected OM-ALI cells. (b) Heatmap comparing AD mock and AD-infected OM-ALI cells.

Additional file 4. Changes in expression of genes involved in innate immune response at 48 h post-infection with SARS-CoV-2. (a) Heatmap comparing healthy mock and healthy infected cells. (b) Heatmap comparing AD mock and AD infected cells.

Additional file 5: Table S1. Significant differentially expressed genes between control mock and AD mock OM-ALI cells. **Table S2**. Significant differentially expressed genes between control mock and control-infected OM-ALI cells. **Table S3**. Significant differentially expressed genes between AD mock and AD-infected OM-ALI cells. **Table S4**. Significant differentially expressed genes between control-infected and AD-infected OM-ALI cells. **Table S5**. Significant ingenuity canonical pathways that are found from analysis of significant differentially expressed genes between control mock and AD mock. **Table S6**. Top 20 upstream regulators among significant differentially expressed genes between control mock and AD mock OM-ALI cells. **Table S7**. Significant ingenuity canonical pathways that are found from analysis of significant differentially expressed genes between control mock and control. **Table S8**. Significant ingenuity canonical pathways that are found from analysis of significant differentially expressed genes between AD mock and AD infected. **Table S9**. Top 20 upstream regulators among significant differentially expressed genes between control mock and control-infected OM-ALI cells. Table S10 Top 20 upstream regulators among significant differentially expressed genes between AD mock and AD-infected OM-ALI cells. **Table S11**: Significant ingenuity canonical pathways that are found from analysis of significant differentially expressed genes between control infected and AD. **Table S12.** Top 20 upstream regulators among significant differentially expressed genes between control-infected and AD-infected OM-ALI cells.

Acknowledgements
We would like to express our gratitude and acknowledge the invaluable technical assistance provided by Mira Utriainen at the BSL 3 facility, Department of Virology, University of Helsinki, and Mirka Tikkanen at the A.I Virtanen Institute for Molecular Medicine, University of Eastern Finland.

Author contributions
KMK, GB, SC, PS, JT, OV and MAS designed the study. MAS, SK, TZ, ZK, LM, RO, LS and NT performed the experiments. OV, JT, KMK provided facility supports. AMK, EP, JK and HL provided biopsies and clinical data. MAS, TH, GB and RL, SK and TZ analyzed the data. MAS wrote the draft of the manuscript. KMK, GB, SK and RL revised the manuscript.

Funding
This work was financially supported by the Academy of Finland (grant number 335524), Sigrid Juselius foundation, and by the University of Eastern Finland. This work was supported by the Ministry of Education, Youth and Sports of the Czech Republic (the Research Infrastructure NanoEnviCZ, LM2018124) and the European Union—European Structural and Investments Funds in the frame of Operational Programme Research Development and Education—project Pro-NanoEnviCz (Project No. CZ.02.1.01/0.0/0.0/16_013/0001821).

Availability of data and materials
The data presented in this study are available upon reasonable request from the corresponding author. RNA sequencing data will be available from the European Genome–phenome Archive (EGA, https://ega-archive.org/) under the The Data Access Committee for Human Olfactory Mucosa Cells (DAC_HOM) at UEF (EGAC00001002527).

Declarations

Ethics approval and consent to participate
Human olfactory biopsies were obtained from cognitively healthy and AD individuals under the approved ethical permit from the Human Research Ethics Committees (HRECs), of Northern Savo Hospital District (permit number 536/2017). Written informed consent was obtained from all subjects and proxy consent from family members of persons with mild AD dementia.

Consent for publication
Not applicable.

Competing interests
The authors declare no competing interests.

Author details
[1]A.I. Virtanen Institute for Molecular Sciences, University of Eastern Finland, 70210 Kuopio, Finland. [2]Department of Virology, Faculty of Medicine, University of Helsinki, 00290 Helsinki, Finland. [3]Charité-Universitätsmedizin Berlin, Corporate Member of Freie Universität Berlin and Humboldt-Universität Zu Berlin, Institute of Virology, 10117 Berlin, Germany. [4]Institute of Molecular Genetics, Czech Academy of Sciences, 142 20 Prague, Czech Republic. [5]Department of Genetic Toxicology and Epigenetics, Institute of Experimental Medicine, Czech Academy of Sciences, 142 20 Prague, Czech Republic. [6]Department of Neurology, Neuro Centre, Kuopio University Hospital, 70210 Kuopio, Finland. [7]Brain Research Unit, Department of Neurology, School of Medicine, University of Eastern Finland, 70210 Kuopio, Finland. [8]Department of Neurology and Geriatrics, Helsinki University Hospital and Neurosciences, Faculty of Medicine, University of Helsinki, 00014 Helsinki, Finland. [9]Department of Otorhinolaryngology, University of Eastern Finland and Kuopio University Hospital, 70210 Kuopio, Finland. [10]Finnadvance, 90220 Oulu, Finland. [11]The Queensland Brain Institute, University of Queensland, Brisbane, Queensland 4072, Australia.

Received: 11 July 2023 Accepted: 30 November 2023
Published online: 14 December 2023

References

1. Luërs JC, Klumann JP, Guntinas-Lichius O. The COVID-19 pandemic and otolaryngology: what it comes down to? Laryngorhinootologie. 2020;99(5):287–91.
2. Eliezer M, Hautefort C, Hamel AL, Verillaud B, Herman P, Houdart E, et al. Sudden and complete olfactory loss of function as a possible symptom of COVID-19. JAMA Otolaryngol Head Neck Surg. 2020;146(7):674–5.
3. Vaira LA, Salzano G, Deiana G, de Riu G. Anosmia and ageusia: common findings in COVID-19 patients. Laryngoscope. 2020;130(7):1787.

4. Doty RL. Olfactory dysfunction in COVID-19: pathology and long-term implications for brain health. Trends Mol Med. 2022;28(9):781–94.
5. Lee Y, Min P, Lee S, Kim SW. Prevalence and duration of acute loss of smell or taste in COVID-19 patients. J Korean Med Sci. 2020;35(18):e174.
6. Tan BKJ, Han R, Zhao JJ, Tan NKW, Quah ESH, Tan CJW, et al. Prognosis and persistence of smell and taste dysfunction in patients with covid-19: meta-analysis with parametric cure modelling of recovery curves. BMJ. 2022;378:e069503. https://doi.org/10.1136/bmj-2021-069503.
7. Stefanou MI, Palaiodimou L, Bakola E, Smyrnis N, Papadopoulou M, Paraskevas GP, et al. Neurological manifestations of long-COVID syndrome: a narrative review. Ther Adv Chronic Dis. 2022;13:204062232210768.
8. Bauer L, Laksono BM, de Vrij FMS, Kushner SA, Harschnitz O, van Riel D. The neuroinvasiveness, neurotropism, and neurovirulence of SARS-CoV-2. Trends Neurosci. 2022;45(5):358–68.
9. Chen Y, Yang W, Chen F, Cui L. COVID-19 and cognitive impairment: neuroinvasive and blood–brain barrier dysfunction. J Neuroinflammation. 2022;19(1):1–14. https://doi.org/10.1186/s12974-022-02579-8.
10. Klingenstein M, Klingenstein S, Neckel PH, Mack AF, Wagner AP, Kleger A, et al. Evidence of SARS-CoV2 entry protein ACE2 in the human nose and olfactory bulb. Cells Tissues Organs. 2020;209(4–6):155–64.
11. Bilinska K, Jakubowska P, von Bartheld CS, Butowt R. Expression of the SARS-CoV-2 entry proteins, ACE2 and TMPRSS2, in cells of the olfactory epithelium: identification of cell types and trends with age. ACS Chem Neurosci. 2020;11(11):1555–62.
12. Fodoulian L, Tuberosa J, Rossier D, Boillat M, Kan C, Pauli V, et al. SARS-CoV-2 receptors and entry genes are expressed in the human olfactory neuroepithelium and brain. iScience. 2020;23(12):101839.
13. Chen M, Shen W, Rowan NR, Kulaga H, Hillel A, Ramanathan M, et al. Elevated ACE-2 expression in the olfactory neuroepithelium: implications for anosmia and upper respiratory SARS-CoV-2 entry and replication. Eur Respir J. 2020;56(3):2001948.
14. Shahbaz MA, de Bernardi F, Alatalo A, Sachana M, Clerbaux LA, Muñoz A, et al. Mechanistic understanding of the olfactory neuroepithelium involvement leading to short-term anosmia in COVID-19 using the adverse outcome pathway framework. Cells. 2022;11(19):3027.
15. de Melo GD, Lazarini F, Levallois S, Hautefort C, Michel V, Larrous F, et al. COVID-19-related anosmia is associated with viral persistence and inflammation in human olfactory epithelium and brain infection in hamsters. Sci Transl Med. 2021;13(596):e8396.
16. Meinhardt J, Radke J, Dittmayer C, Franz J, Thomas C, Mothes R, et al. Olfactory transmucosal SARS-CoV-2 invasion as a port of central nervous system entry in individuals with COVID-19. Nat Neurosci. 2021;24(2):168–75.
17. Alipoor SD, Mirsaeidi M. SARS -CoV-2 cell entry beyond the ACE2 receptor. Mol Biol Rep. 2022;49:10715–27.
18. Cantuti-Castelvetri L, Ojha R, Pedro LD, Djannatian M, Franz J, Kuivanen S, et al. Neuropilin-1 facilitates SARS-CoV-2 cell entry and infectivity. Science (1979). 2020;370(6518):856. https://doi.org/10.1126/science.abd2985.
19. Daly JL, Simonetti B, Klein K, Chen KE, Williamson MK, Antón-Plágaro C, et al. Neuropilin-1 is a host factor for SARS-CoV-2 infection. Science. 2020;370(6518):861–5.
20. Fotuhi M, Mian A, Meysami S, Raji CA. Neurobiology of COVID-19. J Alzheimer's Dis. 2020;76(1):3–19.
21. Xia X, Wang Y, Zheng J. COVID-19 and Alzheimer's disease: how one crisis worsens the other. Transl Neurodegener. 2021;10:15. https://doi.org/10.1186/s40035-021-00237-2.
22. Knopman DS, Amieva H, Petersen RC, Chételat G, Holtzman DM, Hyman BT, et al. Alzheimer disease. Nature Rev Dis Primers. 2021;7(1):1–21.
23. Deture MA, Dickson DW. The neuropathological diagnosis of Alzheimer's disease. Mol Neurodegener. 2019;14(1):1–18. https://doi.org/10.1186/s13024-019-0333-5.
24. Marin C, Vilas D, Langdon C, Alobid I, López-Chacón M, Haehner A, et al. Olfactory dysfunction in neurodegenerative diseases. Curr Allergy Asthma Rep. 2018;18(8):1–19. https://doi.org/10.1007/s11882-018-0796-4.
25. Jung HJ, Shin IS, Lee JE. Olfactory function in mild cognitive impairment and Alzheimer's disease: a meta-analysis. Laryngoscope. 2019;129(2):362–9.
26. Roberts RO, Christianson TJH, Kremers WK, Mielke MM, Machulda MM, Vassilaki M, et al. Association between olfactory dysfunction and amnestic mild cognitive impairment and Alzheimer disease dementia. JAMA Neurol. 2016;73(1):93–101.
27. Woodward MR, Amrutkar CV, Shah HC, Benedict RHB, Rajakrishnan S, Doody RS, et al. Validation of olfactory deficit as a biomarker of Alzheimer disease. Neurol Clin Pract. 2017;7(1):5–14.
28. Lafaille-Magnan ME, Poirier J, Etienne P, Tremblay-Mercier J, Frenette J, Rosa-Neto P, et al. Odor identification as a biomarker of preclinical AD in older adults at risk. Neurology. 2017;89(4):327–35.
29. Lampinen R, Górová V, Avesani S, Liddell JR, Penttilä E, Závodná T, et al. Biometal dyshomeostasis in olfactory mucosa of Alzheimer's disease patients. Int J Mol Sci. 2022;23(8):4123.
30. Lampinen R, FerozeFazaludeen M, Avesani S, Örd T, Penttilä E, Lehtola JM, et al. Single-cell RNA-Seq analysis of olfactory mucosal cells of Alzheimer's disease patients. Cells. 2022;11:676.
31. Sochocka M, Zwolińska K, Leszek J. The infectious etiology of Alzheimer's disease. Curr Neuropharmacol. 2017;15(7):996.
32. Itzhaki RF, Golde TE, Heneka MT, Readhead B. Do infections have a role in the pathogenesis of Alzheimer disease? Nat Rev Neurol. 2020;16(4):193–7.
33. Ciaccio M, lo Sasso B, Scazzone C, Gambino CM, Ciaccio AM, Bivona G, et al. COVID-19 and Alzheimer's disease. Brain Sci. 2021;11(3):305.
34. Chen F, Chen Y, Wang Y, Ke Q, Cui L. The COVID-19 pandemic and Alzheimer's disease: mutual risks and mechanisms. Transl Neurodegener. 2022;11(1):1–18. https://doi.org/10.1186/s40035-022-00316-y.
35. Villa C, Rivellini E, Lavitrano M, Combi R. Can SARS-CoV-2 infection exacerbate Alzheimer's disease? An overview of shared risk factors and pathogenetic mechanisms. J Pers Med. 2022;12(1):29.
36. Wang QQ, Xu R, Volkow ND. Increased risk of COVID-19 infection and mortality in people with mental disorders: analysis from electronic health records in the United States. World Psychiatry. 2021;20(1):124–30.
37. Mavrikaki M, Lee JD, Solomon IH, Slack FJ. Severe COVID-19 is associated with molecular signatures of aging in the human brain. Nat Aging. 2022;2(12):1130–7.
38. Reiken S, Sittenfeld L, Dridi H, Liu Y, Liu X, Marks AR. Alzheimer's-like signaling in brains of COVID-19 patients. Alzheimer's Dementia. 2022;18(5):955–65.
39. Vavougios GD, Nday C, Pelidou SH, Gourgoulianis KI, Stamoulis G, Doskas T, et al. Outside-in induction of the IFITM3 trafficking system by infections, including SARS-CoV-2, in the pathobiology of Alzheimer's disease. Brain Behav Immun Health. 2021;14: 100243.
40. Naughton SX, Raval U, Pasinetti GM. Potential novel role of COVID-19 in Alzheimer's disease and preventative mitigation strategies. J Alzheimers Dis. 2020;76(1):21.
41. Li W, Sun L, Yue L, Xiao S. Alzheimer's disease and COVID-19: interactions, intrinsic linkages, and the role of immunoinflammatory responses in this process. Front Immunol. 2023;14:1120495.
42. Jack CR, Bennett DA, Blennow K, Carrillo MC, Dunn B, Haeberlein SB, et al. 2018 National Institute on Aging-Alzheimer's Association (NIA-AA) Research Framework NIA-AA Research Framework: toward a biological definition of Alzheimer's disease. Alzheimer Dementia. 2018;14:535. https://doi.org/10.1016/j.jalz.2018.02.018.
43. Morris JC, Heyman A, Mohs RC, Hughes JP, van Belle G, Fillenbaum G, et al. The Consortium to Establish a Registry for Alzheimer's Disease (CERAD). Part I. Clinical and neuropsychological assessment of Alzheimer's disease. Neurology. 1989;39(9):1159–1159.
44. Mirra SS, Heyman A, McKeel D, Sumi SM, Crain BJ, Brownlee LM, et al. The Consortium to establish a registry for Alzheimer's disease (CERAD). Neurology. 1991;41(4):479–479.
45. Murrell W, Féron F, Wetzig A, Cameron N, Splatt K, Bellette B, et al. Multipotent stem cells from adult olfactory mucosa. Dev Dyn. 2005;233(2):496–515. https://doi.org/10.1002/dvdy.20360.
46. Benson K, Cramer S, Galla HJ. Impedance-based cell monitoring: barrier properties and beyond. Fluids Barriers CNS. 2013;10(1):1–11. https://doi.org/10.1186/2045-8118-10-5.
47. Wen LJ, Tang C, Cheng WH, Du B, Chen C, Wang M, et al. Genomic monitoring of SARS-CoV-2 uncovers an Nsp1 deletion variant that modulates type I interferon response. Cell Host Microbe. 2021;29(3):489-502.e8.
48. Corman VM, Landt O, Kaiser M, Molenkamp R, Meijer A, Chu DKW, et al. Detection of 2019 novel coronavirus (2019-nCoV) by real-time RT-PCR. Eurosurveillance. 2020;25(3):1.

49. Bolger AM, Lohse M, Usadel B. Trimmomatic: a flexible trimmer for Illumina sequence data. Bioinformatics. 2014;30(15):2114–20.
50. Dobin A, Davis CA, Schlesinger F, Drenkow J, Zaleski C, Jha S, et al. Sequence analysis STAR: ultrafast universal RNA-seq aligner. Bioinformatics. 2013;29(1):15–21.
51. Liao Y, Smyth GK, Shi W. featureCounts: an efficient general purpose program for assigning sequence reads to genomic features. Bioinformatics. 2014;30(7):923–30.
52. Hoffmann M, Kleine-Weber H, Schroeder S, Krüger N, Herrler T, Erichsen S, et al. SARS-CoV-2 cell entry depends on ACE2 and TMPRSS2 and is blocked by a clinically proven protease inhibitor. Cell. 2020;181(2):271-280.e8.
53. Simmons G, Gosalia DN, Rennekamp AJ, Reeves JD, Diamond SL, Bates P. Inhibitors of cathepsin L prevent severe acute respiratory syndrome coronavirus entry. Proc Natl Acad Sci USA. 2005;102(33):11876–81.
54. Coutard B, Valle C, de Lamballerie X, Canard B, Seidah NG, Decroly E. The spike glycoprotein of the new coronavirus 2019-nCoV contains a furin-like cleavage site absent in CoV of the same clade. Antiviral Res. 2020;1:176.
55. Kalejaiye TD, Bhattacharya R, Burt MA, Travieso T, Okafor AE, Mou X, et al. SARS-CoV-2 employ BSG/CD147 and ACE2 receptors to directly infect human induced pluripotent stem cell-derived kidney podocytes. Front Cell Dev Biol. 2022;20(10):737.
56. Essalmani R, Jain J, Susan-Resiga D, Andréo U, Evagelidis A, Derbali RM, et al. Distinctive roles of furin and TMPRSS2 in SARS-CoV-2 infectivity. J Virol. 2022;96(8):e0012822.
57. Butowt R, Bilińska K, von Bartheld C. Why does the omicron variant largely spare olfactory function? Implications for the pathogenesis of anosmia in coronavirus disease 2019. J Infect Dis. 2022;226:1304.
58. Koch J, Uckeley ZM, Doldan P, Stanifer M, Boulant S, Lozach PY. TMPRSS2 expression dictates the entry route used by SARS-CoV-2 to infect host cells. EMBO J. 2021;40(16):e107821. https://doi.org/10.15252/embj.2021107821.
59. Shelton JF, Shastri AJ, Fletez-Brant K, Auton A, Chubb A, Fitch A, et al. The UGT2A1/UGT2A2 locus is associated with COVID-19-related loss of smell or taste. Nat Genet. 2022;54(2):121–4.
60. Miller B, Silverstein A, Flores M, Cao K, Kumagai H, Mehta HH, et al. Host mitochondrial transcriptome response to SARS-CoV-2 in multiple cell models and clinical samples. Sci Rep. 2021;11(1):1–10.
61. Budhraja A, Basu A, Gheware A, Abhilash D, Rajagopala S, Pakala S, et al. Molecular signature of postmortem lung tissue from COVID-19 patients suggests distinct trajectories driving mortality. DMM Dis Models Mech. 2022;15(5):dmm049572.
62. Wyler E, Mösbauer K, Franke V, Diag A, Gottula LT, Arsiè R, et al. Transcriptomic profiling of SARS-CoV-2 infected human cell lines identifies HSP90 as target for COVID-19 therapy. iScience. 2021;24(3):102151.
63. Liu L, Zhang Y, Chen Y, Zhao Y, Shen J, Wu X, et al. Therapeutic prospects of ceRNAs in COVID-19. Front Cell Infect Microbiol. 2022;20(12):1379.
64. Chakraborty C, Sharma AR, Bhattacharya M, Zayed H, Lee SS. Understanding gene expression and transcriptome profiling of COVID-19: an initiative towards the mapping of protective immunity genes against SARS-CoV-2 infection. Front Immunol. 2021;15(12):5284.
65. Meydan C, Madrer N, Soreq H. The neat dance of COVID-19: NEAT1, DANCR, and co-modulated cholinergic RNAs link to inflammation. Front Immunol. 2020;9(11):2638.
66. Fung TS, Liao Y, Liu DX. Regulation of stress responses and translational control by coronavirus. Viruses. 2016;8(7):184.
67. Policard M, Jain S, Rego S, Dakshanamurthy S. Immune characterization and profiles of SARS-CoV-2 infected patients reveals potential host therapeutic targets and SARS-CoV-2 oncogenesis mechanism. Virus Res. 2021;1(301): 198464.
68. Khan M, Yoo SJ, Clijsters M, Backaert W, Vanstapel A, Speleman K, et al. Visualizing in deceased COVID-19 patients how SARS-CoV-2 attacks the respiratory and olfactory mucosae but spares the olfactory bulb. Cell. 2021;184(24):5932-5949.e15.
69. Zazhytska M, Kodra A, Hoagland DA, Frere J, Fullard JF, Shayya H, et al. Non-cell-autonomous disruption of nuclear architecture as a potential cause of COVID-19-induced anosmia. Cell. 2022;185(6):1052-1064.e12.
70. Ren C, Gu X, Li H, Lei S, Wang Z, Wang J, et al. The role of DKK1 in Alzheimer's disease: a potential intervention point of brain damage prevention? Pharmacol Res. 2019;1(144):331–5.
71. Palomer E, Martin-Flores N, Jolly S, Pascual-Vargas P, Benvegnù S, Podpolny M, et al. Epigenetic repression of Wnt receptors in AD: a role for Sirtuin2-induced H4K16ac deacetylation of Frizzled1 and Frizzled7 promoters. Mol Psychiatry. 2022. https://doi.org/10.1101/2021.05.19.444683.
72. Zhuang J, Cai P, Chen Z, Yang Q, Chen X, Wang X, et al. Long noncoding RNA MALAT1 and its target microRNA-125b are potential biomarkers for Alzheimer's disease management via interactions with FOXQ1, PTGS2 and CDK5. Am J Transl Res. 2020;12(9):5940.
73. Husain MA, Laurent B, Plourde M. APOE and Alzheimer's disease: from lipid transport to physiopathology and therapeutics. Front Neurosci. 2021;17(15):85.
74. Brann DH, Tsukahara T, Weinreb C, Lipovsek M, van den Berge K, Gong B, et al. Non-neuronal expression of SARS-CoV-2 entry genes in the olfactory system suggests mechanisms underlying COVID-19-associated anosmia. Sci Adv. 2020;6(31):eabc5801.
75. Ye Q, Zhou J, He Q, Li RT, Yang G, Zhang Y, et al. SARS-CoV-2 infection in the mouse olfactory system. Cell Discov. 2021;7:1–13.
76. Heydel JM, Coelho A, Thiebaud N, Legendre A, le Bon AM, Faure P, et al. Odorant-binding proteins and xenobiotic metabolizing enzymes: Implications in olfactory perireceptor events. Anat Rec. 2013;296(9):1333–45.
77. Cooper KW, Brann DH, Farruggia MC, Bhutani S, Pellegrino R, Tsukahara T, et al. COVID-19 and the chemical senses: supporting players take center stage. Neuron. 2020;107(2):219–33.
78. Bryche B, St Albin A, Murri S, Lacôte S, Pulido C, ArGouilh M, et al. Massive transient damage of the olfactory epithelium associated with infection of sustentacular cells by SARS-CoV-2 in golden Syrian hamsters. Brain Behav Immun. 2020;1(89):579–86.
79. Finlay JB, Brann DH, Abi Hachem R, Jang DW, Oliva AD, Ko T, et al. Persistent post-COVID-19 smell loss is associated with immune cell infiltration and altered gene expression in olfactory epithelium. Sci Transl Med. 2022;14(676):eadd0484. https://doi.org/10.1126/scitranslmed.add0484.
80. de Melo GD, Lazarini F, Levallois S, Hautefort C, Michel V, Larrous F, et al. COVID-19-related anosmia is associated with viral persistence and inflammation in human olfactory epithelium and brain infection in hamsters. Sci Transl Med. 2021;13(596):8396. https://doi.org/10.1126/scitranslmed.abf8396.
81. Pliss A, Kuzmin AN, Prasad PN, Mahajan SD. Mitochondrial dysfunction: a prelude to neuropathogenesis of SARS-CoV-2. ACS Chem Neurosci. 2022;13(3):308–12. https://doi.org/10.1021/acschemneuro.1c00675.
82. Rodriguez-Sevilla JJ, Güerri-Fernádez R, Bertran RB. Is there less alteration of smell sensation in patients with omicron SARS-CoV-2 variant infection? Front Med (Lausanne). 2022;9:1044. https://doi.org/10.3389/fmed.2022.852998/full.
83. Chen M, Pekosz A, Villano JS, Shen W, Zhou R, Kulaga H, et al. Evolution of nasal and olfactory infection characteristics of SARS-CoV-2 variants. bioRxiv. 2022.
84. Rudnicka-Drożak E, Drożak P, Mizerski G, Zaborowski T, Ślusarska B, Nowicki G, et al. Links between COVID-19 and Alzheimer's disease—what do we already know? Int J Environ Res Public Health. 2023;20(3):2146.
85. Evans CE, Miners JS, Piva G, Willis CL, Heard DM, Kidd EJ, et al. ACE2 activation protects against cognitive decline and reduces amyloid pathology in the Tg2576 mouse model of Alzheimer's disease. Acta Neuropathol. 2020;139(3):485.
86. Masood KI, Yameen M, Ashraf J, Shahid S, Faisal Mahmood S, Nasir A, et al. Upregulated type I interferon responses in asymptomatic COVID-19 infection are associated with improved clinical outcome. Sci Rep. 2021;11:22958. https://doi.org/10.1038/s41598-021-02489-4.
87. Hadjadj J, Yatim N, Barnabei L, Corneau A, Boussier J, Smith N, et al. Impaired type I interferon activity and inflammatory responses in severe COVID-19 patients. Science. 2020;369(6504):718–24.
88. Chiricosta L, Gugliandolo A, Mazzon E. SARS-CoV-2 exacerbates beta-amyloid neurotoxicity, inflammation and oxidative stress in Alzheimer's disease patients. Int J Mol Sci. 2021;22(24):13603.
89. Taylor JM, Moore Z, Minter MR, Crack PJ. Type-I interferon pathway in neuroinflammation and neurodegeneration: focus on Alzheimer's disease. J Neural Transm. 2018;125(5):797–807.
90. Vavougios GD, Mavridis T, Artemiadis A, Krogfelt KA, Hadjigeorgiou G. Trained immunity in viral infections, Alzheimer's disease and multiple

sclerosis: a convergence in type I interferon signalling and IFNβ-1a. Biochim Biophys Acta (BBA) Mol Basis Dis. 2022;1868(9):166430.
91. Song L, Chen J, Lo CYZ, Guo Q, Feng J, Zhao XM. Impaired type I interferon signaling activity implicated in the peripheral blood transcriptome of preclinical Alzheimer's disease. EBioMedicine. 2022;82: 104175.
92. Roy ER, Wang B, Wooi WY, Chiu G, Cole A, Yin Z, et al. Type I interferon response drives neuroinflammation and synapse loss in Alzheimer disease. J Clin Investig. 2020;130(4):1912–30.
93. Blanco-Melo D, Nilsson-Payant BE, Liu WC, Uhl S, Hoagland D, Møller R, et al. Imbalanced host response to SARS-CoV-2 drives development of COVID-19. Cell. 2020;181(5):1036-1045e9.
94. Opsteen S, Files JK, Fram T, Erdmann N. The role of immune activation and antigen persistence in acute and long COVID. J Investig Med. 2023; 108155892311580.
95. Cecchini R, Cecchini AL. SARS-CoV-2 infection pathogenesis is related to oxidative stress as a response to aggression. Med Hypotheses. 2020;1(143): 110102.
96. Huang WJ, Zhang X, Chen WW. Role of oxidative stress in Alzheimer's disease. Biomed Rep. 2016;4(5):519.
97. Zhu N, Wang W, Liu Z, Liang C, Wang W, Ye F, et al. Morphogenesis and cytopathic effect of SARS-CoV-2 infection in human airway epithelial cells. Nat Commun. 2020;11(1):1–8.
98. Ahn JH, Kim JM, Hong SP, Choi SY, Yang MJ, Ju YS, et al. Nasal ciliated cells are primary targets for SARS-CoV-2 replication in the early stage of COVID-19. J Clin Invest. 2021;131(13):e148517.
99. Maßberg D, Hatt H. Human olfactory receptors: novel cellular functions outside of the nose. Physiol Rev. 2018;98(3):1739–63. https://doi.org/10.1152/physrev.00013.2017.
100. Flegel C, Manteniotis S, Osthold S, Hatt H, Gisselmann G. Expression profile of ectopic olfactory receptors determined by deep sequencing. PLoS ONE. 2013;8(2):e55368. https://doi.org/10.1371/journal.pone.0055368.
101. Ansoleaga B, Garcia-Esparcia P, Llorens F, Moreno J, Aso E, Ferrer I. Dysregulation of brain olfactory and taste receptors in AD, PSP and CJD, and AD-related model. Neuroscience. 2013;248:369–82.
102. Zhao W, Ho L, Varghese M, Yemul S, Dams-Oconnor K, Gordon W, et al. Decreased level of olfactory receptors in blood cells following traumatic brain injury and potential association with tauopathy. J Alzheimer's Dis. 2013;34(2):417–29. https://doi.org/10.3233/JAD-121894.
103. von Bartheld CS, Butowt R, Hagen MM. Prevalence of chemosensory dysfunction in COVID-19 patients: a systematic review and meta-analysis reveals significant ethnic differences. ACS Chem Neurosci. 2020;11(19):2944.
104. Butowt R, von Bartheld CS. Anosmia in COVID-19: underlying mechanisms and assessment of an olfactory route to brain infection. Neuroscientist. 2021;27(6):582–603.
105. Niemi MEK, Karjalainen J, Liao RG, Neale BM, Daly M, Ganna A, et al. Mapping the human genetic architecture of COVID-19. Nature. 2021;600(7889):472–7.

Publisher's Note

III

Exposure to urban particulate matter alters responses of olfactory mucosal cells to SARS-CoV-2 infection

Shahbaz, M. A, Kuivanen, S*, Mussalo, L*, Afonin, A. M, Kumari, K, Behzadpour, D, Kalapudas, J, Koivisto, A. M, Penttilä, E, Löppönen, H, Jalava, P, Vapalahti, O, Balistreri, G, Lampinen, R*, & Kanninen, K. M*

Environmental Research, 249, 118451, 2024.

Environmental Research 249 (2024) 118451

Contents lists available at ScienceDirect

Environmental Research

journal homepage: www.elsevier.com/locate/envres

Exposure to urban particulate matter alters responses of olfactory mucosal cells to SARS-CoV-2 infection

Muhammad Ali Shahbaz [a], Suvi Kuivanen [b,c,1], Laura Mussalo [a,1], Alexey M. Afonin [a], Kajal Kumari [a], Donya Behzadpour [a], Juho Kalapudas [d], Anne M. Koivisto [d,e,f], Elina Penttilä [g], Heikki Löppönen [g], Pasi Jalava [h], Olli Vapalahti [b], Giuseppe Balistreri [b], Riikka Lampinen [a,1], Katja M. Kanninen [a,*,1]

[a] University of Eastern Finland, A.I. Virtanen Institute for Molecular Sciences, Kuopio, Finland
[b] University of Helsinki, Department of Virology, Faculty of Medicine, Helsinki, Finland
[c] Charité – Universitätsmedizin Berlin, Corporate Member of Freie Universität Berlin and Humboldt-Universität zu Berlin, Institute of Virology, Berlin, Germany
[d] University of Eastern Finland, Brain Research Unit, Department of Neurology, School of Medicine, Kuopio, Finland
[e] Kuopio University Hospital, Department of Neurology, Neuro Centre, Kuopio, Finland
[f] University of Helsinki, Faculty of Medicine, Department of Neurology and Geriatrics, Helsinki University Hospital and Neurosciences, Helsinki, Finland
[g] University of Eastern Finland and Kuopio University Hospital, Department of Otorhinolaryngology, Kuopio, Finland
[h] University of Eastern Finland, Inhalation Toxicology Laboratory, Department of Environmental and Biological Sciences, Kuopio, Finland

ARTICLE INFO

Handling editor: Jose L Domingo

Keywords:
COVID-19
Air pollution
Alzheimer's
Immune response
Oxidative stress
Olfactory mucosa (OM)

ABSTRACT

Respiratory viruses have a significant impact on health, as highlighted by the COVID-19 pandemic. Exposure to air pollution can contribute to viral susceptibility and be associated with severe outcomes, as suggested by recent epidemiological studies. Furthermore, exposure to particulate matter (PM), an important constituent of air pollution, is linked to adverse effects on the brain, including cognitive decline and Alzheimer's disease (AD). The olfactory mucosa (OM), a tissue located at the rooftop of the nasal cavity, is directly exposed to inhaled air and in direct contact with the brain. Increasing evidence of OM dysfunction related to neuropathogenesis and viral infection demonstrates the importance of elucidating the interplay between viruses and air pollutants at the OM. This study examined the effects of subacute exposure to urban PM 0.2 and PM 10–2.5 on SARS-CoV-2 infection using primary human OM cells obtained from cognitively healthy individuals and individuals diagnosed with AD. OM cells were exposed to PM and subsequently infected with the SARS-CoV-2 virus in the presence of pollutants. SARS-CoV-2 entry receptors and replication, toxicological endpoints, cytokine release, oxidative stress markers, and amyloid beta levels were measured. Exposure to PM did not enhance the expression of viral entry receptors or cellular viral load in human OM cells. However, PM-exposed and SARS-CoV-2-infected cells showed alterations in cellular and immune responses when compared to cells infected only with the virus or pollutants. These changes are highly pronounced in AD OM cells. These results suggest that exposure of human OM cells to PM does not increase susceptibility to SARS-CoV-2 infection in vitro, but it can alter cellular immune responses to the virus, particularly in AD. Understanding the interplay of air pollutants and COVID-19 can provide important insight for the development of public health policies and interventions to reduce the negative influences of air pollution exposure.

1. Introduction

The COVID-19 pandemic has presented significant challenges to healthcare systems globally. Notably, COVID-19 is characterized by a wide range of symptoms and complications, including respiratory failure, acute respiratory distress syndrome (ARDS), cardiovascular issues, and neurological complications. Initial reports suggested that 36% of COVID-19 patients exhibited neurological symptoms (Mao et al., 2020). However, recent studies have shown a broad range in the reported prevalence of neurological symptoms in COVID-19, varying from

* Corresponding author.
E-mail address: katja.kanninen@uef.fi (K.M. Kanninen).
[1] Equal contribution.

https://doi.org/10.1016/j.envres.2024.118451
Received 22 November 2023; Received in revised form 1 February 2024; Accepted 7 February 2024
Available online 8 February 2024

7% to 77.8% (Wesselingh, 2023). Anosmia, or loss of the sense of smell, is one of the most reported neurological symptoms associated with COVID-19. A systematic review of 107 studies found that 38.2% of COVID-19 patients reported anosmia (Mutiawati et al., 2021. Although the prevalence decreased in patients infected with the SARS-CoV-2 omicron variant (Butowt et al., 2022), the emergence of reports of long-COVID-19, which includes neurological complications like anosmia, remains a topic of concern (Lopez-Leon et al., 2021). The exact mechanisms of anosmia in COVID-19 are not yet fully understood, but current studies suggest that the virus may directly invade and damage the olfactory epithelium (Butowt and von Bartheld, 2021; Shahbaz et al., 2022).

Air pollution is a major public health concern, and particulate matter (PM) is one of its most harmful components. Air pollution consists of a complex mixture of particles with various sizes and compositions, including PM with a diameter smaller than 10 μm (PM 10), smaller than 2.5 μm (PM2.5), and ultrafine particles (UFP) with a diameter smaller than 0.1 μm. Numerous studies have indicated potential adverse effects of PM exposure on the brain, including cognitive decline and neurodegenerative diseases like Alzheimer's disease (AD). A recent systematic review and meta-analysis found that long-term exposure to air pollution was associated with an increased risk of AD and other forms of dementia (Fu and Yung, 2020; Livingston et al., 2020; Peters et al., 2019). However, the exact mechanisms behind these effects require further investigation.

Epidemiological research has suggested a link between PM levels and an increased incidence of COVID-19 infections in specific geographic areas (Fattorini and Regoli, 2020; Jiang et al., 2020; Li et al., 2020; Linares et al., 2021; Travaglio et al., 2021). Recent systematic reviews have concluded that there is a significant association between chronic exposure to PM10 and PM2.5 and the incidence, risk, severity, and mortality of COVID-19 cases (Marquès and Domingo, 2022), as well as short-term exposure to PM10 and PM2.5 (Yu et al., 2024). Several hypotheses have been proposed regarding how air pollutants, including PM, could increase the severity of COVID-19 infections. However, only a limited number of studies have investigated the interaction between different fractions of PM and SARS-CoV-2 infection in experimental settings. Consequently, the precise pathological events leading to increased severity and mortality are not fully understood and require further research.

PM exposure can affect the interaction of the host with SARS-CoV-2 through various mechanisms. PM can induce oxidative stress and trigger an inflammatory response upon entering the nasal and respiratory system, potentially weakening the host immune defenses and exacerbating COVID-19 severity (Brocke et al., 2022; Cevallos et al., 2017; Valderrama et al., 2022; Zhu et al., 2022; Zosky et al., 2014; Yamamoto et al., 2023). Furthermore, PM has been shown to influence the expression of angiotensin-converting enzyme 2 (ACE2), the main receptor used by SARS-CoV-2 to enter host cells. This alteration in ACE2 expression on host cells could increase susceptibility to SARS-CoV-2 infection and worsen clinical outcomes in exposed individuals. In murine models, it has been demonstrated that ambient PM increases ACE2 expression in the lungs (Zhu et al., 2021a) and alveolar type 2 cells (Sagawa et al., 2021). Furthermore, in vitro studies have indicated that urban PM, diesel PM 2.5, and PM 10 exposure elevate ACE2 levels in pulmonary alveolar epithelial cells (Zhu et al., 2021b), pluripotent stem cell–derived airway epithelial cells (Kim et al., 2020), and human nasal epithelial cells (Miyashita et al., 2023). However, there is limited information on how exposure to the smallest particles affects SARS-CoV-2 infection.

Recent evidence indicates that PM may reach the brain through nasal exposure, directly through the olfactory route (Block and Calderón-Garcidueñas, 2009; Oberdörster et al., 2004). The olfactory mucosa (OM), located at the roof of the nasal cavity, plays a crucial role in the sense of smell, and is directly connected to the brain. Previous studies have demonstrated that PM exposure induces functional alterations in OM cells (Chew et al., 2020; Kim et al., 2022; Mussalo et al., 2023). However, the interaction between PM exposure and SARS-CoV-2 infection at this critical site exposed to inhaled air has received less attention.

Beyond neurological symptoms, a potential link has been suggested between COVID-19 and neurodegenerative disorders, particularly AD (Rudnicka-Drożak et al., 2023). AD is a progressive neurodegenerative disorder characterized by the accumulation of amyloid beta (Aβ) and tau proteins in the brain. AD is among the most common central nervous system (CNS)-associated comorbidities of COVID-19 (Fotuhi et al., 2020; Xia et al., 2021), and dementia patients, including those with AD, are considered more susceptible to severe SARS-CoV-2 infection and mortality (Atkins et al., 2020). It has been demonstrated that the cells of the OM recapitulate pathological changes observed in AD (Lampinen et al., 2022; Rantanen et al., 2022), and SARS-CoV-2 infection in AD OM cells show unique transcriptomic signatures associated with alterations in oxidative stress, inflammation, and antiviral immune response compared to cognitively healthy OM cells (Shahbaz et al., 2023). Given the gaps in knowledge in this research area, this study aims to investigate the link between PM exposure, SARS-CoV-2 infection, and AD in primary human OM cells.

2. Materials and methods

2.1. Human olfactory mucosal cell culture

In this study, we utilized primary OM cell cultures derived from cognitively healthy control subjects (n = 3) and individuals with AD (n = 3). The average age of the cognitively healthy control and AD individuals was 74.3 years and 62.3 years respectively, representing both male and female donors. The study was authorized by the Research Ethics Committee of the Northern Savo Hospital District with permit number 536/2017. All participants gave their written consent to participate in the study. The procedure for recruitment of donors and protocol for collection and processing of biopsies has been previously described in (Lampinen et al., 2022; Shahbaz et al., 2023). In brief, the OM biopsies were collected from the rooftop of the nasal cavity and transferred into PneumaCult - Ex Plus (Stemcell Technologies, #05040) and supplemented with hydrocortisone (final concentration of 96 ng/ml) and 1% Penicillin-Streptomycin (Gibco). The OM tissue sample was then immediately transferred to the BSL2 facility where it underwent mechanical and enzymatic processing to obtain individual cells that were dissociated from each other. Cells obtained from the biopsies were expanded and primary OM cell lines were frozen in liquid nitrogen for later use. Thawed human primary olfactory mucosal (OM) cells were cultivated in supplemented PneumaCult - Ex Plus media for 4–6 days under submerged conditions before plating the cells for exposure. Cells in primary passages 2–3 were used for experiments as described below.

2.2. Particulate matter samples

We utilized urban air PM samples obtained from a sampling campaign conducted in China in 2014. The PM samples were collected at Nanjing University (NJU) Xianlin campus, with detailed information on the collection method, sample origin, PM composition, and size-segregation method available in previous publications (Rönkkö et al., 2021, 2020, 2018). In brief, we used PM 0.2 (diameter<0.2 μm) and PM 10–2.5 (diameter<10 μm and >2.5 μm) fractions collected during the nighttime using a modified Harvard High Volume Cascade Impactor (HVCI) (Sillanpää et al., 2003). The PM samples were stored at −20 °C until the day of experiments. On the day of exposure, the PM samples were suspended in 10% dimethyl sulfoxide (DMSO) in endotoxin-tested water and sonicated for 30 min before being utilized for exposure.

2.3. SARS-CoV2 propagation and purification

The WT strain of SARS-CoV-2, also known as strain B.1, was used in this study. The virus was obtained under a laboratory research permit from Helsinki University Hospital and propagated in VeroE6-TMPRSS2 cells. The viral stock was stored at −80 °C and titrated using plaque assay. The presence of the furin cleavage site in the viral genome was confirmed by next-generation sequencing (Cantuti-Castelvetri et al., 2020). All experiments with the WT strain were conducted in BSL3 facilities at the University of Helsinki.

2.4. PM exposures and SARS-CoV-2 infection

The primary OM cells were seeded at various densities depending on the specific experiment and incubated at 37 °C and 5% CO2 for 24 h. Next, the cells were exposed to either the PM 0.2 or PM 10–2.5 particles, independently (50 μg/ml corresponding to 13.2 μg/cm^2) for 24 h. After exposure, the cell culture plates containing the exposed cells were transferred to a BSL3 facility for infection with the WT-SARS-CoV-2. Prior to infection, most of the media containing the PM 0.2 and PM 10–2.5 particles were transferred to fresh plates and kept in the incubator. The PM-exposed OM cells were inoculated with WT SARS-CoV-2 (1×10^5 Plaque forming units/well (PFUs/well)). Additionally, unexposed OM cells were infected with SARS-CoV-2 (1×10^5 PFUs) to obtain virus-only control. The infected OM cells were incubated for 90 min at 37 °C. After the incubation period with the virus, the media containing the virus was removed from the cells, and the cells were rinsed three times with phosphate-buffered saline (PBS). Finally, the PM-containing media was returned to the respective wells to maintain pollutant exposure throughout the experiment. Media were collected at 1, 24, 48, and 72 h post-infection (hpi) to measure the viral RNA release from infected cells. For cytotoxicity, Enzyme-linked immunosorbent assays (ELISA), and cytokine profiling complete media was collected at 24 and 72 h and treated with 1% Triton X-100 to inactivate SARS-CoV-2. Furthermore, cells were collected in TRI Reagent (Sigma Aldrich) at 24h and 72h for qPCR. Samples were stored at −80 °C. For this study, vehicles (dimethyl sulfoxide (DMSO) in water) and PM-only exposures were also used as experimental controls.

2.5. Quantification of viral RNA after infection

RNA was extracted from media samples collected from various treatments at 1, 24, 48, and 72 h post-infection (hpi) using the QIAamp Viral RNA Minikit (Qiagen) following the manufacturer's protocol. The extracted RNA was subjected to SARS-CoV-2 RT-PCR using primers, a probe, and an in vitro synthesized control for RNA-dependent RNA polymerase (RdRp) as previously described (Corman et al., 2020; Lin et al., 2021). At each time point, the SARS-CoV-2 RNA copies were quantified, and the relative increase in viral load was determined.

2.6. Measurement of cell viability

In our study, we employed the MTT (3-(4,5-dimethylthiazol-2-yl)-2,5-diphenyltetrazolium bromide) tetrazolium reduction assay to evaluate the metabolic activity of cells exposed to various pollutants. We seeded cells into 48-well plates at a density of 20,000 cells per well. Subsequently, these cells were exposed to the pollutants for 24 h, with each treatment having three technical replicates.

Following exposure to PM 0.2 and PM 10–2.5, we collected the culture media and replaced it with media containing 1.2 mM Thiazolyl blue tetrazolium bromide. This mixture was then incubated for approximately 2.5–3 h at 37 °C. After incubation, we removed the media and solubilized the crystal salts that had formed using DMSO. To measure the outcomes, we recorded the absorbances at 595 nm using a Wallac Victor 1420 plate reader (PerkinElmer). Additionally, the background signal, which was measured with DMSO alone, was subtracted from the readings. All data were subsequently normalized to the vehicle-treated cells.

2.7. Measurement of cytotoxicity

We assessed cell damage by quantifying the release of lactate dehydrogenase (LDH) in the collected culture media from different treatments using the CyQUANT™ LDH Cytotoxicity Assay Kit (Invitrogen, #C20301). The absorbance values were measured at both 490 nm and 650 nm with the Wallac Victor 1420 plate reader. As a positive control for cell death, we used cells that had been lysed with Triton-X-100.

2.8. Cytokine profile

A membrane-based sandwich immunoassay, The Proteome Profiler Human XL Cytokine Array Kit (R&D Systems, ARY022B), was used for detecting a total of 105 cytokines, chemokines, and acute phase proteins in the medium samples collected from vehicle, PM 0.2, PM 10–2.5, PM 0.2 and virus, or PM 10–2.5 and virus treated control (n = 3) and AD (n = 3) OM cells at 24 h post infection (hpi). 100 μl medium from each individual were collected and pooled to get one pool of control and AD samples for each treatment. Medium samples were kept on ice and centrifuged at 300×*g* for 5 min until the analysis according to the manufacturer's instructions. Briefly, cytokine membranes were blocked, after which they were incubated with the samples overnight at +4 °C. The next day, the membranes were washed and incubated for 1h with the detection antibody and 30 min with Streptavidin-HRP, after which they were imaged using Bio-Rad ChemiDoc XRS + device (Bio-Rad). Profiles of mean spot pixel density were quantified using Image Lab 5.1 program (Bio-Rad). Spots were circled using the same sized ROI for all the membranes. Negative control spot values were subtracted as background and the results were normalized to the reference spots of all the analyzed membranes. The resulting values represent log2 transformed fold changes. The heatmaps were created using the complex heatmap package (10.1093/bioinformatics/btw313).

2.9. RNA isolation and quantitative real-time PCR (qPCR)

Following exposure to PM and infection with SARS-CoV-2, cellular samples were collected in TRI Reagent and stored at −70 °C until further processing. RNA extraction was carried out in accordance with the manufacturer's protocol. The concentration and purity of the RNA samples were assessed using a NanoDrop 1000 spectrophotometer. Subsequently, cDNA was synthesized from 1 μg of RNA using the High-Capacity Reverse Transcription kit (Applied Biosystems, #4368814).

The relative expression levels of mRNA encoding specific genes were determined in duplicate and analyzed following the manufacturer's guidelines with the StepOnePlus™ Real-Time PCR System (Applied Biosystems, #4376600). For the qPCR assay, 10 ng of cDNA or genomic DNA was employed, and Maxima Probe/ROX qPCR Master Mix (Thermo Scientific, #K0231) was utilized. To normalize the cycle threshold (Ct) values, glyceraldehyde-3-phosphate dehydrogenase (GAPDH) was employed as the internal reference gene. Relative gene expression was calculated using the $2^{-\triangle\triangle Ct}$ method, where Ct indicates the threshold cycle number, and the results were expressed relative to the control conditions. For a list of Taqman gene expression assays employed in this study, please refer to Table S1.

2.10. Enzyme-linked immunosorbent assays for amyloid beta

To assess the levels of secreted $A\beta_{1\text{-}42}$ and $A\beta_{1\text{-}40}$ in OM cells following exposure to PM or infection with SARS-CoV-2 or after both, medium samples of exposed/infected cells were collected and stored at −70 °C until analysis. Right prior to the analysis, the medium samples were supplemented with 1 × complete protease inhibitor cocktail (Roche) and the secreted levels of Aβ were assessed using ELISA kits for

$A\beta_{1\text{-}42}$ (Invitrogen, #KHB3544) and $A\beta_{1\text{-}40}$ Invitrogen, (#KHB3481) as instructed in the kits' manuals. The medium samples were measured as singlets from OM cells derived from n = 3 cognitively healthy individuals and n = 3 individuals with AD.

2.11. Statistical methods and graphical illustrations

The GraphPad Prism 10.0.2 (GraphPad Software Inc.) software was used for the statistical analysis of the data. Statistical analysis methods used for different comparisons are indicated in Figure legends. Error bars in Figs. 1–3 represent standard deviation (SEM). In general, two group comparisons were analyzed by unpaired *t*-test. Multiple group comparisons were analyzed using one-way ANOVA. The graphical illustrations were created with BioRender.com.

3. Results

In the initial phase of our investigation, we directed our focus toward comprehending the repercussions of PM exposure in the absence of viral infection. Specifically, we explored PM's influence on cytotoxicity, oxidative stress, and the mRNA expression of genes encoding for pivotal SARS-CoV-2 entry receptors and proteins (depicted in Fig. 1a). Based on prior literature and our preliminary analyses, we selected doses of PM 0.2 and PM 10–2.5, not expected to cause significant cytotoxicity (Chew et al., 2020). Our experimental protocol involved subjecting OM cells sourced from both cognitively healthy individuals and those afflicted by AD PM 0.2 or PM 10–2.5 for 24 h. Assessment through the MTT assay showed that exposure to PM 0.2 resulted in a statistically significant ($p = 0.041$) yet relatively small increase (8%) in the cellular metabolic activity in control OM cells (Fig. 1a). Like controls, in AD cells PM 0.2 caused a 10% elevation in the metabolic activity of the cells when compared to the vehicle-treated AD cells. PM 10–2.5 exposure did not yield statistically significant deviations in metabolic activity (Fig. 1b). Additionally, to ascertain lack of cytotoxicity, we measured lactate dehydrogenase (LDH) release into the culture medium 24 h post-exposure to PM (Fig. 1c). Results indicated that no other notable changes were observed, thus further confirming the minimal cytotoxic attributes of the selected dose (50 μg/ml).

Although the exposure of OM cells to the selected PM 0.2 and PM 10–2.5 did not cause cytotoxicity, we observed a subtle elevation in oxidative stress markers, *NQO1* (Fig. 1d) and *HMOX1* (Fig. 1e) after 24 h exposure to PM 0.2. However, statistically significant elevation was observed only in *HMOX1* ($p = 0.02$) in control OM cells following exposure to PM 0.2. Furthermore, no significant changes were observed in *NQO1* and *HMOX1* following exposure to PM 10–2.5 for 24 h in control and AD OM cells. Lastly, no relative changes were observed in *NQO1* and *HMOX1* in AD OM cells relative to the control (Supplementary Figs. 1a–b). Substantiating these findings, we validated changes at the mRNA level using Western blot analysis, revealing a replication of the observed protein-level responses to oxidative stress induced by both PM 0.2 and PM 10–2.5 (Supplementary Figs. 2a–b). Notably, the intriguing observation was made that the changes in NQO1 and HMOX1 protein levels mirrored those at the mRNA level.

Next, we studied the potential impact of pre-existing PM exposure on the expression of genes crucial for SARS-CoV-2 entry. This includes genes encoding for the ACE2 receptor, which plays a key role in mediating viral entry, and TMPRSS2, which facilitates the activation of the viral spike protein within infected cells (Hoffmann et al., 2020a). Furthermore, we evaluated the mRNA expression of NRP1, which has been suggested to function as a potential alternative receptor for SARS-CoV-2 (Cantuti-Castelvetri et al., 2020). Our results demonstrated that there was no alteration in the expression of *ACE2* or *NRP1* in either control or AD cells following exposure to PM 0.2 or PM 10–2.5 (Fig. 1f–h). Similarly, *TMPRSS2* expression remained unaltered in control cells exposed to PM 0.2 and PM 10–2.5, whereas AD cells exhibited a significant increase in *TMPRSS2* expression ($p = 0.002$) after exposure to PM 0.2 only (Fig. 1g). However, the disease effect was only observed in *NRP1* expression after treatment with PM 0.2. No alterations were observed in *ACE2* or *TMPRSS2* expression in AD cells relative to control (Supplementary Figs. 1c–e).

Next, to understand how exposure to PM 0.2 and PM 10–2.5 impacts the SARS-CoV-2 infection in the OM cells from cognitively healthy and AD individuals, we conducted an experimental protocol shown in Fig. 2a. After 24 h exposure with either PM 0.2 or PM 10–2.5, the OM cells were subsequently infected with the WT-SARS-CoV-2 virus in the presence of PM. We monitored the responses of these co-exposed OM cells over 72 h.

To assess the viral replication within the infected cells we monitored secreted viral RNA copies released from OM cells at 1, 24, 48, and 72 h post-infection (hpi) (Fig. 2b and c). In OM cultures infected solely with the SARS-CoV-2 virus, viral RNA levels exhibited a time-dependent increase, confirming viral replication and propagation within the infected cells. Notably, one-way ANOVA analysis revealed that the pretreatment and subsequent presence of PM during SARS-CoV-2 infection significantly influenced the viral RNA load in the media collected at 1 hpi from both control and AD OM cells (Supplementary Figs. 3a–b). However, it should be noted that the quantities of viral RNA released from PM-exposed OM cells with subsequent infection, compared to OM cells only infected with the SARS-CoV-2 virus, remained unaltered at later time points, specifically 24, 48, and 72 h (Supplementary Figs. 3c–h) The absence of alterations in viral RNA levels during these later time points suggests that any initial differences were biologically inconsequential. Given previous evidence that ambient air pollutants can act as potential carriers for SARS-CoV-2 (Kayalar et al., 2021), the higher viral load observed at the 1-h time point may indicate that PM particles adhering to OM cells could adsorb viral particles on their surface, leading to an initial increase in viral load. Furthermore, the absence of any discernible effect of PM exposure on ACE2 mRNA expression suggests that there was no enhancement of viral entry into the cells, resulting in similar viral load patterns at the later time points.

Similar to controls, comparable results were observed in AD OM cells when they were exposed to both PM 0.2 and PM 10–2.5 in conjunction with SARS-CoV-2 infection (Fig. 2c). Only minor differences in viral RNA load were noted between the OM cells treated with both types of PM and undergoing SARS-CoV-2 infection, compared to the OM cells treated solely with SARS-CoV-2 in individuals with AD. Taken together, these findings suggest that the combined exposure to PM and the virus had comparable effects in both control and AD OM cells on the propagation of SARS-CoV-2 within the OM cells following infection.

Next, LDH assays were conducted at both 24 and 72 h post-viral infection in OM cells exposed to PM to assess cellular toxicity. At 24 hpi, a slight increase in cytotoxicity was observed in both control and AD cells that were infected simultaneously with PM 0.2 and PM 10–2.5, respectively (Fig. 2d). However, the statistically significant increase in cytotoxicity was only observed in the group exposed to PM 10–2.5 in combination with the virus compared to AD cells exposed to the vehicle ($p = 0.0037$), PM 10–2.5 only ($p = 0.038$), and virus only ($p = 0.0015$) conditions. Notably, the percentage increase in LDH release was minor, ranging from 1 to 2%.

At 72 hpi, both control ($p = 0.002$) and AD ($p = 0.0001$) OM cells infected solely with the virus exhibited significantly elevated levels of LDH release into the media compared to the vehicle control, indicating cytotoxicity (Fig. 2e). The individual PM fractions did not induce cytotoxicity. Consistent with the virus-only treatments, OM cells exposed to PM 0.2 and subsequently infected with SARS-CoV-2 showed an increase in cytotoxicity in both control and AD OM cells. However, this increase was found to be significant in AD OM cells compared to the vehicle ($p = 0.002$) and PM 0.2 only ($p = 0.002$) conditions.

Interestingly, exposure to PM 10–2.5 in AD cells slightly reduced cytotoxicity upon subsequent infection with the virus, as evidenced by significantly lower LDH release compared to the virus-only treatment ($p = 0.002$), although not significantly different from the PM 10–2.5 alone

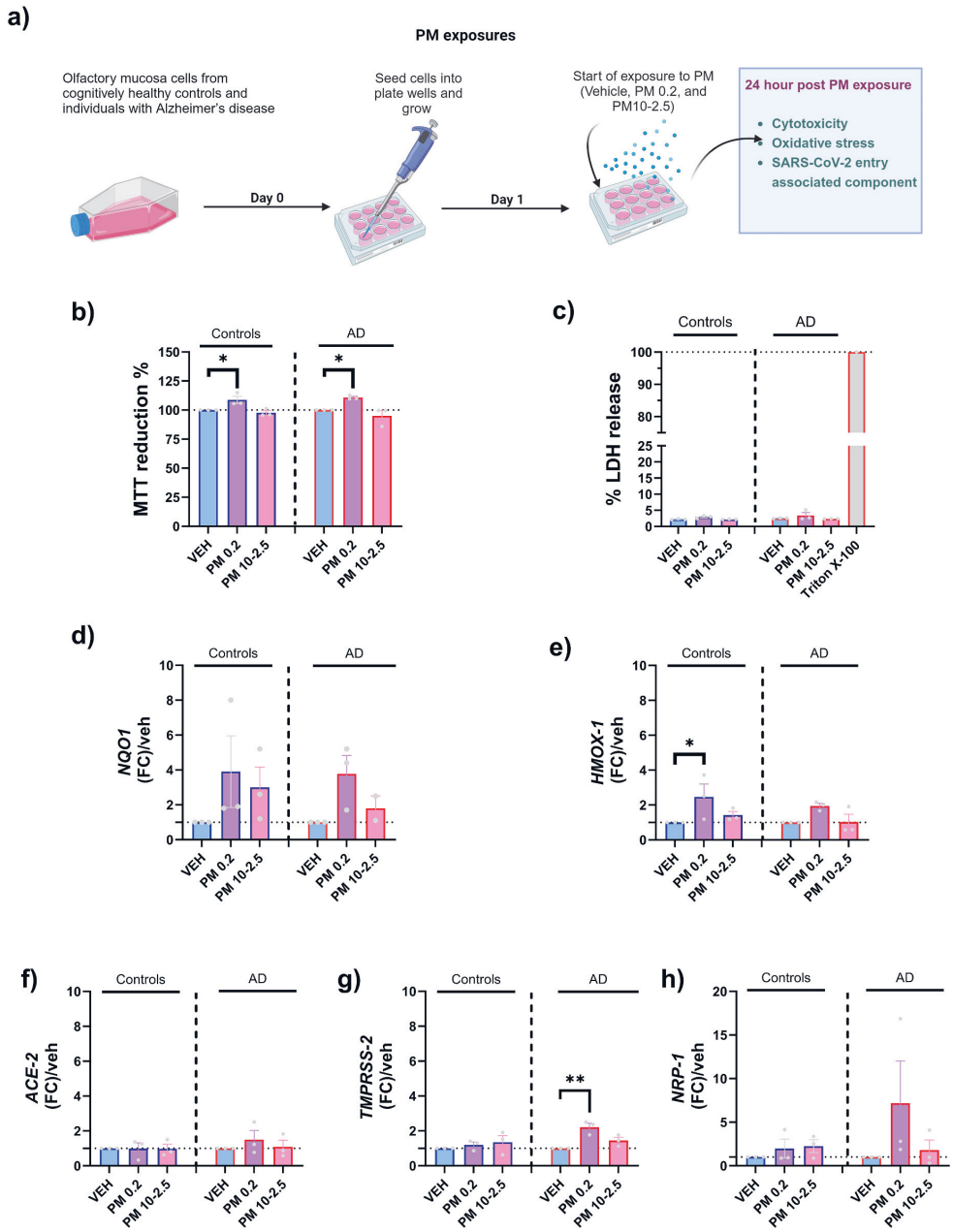

Fig. 1. Effects of 24 h PM 0.2 and PM 10–2.5 exposure on cellular viability, cytotoxicity, oxidative stress, and SARS-CoV-2 entry receptor expression in OM cells from control and AD individuals. (a) Schematic representations of the exposure model. (b) Assessment of cellular viability by measuring the percentage of cellular metabolic activity relative to the vehicle control using the MTT assay. (c) Evaluation of cytotoxicity by measuring lactate dehydrogenase (LDH) release into the cell culture medium. (d) mRNA levels were normalized to the relative vehicle for oxidative stress markers NQO1 and (e) HMOX1, as well as for genes encoding for SARS-CoV-2 entry proteins, (f) ACE2, (g) TMPRSS2, and (h) NRP1. The normalization of gene expression was performed against the housekeeping gene glyceraldehyde-3-phosphate dehydrogenase (GADPH). The graphs display the mean with SEM for n = 3 donors in control and AD OM cells. * Indicates p-values ≤0.05, ** Indicates p-values ≤0.01, as determined by one-way ANOVA with Šídák's multiple comparisons test.

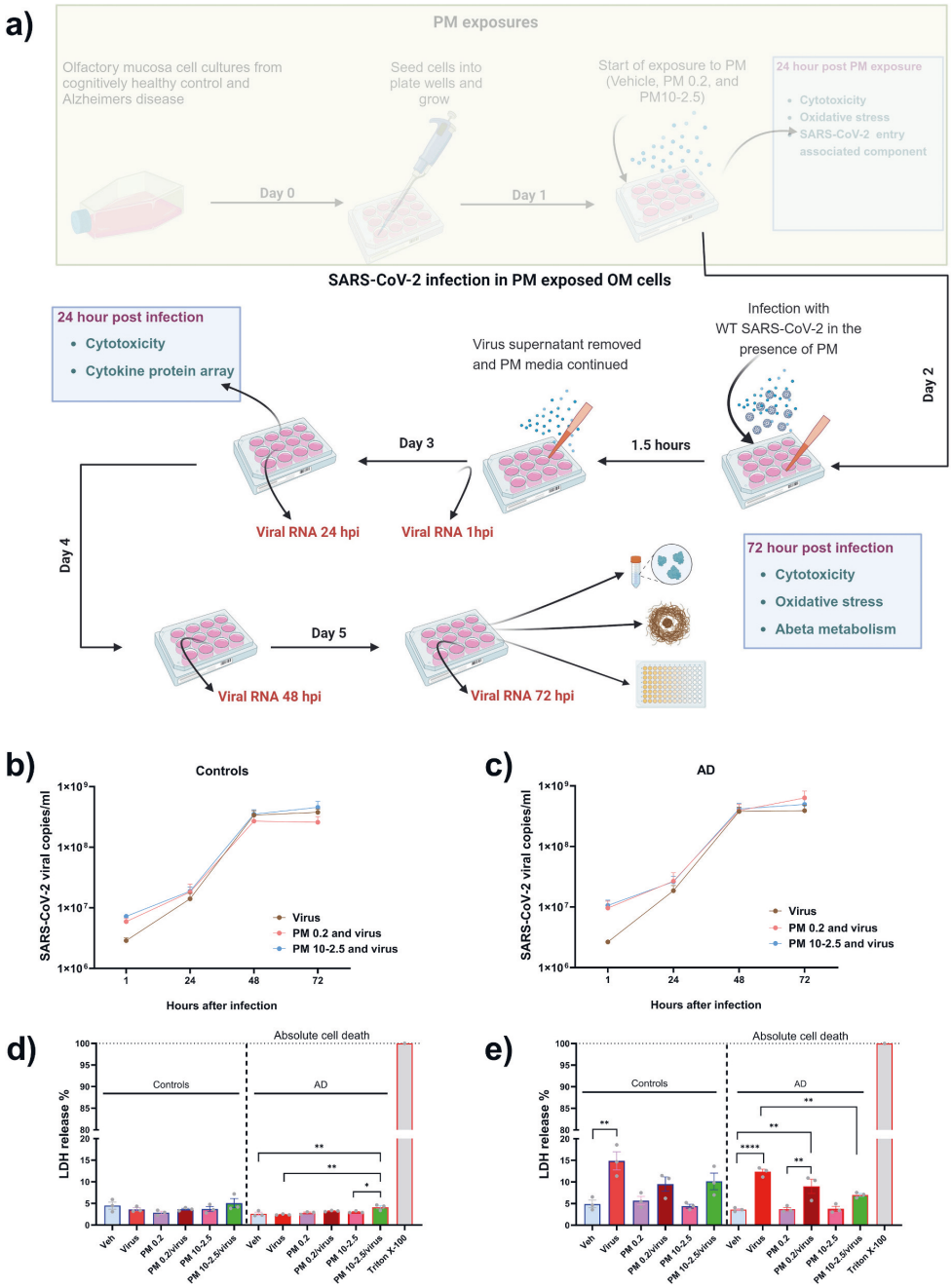

Fig. 2. Effects of PM 0.2 and PM 10–2.5 exposure on SARS-CoV-2 infection and cytotoxicity in OM cells from healthy and AD individuals. (a) Schematic representation of SARS-CoV-2 infection in PM-exposed OM cells. PM 0.2 and PM 10–2.5 exposed OM cultures were assessed for SARS-CoV-2 viral mRNA load in (b) control and (c) AD OM cells at 1, 48, and 72 h post-infection. (d) Cytotoxicity was evaluated by measuring LDH release in the media at 24 h and 72 h post-infection with WT SARS-CoV-2. The graph displays the mean with SEM for n = 3 donors in both control and AD cells. * Indicates p-values ≤0.05, ** Indicates p-values ≤0.01, *** Indicates p-values ≤0.001, as determined by one-way ANOVA with Šídák's multiple comparisons test.

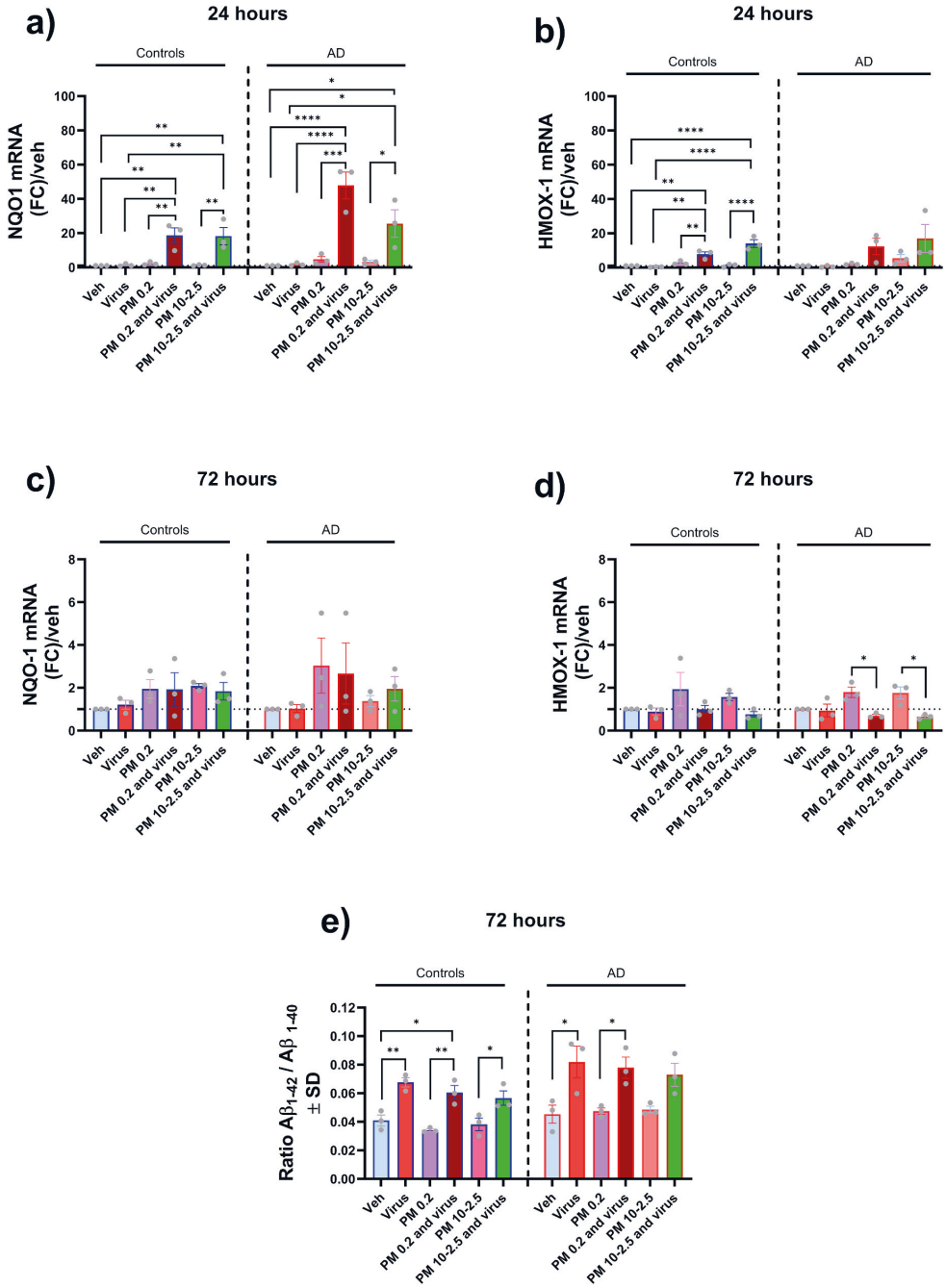

Fig. 3. Effects of concomitant exposure to PM and SARS-CoV-2 on oxidative stress and Aβ metabolism in OM cells from cognitively healthy and AD individuals. The Figure displays the normalized fold mRNA expression levels relative to the vehicle treatment for oxidative stress markers NQO1 and (e, f) HMOX1, at 24 h (a, b) and 72 h (c, d) post-infection in PM-exposed OM cells. Additionally, (e) media collected after 72 h post-infection was utilized to assess the concentrations of Aβ $_{1\text{-}42}$ and Aβ $_{1\text{-}40}$ with ELISA, with the Fig.showing the ratio of Aβ $_{1\text{-}42}$/Aβ $_{1\text{-}40}$. The graph represents the mean with SEM for n = 3 donors in both control and AD cells. * Indicates p-values ≤0.05, ** Indicates p-values ≤0.01, *** Indicates p-values ≤0.001, as determined by one-way ANOVA with Šídák's multiple comparisons test.

treatment. Therefore, our results suggest that at 72 hpi, changes in cellular toxicity in PM 0.2 and virus co-exposed cells were primarily due to viral infection rather than PM exposure, while PM 10–2.5 did influence virus-induced cell death.

Next, our focus shifted towards investigating the effects of concomitant PM and SARS-CoV-2 effects on oxidative stress. Remarkably, after a 24 h PM exposure followed by viral infection, both oxidative stress marker genes, *NQO1* (Fig. 3a, Supplementary Fig. 4a) and *HMOX1* (Fig. 3b, Supplementary Fig. 4b), were increased in expression in PM 0.2 and PM 10–2.5 exposed control cells when compared to cells treated with the virus or PM in isolation. A similar trend was observed in AD cells; however, there was greater variability in the mRNA levels of *HMOX1* among individuals with AD, resulting in the increase not reaching statistical significance. At 72 hpi, a notable decrease in mRNA expression levels for both *NQO1* and *HMOX1* was observed in co-exposed samples, when compared to the 24 hpi. This reduction was particularly substantial; in the case of *NQO1*, there was no statistical difference observed when compared to cells exposed solely to the virus or PM alone. This pattern was consistent in both control and AD OM cells (Fig. 3c, Supplementary Fig. 4c). Moreover, for *HMOX1,* mRNA levels in the co-exposed samples were significantly lower when compared to the respective PM-only treatments (Fig. 3d, Supplementary Fig. 4c).

Next, we focused on amyloid beta (Aβ) metabolism due to its critical relevance in AD pathogenesis. For this purpose, we investigated the effects of both individual and combined exposures on secreted $A\beta_{1\text{-}42}$ and $A\beta_{1\text{-}40}$ by OM cells obtained from cognitively healthy controls and individuals with AD. Our results indicated that the SARS-CoV-2 virus alone led to a significant increase in the $A\beta_{1\text{-}42}/A\beta_{1\text{-}40}$ ratio in both control and AD OM cells (Fig. 3e). Intriguingly, exposure to PM 0.2 and PM 10–2.5 did not produce a significant effect on Aβ secretion when compared to the vehicle treatment. Interestingly, OM cells exposed to PM and subsequently infected with SARS-CoV-2 exhibited a persistent impact of the virus on the secretion of Aβ. The $A\beta_{1\text{-}42}/A\beta_{1\text{-}40}$ ratio in co-exposed control and AD OM cells was significantly higher compared to cells exposed only to PM, and it approximated levels observed in cells solely exposed to the virus.

To determine the effects of treatments on the cytokine profile of the cells, we applied the Proteome Profiler Human XL Cytokine Array to media collected from exposed cells (Supplementary Fig. 5). Exposure to PM 0.2 and PM 10–2.5 together with SARS-CoV-2 infection altered the assessed cellular cytokines and chemokines in a complex manner. Most of the SARS-CoV-2 induced responses in the cytokine profile diminished when control OM cells underwent PM 0.2 pre-treatment (Fig. 4a). Insulin-Like Growth Factor-Binding Protein 3 (IGFBP-3), Trefoil factor 3 (TFF3), and CD14 (log2fc 1.9; 1.23; and 1.12, respectively) were among the top enriched in the SARS-CoV-2 infection of the control OM cells. However, in PM 0.2 and SARS-CoV-2 infected cells there was significant downregulation compared to SARS-CoV-2 alone infected control OM cells. Interestingly, only interferon-associated protein expressions, such as Interferon-Inducible Protein 10 (IP10) was significantly increased (log2fc 2.9) in PM 0.2-treated cells that were subsequently infected with SARS-CoV-2 (Fig. 4a). When cells were treated with SARS-CoV-2 alone, a significant increase in IP10 (log2fc 1.1) was also observed, whereas PM 0.2 treatment alone reduced IP-10 (log2fc −0.6).

Notably, cells treated with both PM 0.2 and SARS-CoV-2 exhibited similar changes in most cytokines expression levels when compared to those treated with PM 0.2 alone. Interleukin-24 (IL-24), IL-31, and transferrin receptor (TFR) (log2fc −2.1; −1.6; and −0.7, respectively) which were downregulated upon PM 0.2 exposure alone were further downregulated (log2fc −2.2; −2.1; −1.6); and among the other most altered cytokines in PM 0.2 and SARS-CoV-2 treated cells. In contrast, Granulocyte-Macrophage Colony-Stimulating Factor (GM-CSF) exhibited a different pattern of expression. When cells were exposed to PM 0.2 alone, GM-CSF displayed a log2fc of 3.8, indicating significant activation of this gene in response to PM 0.2 exposure. However, when cells were co-exposed to both PM 0.2 and SARS-CoV-2, the activation of GM-CSF (log2fc 0.16) appeared to be ineffective.

Like PM 0.2 treatment, pre-treatment with PM 10–2.5 followed by SARS-CoV-2 infection often led to diminished SARS-CoV-2-associated cytokine responses. For instance, the IGFBP-3, TFF3, CD14 which were top 3 altered cytokines in SARS-CoV-2 infection of the control OM cells were found to be severely downregulated (log2fc −0.04; −1.3; and −0.7, respectively) in the PM 10–2.5 pretreated control OM cells after infection with SARS-CoV-2. However, the top 3 cytokines in the PM 10–2.5 and virus-treated cells were IL-31, angiopoietin, and kallikrein 3 (log2fc −2.21; −2.11; and −2.06, respectively). It's noteworthy that these same cytokines were also found to be markedly downregulated in control OM cells when exposed solely to PM 10–2.5.

Next, in AD OM cells we observed a dramatic downregulation in almost all the components of the cytokine profile, suggesting severe alterations in the immune response upon SARS-CoV-2 infection (Fig. 4a). PM 0.2 and SARS-CoV-2 exposure caused significant upregulation in IL-17A and Fibroblast Growth Factor Basic (FGF basic) (log2fc 0.5 and 0.5) as compared to vehicle-treated AD OM cells. Furthermore, IL-24, Retinol-Binding Protein 4 (RBP-4), and IL-31 (log2fc −5; −4.5; and −3.9, respectively) were downregulated the most and followed the response to PM 0.2 alone, where significant downregulation was observed. It is noteworthy that the most differentially expressed cytokines with PM 0.2 exposure alone in AD OM cells, were Resistin (log2fc 3.2), IL-1 receptor antagonist (IL-1ra) (log2fc −3.12), and IL-32 (log2fc 2.9). However, when subsequently infected with SARS-CoV-2, significant alterations (log2fc −1.2; −1.2; and −2) were observed among those as well. Similarly, cytokines that were highly altered by SARS-CoV-2 alone, like GM-CSF, IGFBP-3, and Macrophage Inflammatory Protein 3 alpha (MIP-3α) (log2fc 3.39; 1.8; and −1.5, respectively), also showed a to be ineffective (log2fc 0.01; 0.16; −0.24) in co-exposures. The cytokine profile of AD OM cells, which were exposed to PM 10–2.5 and infected with SARS-CoV-2 either pre- or concomitantly, does not exhibit a significant deviation compared to AD OM cells solely exposed to PM 10–2.5. Although most of the responses associated with SARS-CoV-2 decrease in cells with co-exposure, the overall response is largely like that of cells exposed exclusively to PM 10–2.5. The top 3 altered proteins were RAGE, TfR, and IL-6 (log2fc −2.27; −1.80; and 1.8, respectively). Notably, IL-6 is the most prominently induced cytokine in this context, showing a significant change in expression compared to the response observed in cells exposed to PM 10–2.5 alone and SARS-CoV-2 alone.

To explore the impact of existing AD pathology on inflammation and antiviral immune response in relation to PM and viral treatment, we next compared the relative expression of proteins associated with the inflammation pathway in AD cells to control cells in the different treatment groups as depicted in Fig. 4b. We observed a significantly higher baseline level of expression of the assessed cytokines in AD cells compared to controls when treated with the vehicle alone, indicating an elevation in the baseline of cytokines in AD cells. The top 3 most altered cytokines in vehicle treated AD cells in comparison to control cells were RANTES, RAGE, and endoglin (log2fc 1.94; 1.57; and 1.48, respectively). Furthermore, In AD OM cells infected with the virus, more significant changes were noted in the levels of GM-CSF, TFF3, and RANTES (log2fc 3.52; −2.51; and 2.01) when compared to control cells treated with the virus. This baseline inflammation in AD cells appears to have significantly influenced the cytokine profile in co-treatment conditions as well. In response to PM 0.2 and virus treatment, a general trend of downregulation was observed compared to the treated control cells. The highest alterations were observed in IP10, RBP-4, and kallikrein (log2fc −4.38; −3.09; and −3.07, respectively). In contrast, PM 10–2.5 exposure induced a significantly enriched general cytokine response in AD as compared to the PM 10–2.5 control treatment. Notably, RANTES, Angiogenin, SDF-1a, and IL-6 (log2fc 2.42; 1.8; and 1.5) were among the topmost altered cytokines. In short, a distinct cytokine profile is observed in the SARS-CoV-2 infection with pre- and concomitant treatments of PM 0.2 and PM 10–2.5, in AD OM cells compared to the controls. This complexity suggests an intricate relationship between PM

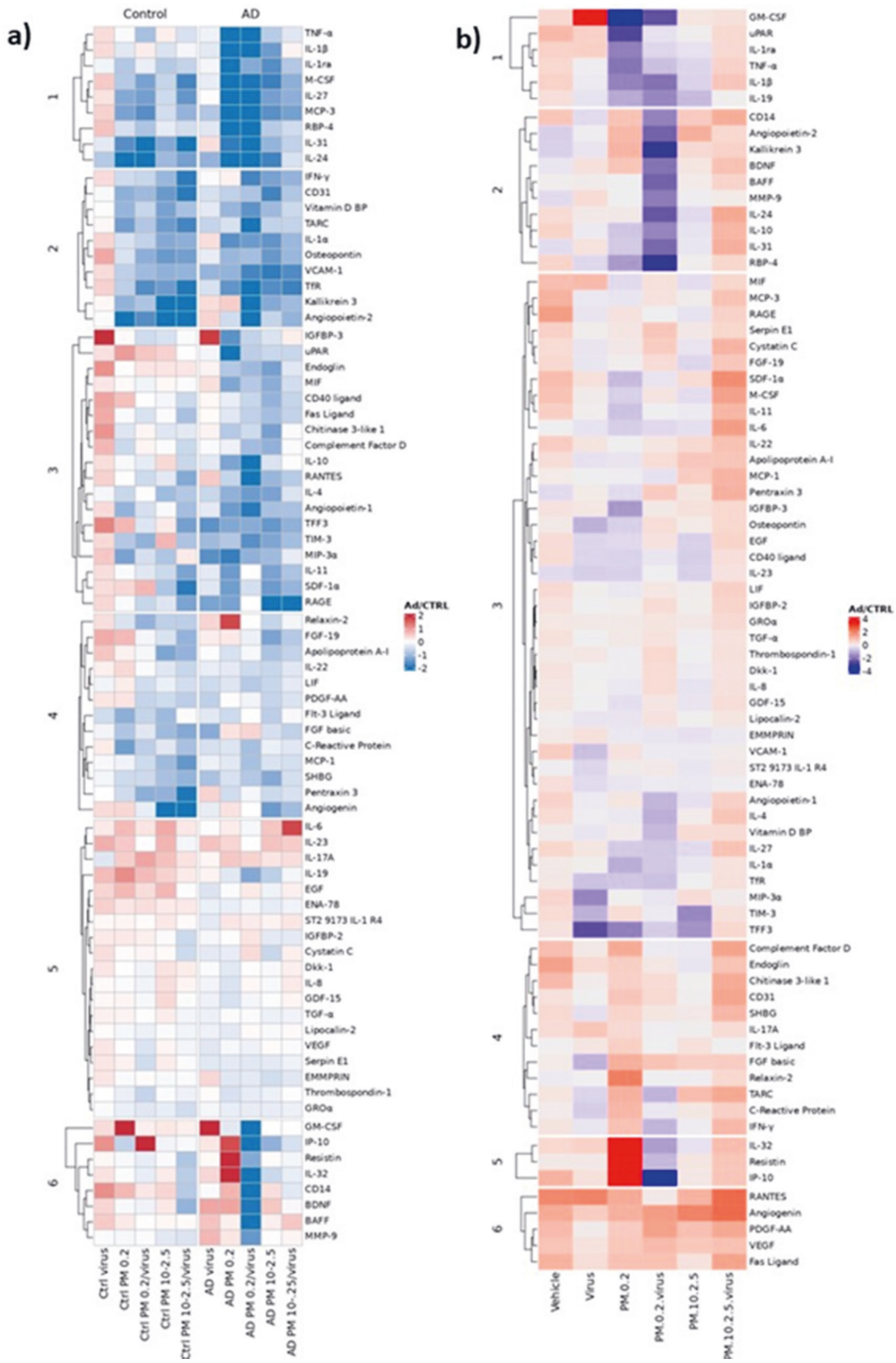

Fig. 4. Impact of PM 0.2 and PM 10–2.5 on SARS-CoV-2-induced cytokine profiles in AD and control cells at 24 h post-infection. Media samples from n = 3 control and n = 3 AD donors were pooled 24 h after subsequent infection with SARS-CoV-2 in PM-exposed cells for cytokine profiling analysis. The Fig.shows (a) a heatmap illustrating log2 fold changes relative to vehicle treatment in control and AD cells respectively, and (b) a heatmap illustrating log2 fold changes in AD cells compared to their respective control exposure.

exposure, viral infection, and the specific pathological alterations in OM cells associated with AD.

4. Discussion

Extensive research has highlighted the role of genetic, environmental, and lifestyle factors in shaping the course and severity of COVID-19 (Samadizadeh et al., 2021). Epidemiological evidence consistently links poor air quality to an increased incidence and severity of COVID-19 (Weaver et al., 2022; Ali and Islam, 2020; Comunian et al., 2020; Hernandez Carballo et al., 2022; Isphording and Pestel, 2021). This study explores the interplay between SARS-CoV-2 infection, PM exposure, and their effects on OM cells.

Previous studies have established that the nasal cavity, particularly the OM, may serve as a site for ultrafine particle translocation and the neurological manifestations of SARS-CoV-2, with PM 10 accumulating in the upper respiratory tract. PM exposure is known to modulate cytokine production, induce oxidative stress, and lead to mitochondrial dysfunction in human OM cells (Chew et al., 2020). Oxidative stress also represents a significant mechanism underlying the adverse effects associated with PM exposure in the context of COVID-19 (Santurtún et al., 2022). In this study, we employed a PM dose of 50 μg/ml to simulate subacute exposure (Jalava et al., 2015; Rönkkö et al., 2018), resulting in a mild induction of oxidative stress without evident cytotoxicity. Interestingly, SARS-CoV-2 infection of the pre-exposed samples revealed that PM did not affect viral entry or replication in primary human OM cells, suggesting that instead, altered cellular responses could contribute to varied COVID-19 outcomes, especially in individuals with AD.

Research has firmly established that ACE2 serves as the primary receptor for the cellular entry of SARS-CoV-2 (Hoffmann et al., 2020b). Studies in mice and human pulmonary alveolar cells demonstrated increased ACE2 expression post-exposure to urban PM (Sagawa et al., 2021; Zhu et al., 2021b). Additionally, exposure to curbside PM10 at concentrations of 10 μg/mL or higher led to increased ACE2 expression in various cell types, including A549, HPNEpCs, and Calu3 cells, while diesel PM10 also raised ACE2 expression in HPNEpCs (Miyashita et al., 2023). However, our results indicate that neither PM 0.2 nor PM 10–2.5 alter the mRNA expression of *ACE2*, *TMPRSS2*, or *NRP1* following a 24 h exposure in primary OM cells. This observation could be partially explained by findings from Botto et al. (2023), which demonstrated that exposure to PM2.5 causes organ-specific changes in the expression of ACE2 and ACE (Botto et al., 2023), and the fact that we used primary cells, instead of immortalized cell lines. Furthermore, the origin of the PM can significantly influence the composition of particles, which, in turn, greatly affects the subsequent effects induced by those particles (Rönkkö et al., 2020, 2021). Furthermore, recent study demonstrated distinctive neurotoxic effects of wood and plastic smoke PM (Tarasenko et al., 2022).

Another proposed mechanism by which PM could influence the SARS-CoV-2 entry involves the formation of a complex between PM and the virus, operating independently of ACE-2 facilitated viral entry (Borisova and Komisarenko, 2021). However, exposure to PM 0.2 or PM 10–2.5 did not appear to influence the susceptibility of OM cells to SARS-CoV-2 infection. Even at 72 hpi, there were no differences in viral load between PM-exposed and unexposed OM cells, whether derived from cognitively healthy individuals or those with AD. Consistent with our study, Brocke et al. (2022), also reported no alteration in the viral load of SARS-CoV-2 infection with exposure to wood smoke particles in human nasal epithelial cells.

Oxidative stress, a central mechanism in pollutant-induced toxicity, arises from reactive oxygen species (ROS) from various PM components (Ghio et al., 2012; Lodovici and Bigagli, 2011). Similarly, viruses, including SARS-CoV-2, are known to induce oxidative stress as a primary pathogenic mechanism, leading to tissue damage and the exacerbation of disease severity (Lee, 2018). A recent study links dysregulated oxidative stress-related genes to severe COVID-19 (Saheb Sharif-Askari et al., 2021). In the context of SARS-CoV-2 infection, the activation of NRF2-regulated enzymes, such as HMOX1 and NQO1, plays a crucial role in suppressing viral replication (Itoh et al., 1999; Ramezani et al., 2018). However, the viral protein NSP14 disrupts the NRF2/HMOX1 axis, compromising this antiviral defense mechanism (Zhang et al., 2022). Moreover, lung biopsy specimens from COVID-19 patients have revealed a suppression of genes associated with the NRF2-dependent antioxidant response, accompanied by an enrichment of genes linked to inflammatory and antiviral pathways (Olagnier et al., 2020). Consistent with the mentioned studies, SARS-CoV-2 alone fails to induce NRF2-associated antioxidant response in the OM cells in the current study. However, co-exposure to PM and the virus increases *HMOX1* and *NQO1* mRNA levels at 24 h. Enhanced cellular toxicity, particularly in AD OM cells pre-treated with PM 10–2.5, suggests transient dysregulation in oxidative stress response leading to cell adversity in AD OM cells exposed to PM 10–2.5. Intriguingly, at 72 hpi, the mRNA levels of *HMOX1* returned to the baseline but were also significantly lower than the PM-only treatments. However, co-exposed cells showed comparable toxicity to SARS-CoV-2 alone, but notably higher than PM-only treated cells. This suggests potential SARS-CoV-2-induced suppression of NRF2-dependent antioxidants, compromising immune defense and elevating cell toxicity.

Given that Aβ is one of the most important pathological hallmarks associated with AD (Hardy and Selkoe, 2002), we were interested to assess whether the exposures affect the production of this toxic peptide and measured the ratio of $A\beta_{1\text{-}42}/A\beta_{1\text{-}40}$, which is used as a marker of amyloid plaque formation or disease progression in AD (Lehmann et al., 2018). SARS-CoV-2 infection increased the $A\beta_{1\text{-}42}/A\beta_{1\text{-}40}$ ratio at 72 hpi in both AD and control cells. However, our results indicated that PM exposure did not alter the SARS-CoV-2-associated effects on the $A\beta_{1\text{-}42}/A\beta_{1\text{-}40}$ ratio. While our study did not directly investigate the mechanisms involved, research has suggested a complex relationship between SARS-CoV-2 infections and Aβ metabolism, potentially contributing to neurodegenerative processes (Caradonna et al., 2022; Idrees and Kumar, 2021; Shen et al., 2022). For instance, a recent study revealed the interaction of the SARS-CoV-2 N and S proteins with $A\beta_{1\text{-}42}$ and ACE-2 receptor, potentially influencing the entry of the virus in a mouse model (Hsu et al., 2021).

It has been reported that an effective antiviral response contributes to viral clearance and improves clinical outcomes (Hadjadj et al., 2020; Masood et al., 2021). However, in individuals with underlying AD, inflammation and impaired immune function can increase the risk of severe disease outcomes (Chiricosta et al., 2021). In our study, the AD OM cells already without any viral infection showed a slight basal enrichment of innate immune response elements. Furthermore, baseline levels of RAGE and RANTES levels were significantly higher in untreated AD OM cells compared to controls. RAGE is associated with Aβ production, oxidative stress, and synaptic dysfunction as reviewed in (Cai et al., 2016), and alterations of RANTES, a neuroinflammatory chemokine (Azizi et al., 2015), suggests an enhanced immune response and oxidative stress in AD OM cells.

Numerous studies have explored SARS-CoV-2 impact on the OM in vivo and ex vivo, suggesting damage to the epithelium, subsequent immune responses, and functional impairment (Bryche et al., 2020; de Melo et al., 2021; Khan et al., 2021; Ye et al., 2021; Zazhytska et al., 2022; Shahbaz et al., 2022). Inflammation, immune cell infiltration, and altered cytokine levels during infection contribute to olfactory dysfunction (Pozharskaya and Lane, 2013; Bryche et al., 2020; de Melo et al., 2021; Torabi et al., 2020). Notably, elevated interferon-gamma (IFN-γ) levels have been detected in infected OM samples, indicating an active antiviral gene expression response (Zazhytska et al., 2022). Epithelial cells, along with immune cells, express cytokines and initiate immune responses during infection (reviewed in (Hsu et al., 2022). Therefore, understanding the cytokine response in OM cells is crucial for insights into site-specific immune reactions during early infection.

Our study highlights distinct cytokine and chemokine responses in OM cells during SARS-CoV-2 infection. In cognitively healthy controls, infection led to a slight increase in typical SARS-CoV-2-associated cytokines, including IL-6, IL-8, MCP-3, TNF-alpha, IL1, GM-CSF, and IFN-γ (log2 fold change >0.5), while IP-10 was significantly upregulated. In addition, mucous secretory proteins IGFBP-3, and TFF3, along with CD14 were prominently upregulated. (Federico et al., 1999; Gamage et al., 2022).IGFBP-3, known to inhibit epithelial cell growth, shows elevation in severely infected COVID-19 lung epithelial cells (Lipskaia et al., 2022). Furthermore, TFF3 and CD14 are implicated at enhancing ciliary function, potentially to aid in viral clearance and support tissue repair processes (LeSimple et al., 2012)and initiation of the innate immune response towards viral infection (Di Gioia and Zanoni, 2015), respectively.

In SARS-CoV-2 infected AD OM cells, a distinct modulation of several cytokines and chemokines associated with the antiviral immune response was observed, displaying either slight alterations or significant downregulation compared to control infected cells. Notably, an elevation in GM-CSF levels was identified in infected AD OM cells, aligning with reports of increased circulating GM-CSF in COVID-19 patients compared to healthy controls (Huang et al., 2020). These findings suggest that the underlying pathology of AD may contribute to changes in cellular responses and sensitize the innate immune system, potentially influencing the inflammatory and antiviral immune response to SARS-CoV-2 infection in AD cells.

Expanding our exploration to the impact of pre-exposure to PM 0.2, and PM 10–2.5 on SARS-CoV-2 responses, our study aligns with prior research linking PM exposure to immune suppression and alterations in cytokine production (Mishra et al., 2020; Croft et al., 2021; Marín-Palma et al., 2023), and antiviral response gene expression (Brocke et al., 2022). Interestingly, irrespective of the size fraction of PM, pre-exposure caused downregulation in most of SARS-CoV-2-associated cytokines in both control and AD OM cells as compared to SARS-CoV-2 alone. However, a notable exception was observed with PM 0.2 treatment, which significantly elevated the response of IP10 after SARS-CoV-2 infection in control cells. Prior literature suggests the IP10 levels are associated with the critical illness, inflammation of the nervous system (Gudowska-Sawczuk and Mroczko, 2022), and anosmia as observed in patients with acute olfactory loss in COVID19 (de Melo et al., 2021). In contrast to control, IP10 levels were observed to be higher in AD OM cells at the baseline, and PM 0.2 exposure caused a severe upregulation in IP10 levels. However, upon subsequent infection, the immune system might undergo modulation or regulation to prevent excessive inflammation. This downregulation could be a regulatory mechanism to avoid immune overactivity, which can sometimes contribute to tissue damage. This is further supported by the fact that baseline levels of SARS-CoV-2 associated genes were higher in AD cells as compared to controls. Consequently, AD cells exhibited a milder response to SARS-CoV-2 infection compared to controls. However, in SARS-CoV-2 infection following PM 0.2 treatment, cells underwent modulation with a severe downregulation in SARS-CoV-2-associated immune responses and most of the cytokine profiles. Similar downregulation was observed in PM 10–2.5 pre-exposed control and AD OM cells, notably IL-6, contrasting with its upregulation in PM 10-2.5-exposed AD OM cells. This heightened IL-6 production in AD cells, potentially influenced by PM exposure, could contribute to the inflammatory response observed in COVID-19 infection. Elevated IL-6 production, positively correlated with COVID-19 severity and viral RNA detection, which may contribute to SARS-CoV-2 pathogenesis, with critically ill patients showing notably higher levels than mild cases (Zhang et al., 2020; Chen et al., 2020; Han et al., 2020; Avila-Nava et al., 2021; Zhang et al., 2020; Chen et al., 2020; Han et al., 2020; Avila-Nava et al., 2021).

This distinct response in AD cells, exacerbated by exposure to PM fractions, highlights the intricate interplay between environmental exposure and SARS-CoV-2 outcomes, providing valuable insights into both control and AD scenarios. While this study sheds light on the interplay between air pollution, nasal immune responses, and susceptibility to respiratory infections, it has limitations. It is primarily focused on PM 0.2 and PM 10–2.5 interactions with SARS-CoV-2 in OM cells based on the physiological relevance, however, the broader spectrum of air pollutants and their varied impacts on immune responses remain unexplored. The research also lacked a comprehensive analysis of the entire immune response, particularly adaptive immune responses, and focused solely on OM cells, providing a simplified model of SARS-CoV-2 infection. Future studies should address these limitations, exploring diverse pollutants, comprehensive immune responses, various immune cells, and employing more complex models to enhance our understanding of the intricate relationship between environmental pollution and susceptibility to respiratory infections across diverse populations and pathogens.

5. Conclusion

Overall, our data demonstrates that acute exposure to PM 0.2 and PM 10–2.5 does not alter the expression of ACE-2, or viral replication up to 72 hpi in OM cells derived from cognitively healthy controls and individuals with AD. However, pre-exposure to PM 0.2 and PM 10–2.5 induces alterations in cellular responses to SARS-CoV-2, including oxidative stress and cytotoxicity. Additionally, there is a discernible downregulation of key cytokines and chemokines associated with innate and antiviral immune responses, implying a potential modulation in the host cell response. Moreover, the altered immune response and inflammation pathways observed between control and AD cells following SARS-CoV-2 infection in the presence of PM 0.2 and PM 10–2.5 suggests a complex interplay between underlying disease pathology and PM exposure, possibly contributing to the variability in the severity and manifestations of COVID-19 outcomes. These findings underscore the importance of considering both environmental factors and individual health conditions in understanding the nuanced responses to SARS-CoV-2, providing valuable insights for future research and public health considerations.

CRediT authorship contribution statement

Muhammad Ali Shahbaz: Writing – review & editing, Writing – original draft, Methodology, Investigation, Formal analysis, Conceptualization. **Suvi Kuivanen:** Resources, Methodology, Investigation. **Laura Mussalo:** Writing – review & editing, Methodology, Investigation. **Alexey M. Afonin:** Validation, Formal analysis. **Kajal Kumari:** Visualization, Formal analysis. **Donya Behzadpour:** Investigation. **Juho Kalapudas:** Resources. **Anne M. Koivisto:** Resources. **Elina Penttilä:** Resources. **Heikki Löppönen:** Resources. **Pasi Jalava:** Resources, Conceptualization. **Olli Vapalahti:** Resources, Conceptualization. **Giuseppe Balistreri:** Resources, Conceptualization. **Riikka Lampinen:** Writing – review & editing, Supervision, Investigation, Formal analysis, Conceptualization. **Katja M. Kanninen:** Writing – review & editing, Visualization, Resources, Funding acquisition, Conceptualization.

Declaration of competing interest

The authors declare the following financial interests/personal relationships which may be considered as potential competing interests: Katja Kannienen reports financial support was provided by Research Council of Finland. Katja Kannienen reports financial support was provided by Sigrid Jusélius Foundation. If there are other authors, they declare that they have no known competing financial interests or personal relationships that could have appeared to influence the work reported in this paper.

Data availability

Data will be made available on request.

Acknowledgements

The authors would like to thank Academy of Finland for (grant number 335524) and Sigrid Juselius foundation for funding this work.

Appendix A. Supplementary data

Supplementary data to this article can be found online at https://doi.org/10.1016/j.envres.2024.118451.

References

Ali, N., Islam, F., 2020. The effects of air pollution on COVID-19 infection and mortality—a review on recent evidence. Front. Public Health 8, 580057. https://doi.org/10.3389/FPUBH.2020.580057/BIBTEX.

Atkins, J.L., Masoli, J.A.H., Delgado, J., Pilling, L.C., Kuo, C.-L., Kuchel, G.A., Melzer, D., 2020. Preexisting comorbidities predicting COVID-19 and mortality in the UK biobank community cohort. J. Gerontol.: Series A 75, 2224–2230. https://doi.org/10.1093/gerona/glaa183.

Avila-Nava, A., Cortes-Telles, A., Torres-Erazo, D., López-Romero, S., Chim Aké, R., Gutiérrez Solis, A.L., 2021. Serum IL-6: a potential biomarker of mortality among SARS-CoV-2 infected patients in Mexico. Cytokine 143. https://doi.org/10.1016/J.CYTO.2021.155543.

Azizi, G., Navabi, S.S., Al-Shukaili, A., Seyedzadeh, M.H., Yazdani, R., Mirshafiey, A., 2015. The role of inflammatory mediators in the pathogenesis of alzheimer's disease. Sultan Qaboos Univ Med J 15, e305–e316. https://doi.org/10.18295/SQUMJ.2015.15.03.002.

Block, M.L., Calderón-Garcidueñas, L., 2009. Air pollution: mechanisms of neuroinflammation and CNS disease. Trends Neurosci. 32, 506–516. https://doi.org/10.1016/j.tins.2009.05.009.

Borisova, T., Komisarenko, S., 2021. Air pollution particulate matter as a potential carrier of SARS-CoV-2 to the nervous system and/or neurological symptom enhancer: arguments in favor. Environ. Sci. Pollut. Control Ser. 28, 40371–40377. https://doi.org/10.1007/s11356-020-11183-3.

Botto, L., Lonati, E., Russo, S., Cazzaniga, E., Bulbarelli, A., Palestini, P., 2023. Effects of PM2.5 exposure on the ACE/ACE2 pathway: possible implication in COVID-19 pandemic. Int. J. Environ. Res. Publ. Health 20, 4393. https://doi.org/10.3390/ijerph20054393.

Brocke, S.A., Billings, G.T., Taft-Benz, S., Alexis, N.E., Heise, M.T., Jaspers, I., 2022. Woodsmoke particle exposure prior to SARS-CoV-2 infection alters antiviral response gene expression in human nasal epithelial cells in a sex-dependent manner. Am. J. Physiol. Lung Cell Mol. Physiol. 322, L479–L494. https://doi.org/10.1152/ajplung.00362.2021.

Bryche, B., St Albin, A., Murri, S., Lacôte, S., Pulido, C., Ar Gouilh, M., Lesellier, S., Servat, A., Wasniewski, M., Picard-Meyer, E., Monchatre-Leroy, E., Volmer, R., Rampin, O., Le Goffic, R., Marianneau, P., Meunier, N., 2020. Massive transient damage of the olfactory epithelium associated with infection of sustentacular cells by SARS-CoV-2 in golden Syrian hamsters. Brain Behav. Immun. 89, 579–586. https://doi.org/10.1016/J.BBI.2020.06.032.

Butowt, R., Bilińska, K., von Bartheld, C., 2022. Why does the omicron variant largely spare olfactory function? Implications for the pathogenesis of anosmia in coronavirus disease 2019. J. Infect. Dis. 226, 1304–1308. https://doi.org/10.1093/infdis/jiac113.

Butowt, R., von Bartheld, C.S., 2021. Anosmia in COVID-19: underlying mechanisms and assessment of an olfactory route to brain infection. Neuroscientist 27, 582–603. https://doi.org/10.1177/1073858420956905.

Cai, Z., Liu, N., Wang, C., Qin, B., Zhou, Y., Xiao, M., Chang, L., Yan, L.J., Zhao, B., 2016. Role of RAGE in alzheimer's disease. Cell. Mol. Neurobiol. 36, 483–495. https://doi.org/10.1007/S10571-015-0233-3.

Cantuti-Castelvetri, L., Ojha, R., Pedro, L.D., Djannatian, M., Franz, J., Kuivanen, S., van der Meer, F., Kallio, K., Kaya, T., Anastasina, M., Smura, T., Levanov, L., Szirovicza, L., Tobi, A., Kallio-Kokko, H., Österlund, P., Joensuu, M., Meunier, F.A., Butcher, S.J., Winkler, M.S., Mollenhauer, B., Helenius, A., Gokce, O., Teesalu, T., Hepojoki, J., Vapalahti, O., Stadelmann, C., Balistreri, G., Simons, M., 2020. Neuropilin-1 facilitates SARS-CoV-2 cell entry and infectivity. Science 370, 856–860. https://doi.org/10.1126/science.abd2985, 1979.

Caradonna, A., Patel, T., Toleska, M., Alabed, S., Chang, S.L., 2022. Meta-analysis of APP expression modulated by SARS-CoV-2 infection via the ACE2 receptor. Int. J. Mol. Sci. 23, 1182. https://doi.org/10.3390/ijms23031182.

Cevallos, V.M., Díaz, V., Sirois, C.M., 2017. Particulate matter air pollution from the city of Quito, Ecuador, activates inflammatory signaling pathways *in vitro*. Innate Immun. 23, 392–400. https://doi.org/10.1177/1753425917699864.

Chen, X., Zhao, B., Qu, Y., Chen, Y., Xiong, J., Feng, Y., Men, D., Huang, Q., Liu, Y., Yang, B., Ding, J., Li, F., 2020. Detectable serum severe acute respiratory syndrome coronavirus 2 viral load (RNAemia) is closely correlated with drastically elevated interleukin 6 level in critically ill patients with coronavirus disease 2019. Clin. Infect. Dis. 71, 1937–1942. https://doi.org/10.1093/CID/CIAA449.

Chew, S., Lampinen, R., Saveleva, L., Korhonen, P., Mikhailov, N., Grubman, A., Polo, J. M., Wilson, T., Komppula, M., Rönkkö, T., Gu, C., Mackay-Sim, A., Malm, T., White, A.R., Jalava, P., Kanninen, K.M., 2020. Urban air particulate matter induces mitochondrial dysfunction in human olfactory mucosal cells. Part. Fibre Toxicol. 17, 18. https://doi.org/10.1186/s12989-020-00352-4.

Chiricosta, L., Gugliandolo, A., Mazzon, E., 2021. SARS-CoV-2 exacerbates beta-amyloid neurotoxicity, inflammation and oxidative stress in alzheimer's disease patients. Int. J. Mol. Sci. 22 https://doi.org/10.3390/IJMS222413603.

Comunian, S., Dongo, D., Milani, C., Palestini, P., 2020. Air pollution and COVID-19: the role of particulate matter in the spread and increase of COVID-19's morbidity and mortality. Int. J. Environ. Res. Publ. Health 17, 4487. https://doi.org/10.3390/ijerph17124487.

Corman, V.M., Landt, O., Kaiser, M., Molenkamp, R., Meijer, A., Chu, D.K., Bleicker, T., Brünink, S., Schneider, J., Schmidt, M.L., Mulders, D.G., Haagmans, B.L., van der Veer, B., van den Brink, S., Wijsman, L., Goderski, G., Romette, J.-L., Ellis, J., Zambon, M., Peiris, M., Goossens, H., Reusken, C., Koopmans, M.P., Drosten, C., 2020. Detection of 2019 novel coronavirus (2019-nCoV) by real-time RT-PCR. Euro Surveill. 25 https://doi.org/10.2807/1560-7917.ES.2020.25.3.2000045.

Croft, D.P., Burton, D.S., Nagel, D.J., Bhattacharya, S., Falsey, A.R., Georas, S.N., Hopke, P.K., Johnston, C.J., Kottmann, R.M., Litonjua, A.A., Mariani, T.J., Rich, D. Q., Thevenet-Morrison, K., Thurston, S.W., Utell, M.J., McCall, M.N., 2021. The effect of air pollution on the transcriptomics of the immune response to respiratory infection. Sci. Rep. 11 (1 11), 1–14. https://doi.org/10.1038/s41598-021-98729-8, 2021.

de Melo, G.D., Lazarini, F., Levallois, S., Hautefort, C., Michel, V., Larrous, F., Verillaud, B., Aparicio, C., Wagner, S., Gheusi, G., Kergoat, L., Kornobis, E., Donati, F., Cokelaer, T., Hervochon, R., Madec, Y., Roze, E., Salmon, D., Bourhy, H., Lecuit, M., Lledo, P.-M., 2021. COVID-19–related anosmia is associated with viral persistence and inflammation in human olfactory epithelium and brain infection in hamsters. Sci. Transl. Med. 13 https://doi.org/10.1126/scitranslmed.abf8396.

Di Gioia, M., Zanoni, I., 2015. Toll-like receptor co-receptors as master regulators of the immune response. Mol. Immunol. 63, 143–152. https://doi.org/10.1016/J.MOLIMM.2014.05.008.

Fattorini, D., Regoli, F., 2020. Role of the chronic air pollution levels in the Covid-19 outbreak risk in Italy. Environ. Pollut. 264, 114732 https://doi.org/10.1016/j.envpol.2020.114732.

Federico, G., Maremmani, C., Cinquanta, L., Baroncelli, G.I., Fattori, B., Saggese, G., 1999. Mucus of the human olfactory epithelium contains the insulin-like growth factor-I system which is altered in some neurodegenerative diseases. Brain Res. 835, 306–314. https://doi.org/10.1016/S0006-8993(99)01614-5.

Fotuhi, M., Mian, A., Meysami, S., Raji, C.A., 2020. Neurobiology of COVID-19. J. Alzheim. Dis. 76, 3–19. https://doi.org/10.3233/JAD-200581.

Fu, P., Yung, K.K.L., 2020. Air pollution and alzheimer's disease: a systematic review and meta-analysis. J. Alzheim. Dis. 77, 701–714. https://doi.org/10.3233/JAD-200483.

Gamage, A.M., Tan, K. Sen, Chan, W.O.Y., Lew, Z.Z.R., Liu, J., Tan, C.W., Rajagopalan, D., Lin, Q.X.X., Tan, L.M., Venkatesh, P.N., Ong, Y.K., Thong, M., Lin, R.T.P., Prabhakar, S., Wang, D.Y., Wang, L.-F., 2022. Human nasal epithelial cells sustain persistent SARS-CoV-2 infection *in vitro* , despite eliciting a prolonged antiviral response. mBio 13. https://doi.org/10.1128/mbio.03436-21.

Ghio, A.J., Carraway, M.S., Madden, M.C., 2012. Composition of air pollution particles and oxidative stress in cells, tissues, and living systems. J. Toxicol. Environ. Health, Part A B 15, 1–21. https://doi.org/10.1080/10937404.2012.632359.

Gudowska-Sawczuk, M., Mroczko, B., 2022. What is currently known about the role of CXCL10 in SARS-CoV-2 infection? Int. J. Mol. Sci. 23 https://doi.org/10.3390/IJMS23073673.

Hadjadj, J., Yatim, N., Barnabei, L., Corneau, A., Boussier, J., Smith, N., Péré, H., Charbit, B., Bondet, V., Chenevier-Gobeaux, C., Breillat, P., Carlier, N., Gauzit, R., Morbieu, C., Pène, F., Marin, N., Roche, N., Szwebel, T.A., Merkling, S.H., Treluyer, J.M., Veyer, D., Mouthon, L., Blanc, C., Tharaux, P.L., Rozenberg, F., Fischer, A., Duffy, D., Rieux-Laucat, F., Kernéis, S., Terrier, B., 2020. Impaired type I interferon activity and inflammatory responses in severe COVID-19 patients. Science 369, 718–724. https://doi.org/10.1126/SCIENCE.ABC6027.

Han, H., Ma, Q., Li, C., Liu, R., Zhao, L., Wang, W., Zhang, P., Liu, X., Gao, G., Liu, F., Jiang, Y., Cheng, X., Zhu, C., Xia, Y., 2020. Profiling serum cytokines in COVID-19 patients reveals IL-6 and IL-10 are disease severity predictors. Emerg. Microb. Infect. 9, 1123–1130. https://doi.org/10.1080/22221751.2020.1770129.

Hardy, J., Selkoe, D.J., 2002. The amyloid hypothesis of alzheimer's disease: progress and problems on the road to therapeutics. Science 297, 353–356. https://doi.org/10.1126/science.1072994, 1979.

Hernandez Carballo, I., Bakola, M., Stuckler, D., 2022. The impact of air pollution on COVID-19 incidence, severity, and mortality: a systematic review of studies in Europe and North America. Environ. Res. 215, 114155 https://doi.org/10.1016/J.ENVRES.2022.114155.

Hoffmann, M., Kleine-Weber, H., Schroeder, S., Krüger, N., Herrler, T., Erichsen, S., Schiergens, T.S., Herrler, G., Wu, N.H., Nitsche, A., Müller, M.A., Drosten, C., Pöhlmann, S., 2020a. SARS-CoV-2 cell entry depends on ACE2 and TMPRSS2 and is blocked by a clinically proven protease inhibitor. Cell 181, 271–280.e8. https://doi.org/10.1016/j.cell.2020.02.052.

Hoffmann, M., Kleine-Weber, H., Schroeder, S., Krüger, N., Herrler, T., Erichsen, S., Schiergens, T.S., Herrler, G., Wu, N.-H., Nitsche, A., Müller, M.A., Drosten, C., Pöhlmann, S., 2020b. SARS-CoV-2 cell entry depends on ACE2 and TMPRSS2 and is blocked by a clinically proven protease inhibitor. Cell 181, 271–280.e8. https://doi.org/10.1016/j.cell.2020.02.052.

Hsu, J.T.-A., Tien, C.-F., Yu, G.-Y., Shen, S., Lee, Y.-H., Hsu, P.-C., Wang, Y., Chao, P.-K., Tsay, H.-J., Shie, F.-S., 2021. The effects of aβ1-42 binding to the SARS-CoV-2 spike

protein S1 subunit and angiotensin-converting enzyme 2. Int. J. Mol. Sci. 22, 8226. https://doi.org/10.3390/ijms22158226.
Hsu, R.J., Yu, W.C., Peng, G.R., Ye, C.H., Hu, S.Y., Chong, P.C.T., Yap, K.Y., Lee, J.Y.C., Lin, W.C., Yu, S.H., 2022. The role of cytokines and chemokines in severe acute respiratory syndrome coronavirus 2 infections. Front. Immunol. 13, 832394 https://doi.org/10.3389/FIMMU.2022.832394/BIBTEX.
Huang, C., Wang, Y., Li, X., Ren, L., Zhao, J., Hu, Y., Zhang, L., Fan, G., Xu, J., Gu, X., Cheng, Z., Yu, T., Xia, J., Wei, Y., Wu, W., Xie, X., Yin, W., Li, H., Liu, M., Xiao, Y., Gao, H., Guo, L., Xie, J., Wang, G., Jiang, R., Gao, Z., Jin, Q., Wang, J., Cao, B., 2020. Clinical features of patients infected with 2019 novel coronavirus in Wuhan, China. Lancet 395, 497–506. https://doi.org/10.1016/S0140-6736(20)30183-5.
Idrees, D., Kumar, V., 2021. SARS-CoV-2 spike protein interactions with amyloidogenic proteins: potential clues to neurodegeneration. Biochem. Biophys. Res. Commun. 554, 94–98. https://doi.org/10.1016/j.bbrc.2021.03.100.
Isphording, I.E., Pestel, N., 2021. Pandemic meets pollution: poor air quality increases deaths by COVID-19. J. Environ. Econ. Manag. 108, 102448 https://doi.org/10.1016/J.JEEM.2021.102448.
Itoh, K., Ishii, T., Wakabayashi, N., Yamamoto, M., 1999. Regulatory mechanisms of cellular response to oxidative stress. Free Radic. Res. 31, 319–324. https://doi.org/10.1080/10715769900300881.
Jalava, P.I., Wang, Q., Kuuspalo, K., Ruusunen, J., Hao, L., Fang, D., Väisänen, O., Ruuskanen, A., Sippula, O., Happo, M.S., Uski, O., Kasurinen, S., Torvela, T., Koponen, H., Lehtinen, K.E.J., Komppula, M., Gu, C., Jokiniemi, J., Hirvonen, M.-R., 2015. Day and night variation in chemical composition and toxicological responses of size segregated urban air PM samples in a high air pollution situation. Atmos. Environ. 120, 427–437. https://doi.org/10.1016/j.atmosenv.2015.08.089.
Jiang, Y., Wu, X.-J., Guan, Y.-J., 2020. Effect of ambient air pollutants and meteorological variables on COVID-19 incidence. Infect. Control Hosp. Epidemiol. 41, 1011–1015. https://doi.org/10.1017/ice.2020.222.
Kayalar, Ö., Arı, A., Babuççu, G., Konyalılar, N., Doğan, Ö., Can, F., Şahin, Ü.A., Gaga, E. O., Levent Kuzu, S., Arı, P.E., Odabaşı, M., Taşdemir, Y., Sıddık Cindoruk, S., Esen, F., Sakın, E., Çalışkan, B., Tecer, L.H., Fıçıcı, M., Altın, A., Onat, B., Ayvaz, C., Uzun, B., Saral, A., Döğeroğlu, T., Malkoç, S., Üzmez, Ö.Ö., Kunt, F., Aydın, S., Kara, M., Yaman, B., Doğan, G., Olgun, B., Dokumacı, E.N., Güllü, G., Uzunpınar, E. S., Bayram, H., 2021. Existence of SARS-CoV-2 RNA on ambient particulate matter samples: a nationwide study in Turkey. Sci. Total Environ. 789, 147976 https://doi.org/10.1016/j.scitotenv.2021.147976.
Khan, M., Yoo, S.J., Clijsters, M., Backaert, W., Vanstapel, A., Speleman, K., Lietaer, C., Choi, S., Hether, T.D., Marcelis, L., Nam, A., Pan, L., Reeves, J.W., Van Bulck, P., Zhou, H., Bourgeois, M., Debaveye, Y., De Munter, P., Gunst, J., Jorissen, M., Lagrou, K., Lorent, N., Neyrinck, A., Peetermans, M., Thal, D.R., Vandenbriele, C., Wauters, J., Mombaerts, P., Van Gerven, L., 2021. Visualizing in deceased COVID-19 patients how SARS-CoV-2 attacks the respiratory and olfactory mucosae but spares the olfactory bulb. Cell 184. https://doi.org/10.1016/J.CELL.2021.10.027, 5932-5949.e15.
Kim, B.-Y., Park, J.Y., Cho, K.J., Bae, J.H., 2022. Effects of urban particulate matter on the olfactory system in a mouse model. Am J Rhinol Allergy 36, 81–90. https://doi.org/10.1177/19458924211026416.
Kim, J.-H., Kim, J., Kim, W.J., Choi, Y.H., Yang, S.-R., Hong, S.-H., 2020. Diesel particulate matter 2.5 induces epithelial-to-mesenchymal transition and upregulation of SARS-CoV-2 receptor during human pluripotent stem cell-derived alveolar organoid development. Int. J. Environ. Res. Publ. Health 17, 8410. https://doi.org/10.3390/ijerph17228410.
Lampinen, R., Fazaludeen, M.F., Avesani, S., Örd, T., Penttilä, E., Lehtola, J.M., Saari, T., Hannonen, S., Saveleva, L., Kaartinen, E., Acosta, F.F., Cruz-Haces, M., Löppönen, H., Mackay-Sim, A., Kaikkonen, M.U., Koivisto, A.M., Malm, T., White, A. R., Giugno, R., Chew, S., Kanninen, K.M., 2022. Single-cell RNA-seq analysis of olfactory mucosal cells of alzheimer's disease patients. Cells 11, 676. https://doi.org/10.3390/CELLS11040676/S1.
Lee, C., 2018. Therapeutic modulation of virus-induced oxidative stress via the nrf2-dependent antioxidative pathway. Oxid. Med. Cell. Longev. 2018, 1–26. https://doi.org/10.1155/2018/6208067.
Lehmann, S., Delaby, C., Boursier, G., Catteau, C., Ginestet, N., Tiers, L., Maceski, A., Navucet, S., Paquet, C., Dumurgier, J., Vanmechelen, E., Vanderstichele, H., Gabelle, A., 2018. Relevance of aβ42/40 ratio for detection of alzheimer disease pathology in clinical routine: the PLMR scale. Front. Aging Neurosci. 10 https://doi.org/10.3389/fnagi.2018.00138.
LeSimple, P., Van Seuningen, I., Buisine, M.P., Copin, M.C., Hinz, M., Hoffmann, W., Hajj, R., Brody, S.L., Coraux, C., Puchelle, E., 2012. Trefoil Factor Family 3 Peptide Promotes Human Airway Epithelial Ciliated Cell Differentiation, pp. 296–303. https://doi.org/10.1165/RCMB.2006-0270OC, 10.1165/rcmb.2006-0270OC36.
Li, H., Xu, X.-L., Dai, D.-W., Huang, Z.-Y., Ma, Z., Guan, Y.-J., 2020. Air pollution and temperature are associated with increased COVID-19 incidence: a time series study. Int. J. Infect. Dis. 97, 278–282. https://doi.org/10.1016/j.ijid.2020.05.076.
Lin, J., Tang, C., Wei, Han-cheng, Du, B., Chen, C., Wang, M., Zhou, Y., Yu, M., Cheng, L., Kuivanen, S., Ogando, N.S., Levanov, L., Zhao, Y., Li, C., Zhou, R., Li, Z., Zhang, Yiming, Sun, K., Wang, C., Chen, Li, Xiao, X., Zheng, X., Chen, S., Zhou, Z., Yang, R., Zhang, D., Xu, M., Song, J., Wang, D., Li, Y., Lei, S., Zeng, W., Yang, Q., He, P., Zhang, Yaoyao, Zhou, L., Cao, L., Luo, F., Liu, H., Wang, L., Ye, F., Zhang, M., Li, M., Fan, W., Li, X., Li, K., Ke, B., Xu, J., Yang, H., He, S., Pan, M., Yan, Y., Zha, Y., Jiang, L., Yu, C., Liu, Y., Xu, Z., Li, Q., Jiang, Y., Sun, J., Hong, W., Wei, Hongping, Lu, G., Vapalahti, O., Luo, Y., Wei, Y., Connor, T., Tan, W., Snijder, E.J., Smura, T., Li, W., Geng, J., Ying, B., Chen, Lu, 2021. Genomic monitoring of SARS-CoV-2 uncovers an Nsp1 deletion variant that modulates type I interferon response. Cell Host Microbe 29, 489–502.e8. https://doi.org/10.1016/j.chom.2021.01.015.
Linares, C., Belda, F., López-Bueno, J.A., Luna, M.Y., Sánchez-Martínez, G., Hervella, B., Culqui, D., Díaz, J., 2021. Short-term associations of air pollution and meteorological variables on the incidence and severity of COVID-19 in Madrid (Spain): a time series study. Environ. Sci. Eur. 33, 107. https://doi.org/10.1186/s12302-021-00548-1.
Lipskaia, L., Maisonnasse, P., Fouillade, C., Sencio, V., Pascal, Q., Flaman, J.M., Born, E., Londono-Vallejo, A., Le Grand, R., Bernard, D., Trottein, F., Adnot, S., 2022. Evidence that SARS-CoV-2 induces lung cell senescence: potential impact on COVID-19 lung disease. Am. J. Respir. Cell Mol. Biol. 66, 107–111. https://doi.org/10.1165/RCMB.2021-0205LE.
Livingston, G., Huntley, J., Sommerlad, A., Ames, D., Ballard, C., Banerjee, S., Brayne, C., Burns, A., Cohen-Mansfield, J., Cooper, C., Costafreda, S.G., Dias, A., Fox, N., Gitlin, L.N., Howard, R., Kales, H.C., Kivimäki, M., Larson, E.B., Ogunniyi, A., Orgeta, V., Ritchie, K., Rockwood, K., Sampson, E.L., Samus, Q., Schneider, L.S., Selbæk, G., Teri, L., Mukadam, N., 2020. Dementia prevention, intervention, and care: 2020 report of the Lancet Commission. Lancet 396, 413–446. https://doi.org/10.1016/S0140-6736(20)30367-6/ATTACHMENT/DFC82F21-55AB-4950-8828-93F27077EF6D/MMC1.PDF.
Lodovici, M., Bigagli, E., 2011. Oxidative stress and air pollution exposure. J. Toxicol. 2011, 1–9. https://doi.org/10.1155/2011/487074.
Lopez-Leon, S., Wegman-Ostrosky, T., Perelman, C., Sepulveda, R., Rebolledo, P.A., Cuapio, A., Villapol, S., 2021. More than 50 long-term effects of COVID-19: a systematic review and meta-analysis. Sci. Rep. 11, 16144 https://doi.org/10.1038/s41598-021-95565-8.
Mao, L., Jin, H., Wang, M., Hu, Y., Chen, S., He, Q., Chang, J., Hong, C., Zhou, Y., Wang, D., Miao, X., Li, Y., Hu, B., 2020. Neurologic manifestations of hospitalized patients with coronavirus disease 2019 in wuhan, China. JAMA Neurol. 77, 683. https://doi.org/10.1001/jamaneurol.2020.1127.
Marín-Palma, D., Tabares-Guevara, J.H., Zapata-Cardona, M.I., Zapata-Builes, W., Taborda, N., Rugeles, M.T., Hernandez, J.C., 2023. PM10 promotes an inflammatory cytokine response that may impact SARS-CoV-2 replication in vitro. Front. Immunol. 14, 1161135 https://doi.org/10.3389/FIMMU.2023.1161135/BIBTEX.
Marquès, M., Domingo, J.L., 2022. Positive association between outdoor air pollution and the incidence and severity of COVID-19. A review of the recent scientific evidences. Environ. Res. 203, 111930 https://doi.org/10.1016/j.envres.2021.111930.
Masood, K.I., Yameen, M., Ashraf, J., Shahid, S., Mahmood, S.F., Nasir, A., Nasir, N., Jamil, B., Ghanchi, N.K., Khanum, I., Razzak, S.A., Kanji, A., Hussain, R., E. Rottenberg, M., Hasan, Z., 2021. Upregulated type I interferon responses in asymptomatic COVID-19 infection are associated with improved clinical outcome. Sci. Rep. 11 (1 11), 1–14. https://doi.org/10.1038/s41598-021-02489-4, 2021.
Mishra, R., Krishnamoorthy, P., Gangamma, S., Raut, A.A., Kumar, H., 2020. Particulate matter (PM10) enhances RNA virus infection through modulation of innate immune responses. Environ. Pollut. 266 https://doi.org/10.1016/J.ENVPOL.2020.115148.
Miyashita, L., Foley, G., Semple, S., Gibbons, J.M., Pade, C., McKnight, Á., Grigg, J., 2023. Curbside particulate matter and susceptibility to SARS–CoV-2 infection. J. Allergy Clin. Immunol.: Global 2, 100141. https://doi.org/10.1016/j.jacig.2023.100141.
Mussalo, L., Avesani, S., Shahbaz, M.A., Závodná, T., Saveleva, L., Järvinen, A., Lampinen, R., Belaya, I., Krejčík, Z., Ivanova, M., Hakkarainen, H., Kalapudas, J., Penttilä, E., Löppönen, H., Koivisto, A.M., Malm, T., Topinka, J., Giugno, R., Aakko-Saksa, P., Chew, S., Rönkkö, T., Jalava, P., Kanninen, K.M., 2023. Emissions from modern engines induce distinct effects in human olfactory mucosa cells, depending on fuel and aftertreatment. Sci. Total Environ. 905, 167038 https://doi.org/10.1016/j.scitotenv.2023.167038.
Mutiawati, E., Fahriani, M., Mamada, S.S., Fajar, J.K., Frediansyah, A., Maliga, H.A., Ilmawan, M., Emran, T. Bin, Ophinni, Y., Ichsan, I., Musadir, N., Rabaan, A.A., Dhama, K., Syahrul, S., Nainu, F., Harapan, H., 2021. Anosmia and Dysgeusia in SARS-CoV-2 Infection: Incidence and Effects on COVID-19 Severity and Mortality, and the Possible Pathobiology Mechanisms - a Systematic Review and Meta-Analysis, vol. 10. F1000Res, p. 40. https://doi.org/10.12688/f1000research.28393.1.
Oberdörster, G., Sharp, Z., Atudorei, V., Elder, A., Gelein, R., Kreyling, W., Cox, C., 2004. Translocation of inhaled ultrafine particles to the brain. Inhal. Toxicol. 16, 437–445. https://doi.org/10.1080/08958370490439597.
Olagnier, D., Farahani, E., Thyrsted, J., Blay-Cadanet, J., Herengt, A., Idorn, M., Hait, A., Hernaez, B., Knudsen, A., Iversen, M.B., Schilling, M., Jørgensen, S.E., Thomsen, M., Reinert, L.S., Lappe, M., Hoang, H.-D., Gilchrist, V.H., Hansen, A.L., Ottosen, R., Nielsen, C.G., Møller, C., van der Horst, D., Peri, S., Balachandran, S., Huang, J., Jakobsen, M., Svenningsen, E.B., Poulsen, T.B., Bartsch, L., Thielke, A.L., Luo, Y., Alain, T., Rehwinkel, J., Alcamí, A., Hiscott, J., Mogensen, T.H., Paludan, S.R., Holm, C.K., 2020. SARS-CoV2-mediated suppression of NRF2-signaling reveals potent antiviral and anti-inflammatory activity of 4-octyl-itaconate and dimethyl fumarate. Nat. Commun. 11, 4938. https://doi.org/10.1038/s41467-020-18764-3.
Peters, R., Ee, N., Peters, J., Booth, A., Mudway, I., Anstey, K.J., 2019. Air pollution and dementia: a systematic review. J. Alzheim. Dis. 70, S145–S163. https://doi.org/10.3233/JAD-180631.
Pozharskaya, T., Lane, A.P., 2013. Interferon gamma causes olfactory dysfunction without concomitant neuroepithelial damage. Int. Forum. Allergy Rhinol. 3, 861–865. https://doi.org/10.1002/ALR.21226.
Ramezani, A., Nahad, M.P., Faghihloo, E., 2018. The role of Nrf2 transcription factor in viral infection. J. Cell. Biochem. 119, 6366–6382. https://doi.org/10.1002/jcb.26897.
Rantanen, L.M., Bitar, M., Lampinen, R., Stewart, R., Quek, H., Oikari, L.E., Cuní-López, C., Sutharsan, R., Thillaiyampalam, G., Iqbal, J., Russell, D., Penttilä, E., Löppönen, H., Lehtola, J.-M., Saari, T., Hannonen, S., Koivisto, A.M., Haupt, L.M., Mackay-Sim, A., Cristino, A.S., Kanninen, K.M., White, A.R., 2022. An alzheimer's

disease patient-derived olfactory stem cell model identifies gene expression changes associated with cognition. Cells 11, 3258. https://doi.org/10.3390/cells11203258.
Rönkkö, T.J., Hirvonen, M.-R., Happo, M.S., Ihantola, T., Hakkarainen, H., Martikainen, M.-V., Gu, C., Wang, Q., Jokiniemi, J., Komppula, M., Jalava, P.I., 2021. Inflammatory responses of urban air PM modulated by chemical composition and different air quality situations in Nanjing, China. Environ. Res. 192, 110382 https://doi.org/10.1016/j.envres.2020.110382.
Rönkkö, T.J., Hirvonen, M.-R., Happo, M.S., Leskinen, A., Koponen, H., Mikkonen, S., Bauer, S., Ihantola, T., Hakkarainen, H., Miettinen, M., Orasche, J., Gu, C., Wang, Q., Jokiniemi, J., Sippula, O., Komppula, M., Jalava, P.I., 2020. Air quality intervention during the Nanjing youth olympic games altered PM sources, chemical composition, and toxicological responses. Environ. Res. 185, 109360 https://doi.org/10.1016/j.envres.2020.109360.
Rönkkö, T.J., Jalava, P.I., Happo, M.S., Kasurinen, S., Sippula, O., Leskinen, A., Koponen, H., Kuuspalo, K., Ruusunen, J., Väisänen, O., Hao, L., Ruuskanen, A., Orasche, J., Fang, D., Zhang, L., Lehtinen, K.E.J., Zhao, Y., Gu, C., Wang, Q., Jokiniemi, J., Komppula, M., Hirvonen, M.-R., 2018. Emissions and atmospheric processes influence the chemical composition and toxicological properties of urban air particulate matter in Nanjing, China. Sci. Total Environ. 639, 1290–1310. https://doi.org/10.1016/j.scitotenv.2018.05.260.
Rudnicka-Drożak, E., Drożak, P., Mizerski, G., Zaborowski, T., Ślusarska, B., Nowicki, G., Drożak, M., 2023. Links between COVID-19 and alzheimer's disease—what do we already know? Int. J. Environ. Res. Publ. Health 20, 2146. https://doi.org/10.3390/ijerph20032146.
Sagawa, T., Tsujikawa, T., Honda, A., Miyasaka, N., Tanaka, M., Kida, T., Hasegawa, K., Okuda, T., Kawahito, Y., Takano, H., 2021. Exposure to particulate matter upregulates ACE2 and TMPRSS2 expression in the murine lung. Environ. Res. 195, 110722 https://doi.org/10.1016/j.envres.2021.110722.
Saheb Sharif-Askari, N., Saheb Sharif-Askari, F., Mdkhana, B., Hussain Alsayed, H.A., Alsafar, H., Alrais, Z.F., Hamid, Q., Halwani, R., 2021. Upregulation of oxidative stress gene markers during SARS-COV-2 viral infection. Free Radic. Biol. Med. 172, 688–698. https://doi.org/10.1016/j.freeradbiomed.2021.06.018.
Samadizadeh, S., Masoudi, M., Rastegar, M., Salimi, V., Shahbaz, M.B., Tahamtan, A., 2021. COVID-19: why does disease severity vary among individuals? Respir. Med. 180, 106356 https://doi.org/10.1016/j.rmed.2021.106356.
Santurtún, A., Colom, M.L., Fdez-Arroyabe, P., Real, Á. del, Fernández-Olmo, I., Zarrabeitia, M.T., 2022. Exposure to particulate matter: direct and indirect role in the COVID-19 pandemic. Environ. Res. 206, 112261 https://doi.org/10.1016/j.envres.2021.112261.
Shahbaz, M.A., De Bernardi, F., Alatalo, A., Sachana, M., Clerbaux, L.-A., Muñoz, A., Parvatam, S., Landesmann, B., Kanninen, K.M., Coecke, S., 2022. Mechanistic understanding of the olfactory neuroepithelium involvement leading to short-term anosmia in COVID-19 using the adverse outcome pathway framework. Cells 11, 3027. https://doi.org/10.3390/cells11193027.
Shahbaz, M.A., Kuivanen, S., Lampinen, R., Mussalo, L., Hron, T., Závodná, T., Ojha, R., Krejčík, Z., Saveleva, L., Tahir, N.A., Kalapudas, J., Koivisto, A.M., Penttilä, E., Löppönen, H., Singh, P., Topinka, J., Vapalahti, O., Chew, S., Balistreri, G., Kanninen, K.M., 2023. Human-derived air–liquid interface cultures decipher Alzheimer's disease–SARS-CoV-2 crosstalk in the olfactory mucosa. J. Neuroinflammation 20, 1–23. https://doi.org/10.1186/S12974-023-02979-4.
Shen, W.-B., Elahi, M., Logue, J., Yang, Penghua, Baracco, L., Reece, E.A., Wang, B., Li, L., Blanchard, T.G., Han, Z., Rissman, R.A., Frieman, M.B., Yang, Peixin, 2022. SARS-CoV-2 invades cognitive centers of the brain and induces Alzheimer's-like neuropathology. bioRxiv. https://doi.org/10.1101/2022.01.31.478476, 2022.01.31.478476.
Sillanpää, M., Hillamo, R., Mäkelä, T., Pennanen, A.S., Salonen, R.O., 2003. Field and laboratory tests of a high volume cascade impactor. J. Aerosol Sci. 34, 485–500. https://doi.org/10.1016/S0021-8502(02)00214-8.
Tarasenko, A., Pozdnyakova, N., Paliienko, K., Borysov, A., Krisanova, N., Pastukhov, A., Stanovyi, O., Gnatyuk, O., Dovbeshko, G., Borisova, T., 2022. A comparative study of wood sawdust and plastic smoke particulate matter with a focus on spectroscopic, fluorescent, oxidative, and neuroactive properties. Environ. Sci. Pollut. Control Ser. 29, 38315–38330. https://doi.org/10.1007/S11356-022-18741-X/TABLES/3.
Torabi, A., Mohammadbagheri, E., Akbari Dilmaghani, N., Bayat, A.H., Fathi, M., Vakili, K., Alizadeh, R., Rezaeimirghaed, O., Hajiesmaeili, M., Ramezani, M., Simani, L., Aliaghaei, A., 2020. Proinflammatory cytokines in the olfactory mucosa result in COVID-19 induced anosmia. ACS Chem. Neurosci. 11, 1909–1913. https://doi.org/10.1021/ACSCHEMNEURO.0C00249/ASSET/IMAGES/LARGE/CN0C00249_0001.JPEG.
Travaglio, M., Yu, Y., Popovic, R., Selley, L., Leal, N.S., Martins, L.M., 2021. Links between air pollution and COVID-19 in England. Environ. Pollut. 268, 115859 https://doi.org/10.1016/j.envpol.2020.115859.
Valderrama, A., Ortiz-Hernández, P., Agraz-Cibrián, J.M., Tabares-Guevara, J.H., Gómez, D.M., Zambrano-Zaragoza, J.F., Taborda, N.A., Hernandez, J.C., 2022. Particulate matter (PM10) induces in vitro activation of human neutrophils, and lung histopathological alterations in a mouse model. Sci. Rep. 12, 7581. https://doi.org/10.1038/s41598-022-11553-6.
Weaver, A.K., Head, J.R., Gould, C.F., Carlton, E.J., Remais, J.V., 2022. Environmental factors influencing COVID-19 incidence and severity. Annu. Rev. Publ. Health 43, 271–291. https://doi.org/10.1146/annurev-publhealth-052120-101420.
Wesselingh, R., 2023. Prevalence, pathogenesis and spectrum of neurological symptoms in COVID-19 and post-COVID-19 syndrome: a narrative review. Med. J. Aust. 219, 230–236. https://doi.org/10.5694/MJA2.52063.
Xia, X., Wang, Y., Zheng, J., 2021. COVID-19 and Alzheimer's disease: how one crisis worsens the other. Transl. Neurodegener. 10, 15. https://doi.org/10.1186/s40035-021-00237-2.
Yamamoto, A., Sly, P.D., Chew, K.Y., Khachatryan, L., Begum, N., Yeo, A.J., Vu, L.D., Short, K.R., Cormier, S.A., Fantino, E., 2023. Environmentally persistent free radicals enhance SARS-CoV-2 replication in respiratory epithelium. Exp Biol Med (Maywood) 248, 271–279. https://doi.org/10.1177/15353702221142616.
Ye, Q., Zhou, J., He, Q., Li, R.T., Yang, G., Zhang, Y., Wu, S.J., Chen, Q., Shi, J.H., Zhang, R.R., Zhu, H.M., Qiu, H.Y., Zhang, T., Deng, Y.Q., Li, X.F., Liu, J.F., Xu, P., Yang, X., Qin, C.F., 2021. SARS-CoV-2 infection in the mouse olfactory system. Cell Discovery 7 (1 7), 1–13. https://doi.org/10.1038/s41421-021-00290-1, 2021.
Yu, K., Zhang, Q., Wei, Y., Chen, R., Kan, H., 2024. Global association between air pollution and COVID-19 mortality: a systematic review and meta-analysis. Sci. Total Environ. 906, 167542 https://doi.org/10.1016/J.SCITOTENV.2023.167542.
Zazhytska, M., Kodra, A., Hoagland, D.A., Frere, J., Fullard, J.F., Shayya, H., McArthur, N.G., Moeller, R., Uhl, S., Omer, A.D., Gottesman, M.E., Firestein, S., Gong, Q., Canoll, P.D., Goldman, J.E., Roussos, P., tenOever, B.R., Overdevest, Jonathan B., Lomvardas, S., 2022. Non-cell-autonomous disruption of nuclear architecture as a potential cause of COVID-19-induced anosmia. Cell 185. https://doi.org/10.1016/j.cell.2022.01.024, 1052-1064.e12.
Zhang, J., Hao, Y., Ou, W., Ming, F., Liang, G., Qian, Y., Cai, Q., Dong, S., Hu, S., Wang, W., Wei, S., 2020. Serum interleukin-6 is an indicator for severity in 901 patients with SARS-CoV-2 infection: a cohort study. J. Transl. Med. 18, 1–8. https://doi.org/10.1186/S12967-020-02571-X/FIGURES/3.
Zhang, S., Wang, J., Wang, L., Aliyari, S., Cheng, G., 2022. SARS-CoV-2 virus NSP14 Impairs NRF2/HMOX1 activation by targeting Sirtuin 1. Cell. Mol. Immunol. 19, 872–882. https://doi.org/10.1038/s41423-022-00887-w.
Zhu, P., Zhang, W., Feng, F., Qin, L., Ji, W., Li, D., Liang, R., Zhang, Y., Wang, Y., Li, M., Wu, W., Jin, Y., Duan, G., 2022. Role of angiotensin-converting enzyme 2 in fine particulate matter-induced acute lung injury. Sci. Total Environ. 825, 153964 https://doi.org/10.1016/j.scitotenv.2022.153964.
Zhu, T.-Y., Qiu, H., Cao, Q.-Q., Duan, Z.-L., Liu, F.-L., Song, T.-Z., Liu, Y., Fang, Y.-Q., Wu, G.-M., Zheng, Y.-T., Ding, W.-J., Lai, R., Jin, L., 2021a. Particulate matter exposure exacerbates susceptibility to SARS-CoV-2 infection in humanized ACE2 mice. Zool. Res. 42, 335–338. https://doi.org/10.24272/j.issn.2095-8137.2021.088.
Zhu, T.-Y., Qiu, H., Cao, Q.-Q., Duan, Z.-L., Liu, F.-L., Song, T.-Z., Liu, Y., Fang, Y.-Q., Wu, G.-M., Zheng, Y.-T., Ding, W.-J., Lai, R., Jin, L., 2021b. Particulate matter exposure exacerbates susceptibility to SARS-CoV-2 infection in humanized ACE2 mice. Zool. Res. 42, 335–338. https://doi.org/10.24272/j.issn.2095-8137.2021.088.
Zosky, G.R., Iosifidis, T., Perks, K., Ditcham, W.G.F., Devadason, S.G., Siah, W.S., Devine, B., Maley, F., Cook, A., 2014. The concentration of iron in real-world geogenic PM10 is associated with increased inflammation and deficits in lung function in mice. PLoS One 9, e90609. https://doi.org/10.1371/journal.pone.0090609.

MUHAMMAD ALI SHAHBAZ

Air pollution exposures and disease pathologies alter infection susceptibility, progression, and outcomes. This thesis investigated how urban particulate matter (PM) affects cellular responses, influencing susceptibility to bacterial and viral pathogens. Additionally, it assessed the impact of SARS-CoV-2 infection on the olfactory mucosa (OM), a potential brain entry site of inhaled agents, and linked to Alzheimer's Disease (AD) pathology. The thesis also investigated how PM-induced cellular changes and AD pathology affect cellular responses to SARS-CoV-2 infection in OM cells.

UNIVERSITY OF
EASTERN FINLAND

uef.fi

PUBLICATIONS OF
THE UNIVERSITY OF EASTERN FINLAND
Dissertations in Health Sciences

ISBN 978-952-61-5235-6
ISSN 1798-5706